CORRELATION OF THE TIOGA BENTONITES USING RHYOLITIC MELT INCLUSIONS FOUND IN QUARTZ PHENOCRYSTS AS GEOCHEMICAL FINGERPRINTS

A thesis presented to the Faculty
of the State University of New York
at Albany
in partial fulfillment of the requirements
for the degree
of Master of Science

College of Science and Mathematics
Department of Geological Sciences

John W. Waechter

1993

State University of New York at Albany

College of Science and Mathematics

Department of Geological Sciences

The thesis for the master's degree submitted by

John W. Waechter

under the title

CORRELATION OF THE TIOGA BENTONITES USING RHYOLITIC MELT INCLUSIONS FOUND IN QUARTZ PHENOCRYSTS AS GEOCHEMICAL FINGERPRINTS

has been read by the undersigned. It is hereby recommended for acceptance by the Faculty with credit to the amount of 6 semester hours.

(Signed) John W. Delano
John W. Delano, Advisor

(Date) 19 April 1993

(Signed) William S. F. Kidd

(Date) 19th April 1993

(Signed) Mary K. Roden
Mary K. Roden

(Date) April 19, 1993

Recommendation accepted by the Dean of Graduate Studies for the Academic Council

(Signed) _____

(Date) _____

CORRELATION OF THE TIOGA BENTONITES USING RHYOLITIC MELT INCLUSIONS FOUND IN QUARTZ PHENOCRYSTS AS GEOCHEMICAL FINGERPRINTS

Abstract of

a thesis presented to the Faculty

of the State University of New York

at Albany

in partial fulfillment of the requirements

for the degree

of Master of Science

College of Science and Mathematics

Department of Geological Sciences

John W. Waechter

1993

ABSTRACT

The Tioga bentonites were first noted by Fettke in 1931 from well cuttings in the Tioga gas fields of Tioga County, Pennsylvania. They have been used by many investigators (Oliver, 1954, 1956; Dennison, 1963; Dennison and Textoris, 1967, 1978; Epstein, 1986; Smith and Way, 1983; Way et al., 1986) as a time-plane to correlate stratigraphic units from eastern Pennsylvania to Illinois and from southern Ontario to Virginia. The Tioga bentonites are recognized as seven major volcanic ash layers labeled Tioga-A - Tioga-G as well as several minor layers labeled Tioga-A1 - Tioga-A3 (Way et al., 1986). They occur within the Onondaga (Middle Devonian) limestone and the Marcellus (Middle Devonian) shale, and by definition mark the top of the Onesquethaw stage (Dennison 1960). The Tioga bentonites are Eifelian (Middle Devonian) and the Tioga-B layer has been recently dated as 390.0 Ma $\pm$0.5 Ma (Roden et al., 1990) using U-Pb analysis of monazite phenocrysts.

The Tioga bentonites have been inferred to cover $\approx$264,180 km^2 of the Appalachian basin of the northeast United States (Dennison and Textoris, 1987) and occur in two dissimilar stratigraphic units; hence the need for precise correlation is paramount. High precision electron microprobe analysis of the rhyolitic melt (i.e., glass) inclusions found in the quartz phenocrysts allows for the geochemical fingerprinting of individual bentonite layers.

Using this technique, only four out of fourteen localities previously reported as the Tioga bentonites geochemically correlated to bentonite layers present at Frankstown, PA. The absence of bentonite layers containing quartz phenocrysts with melt inclusions at the ten other sample locations indicate that bentonite layers equivalent to FP-12 and FP-9 may be absent. This implies that the Tioga group of bentonites may consist of more than the seven major bentonite layers as previously reported. The geochemical analyses of the rhyolitic melt inclusions of this study indicate that the eruptions responsible for the Tioga bentonites (as restricted here) are from a heterogeneous (i.e., zoned) magma chamber.

CORRELATION OF THE TIOGA BENTONITES USING RHYOLITIC MELT INCLUSIONS FOUND IN QUARTZ PHENOCRYSTS AS GEOCHEMICAL FINGERPRINTS

A thesis presented to the Faculty
of the State University of New York
at Albany
in partial fulfillment of the requirements
for the degree
of Master of Science

College of Science and Mathematics
Department of Geological Sciences

John W. Waechter

1993

ACKNOWLEDGMENTS

Without the support and encouragement of many people, this endeavor would not have been possible.

First and foremost, I would like to thank my advisor, John Delano, who introduced me to the Tioga bentonites. His encouragement and financial support enabled me to progress on this project without impediment. It was through his critical reviews that allowed this thesis to mature from a skeleton to what it is now.

I am also grateful to Bill Kidd for "turning me on" to geology and rescuing me from the grips of the Chemistry Department and to Mary Roden for all the resources and encouragement she provided me. A debt of gratitude is also owed to the "bentonite group", thanks for the ideas, suggestions, and lively discussions. I appreciate the time and effort provided by Dave Wark and the use of the electron microprobe facilities at R.P.I. To the entire faculty and all of the graduate students who have made my journey here an enjoyable one, I am extremely grateful. I would also like to thank Bob Osbourne of the State Department of Transportation for his time and information and to all the quarry superintendents who gave me access to their quarries.

I particularly would like to acknowledge Ben Hanson. What can I say, you showed me how to use the probe, spent many evenings helping and encouraging, and had some great conversations around the fire in Pennsylvania. None of it will be forgotten.

Lastly, I would like to thank my parents for instilling the value to dream and to Kelly for helping those dreams become reality.

TABLE OF CONTENTS

LIST OF TABLES

LIST OF FIGURES

LIST OF APPENDICIES

1.1 BENTONITES

The term "bentonite" was first introduced in 1898 by Knight (Knight, 1898) for the soap-like clays found in the Benton shale, which is a Cretaceous deposit in eastern Wyoming (Smith and Way, 1983). They are primarily composed of the mineral smectite which gives them a thixotropic characteristic (Roen and Hosterman, 1982). As a result of this unique property, they are valued in industry, primarily for drilling mud, foundry sand bonds, and pelletizing taconite iron ore (Roen and Hosterman, 1982).

Bentonites are altered and compacted layers of volcanic ash and debris ejected during plinian eruptions. These layers are often deposited over large geographic areas and represent geologically instantaneous deposits. If preserved, they define a chronostratigraphic unit or time-plane that affords a relative time precision that is seven to eight orders of magnitude better than isotopic dating methods (e.g., ± 1 month vs ± 1 Ma).

Because of their importance as a stratigraphic correlative tool, many investigators have attempted to correlate individual bentonites over large geographical areas. The methods used by previous investigators to derive these correlations have included: 1) paleontology; 2) apatite chemistry; 3) bulk bentonite "clay" chemistry; 4) petrology; and 5) zircon morphology. However, difficulties in these methods (i.e., detrital contamination,

bioturbation, diagenetic mobility of elements during alteration, and hydrodynamic sorting during deposition) have often complicated attempts to accurately correlate individual bentonite layers over great distances. These difficulties have stimulated the use of a new technique in geochemical identification of individual bentonite layers that relies on high precision electron microprobe analyses of rhyolitic melt inclusions (i.e., glass) that occur in quartz phenocrysts (Schirnick and Delano, 1990, 1991; Hanson et al., 1991; Lindstrom et al., 1992). This technique gives a geochemical fingerprint of individual bentonite layers that is consistant and repeatable, can be graphically represented, and statistically resolved.

1.2 THE TIOGA BENTONITES

The name Tioga bentonite was proposed by Fettke (1931) for the "...Thin, but persistent seam of brown micaceous bentonite shale occurring at or near the boundary between the Hamilton group and the Onondaga formation...". He later observed the brown micaceous shale throughout the Appalachian basin in Pennsylvania and noted its importance as a time marker (Ebright et al., 1949). James Hall had recognized this bentonite in 1843 at Seneca, New York and described it as a clay parting near the top of the Onondaga limestone (Hall, 1843). Oliver recognized the Tioga bentonite just below the Marcellus shale (Hamilton group) in western New York. He postulated that the Devonian shales drop lower in section eastward and predicted that the Tioga bentonite transgresses from the Onondaga limestone into the Union Springs member of the Hamilton group east of Cherry Valley, New York (Oliver, 1954, 1956). Designation of the Tioga bentonite as the top of the Onesquethaw stage of the Devonian system by Dennison (1961) has been followed by later investigators (Rickard, 1964, 1975; Oliver et al., 1967, 1969).

In actuality, the Tioga "bentonite" consists of at least seven major layers that are preserved in the northeastern portion of the Appalachian basin. The total extent of the Tioga bentonites is approximately 102,000 square miles (Figure 1.1; Dennison and Textoris, 1987).

Most investigators have named the layers Tioga-A through Tioga-G with some investigators (Smith and Way, 1983; Way et al., 1986) labeling other layers observed directly beneath Tioga-A as Tioga-A1 through Tioga-A3.

The age of the Tioga-B layer has recently been determined (Roden et al., 1990) as 390.0 Ma $\pm$0.5 Ma by U-Pb techniques on monazite phenocrysts. The clay mineralogy has been described by Weaver (1956). Dennison and Textoris (1970, 1971, 1978) reported on the petrology of the Tioga bentonites and used the petrological characteristics to aid in their stratigraphic inference of the Tioga bentonite occurrence throughout much of the Appalachian basin.

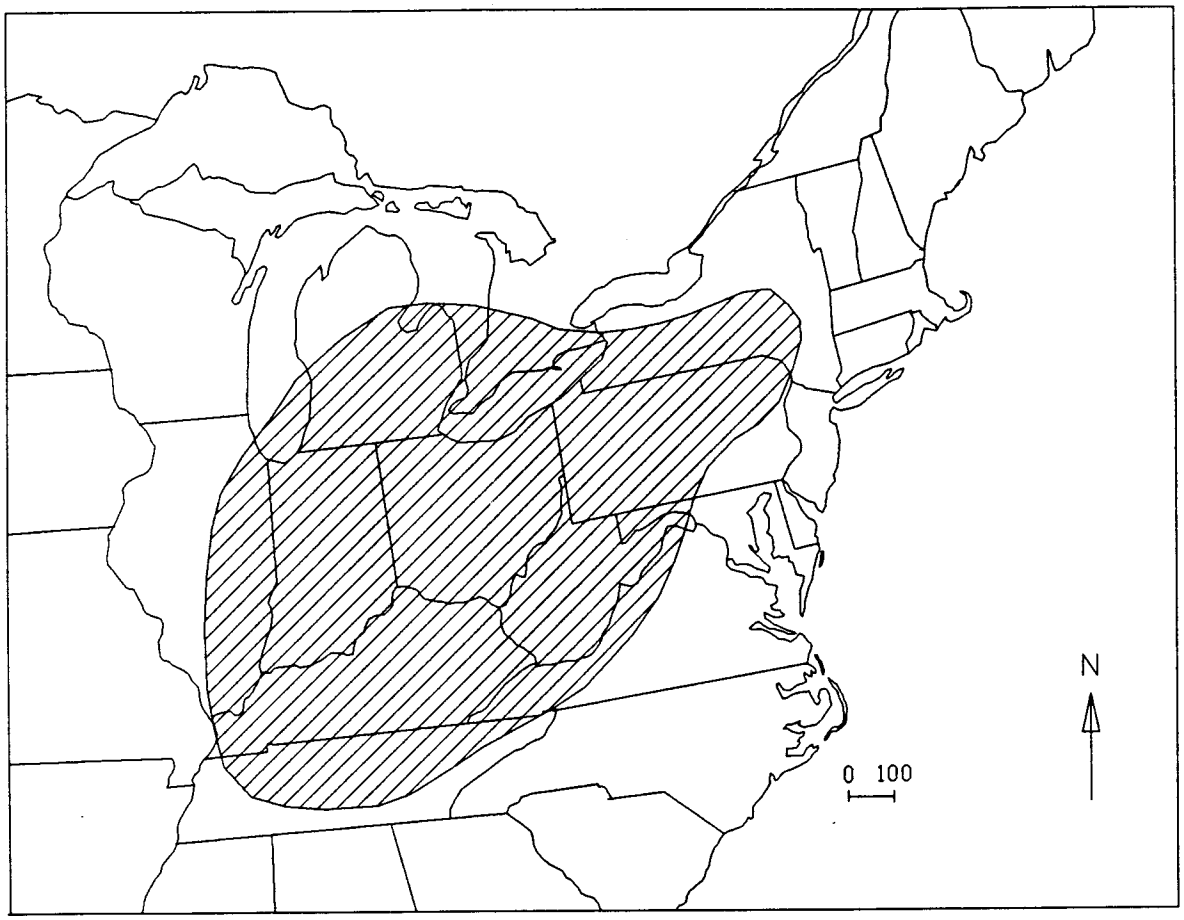

Figure 1.1 Map of the northeastern United States. The hatched area indicates the aerial extent of the Tioga bentonites as reported by other investigators.

1.3 PURPOSE OF STUDY

Because the Tioga bentonites have been reported to occur over a large area and are in two dissimilar stratigraphic units (i.e., the upper Onondaga limestone and the lower Marcellus shale), the need for their precise correlation is paramount. The purpose of this study is to quantitatively verify previously reported correlations of the Tioga bentonites based on other methods, using here the geochemical fingerprinting of pristine glass in melt inclusions contained in quartz phenocrysts.

To perform this quantitative check of previous investigators, the following methodology was used. First, a location central to the area of study was chosen. Detailed sampling of this locality and analyses of these samples were done to obtain a geochemical database to be used as a reference standard. Second, fourteen other localities were sampled, analyzed, and the results compared to the reference database obtained from the central locality. The sample comparisons were then used to verify or refute the equivalency of specific bentonite layers proposed by other investigators.

1.4 GEOLOGICAL SETTING

A thorough understanding of the Acadian Orogeny (≈390 Ma) and its effects in the Appalachians is incomplete due to the lack of stratigraphic continuity, metamorphic and plutonic overprint, and complex structural features (Osberg et al., 1989). There is Silurian-Devonian cover in New England which was not severely affected by the Alleghanian orogeny that allows the study of the Acadian (Osberg et al., 1989). Bradley (1989) supports the theory of McKerrow and Ziegler (1971) that subduction zones dipped east and west beneath the North American and Avalonian margins (Figure 1.2).

Volcanics associated with the Acadian Orogeny include the Piscataquis Volcanic Belt and the Coastal Volcanic Belt (Figure 1.3). Due to incomplete stratigraphic continuity and the effects caused by the Alleghanian Orogeny (≈330 Ma) on the rocks south of New England, the southern extent of these volcanics is unknown.

The Piscataquis Volcanic Belt occurs from Pridolian (414 - 408 Ma) to Gedinnian (408 - 401 Ma) and from Siegenian (401 - 394 Ma) to Emsian (395 - 387 Ma; Osberg et al., 1989). The earlier volcanics consist of andesites with smaller amounts of basalt, dacite, rhyolite, tuff, and ash-flow tuff (Boucot et al., 1964; Hall, 1970; Sargent and Hon, 1981). Laurent and Belanger (1984) believe that these volcanics originated in a compressive intraplate

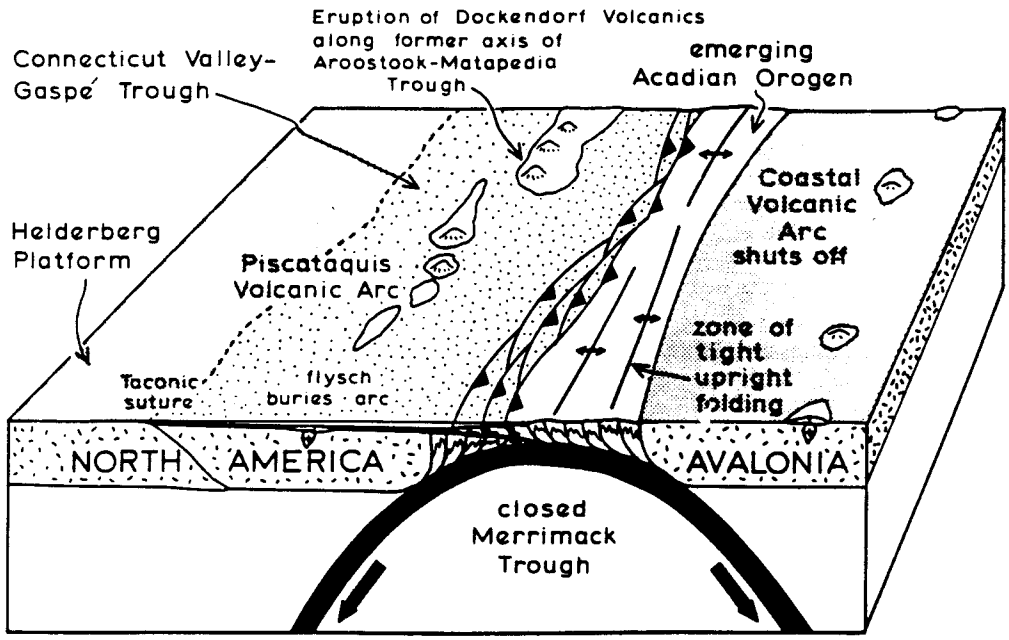

Figure 1.2. Proposed reconstruction of the Acadian Orogen in early Devonian times. From Bradley (1989).

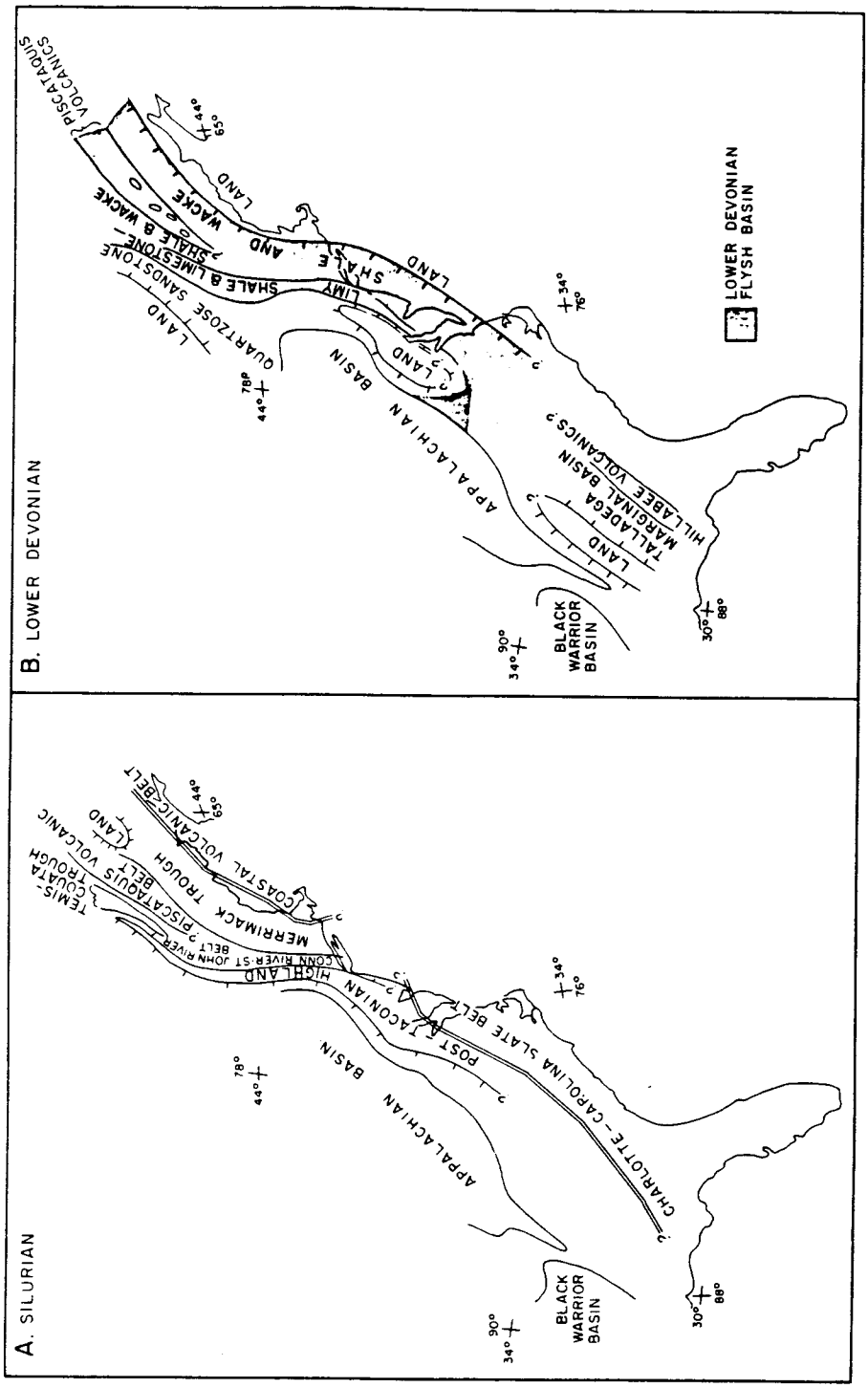

Figure 1.3. Paleogeography for the Silurian (A) and Lower Devonian (B). Double lines indicate the approximate position of an ocean. From Osberg and others (1989).

continental environment . The younger volcanics are rhyolite flows, ash-flow tuffs, and tuffs (Rankin, 1968; Boucot, 1969). Hon et al. (1981) suggest that the geochemical analyses of these rocks indicate that they were derived from a crustal source.

Shride (1976) described the Southern Coastal Volcanic Belt as consisting of basalts, andesites, rhyolites, and tuffs. Geochemical analyses (Gates and Moench, 1981; Pinette, 1983) indicate that these volcanics straddle the boundary between the calc-alkalic and tholeiitic rock series (Osberg et al., 1989).

Bentonites that occur in Early Devonian (i.e., Esopus and Cherry Valley bentonites; Hanson et al., 1991) through the Middle Devonian (i.e., Tioga bentonites) are the only remnants of Acadian volcanism south of New England and north of North Carolina. Dennison and Textoris (1978) place the source of the Tioga bentonites in northeastern Virginia near Fredericksburg. More recently, Osbourne (personal communication, 1992) believes the source lies farther north in New Hampshire.

1.5 DEPOSITIONAL ENVIRONMENT

The Tioga bentonites occur near and at the top of the Selinsgrove limestone (Middle Devonian, Onondaga equivalent) and near the base of the Marcellus shale (Middle Devonian) of the Hamilton group.

The Selinsgrove limestone (referred to as the Needmore formation by Inners, 1975), is a medium gray, argillaceous limestone representing a subtidal marine environment (Feldman, 1980). The Selinsgrove limestone grades into the Marcellus shale. This change is observed by the introduction of black, silty, carbonaceous shales interbedded with the silty limestone beds of the Selinsgrove (Inners, 1975). The limestone beds decrease in size from several meters to thin lenticular beds of several centimeters.

The Marcellus shale is a black fissile shale that is the basal member of the Hamilton group. It represents the first major phase of siliciclastic sedimentation from the Acadian Orogen (Brett, 1986). Dennison (1976) interprets the change from the shallow water limestones (i.e., Selinsgrove) of the Appalachian foreland basin to the black shales (i.e., Hamilton group) as a sea level rise. This interpretation differs from Bradley (1989) where the loading of the North American shelf with the advancing Avalonia would drown the shelf and foreland basin by lithospheric flexure.

2.1 THE RHYOLITIC MELT INCLUSIONS AS A CORRELATING TOOL

Rhyolitic melt inclusions that occur in quartz phenocrysts (Figure 2.1) represent magma that became trapped during phenocryst growth shortly before eruption (e.g., Druitt et al., 1982; Melson, 1983; Roedder et al., 1984). During eruption, the trapped magma contained within the quartz host was quenched to a glass. The glass was then protected and preserved from alteration by the durability (physical and chemical) of the quartz host. This glass will remain pristine unless the integrity of the host is violated (i.e., by microfracturing) or heated for a sufficient time-interval to cause devitrification. Because the melt inclusion represents the geochemical composition of the magma just prior to eruption, each bentonite layer (i.e., volcanic event) will contain quartz phenocrysts with melt inclusions of distinctive geochemical composition. It is this principle of each bentonite layer possessing a distinguishable composition of melt inclusion that allows individual bentonite layers to be geochemically fingerprinted. The capability of the this technique has been demonstrated on Ordovician k-bentonites (Schirnick and Delano, 1990, 1991) and on other Devonian bentonites (Hanson et al., 1992).

Melt inclusions found to occur within quartz phenocrysts of the Tioga bentonites are observed to be of various shapes. These include; cubic to elongated cubic with

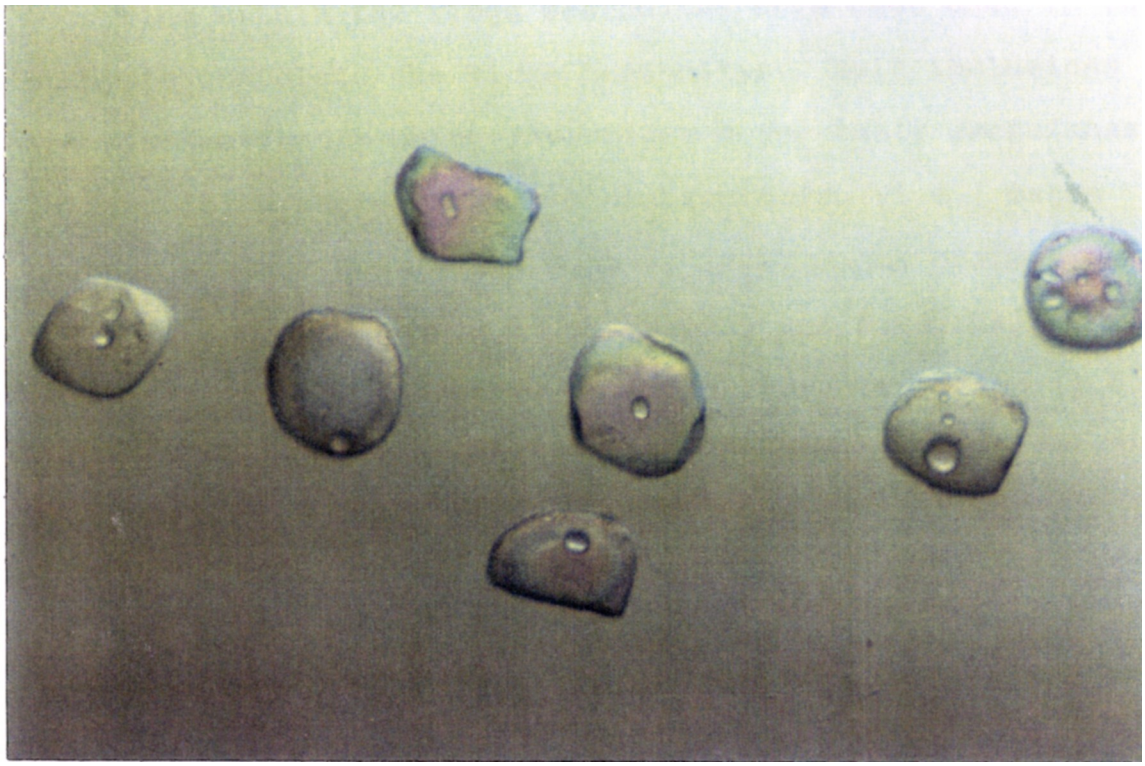

Figure 2.1. Quartz phenocrysts that contain rhyolitic melt (i.e., glass) inclusions. This sample is from bentonite FP-12 at Frankstown, Pennsylvania. Field of view is 4mm.

rounded edges, spherical, elliptical, and kidney shaped (Figures 2.2 and 2.3). The sizes of the melt inclusions vary from 5 microns to 120 microns with an average size of 60-80 microns. While the size-range seems to have a normal distribution, the distribution of geometric shapes appears to be random.

The geochemical compositions of melt inclusions occurring within the Tioga bentonites have been used in this study to correlate the Tioga bentonites. Melt inclusions are also currently being investigated for their usefulness in describing magma chamber characteristics (i.e., magma chamber zoning; Hervig and Dunbar, 1992; magma chamber volatile content; Hervig et al., 1992) and have the potential to describe other volcanic characteristics (i.e., eruption dynamics and magma chamber replenishment).

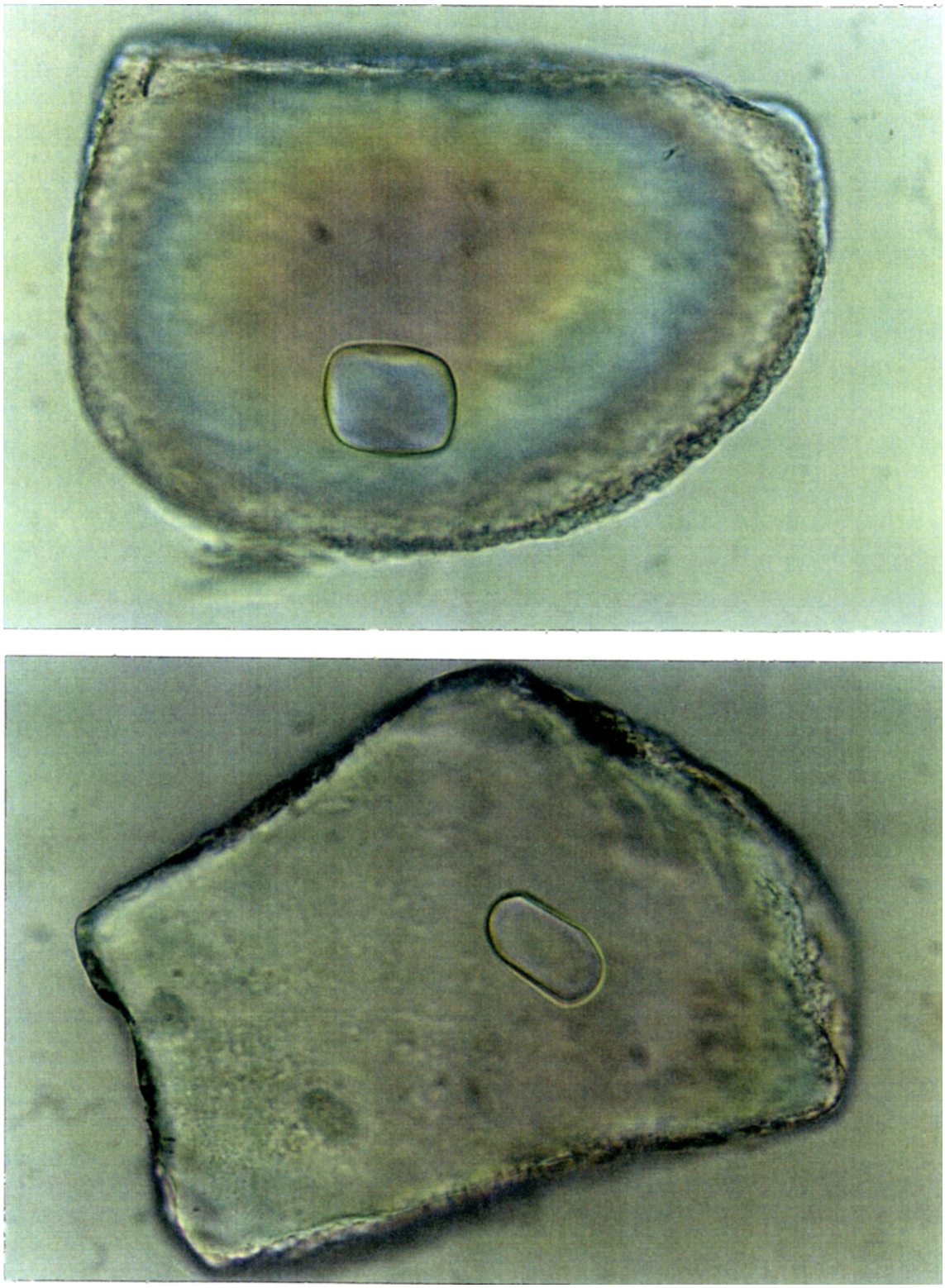

Figure 2.2. Photomicrographs of quartz phenocrysts containing rhyolitic melt inclusions demonstrating the cubic shape with round edges (top) and elongated cubic with round edges (bottom) types. Field of view is 400 microns in both photomicrographs.

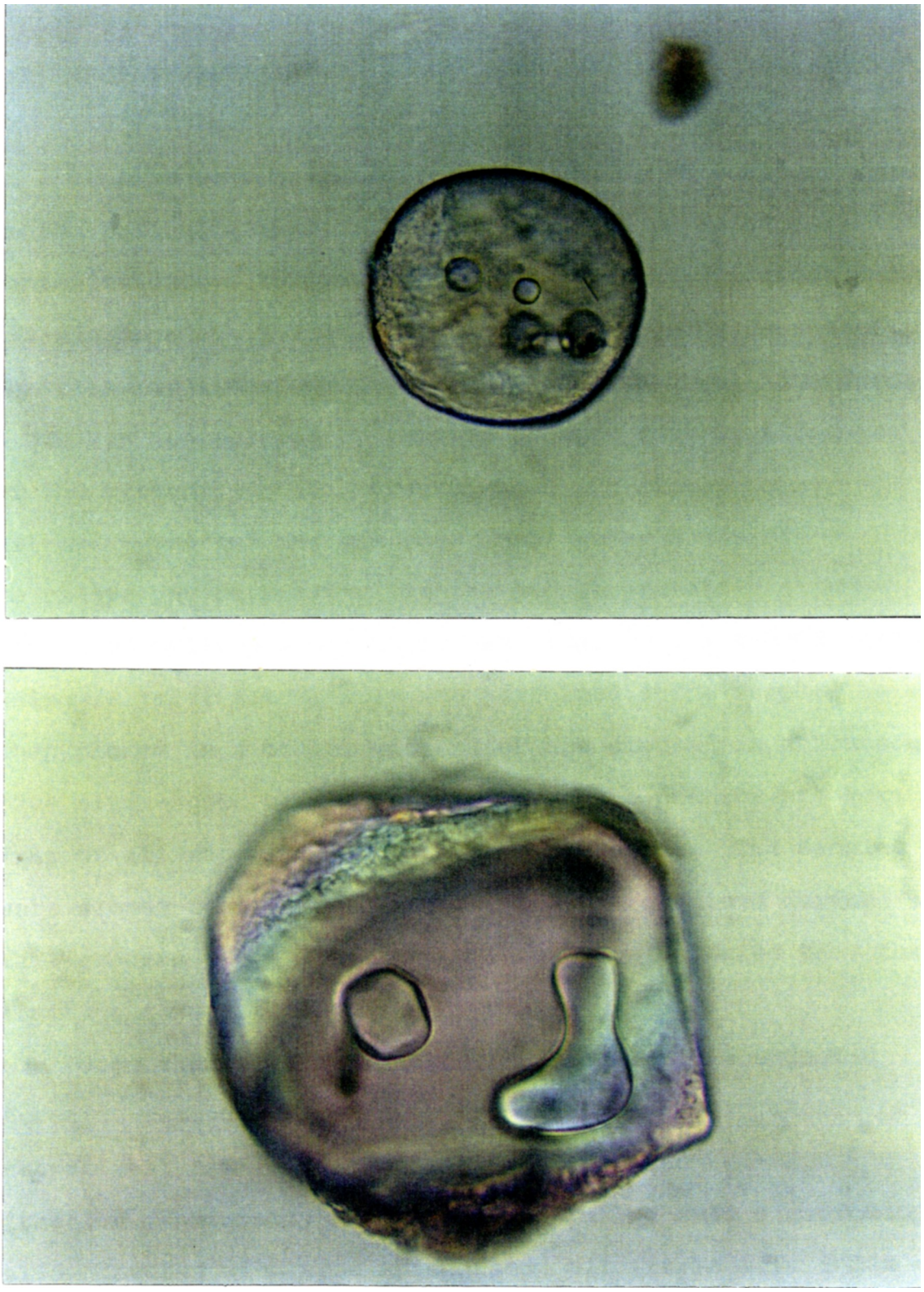

Figure 2.3. Photomicrographs of quartz phenocrysts containing melt inclusions demonstrating the spherical type (top) and kidney shaped (bottom) types that occur. Field of view is 700 microns for the top photomicrograph and 400 microns for the bottom photomicrograph.

2.2 SAMPLE PREPARATION

Samples were prepared for electron microprobe analyses in the following manner. Several hundred grams of bulk bentonite were first washed through a 105-micron sieve and a 350-micron sieve. The latter excluded large fragments of shale and/or limestone. The fraction within the 105-micron sieve was manipulated by hand to promote further breakdown of the bentonite. This greater than 105-micron sample was allowed to reflux for one hour in 12 molar hydrochloric acid to remove any carbonate. If the sample contained a large amount of sulfide minerals or was lithified, a second reflux using 16 molar nitric acid was performed. The samples were then placed in a beaker with water and cleaned in a Branson 5200 ultra-sonic cleaner until the quartz phenocrysts were free of all material (e.g., 48 to 168 hours). The samples were sieved repeatedly using the 105-micron sieve during this process until microscopic inspection revealed that the fraction consisted of clean crystals.

Once cleaned, the sample was dried and the magnetic fraction removed by a Frantz isodynamic magnetic separator set at a 3^{o} tilt and a 10^{o} inclination. The non-magnetic fraction (dominantly quartz) was sprinkled onto a microscope slide covered with type A immersion oil (refractive index = 1.518) obtained from Wards Scientific. The quartz phenocrysts that contained optically homogeneous melt inclusions (Schirnick, 1991) were handpicked.

To mount the quartz phenocrysts, a piece of parafilm type laboratory film was placed on a microscope slide and individual quartz phenocrysts were placed on it with separations of approximately one half inch between crystals. A 0.25-inch (outside diameter) piece of aluminum tubing was placed over each quartz phenocryst. Each tube was three quarters filled with Hillquist brand thin section epoxy types A and B prepared using the manufacturer's instructions. Once the epoxy cured, the mounted samples were carefully ground using a Buehler hand grinding board with 240, 320, 400, and 600 grit grinding strips, successively, to expose the melt inclusion. A final polish was obtained using 0.3-micron alpha alumina polishing compound.

2.3 SAMPLE ANALYSES

Mounted samples were carbon-coated and analyzed on the electron microprobe located at the Department of Earth and Environmental Sciences at the Rensselaer Polytechnic Institute. It is a JEOL 733 Superprobe that uses five wavelength-dispersive spectrometers with on-line data reduction using Bence-Albee matrix corrections. The high precision analyses of Ti, Al, Fe, Cl, and Mg (one element per spectrometer) were obtained using an accelerating voltage of 15 kv, cup current of 40 nanoampres and a beam width of 10 to 20 microns. Counting time for each element was 140 seconds at the peak position and 70 seconds at each background position on both sides of the peak for every analysis. Data was collected for all five elements simultaneously.

The data obtained was the K-value, which is a weight fraction of the elemental oxide without the Bence-Albee matrix correction. The K-values were converted to the elemental abundances by multiplying the K-value by a beta factor. The beta factor for each element was obtained by the ratio of the K-value to the known elemental abundance in various standards. The beta factors used were: for TiO_2, 1.12; MgO, 1.15; Cl, 1.26; FeO, 1.14; and Al_2O_3, 1.07.

3.1 OUTLINE OF METHODOLOGY

To geochemically correlate the Tioga bentonites over a portion of previously recorded occurrences, the following method was used. A location central to the area of study was chosen to provide a database or analytical standard to match all other localities. Once this analytical database was defined, other reported localities of the Tioga bentonites were sampled and analyzed. The results of these analyses were compared to the analytical database obtained from the central locality to determine if a match existed. This match is based both upon graphical representation and statistical analyses of the data.

An abandoned sand quarry at Frankstown, Pennsylvania was chosen as the central locality (Figure 3.1). This location was chosen for its easy access to the major bentonite layers of the Tioga and because it is unanimously considered by other investigators (Way et al., 1986) to contain the Tioga bentonites. Once this locality was carefully sampled and a detailed stratigraphic column was completed, fourteen other localities (Figure 3.1) were sampled and analyzed. These other localities include: Lancaster, NY; Seneca Falls, NY; Marcellus, NY; Jamesville, NY; Cherry Valley, NY; East Stroudsburg, PA; Bowmanstown, PA; Selinsgrove Junction, PA; Dalmatia, PA; Midway, PA; Everett, PA; Newton Hamilton, PA; Tipton, PA; and Castalia, OH (Figure 3.1).

1 LANCASTER
2 SENECA FALLS
3 MARCELLUS
4 JAMESVILLE
5 CHERRY VALLEY
6 EAST STROUDSBURG
7 BOWMANSTOWN
8 SELINSGROVE JUNCTION
9 DALMATIA
10 MIDWAY
11 NEWTON HAMILTON
12 EVERETT
13 FRANKSTOWN
14 TIPTON
15 CASTALIA

Figure 3.1. Map of northeastern United States showing localities sampled and geochemically analyzed for this study. The scale bar is in km.

3.2 FRANKSTOWN, PA AS A GEOCHEMICAL DATABASE

The outcrop at Frankstown, PA (40° 26′ 53" N, 78° 20′ 53" W) is in an abandoned sand quarry. Access to the quarry is off State Route 2020 which is located one mile south of State Route 22 (Figure 3.2). At the southeastern portion of the quarry the Marcellus shale (Middle Devonian) is exposed and dips 25° north (Figure 3.2). The floor of the quarry is composed of eroded sand from the friable Oriskany sandstone (Middle Devonian). The Oriskany/Onondaga and Onandaga/Marcellus contacts are not presently exposed (1992). Twelve distinct bentonite layers are recognized and are designated FP-1 through FP-12. The first four bentonites (FP-1, FP-2, FP-3, and FP-4) were discovered by digging a trench to a depth of five feet in the quarry floor. Bentonites FP-5 through FP-12 are accessible without trenching and correspond to those noted by Way et al. (1986) as Tioga-A3 through Tioga-G (Figure 3.3).

The Marcellus shale is a black fissile shale inter-bedded with gray arenaceous limestones. These limestone beds vary in thickness from 10 cm to 50 cm. The Marcellus shale, which is the base of the Hamilton group represents the first major phase of silicic sedimentation from the Acadian orogeny (Brett, 1991). The bentonites that are determined by previous investigators (Way et al., 1986) as the Tioga bentonites (Figures 3.3 - 3.7) are all within the Marcellus shale (Figures 3.8 and 3.9).

FRANKSTOWN QUADRANGLE
PENNSYLVANIA—BLAIR CO.
7.5 MINUTE SERIES (TOPOGRAPHIC)

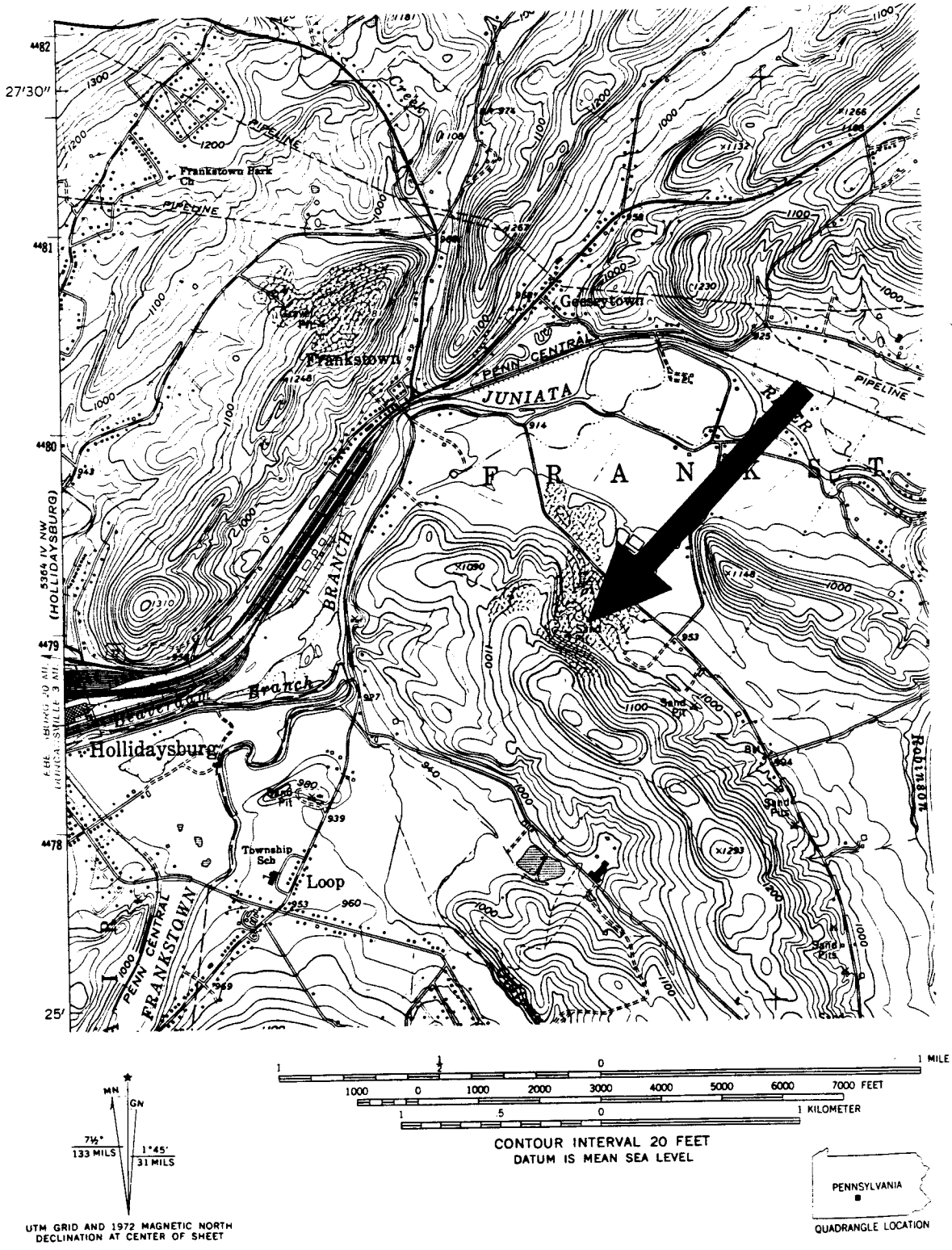

Figure 3.2. 7.5 minute quadrangle map of Frankstown, PA showing the location of the abandoned sand quarry.

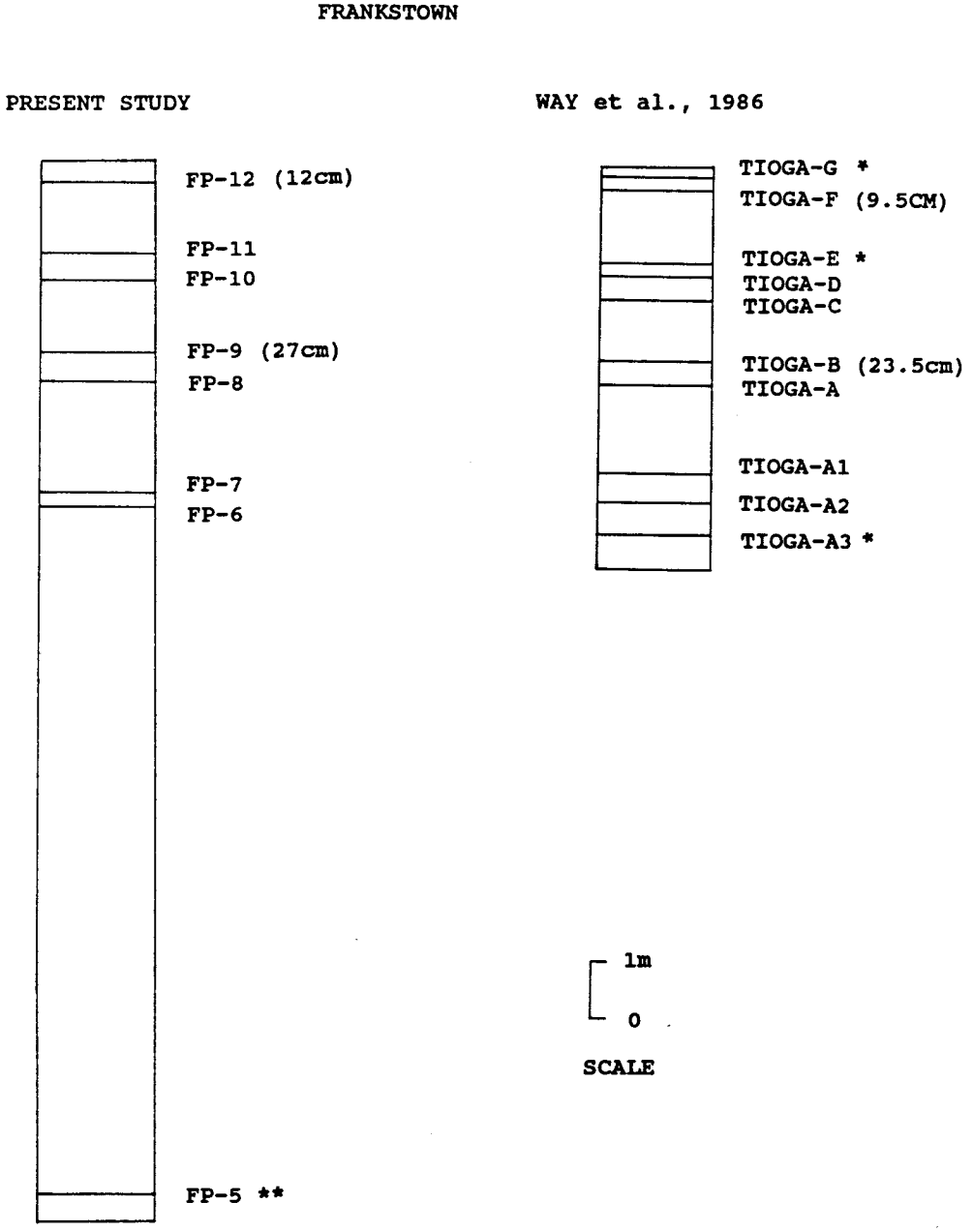

Figure 3.3. Schematic diagram showing the bentonite designations of this study and of previous studies by Way et al. (1986) for the Frankstown, PA outcrop. * indicates that this bentonite was not recognized by this investigator and ** indicates that this bentonite was not recognized by Way et al. (1986).

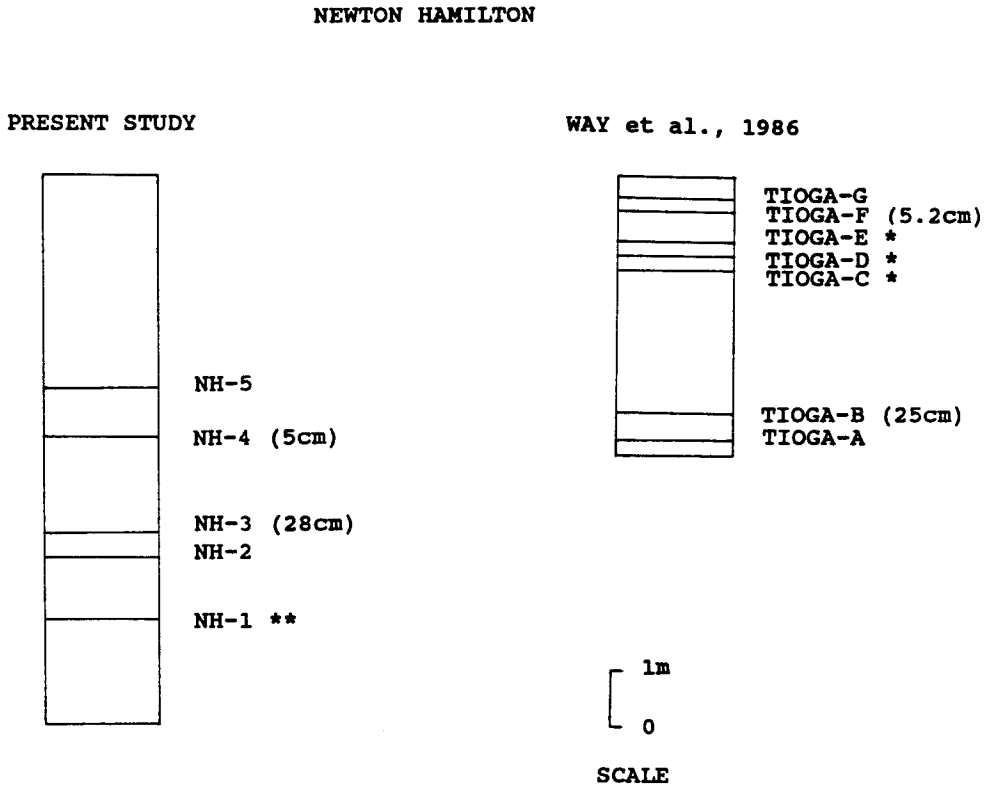

Figure 3.4. Schematic diagram showing the bentonite designations of this study and of previous studies by Way et al. (1986) for the Newton Hamilton, PA outcrop. * indicates that this bentonite was not recognized by this investigator and ** indicates that this bentonite was not recognized by Way et al. (1986).

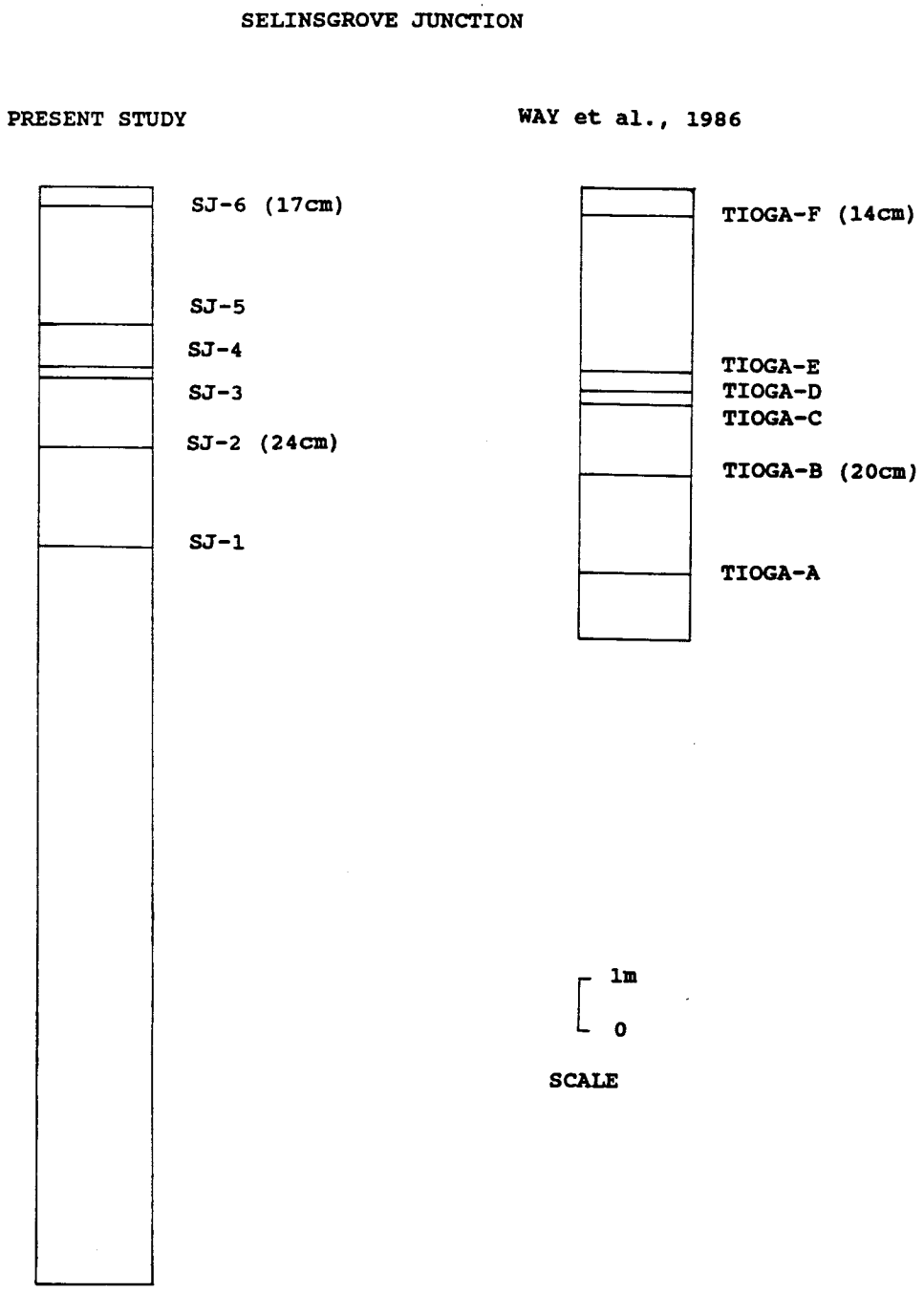

Figure 3.5. Schematic diagram showing the bentonite designations of this study and of previous studies by Way et al. (1986) for the Selinsgrove Junction, PA outcrop.

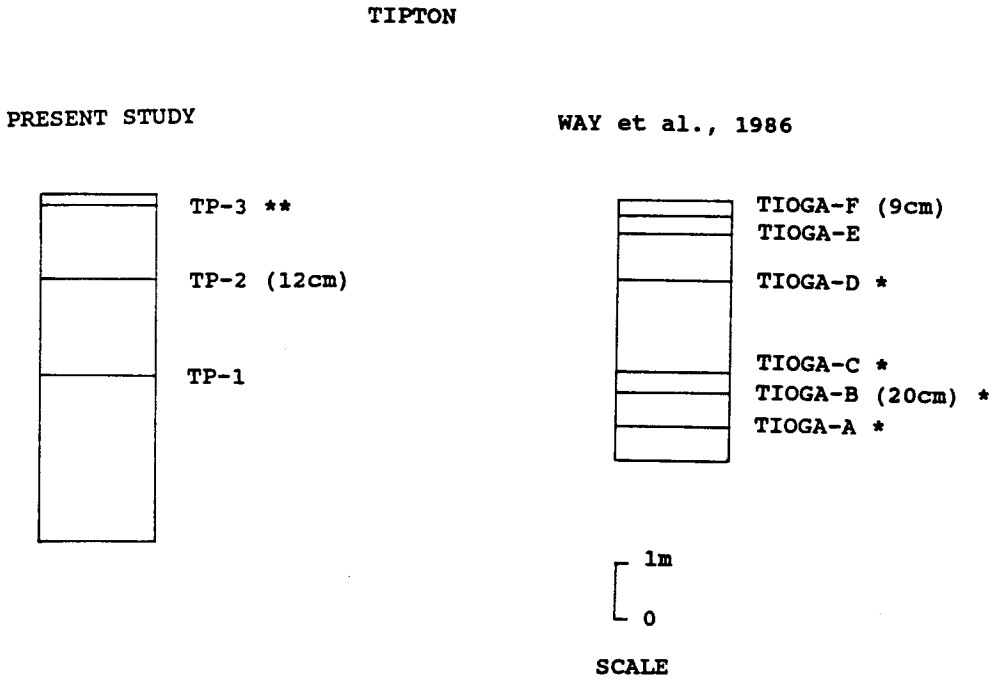

Figure 3.6.. Schematic diagram showing the bentonite designations of this study and of previous studies by Way et al. (1986) of the Tipton, PA outcrop. * indicates that this bentonite was not recognized by this investigator and ** indicates that this bentonite was not recognized by Way et al. (1986).

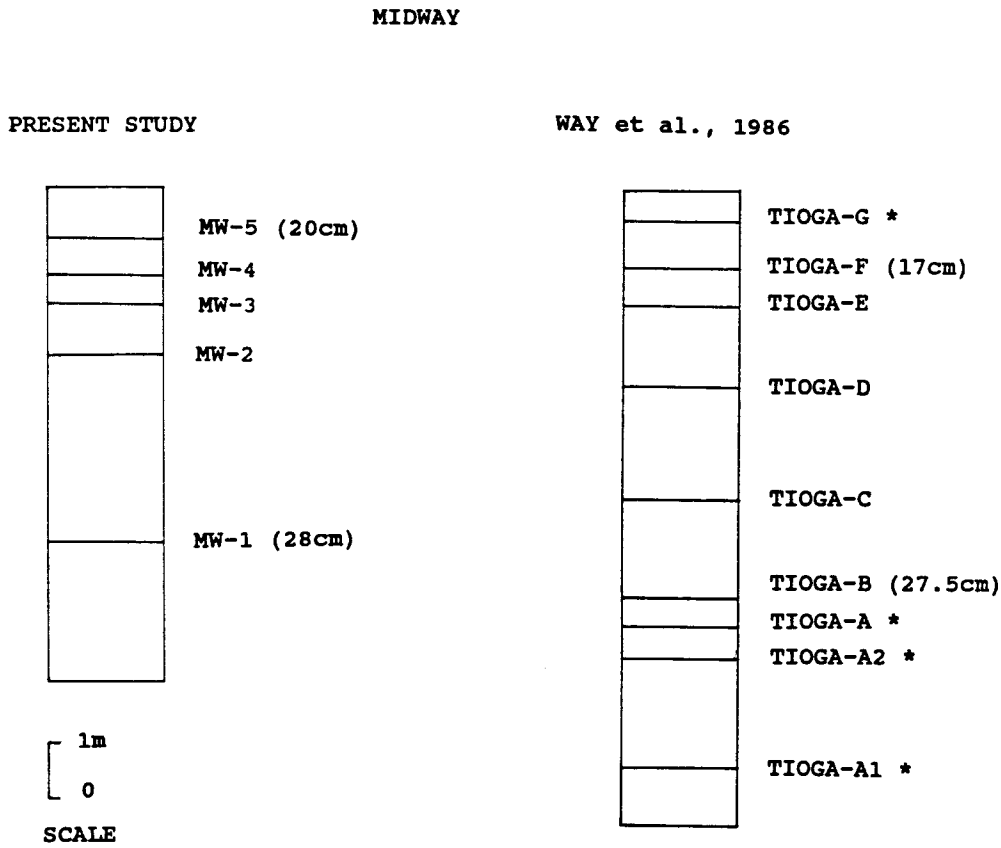

Figure 3.7. Schematic diagram showing the bentonite designations of this study and of previous studies by Way et al. (1986) of the Midway, PA outcrop. * indicates that this bentonite was not recognized by this investigator.

Figure 3.8. Photograph of the Marcellus shale (Middle Devonian) outcrop in the sand quarry at Frankstown, PA. the central location for this study. Arrow indicates bentonite FP-9.

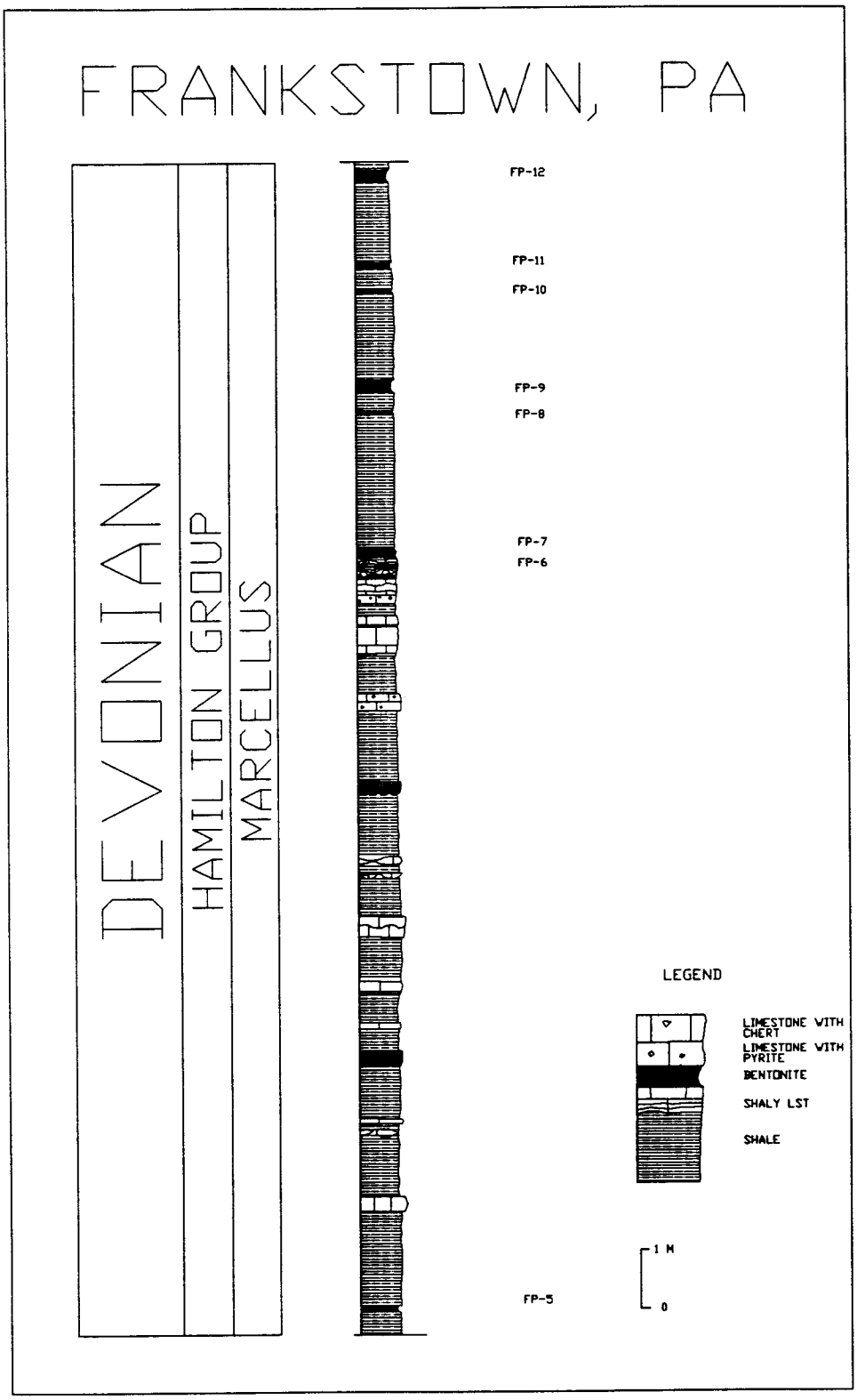

Figure 3.9. Stratigraphic column of the outcrop at Frankstown, PA constructed by this investigator.

Three bentonites (FP-8, FP-9, and FP-12) at this locality contained quartz phenocrysts with melt inclusions. Geochemical analyses of these melt inclusions indicated that all three bentonites could be distinguished by graphical representation. Ternary diagrams of Mg*10-Ti*-Fe and Mg-Ti-Cl (Figure 3.10 and 3.11) along with X-Y plots of wt % MgO vs Cl, TiO_2 vs FeO, Mgo vs FeO, TiO_2 vs Cl, FeO vs Cl, and MgO vs TiO_2 (Figures 3.12 - 3.17) demonstrate the distinctiveness of the individual bentonites. The Yellowstone rhyolite standard (USNM 72854) was analyzed during each electron microprobe session for calibration purposes. Notice the tight cluster of bentonite FP-12 in the FeO vs Cl plot (Figure 3.16) and its rather linear trend in the MgO vs TiO_2 plot (Figure 3.17). These characteristics are diagnostic for this bentonite.

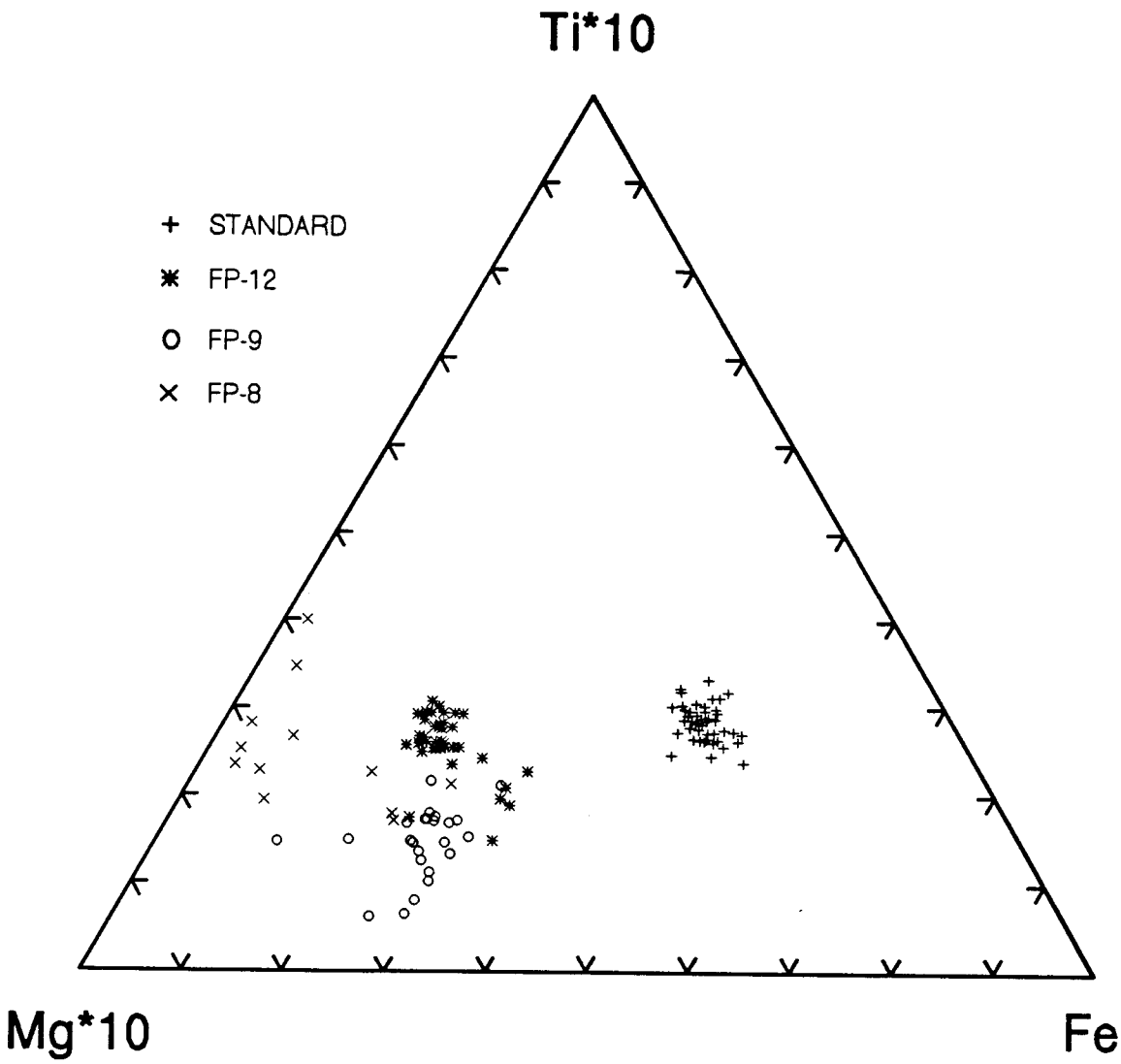

Figure 3.10. Ternary diagram of Mg*10-Ti*10-Fe. Symbols used are: pluses indicate the Yellowstone rhyolite standard; asterisks indicate bentonite FP-12; circles indicate bentonite FP-9; and X's indicate bentonite FP-8.

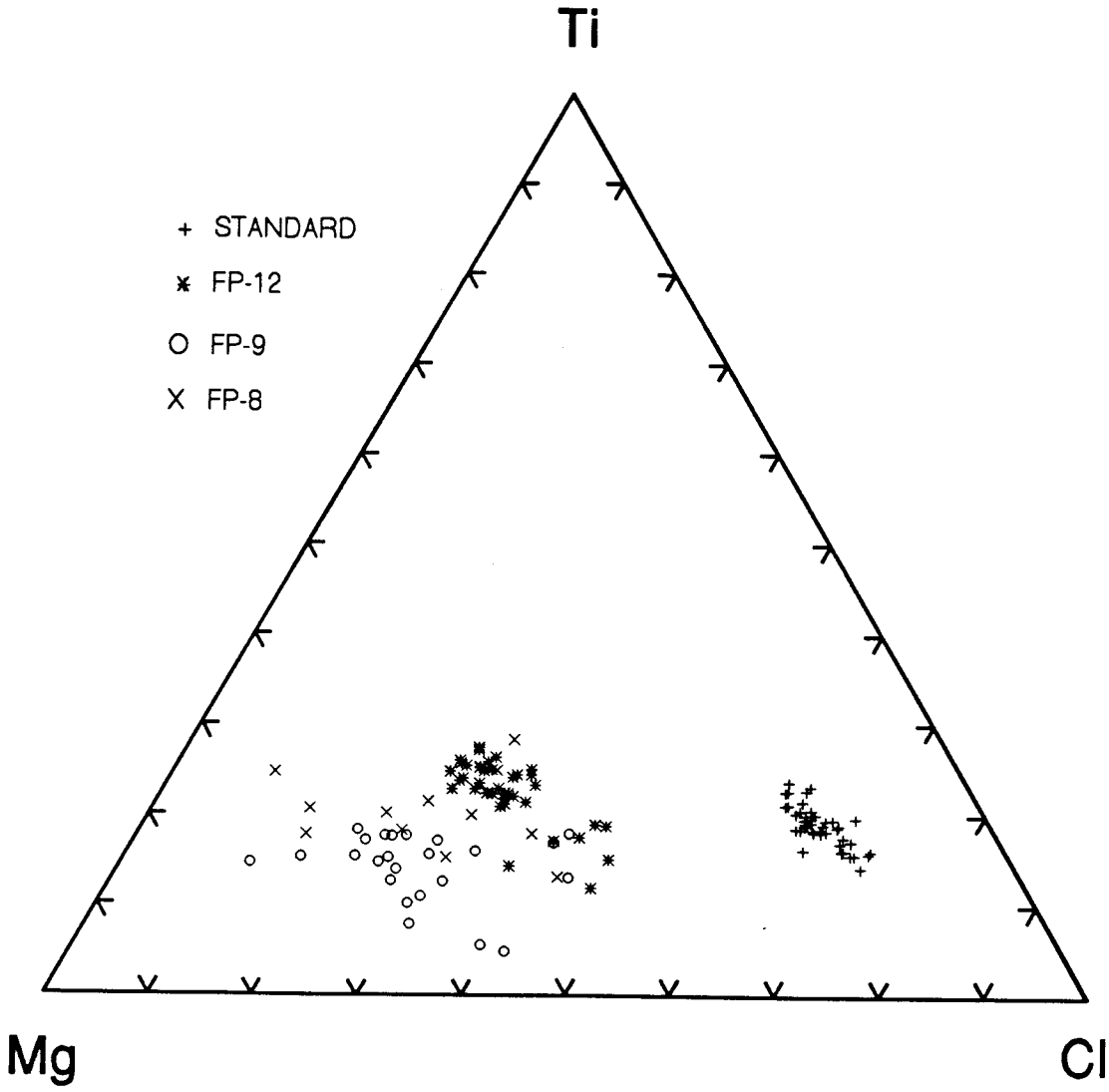

Figure 3.11. Ternary diagram of Mg-Ti-Cl. Symbols used are: pluses indicate the Yellowstone rhyolite standard; asterisks indicated bentonite FP-12; circles indicate bentonite FP-9; and X's indicate bentonite FP-8.

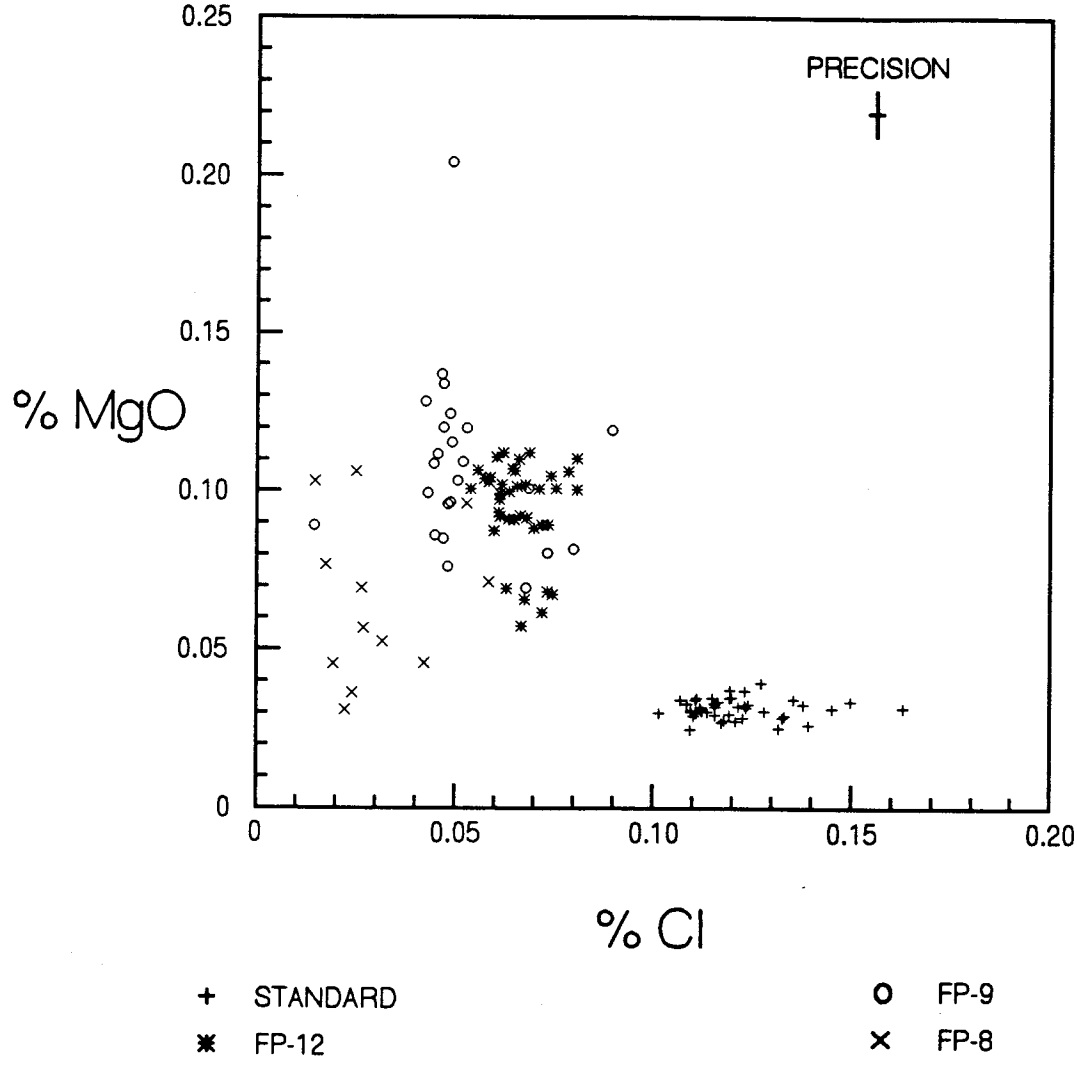

Figure 3.12. X-Y plot of wt % MgO vs Cl. Symbols used are: pluses indicate the Yellowstone rhyolite standard; asterisks indicate bentonite FP-12; circles indicate bentonite FP-9; and X's indicate bentonite FP-8.

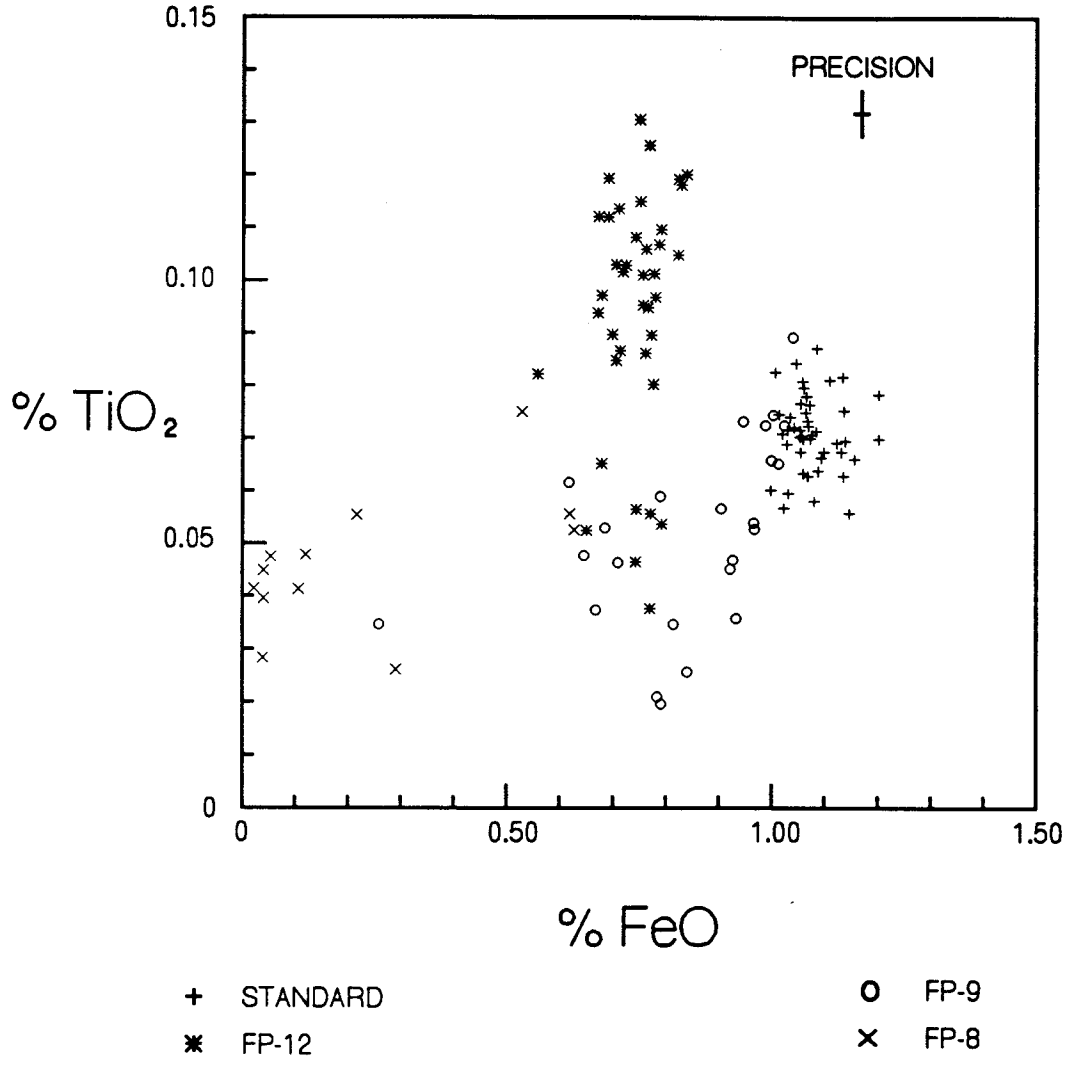

Figure 3.13. X-Y plot of wt % TiO_2 vs FeO. Symbols used are: pluses indicate the Yellostone rhyolite standard; asterisks indicate bentonite FP-12; circles indicate bentonite FP-9; and X's indicate bentonite FP-8.

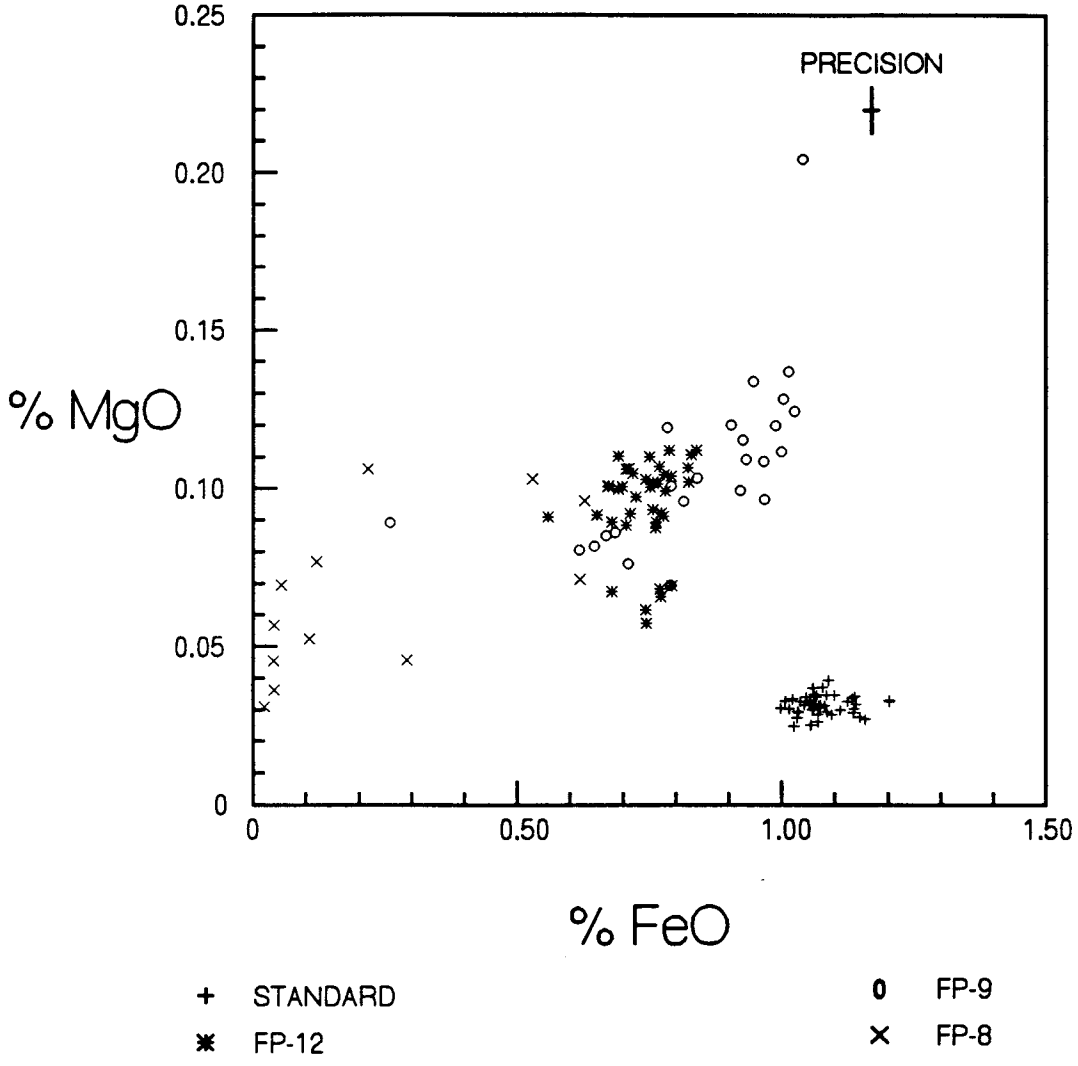

Figure 3.14. X-Y plot of wt % MgO vs FeO. Symbols used are: pluses indicate the Yellowstone rhyolite standard; asterisks indicate bentonite FP-12; circles indicate bentonite FP-9; and X's indicate bentonite FP-8..

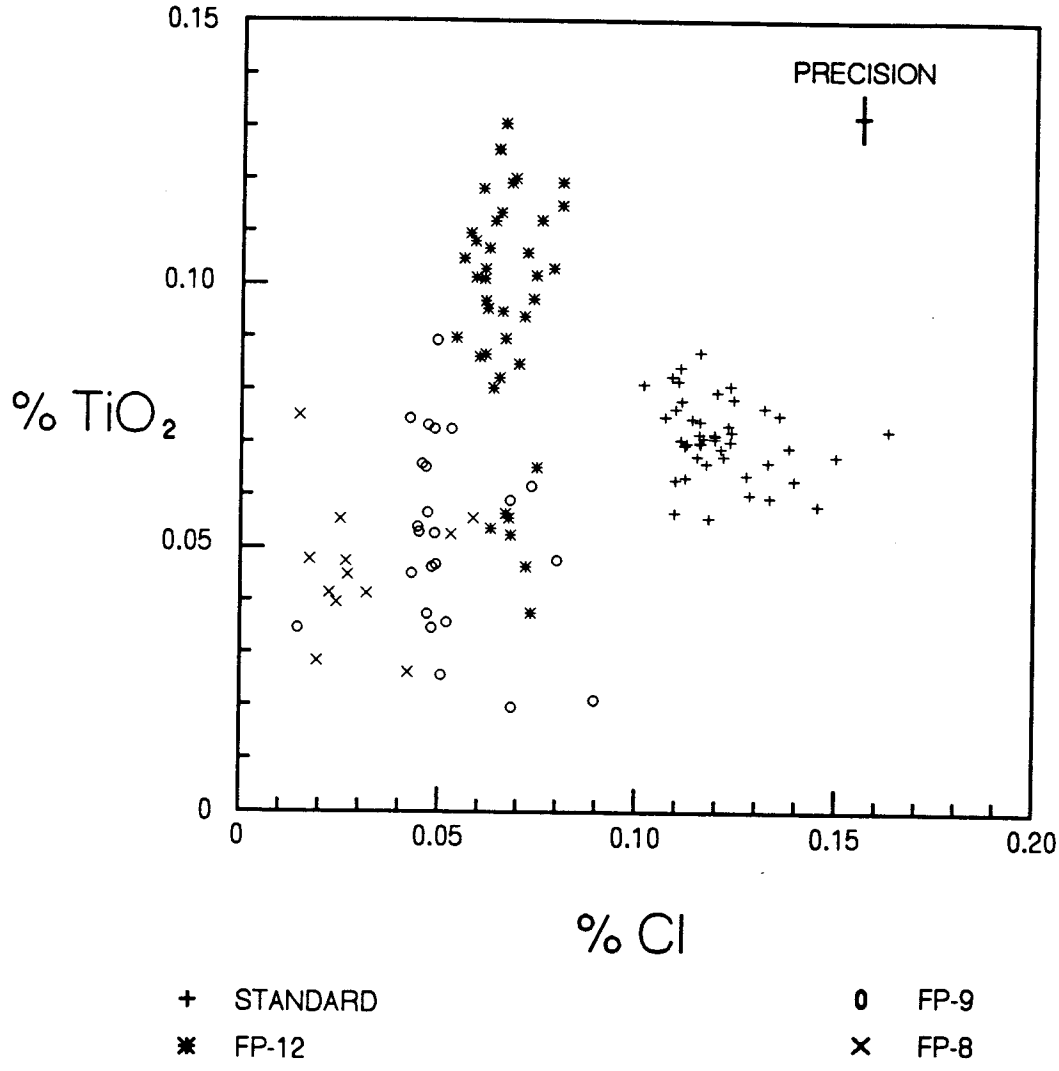

Figure 3.15. X-Y plot of wt % TiO_2 vs Cl. Symbols used are: pluses indicate the Yellowstone rhyolite standard; asterisks indicate bentonite FP-12; circles indicate bentonite FP-9; and X's indicate bentonite FP-8.

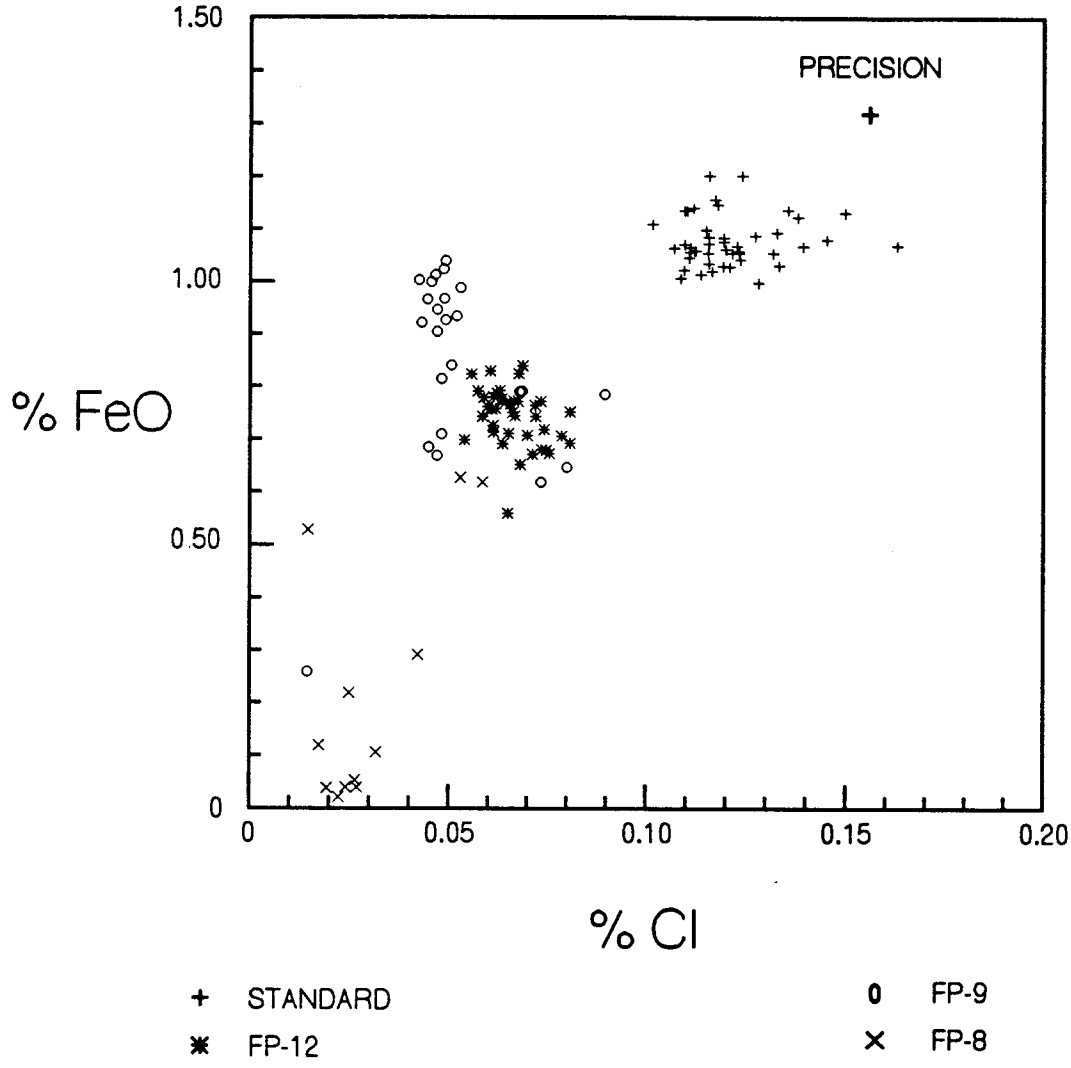

Figure 3.16. X-Y plot of wt % FeO vs Cl. Symbols used are: pluses indicate the Yellowstone rhyolite standard; asterisks indicate bentonite FP-12; circles indicate bentonite FP-9; and X's indicate bentonite FP-8.

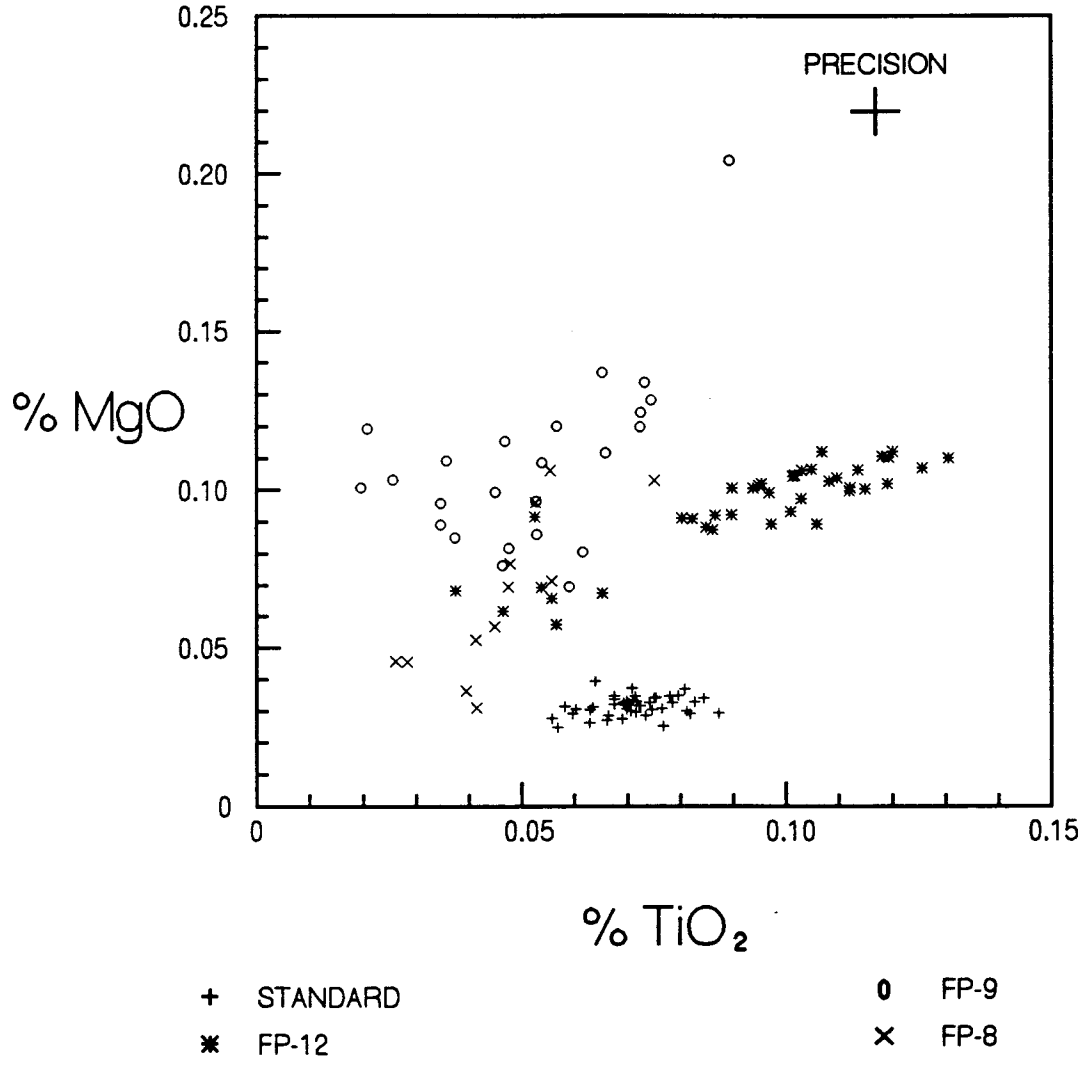

Figure 3.17. X-Y plot of wt % MgO vs TiO2. Symbols used are: pluses indicate the Yellowstone rhyolite; asterisks indicate bentonite FP-12; circles indicate bentonite FP-9; and X's indicate bentonite FP-8.

4.1 CORRELATIONS TO BENTONITE FP-12

Bentonite FP-12 at Frankstown, PA was geochemically correlated to three localities out of the fourteen sampled. Those three localities are: Tipton, PA; Newton Hamilton, PA; and Selinsgrove Junction, PA (Figure 4.1). The aerial extent defined by these occurrences is approximately 2590 km^2 (Figure 4.2).

Tipton, PA

The outcrop at Tipton (40^o 38′ 54" N, 78^o 16′ 14" W) is a roadcut in a private salvage yard (Figure 4.3) located east of Old State Route 220 and south of the bridge over the Pennsylvania Railroad (Figure 4.4). Three bentonites are recognized at this location and are designated TP-1, TP-2, and TP-3. Bentonites TP-2 and TP-3 occur in the Marcellus shale and bentonite TP-1 occurs within the Selinsgrove limestone (Figure 4.4). All three bentonites are red-brown in color and are a soft clay lithology.

Way and Smith (1986) recognized six bentonites at this outcrop. As demonstrated by the geochemical correlation made by this study, they incorrectly designated the bentonite TP-2 as Tioga-D (it actually is Tioga-F, Figure 3.3). The geochemical analyses of melt inclusions that occur in this bentonite (TP-2) indicate that it is equivalent to FP-12 at Frankstown, PA (Figure 4.36).

PENNSYLVANIA

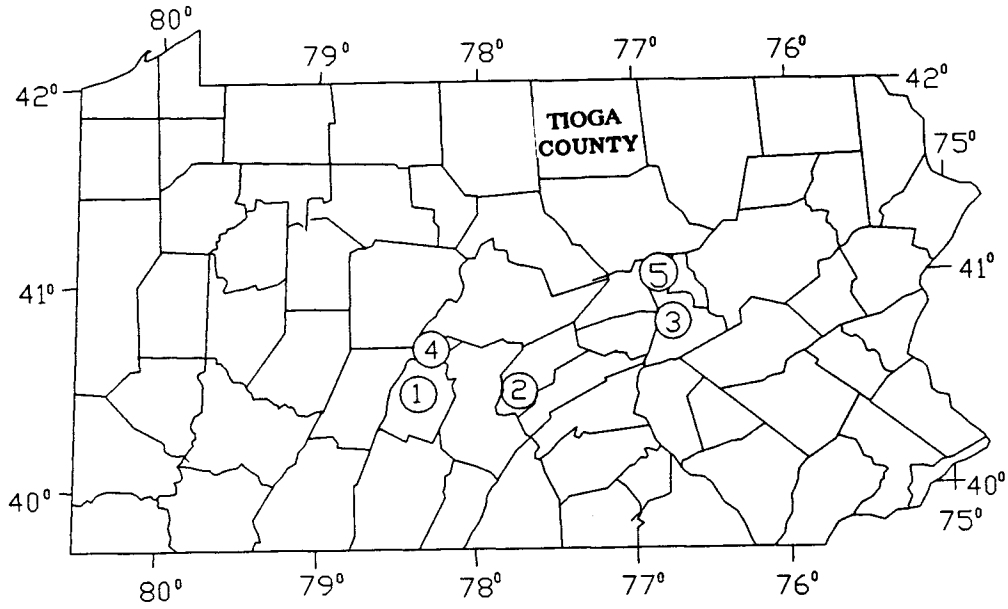

1. FRANKSTOWN

2. NEWTON HAMILTON

3. SELINSGROVE JUNCTION

4. TIPTON

5. ZEIGLER PIT

(390.0 +0.5 Ma Age Location; Roden et al., 1990)

Figure 4.1. Map of Pennsylvania showing the locations of Frankstown, Tipton, Newton Hamilton, and Selinsgrove Junction. Also shown is the Zeigler Pit locality were the Tioga-B bentonite was dated as 390.0 Ma ±0.5 Ma by Roden et al. (1990).

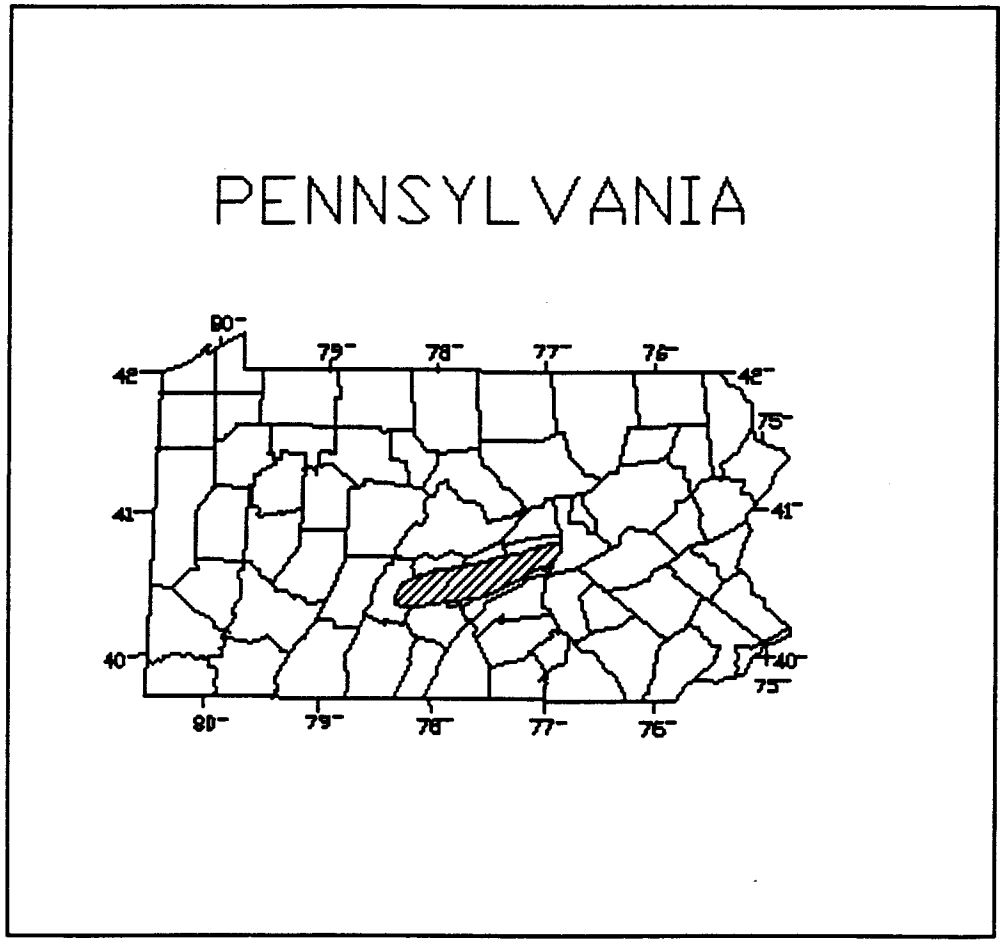

Figure 4.2. Map of Pennsylvania with hatched area indicating the aerial extent of bentonites equivalent to FP-12.

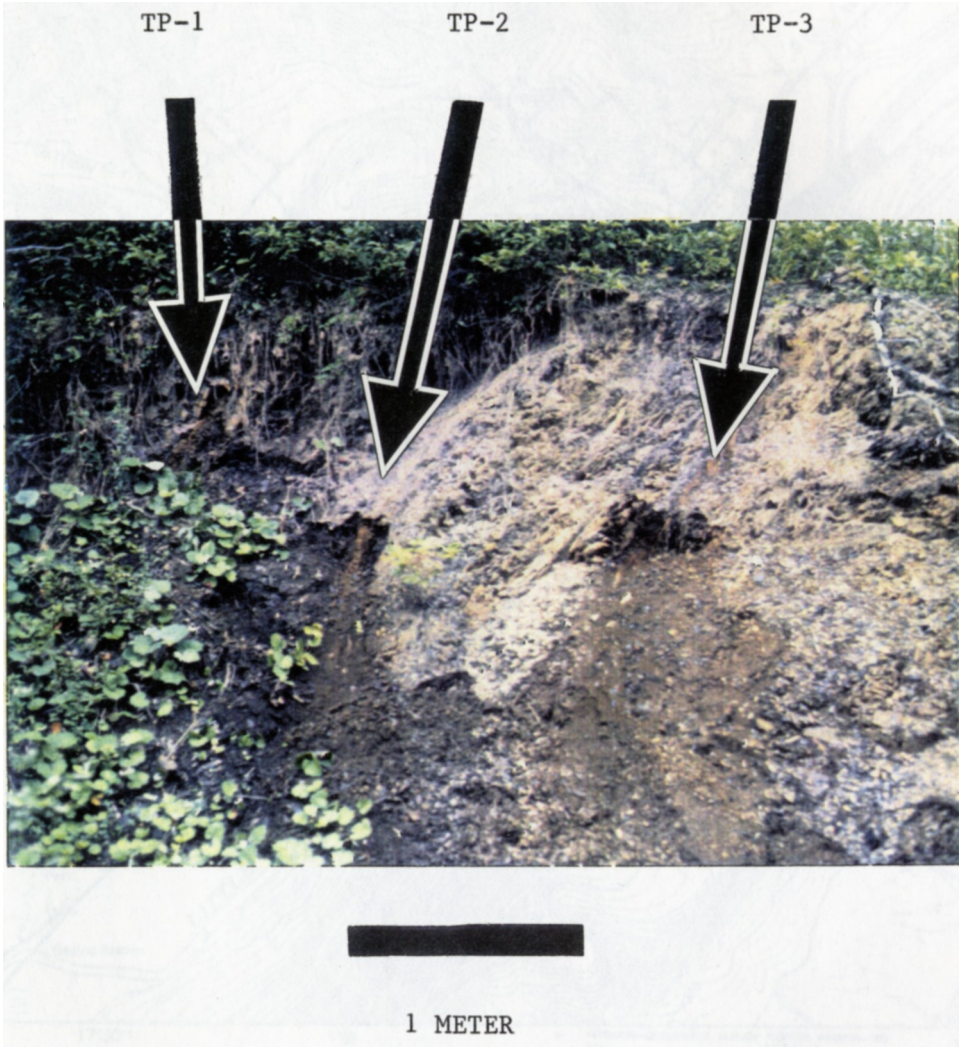

Figure 4.3. Photograph showing the outcrop of Marcellus shale and Selinsgrove limestone at Tipton, PA. Note the arrows indicating bentonites TP-1, TP-2, and TP-3 and the scale bar of 1 meter.

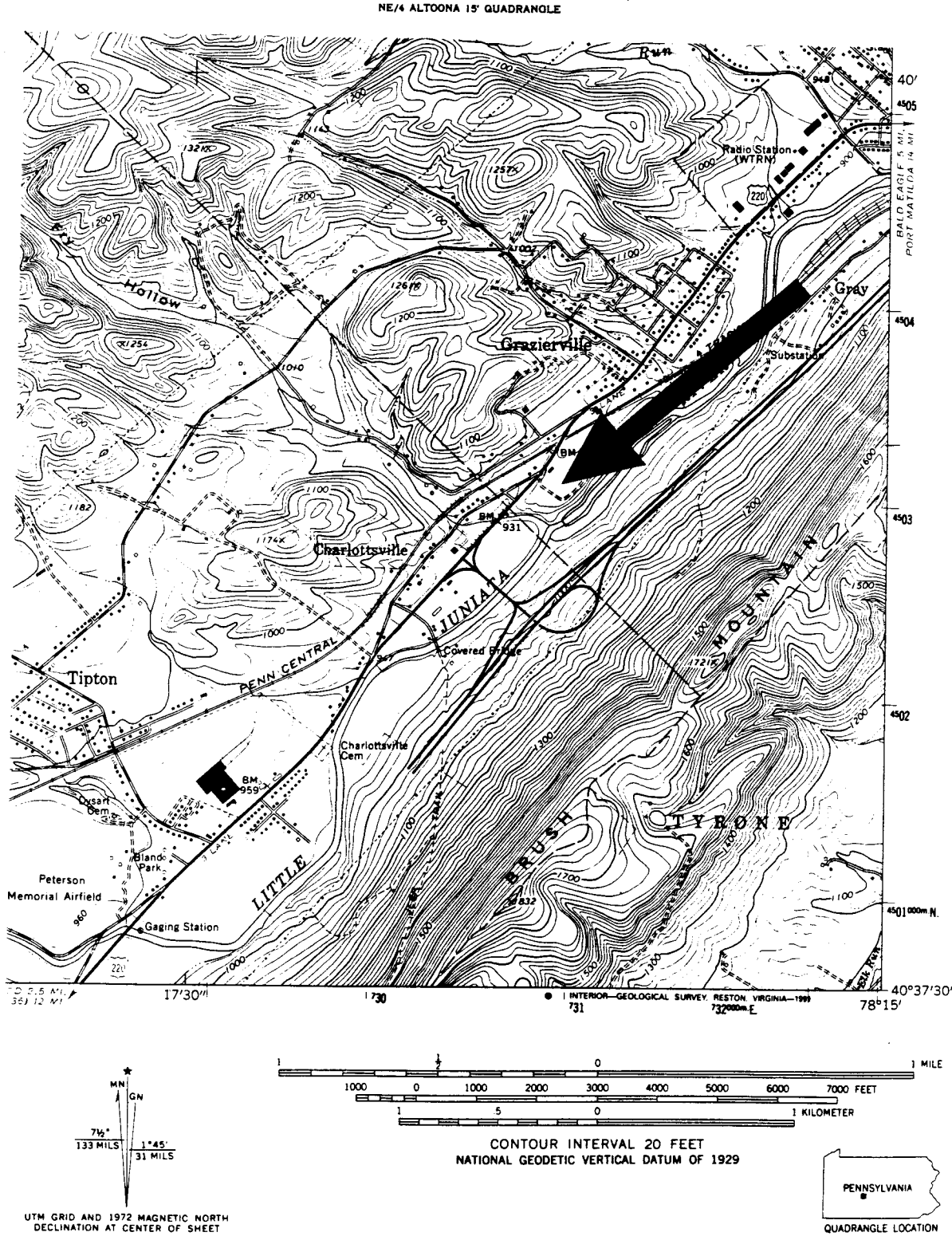

Figure 4.4. 7.5 minute quadrangle map of Tipton, PA showing the location of the Tipton outcrop.

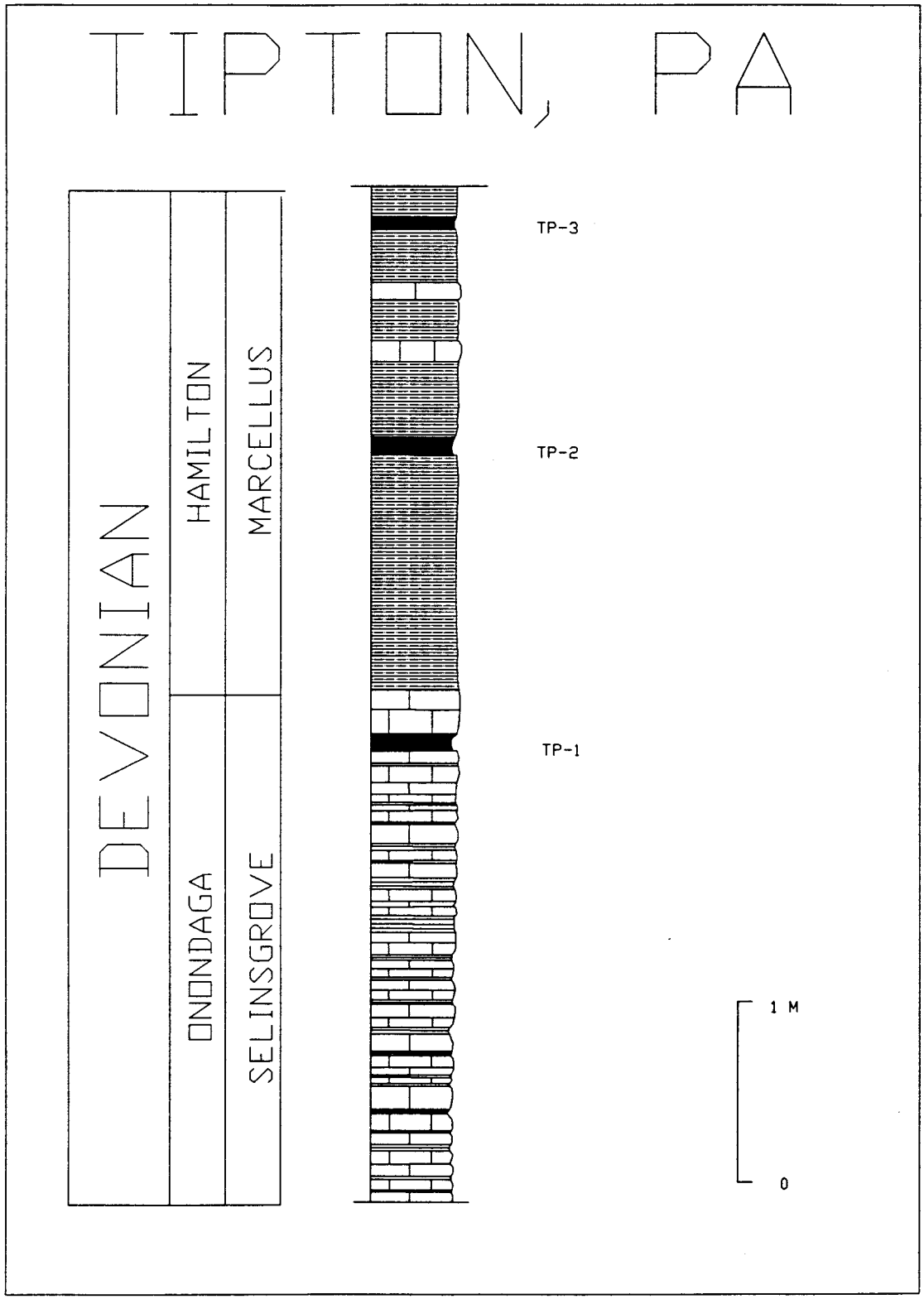

Figure 4.5. Stratigraphic column of the Tipton, PA outcrop constructed by this investigator.

This correlation is demonstrated by the ternary diagrams of Mg-Ti-Cl and Mg*10-Ti*10-Fe (Figure 4.6 and 4.7) and the X-Y plots of MgO vs Cl, TiO_2 vs FeO, MgO vs FeO, TiO_2 vs Cl, FeO vs Cl, and MgO vs TiO_2 (Figures 4.8 - 4.13). Note the tight clustering of the data from bentonite TP-2 with bentonite FP-12 on all the diagrams.

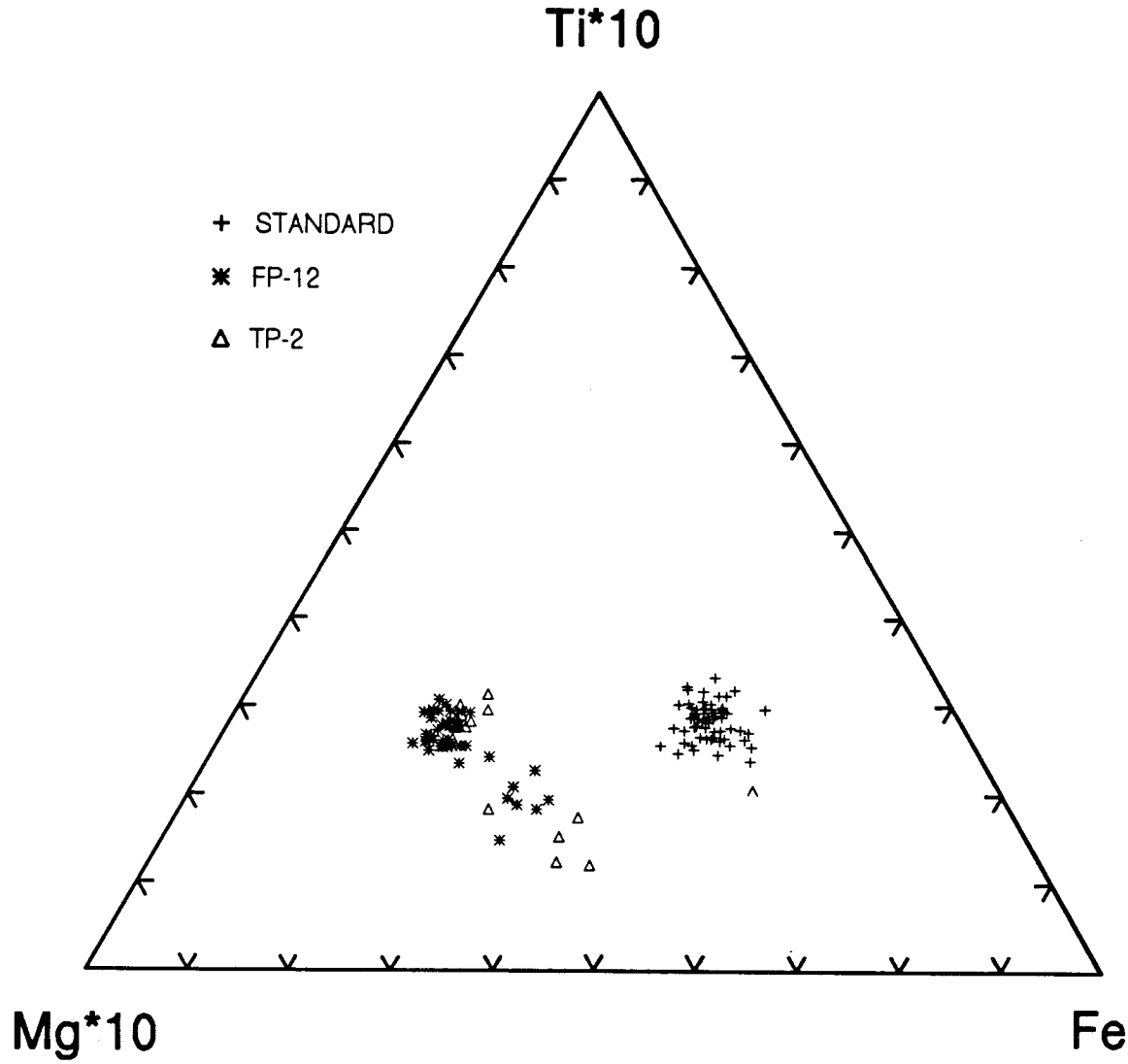

Figure 4.6. Ternary diagram of Mg*10-Ti*10-Fe. The symbols used are: pluses indicate the Yellowstone rhyolite standard; asterisks indicate bentonite FP-12; and triangles indicate bentonite TP-2.

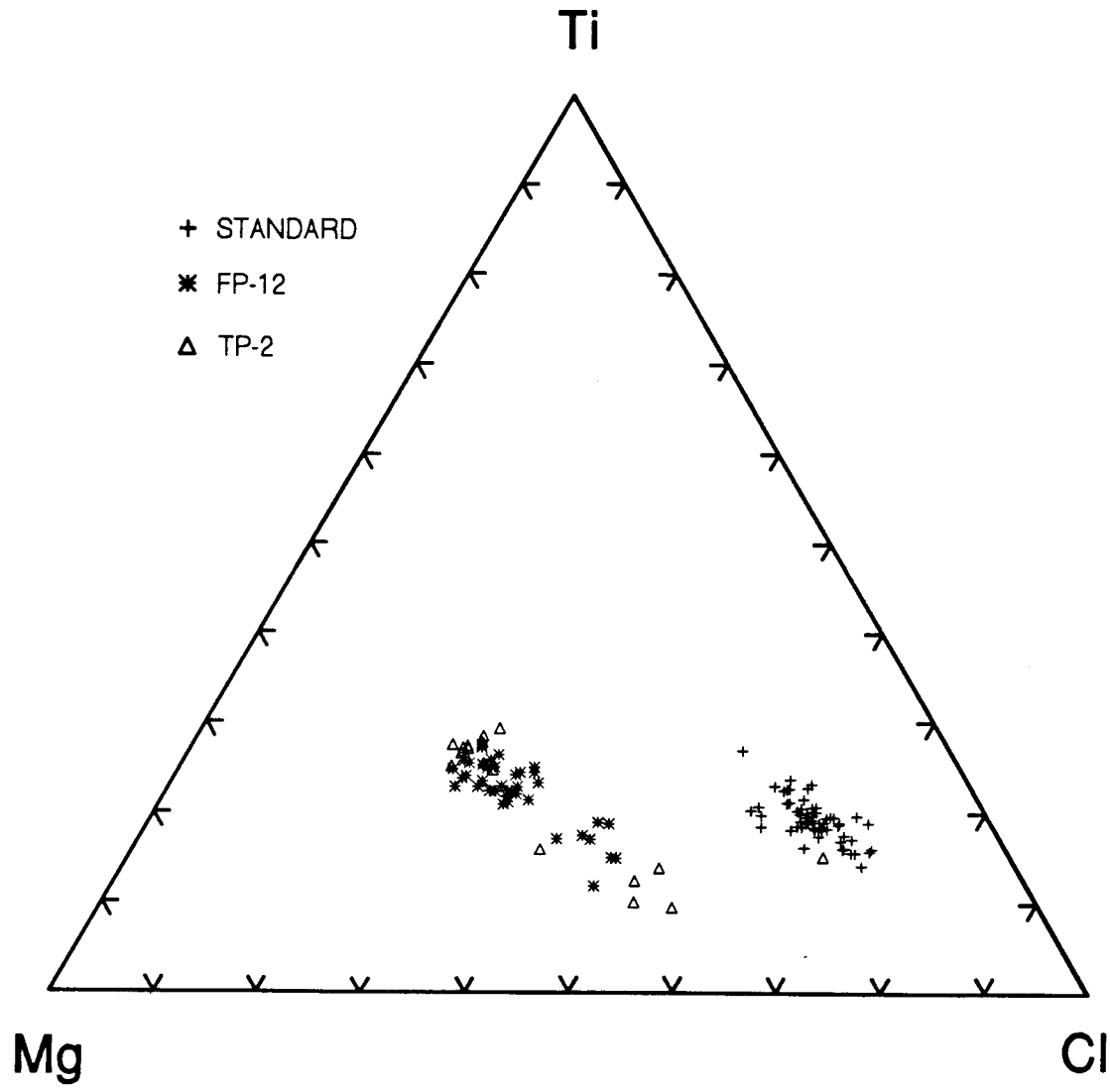

Figure 4.7. Ternary diagram of Mg-Ti-Cl. The symbols used are: pluses indicate the Yellowstone rhyolite standard; asterisks indicate bentonite FP-12; and triangles indicate bentonite TP-2.

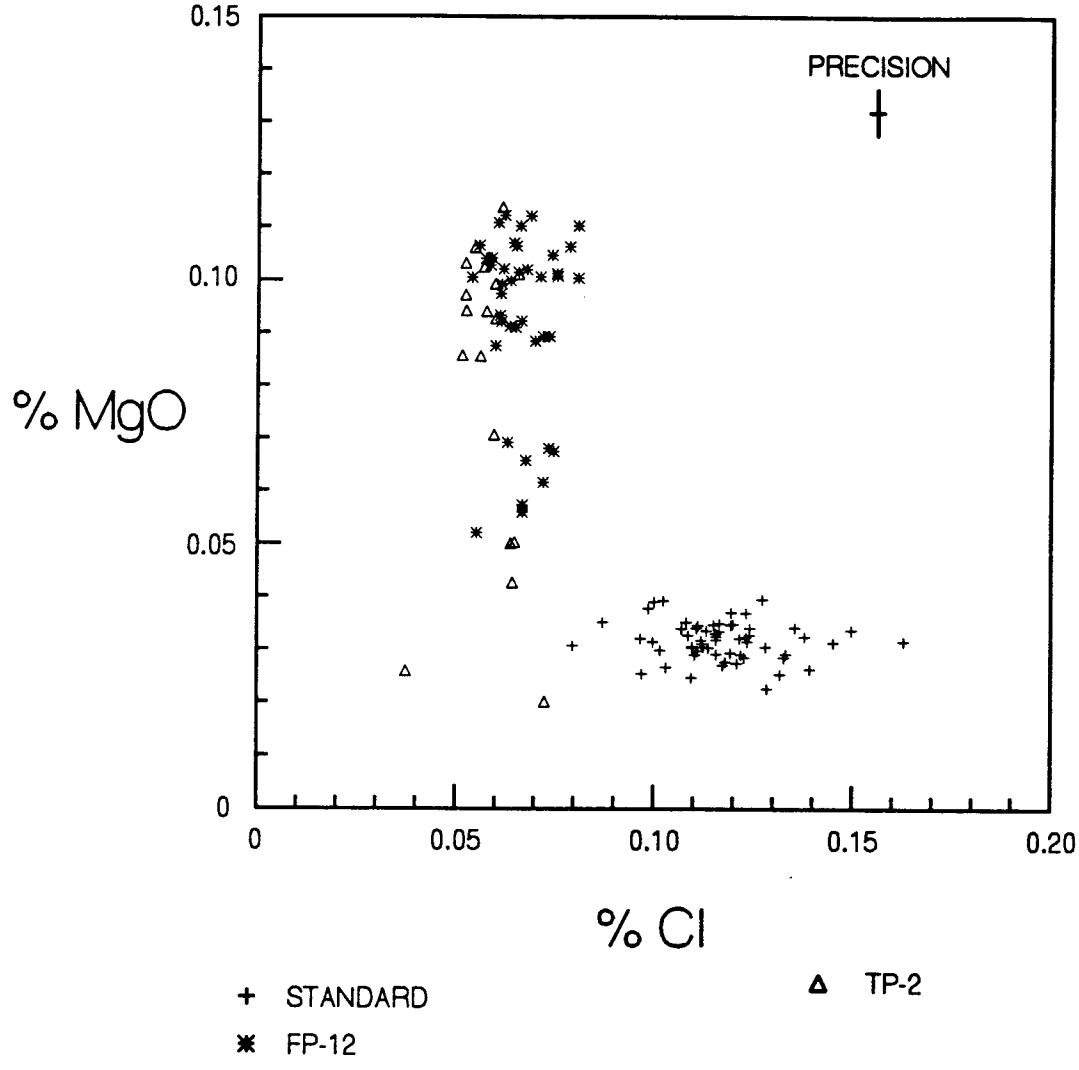

Figure 4.8. X-Y plot of wt % MgO vs Cl. Symbols used are: pluses indicate the Yellowstone rhyolite standard; asterisks indicate bentonite FP-12; and triangles indicate bentonite TP-2.

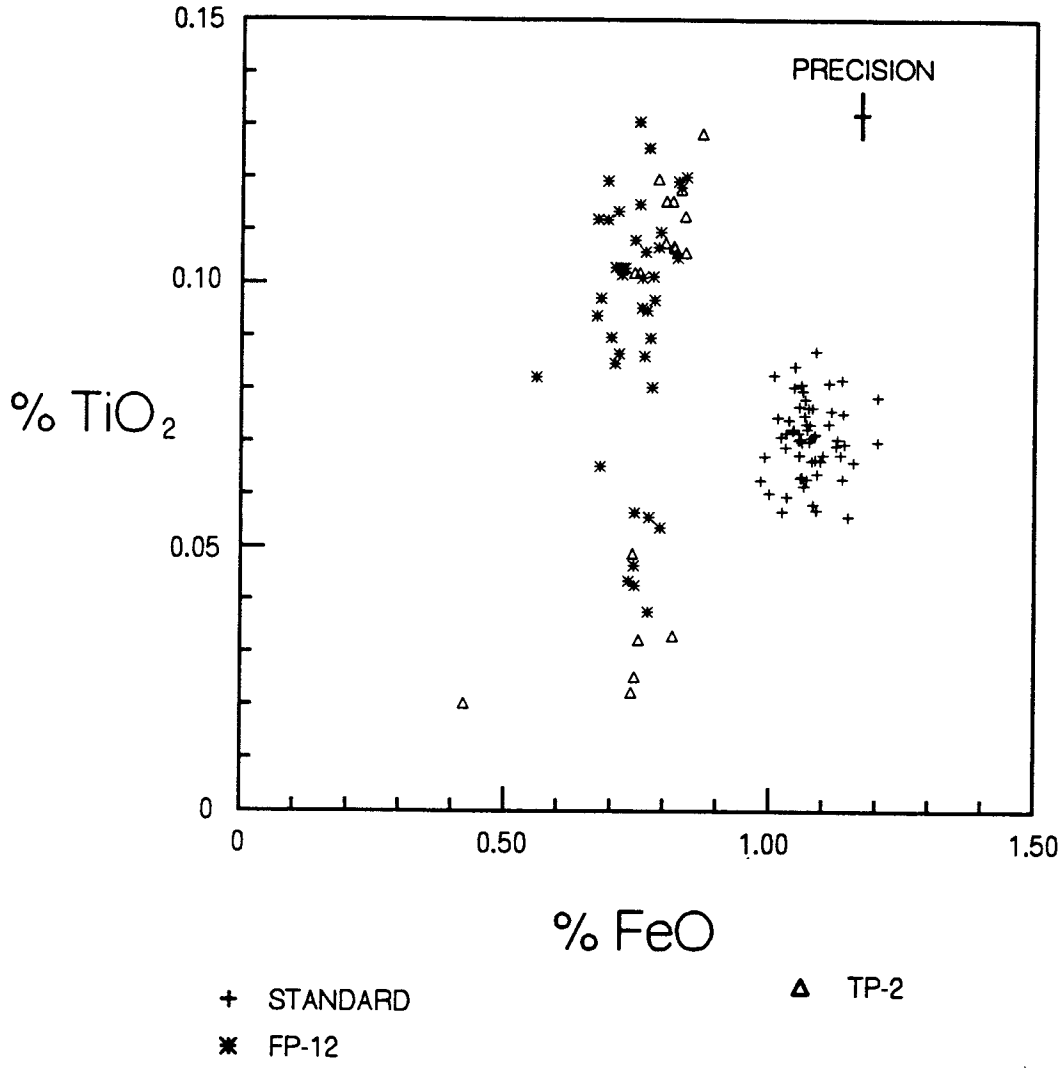

Figure 4.9. X-Y plot of wt % TiO_2 vs FeO. Symbols used are: pluses indicate the Yellowstone rhyolite standard; asterisks indicate bentonite FP-12; and triangles indicate bentonite TP-2.

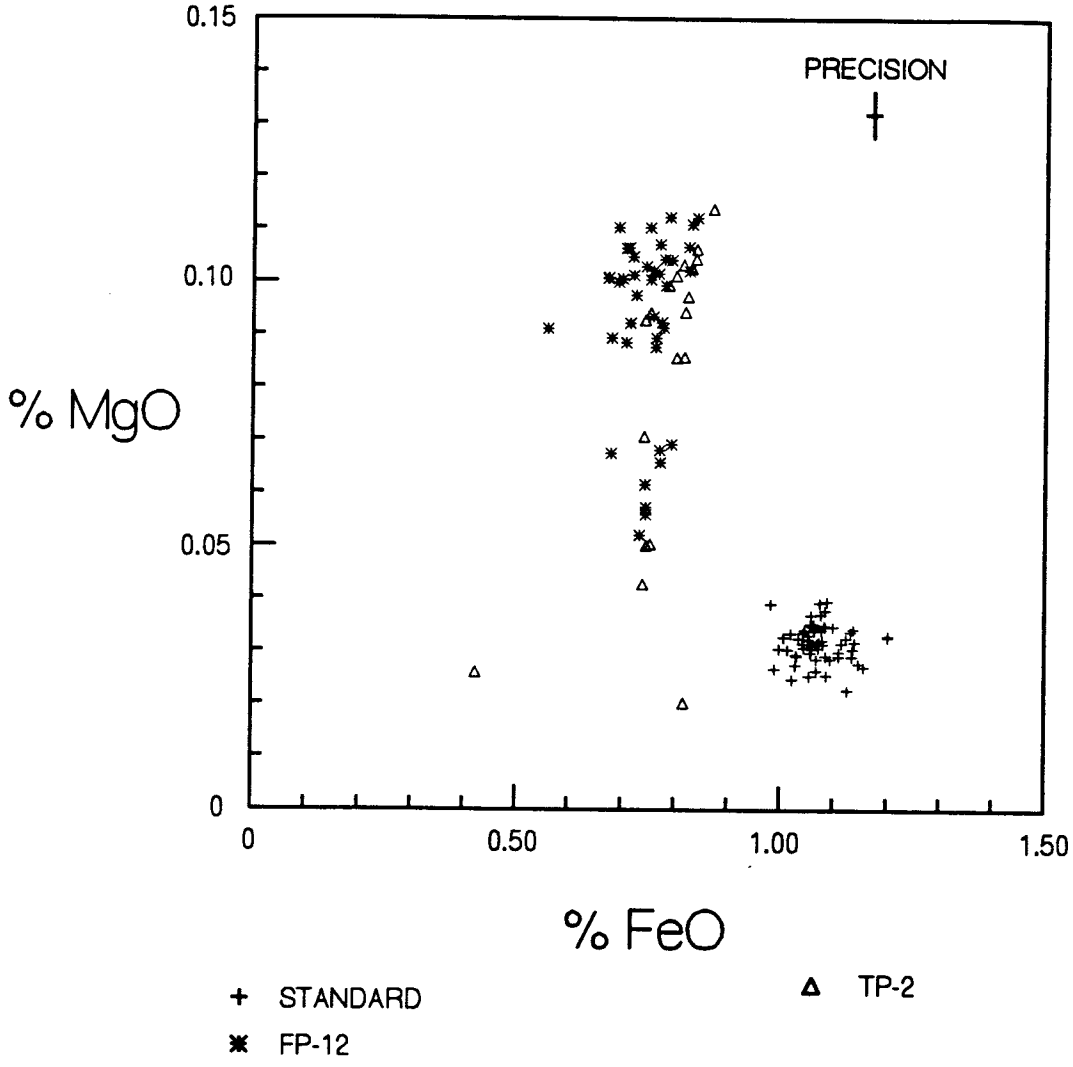

Figure 4.10. X-Y plot of wt % MgO vs FeO. Symbols used are: pluses indicate the Yellowstone rhyolite standard; asterisks indicate bentonite FP-12; and triangles indicate bentonite TP-2.

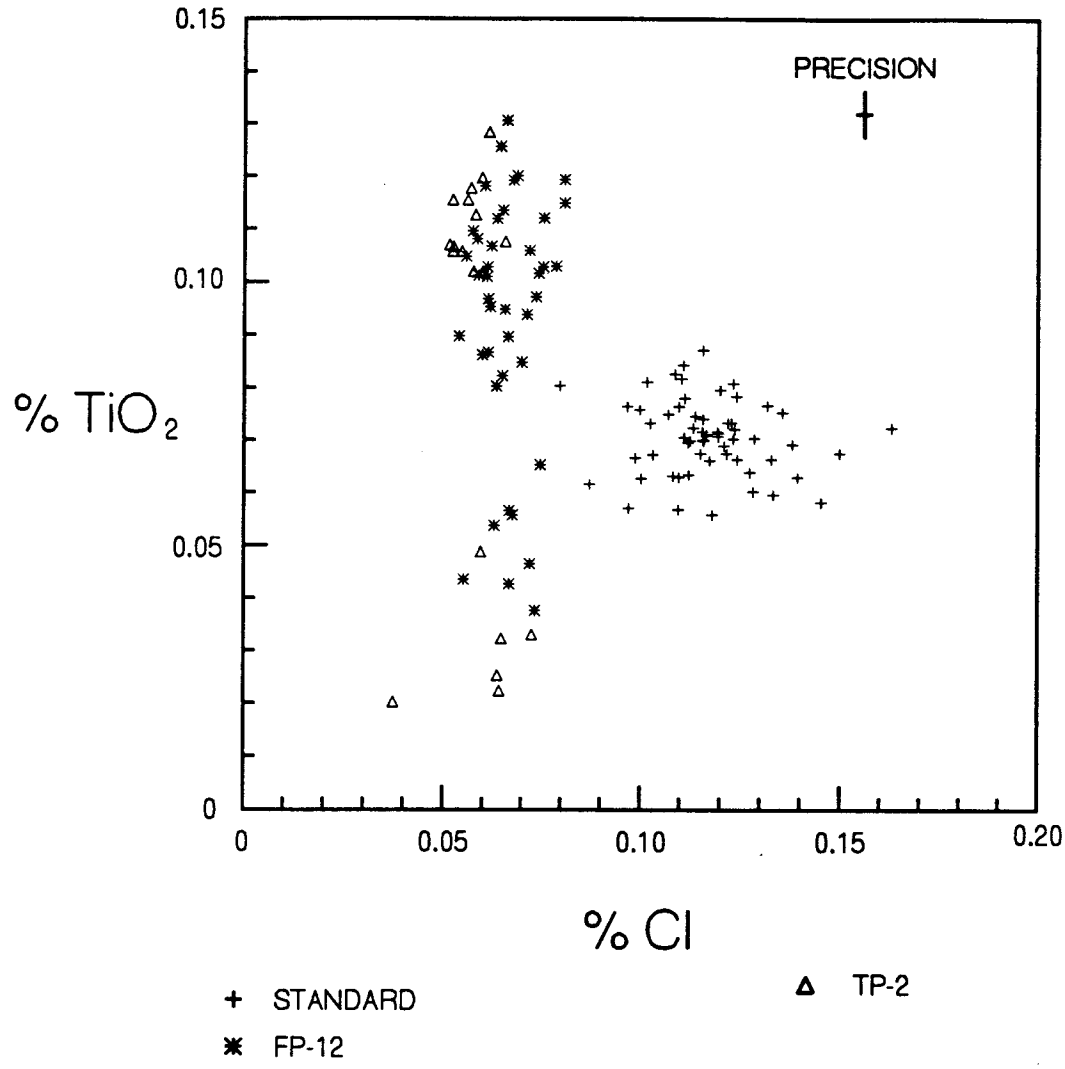

Figure 4.11. X-Y plot of wt % TiO_2 vs Cl. Symbols used are: pluses indicate the Yellowstone rhyolite standard; asterisks indicate bentonite FP-12; and triangles indicate bentonite TP-2.

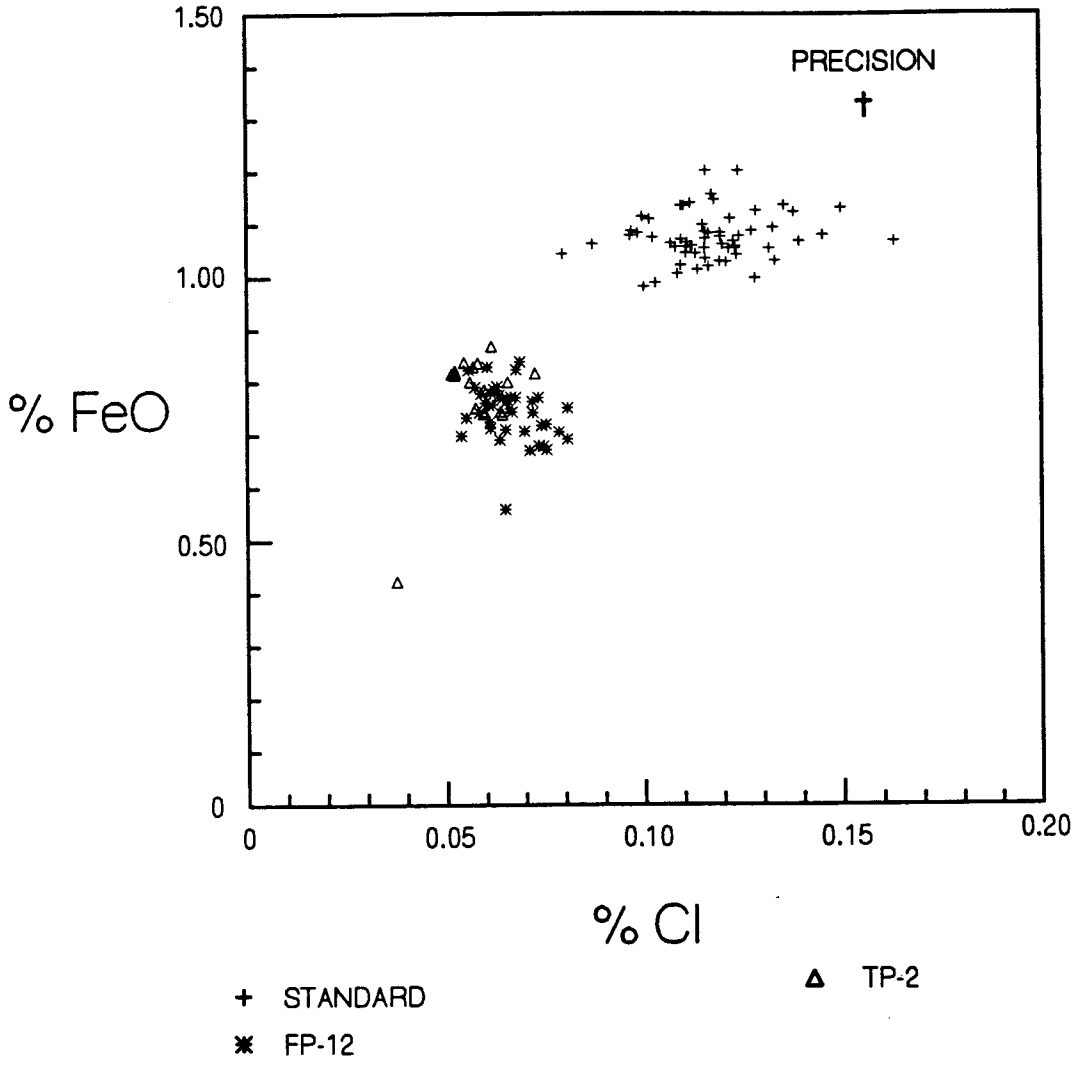

Figure 4.12. X-Y plot of wt % FeO vs Cl. Symbols used are: pluses indicate the Yellowstone rhyolite standard; asterisks indicate bentonite FP-12; and triangles indicate bentonite TP-2.

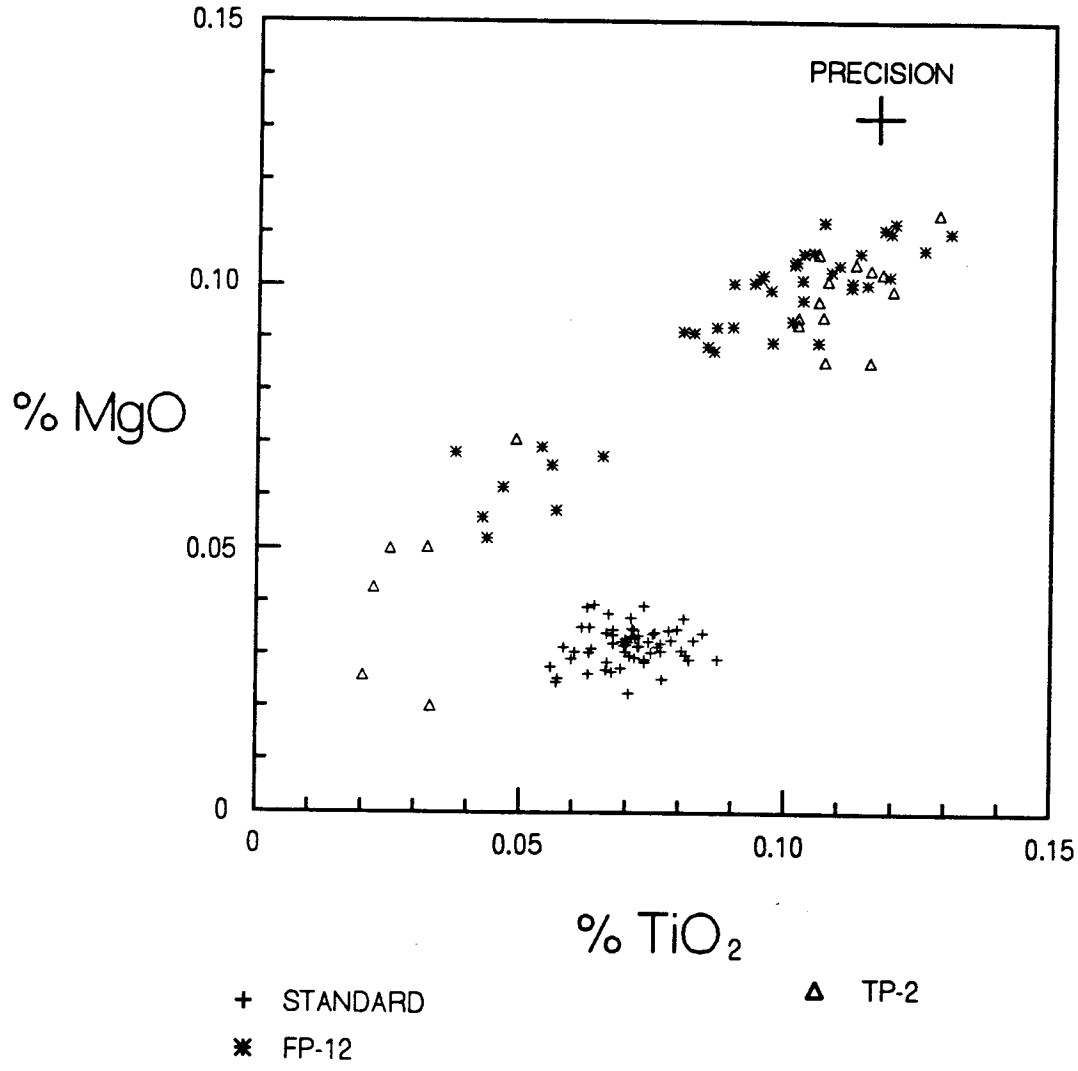

Figure 4.13. X-Y plot of wt % MgO vs TiO_2. Symbols used are: pluses indicate the Yellowstone rhyolite standard; asterisks indicate bentonite FP-12; and triangles indicate bentonite TP-2.

Newton Hamilton, PA

The exposure at Newton Hamilton (40° 23′ 00" N, 77° 51′ 01" W) is accessible by walking one mile southwest along the railroad tracks from the underpass in downtown Newton Hamilton (Figure 4.14). Five bentonites are recognized at this locality as compared to seven reported by Way and Smith (1986, Figure 3.3). Bentonites NH-1, NH-2, and NH-3 occur in the Selinsgrove limestone (Figures 4.15 and 4.16) and bentonites NH-4 and NH-5 occur within the Marcellus shale (Figures 4.15 and 4.16).

These bentonites are a tan color and occur as a hardened clay that is slightly lithified. The geochemical analyses of melt inclusions from bentonite NH-4 appear equivalent to those in FP-12 at Frankstown, PA (Figure 4.36). This is represented by the ternary diagrams of Mg*10-Ti*10-Fe and Mg-Ti-Cl (Figure 4.17 and 4.18) and the X-Y plots of MgO vs Cl, TiO_2 vs FeO, MgO vs FeO, TiO_2 vs Cl, FeO vs Cl, and MgO vs TiO_2 (Figures 4.19 - 4.24). Note the tight grouping represented in all the graphs especially in the plot of wt % FeO vs Cl (Figure 4.23).

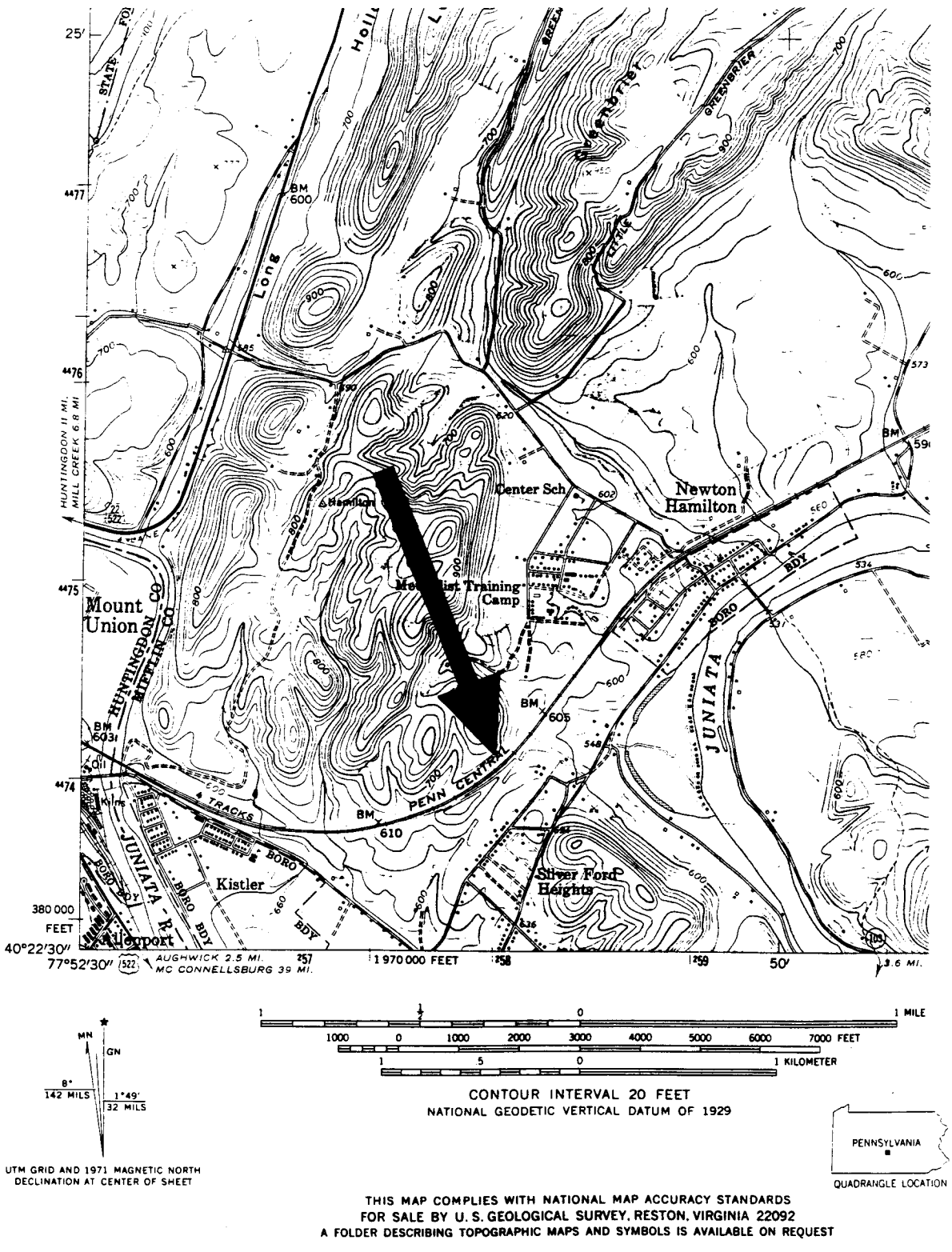

Figure 4.14. 7.5 minute quadrangle map of Newton Hamilton, PA showing the location of the railroad cut south of downtown Newton Hamilton.

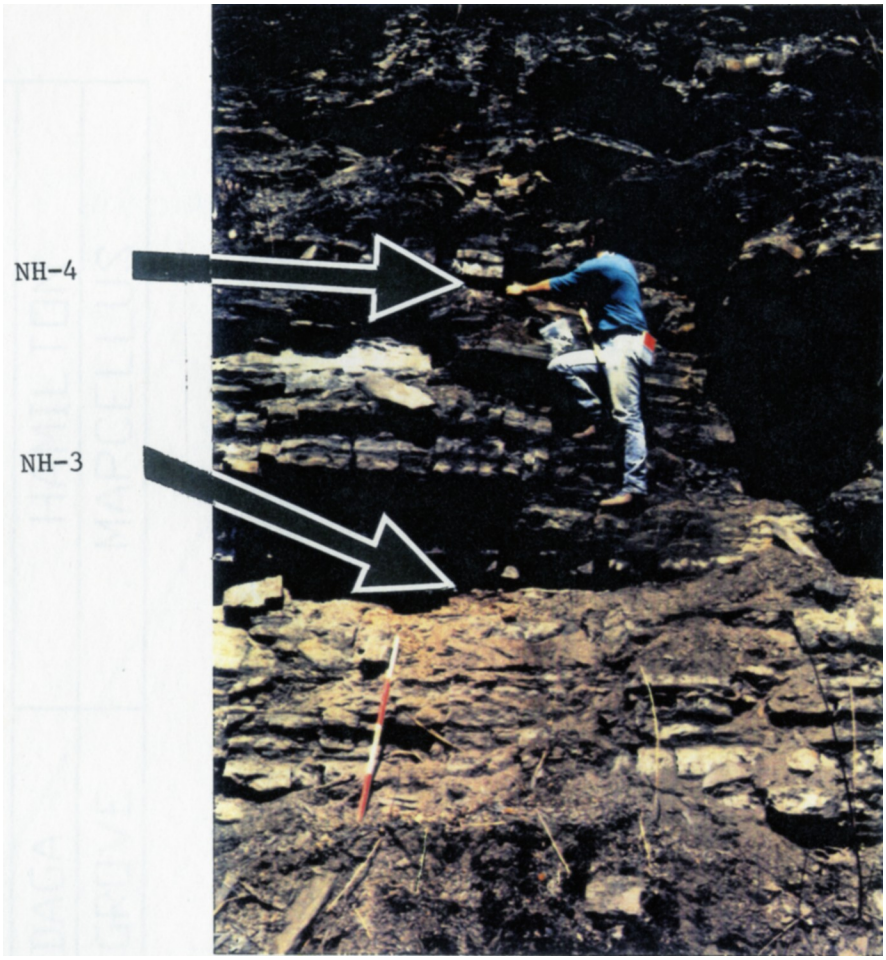

Figure 4.15 Photograph showing the Selinsgrove (Middle Devonian) limestone member and the Marcellus shale (Middle Devonian) at the Newton Hamilton exposure. Note the arrows indicating bentonites NH-3 and NH-4. The markings on the scale bar are in feet.

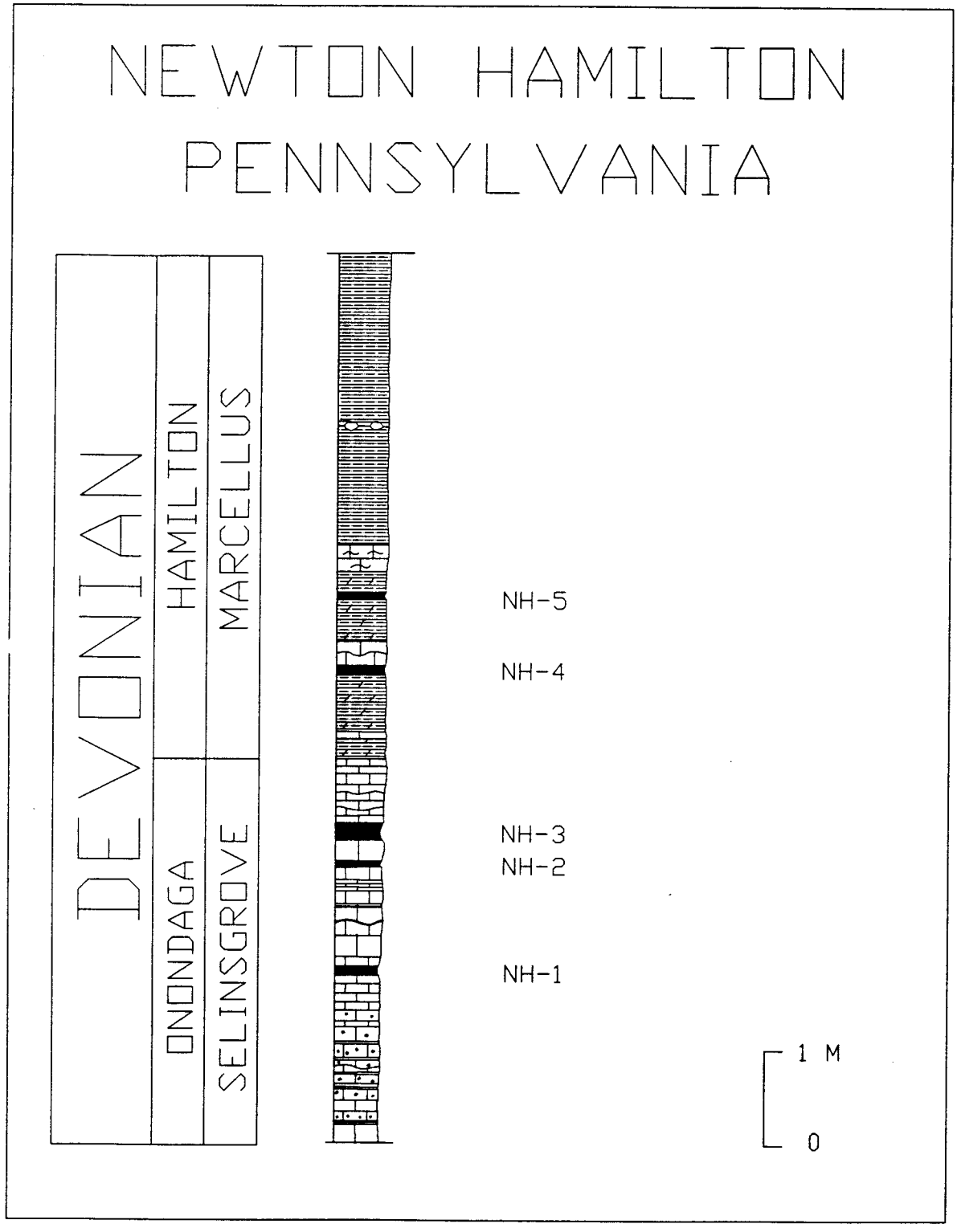

Figure 4.16. Stratigraphic column of the railroad cut at Newton Hamilton, PA constructed by this investigator.

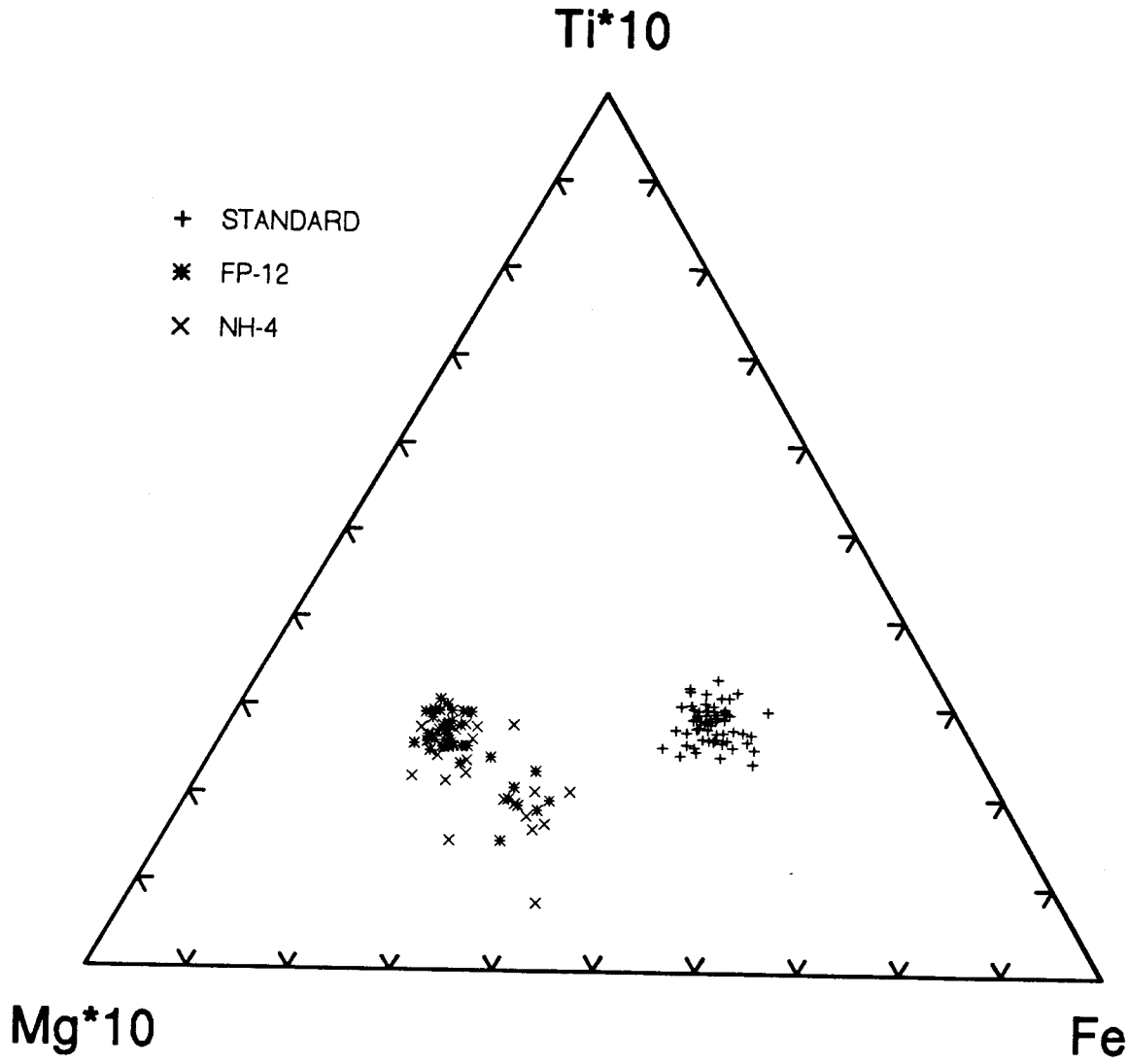

Figure 4.17. Ternary diagram of Mg*10-Ti*10-Fe. The symbols used are: pluses indicate the Yellowstone rhyolite standard; asterisks indicate bentonite FP-12; and X's indicate bentonite NH-4.

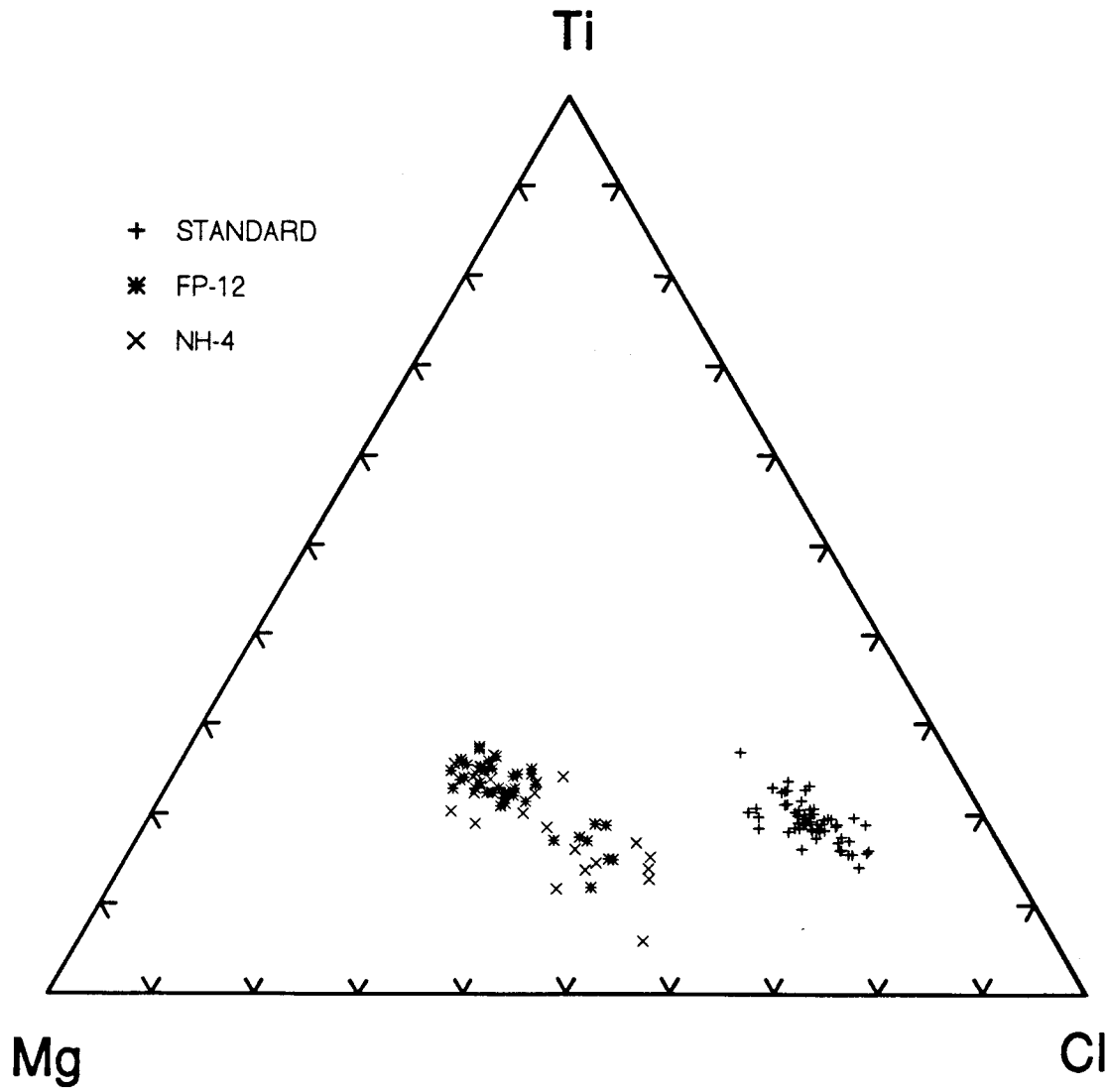

Figure 4.18. Ternary diagram of Mg-Ti-Cl. Symbols used are: pluses indicate the Yellowstone rhyolite standard; pluses indicate bentonite FP-12; and X's indicate bentonite NH-4.

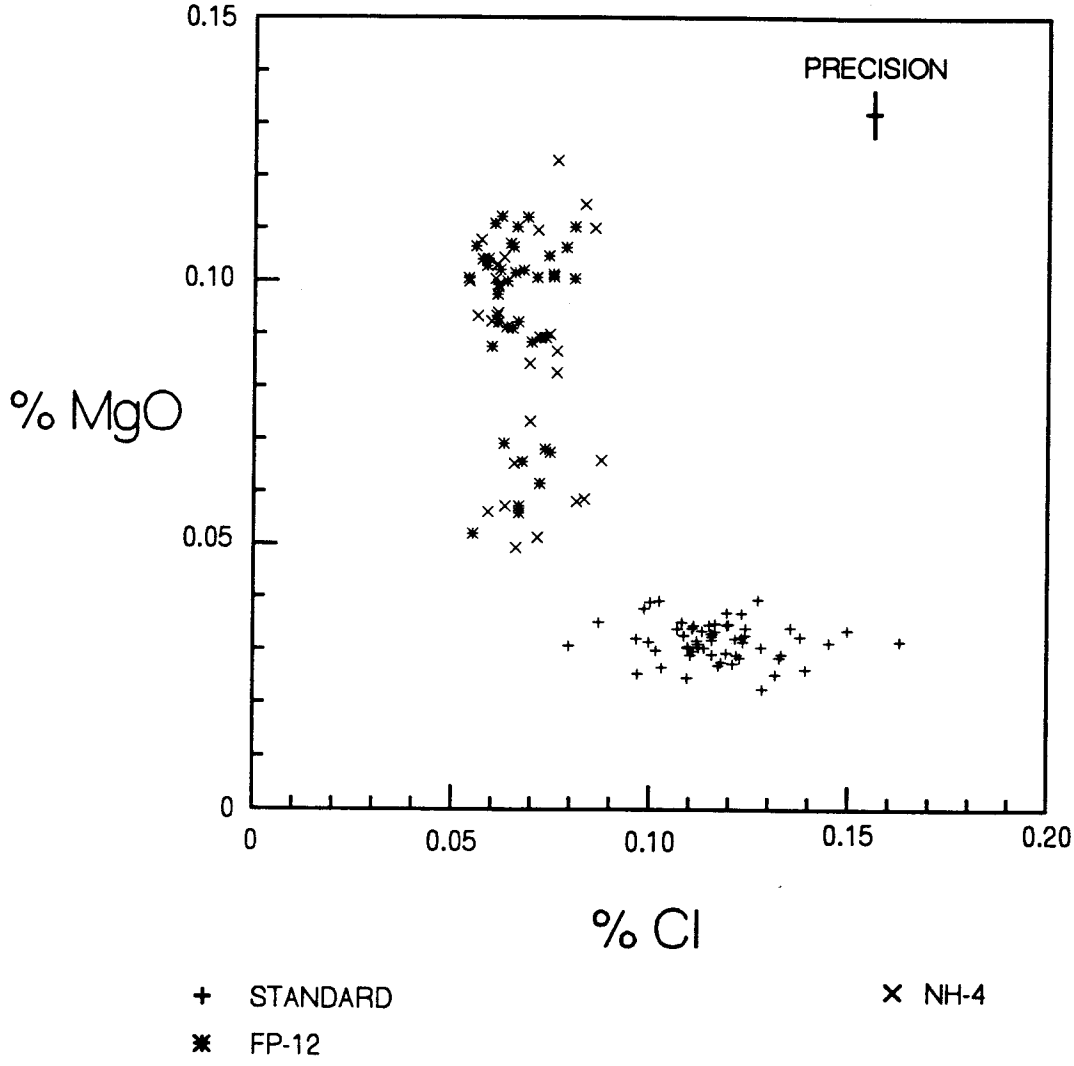

Figure 4.19. X-Y plot of wt % MgO vs Cl. The symbols used are: pluses indicate the Yellowstone rhyolite standard; asterisks indicate bentonite FP-12; and X's indicate bentonite NH-4.

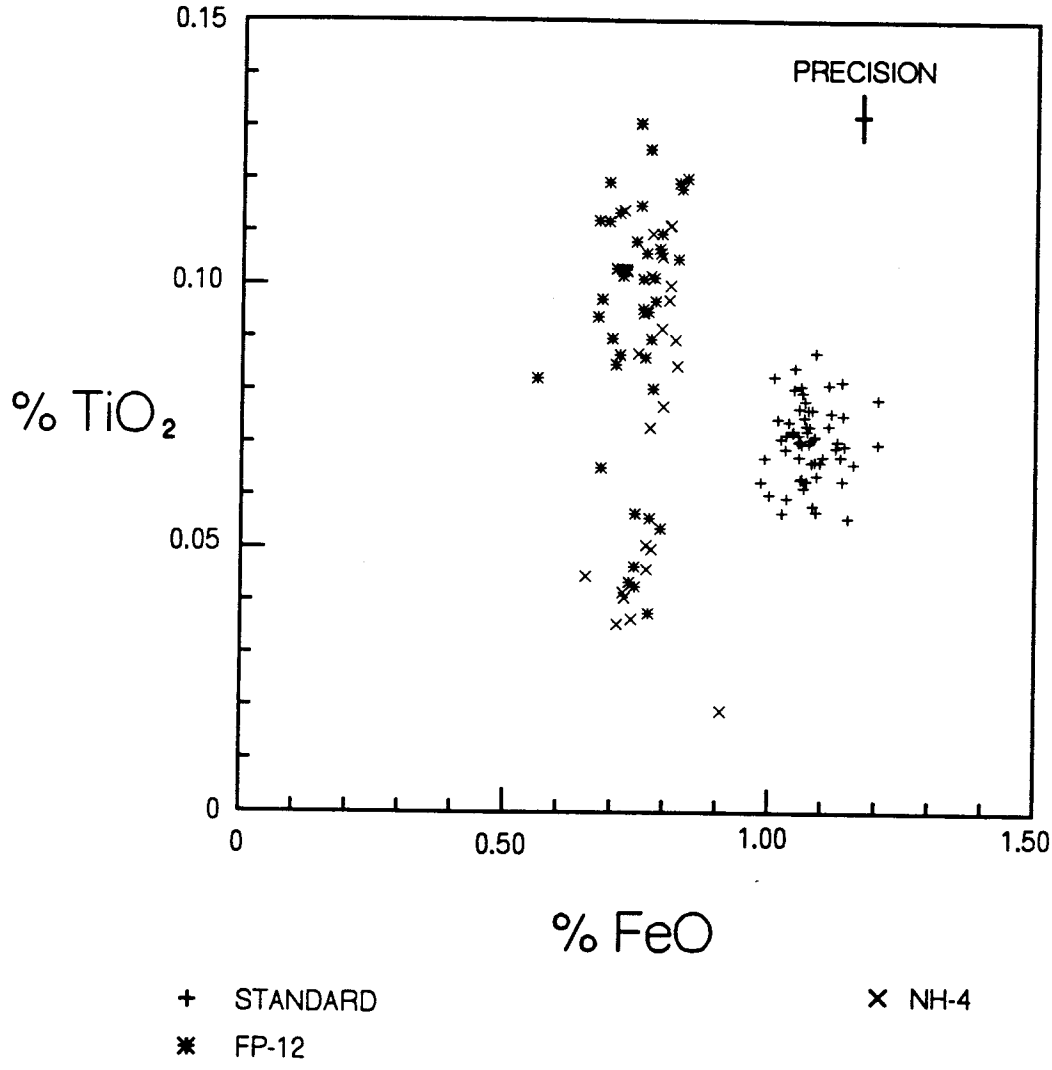

Figure 4.20. X-Y plot of wt % TiO_2 vs FeO. Symbols used are: pluses indicate the Yellowstone rhyolite standard; asterisks indicate bentonite FP-12; and X's indicate bentonite NH-4.

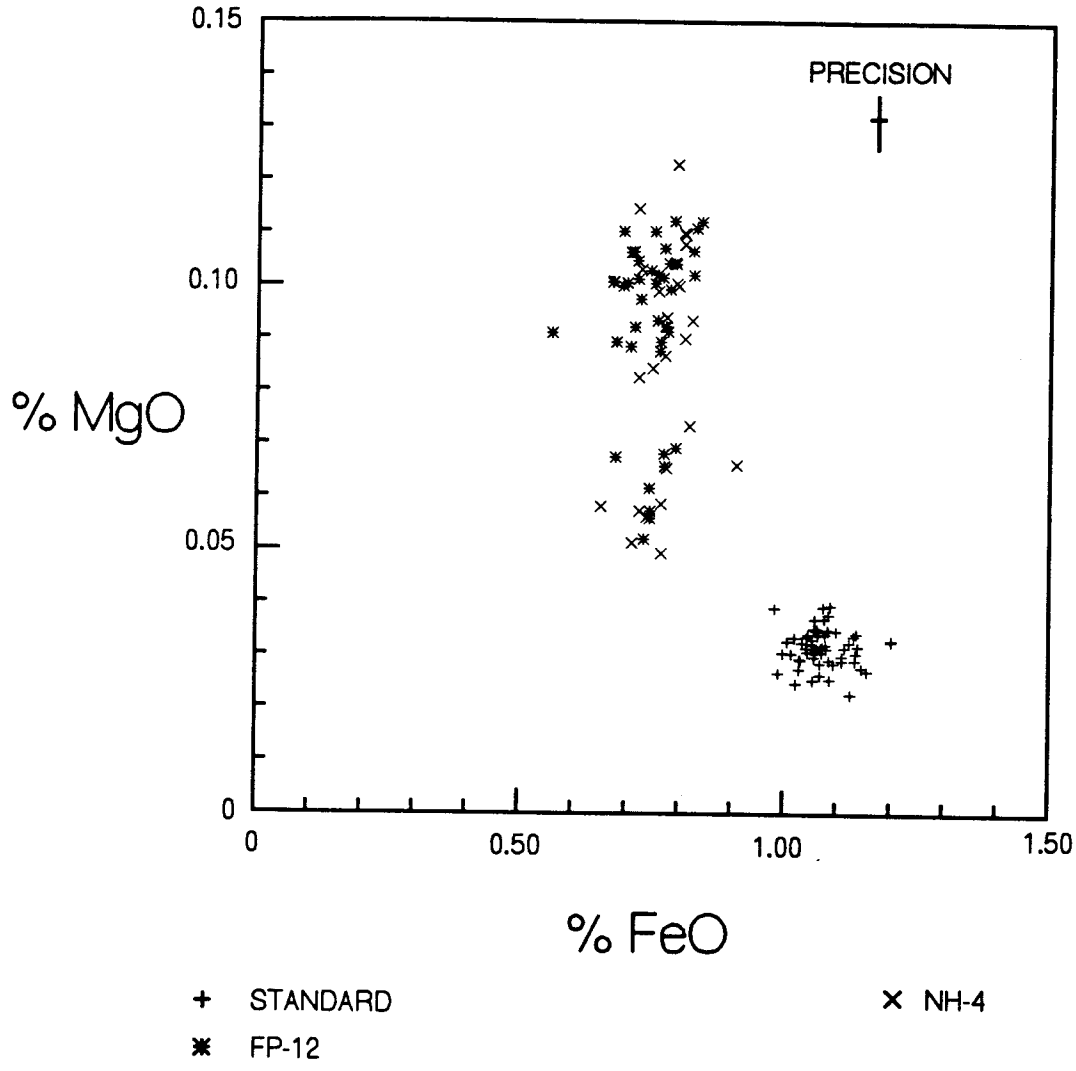

Figure 4.21. X-Y plot of wt % MgO vs Feo. The symbols used are: pluses indicate the Yellowstone rhyolite standard; asterisks indicate bentonite FP-12; and X's indicate bentonite NH-4.

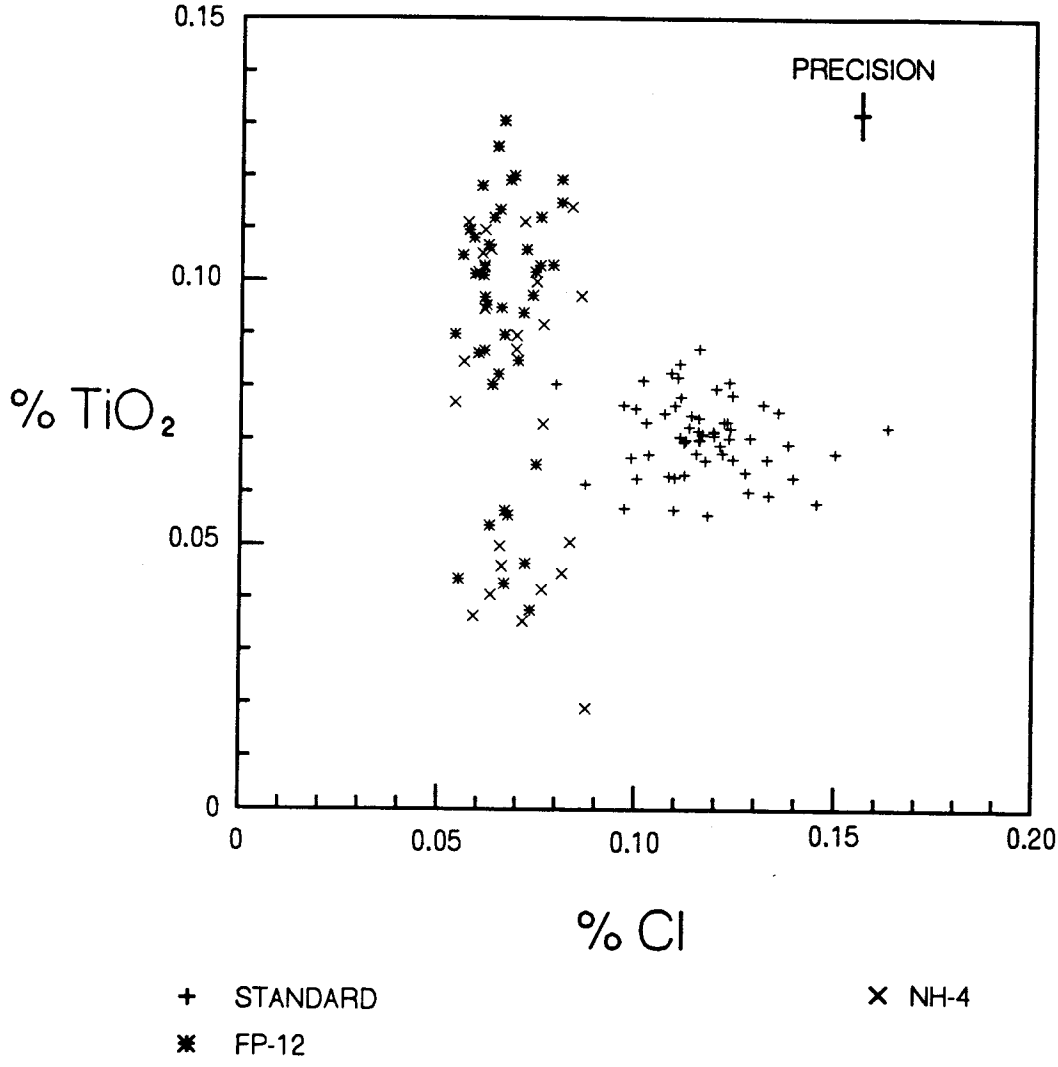

Figure 4.22. X-Y plot of wt % TiO_2 vs Cl. Symbols used are: pluses indicate the Yellowstone rhyolite standard; asterisks indicate bentonite FP-12; and X's indicate bentonite NH-4.

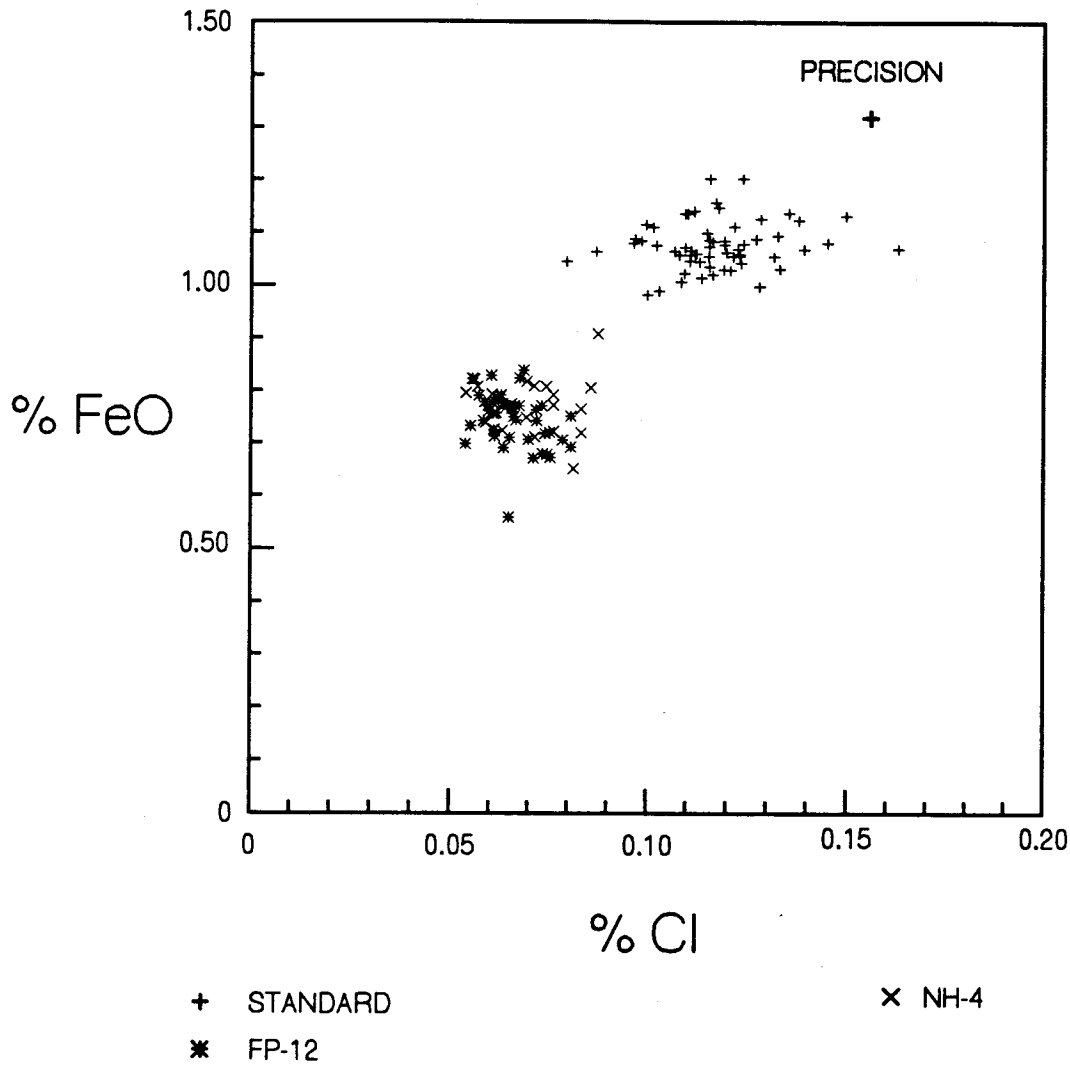

Figure 4.23. X-Y plot of wt % FeO vs Cl. The symbols used are: pluses indicate the Yellowstone rhyolite standard; asterisks indicate bentonite FP-12; and X's indicate bentonite NH-4.

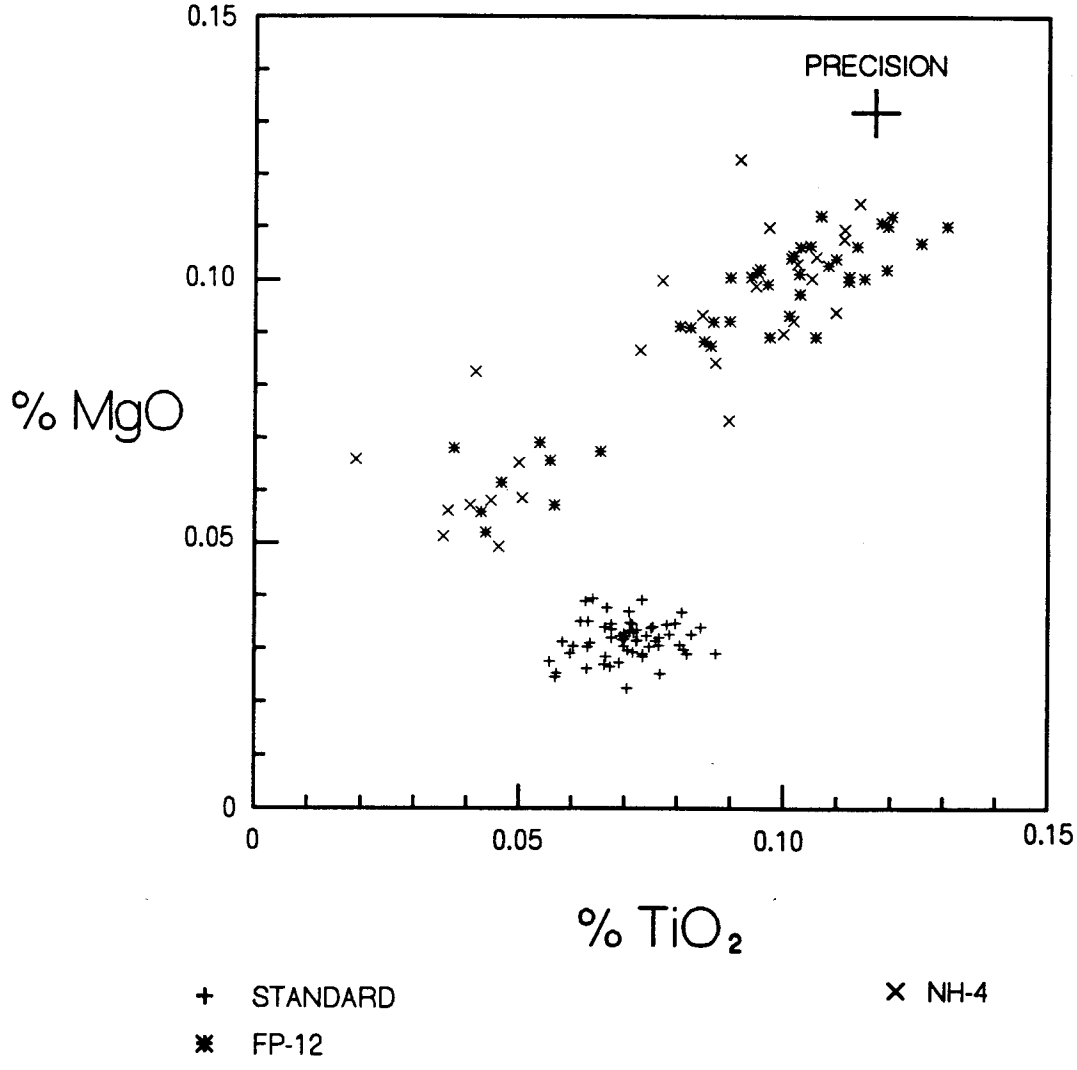

Figure 4.24. X-Y plot of wt % MgO vs TiO_2. Symbols used are: pluses indicate the Yellowstone rhyolite standard; asterisks indicate bentonite FP-12; and X's indicate bentonite NH-4.

Selinsgrove Junction, PA

The exposure at Selinsgrove Junction (40° 47′ 57" N, 76° 50′ 28" W) is a railroad cut along the eastern bank of the Susquehanna River just south of the city Selinsgrove Junction (Figure 4.25). Access to the outcrop is gained by walking 0.5 mile south along the railroad tracks from the railroad bridge that crosses the river (Figure 4.26). Six bentonites are recognized at this locality which correspond in some degree to those noted by Way and coworkers (1986) shown in Figure 3.3. Four bentonites designated SJ-1, SJ-2, SJ-3, and SJ-4 occur in the Selinsgrove limestone and bentonites SJ-5 and SJ-6 occur within the Marcellus shale (Figure 4.27).

The bentonites at this locality are gray in color (SJ-1 through SJ-5) or black (SJ-6) and occur as a strongly lithified claystone. Geochemical analyses of the melt inclusions that occur in bentonite SJ-6 correlate to those found in FP-12 at Frankstown, PA (Figure 4.36). The ternary diagrams of Mg*10-Ti*10-Fe and Mg-Ti-Cl (Figures 4.28 and 4.29) along with X-Y plots of MgO vs Cl, TiO_2 vs FeO, MgO vs FeO, MgO vs TiO_2, and FeO vs Cl (Figures 4.30 - 4.35) illustrate this correlation.

The bentonites at these three localities (i.e., Selinsgrove Junction, Tipton, and Newton Hamilton) that appear to correlate with the bentonite FP-12 at Frankstown, all occur within the Marcellus Shale (figure 4.36). Although the thicknesses of the bentonites at all four

localities (i.e., Frankstown, Selinsgrove Junction, Newton Hamilton, and Tipton) are each approximately 15 cm, they vary in color and degree of lithofication. Mineralogically, all four bentonites contained quartz, zircon, feldspar, apatite, and varying amounts of biotite and pyrite (Table 4.1). Only by the quantitative geochemical analyses could these bentonites be accurately correlated (Figures 4.37 - 4.44). Note that the analyses are not only tightly grouped but also have identical trends in each X-Y plot.

Figure 4.25. Photograph showing the outcrop at Selinsgrove Junction, PA. Note the arrow pointing to bentonite SJ-2. The markings on the scale bar are in feet.

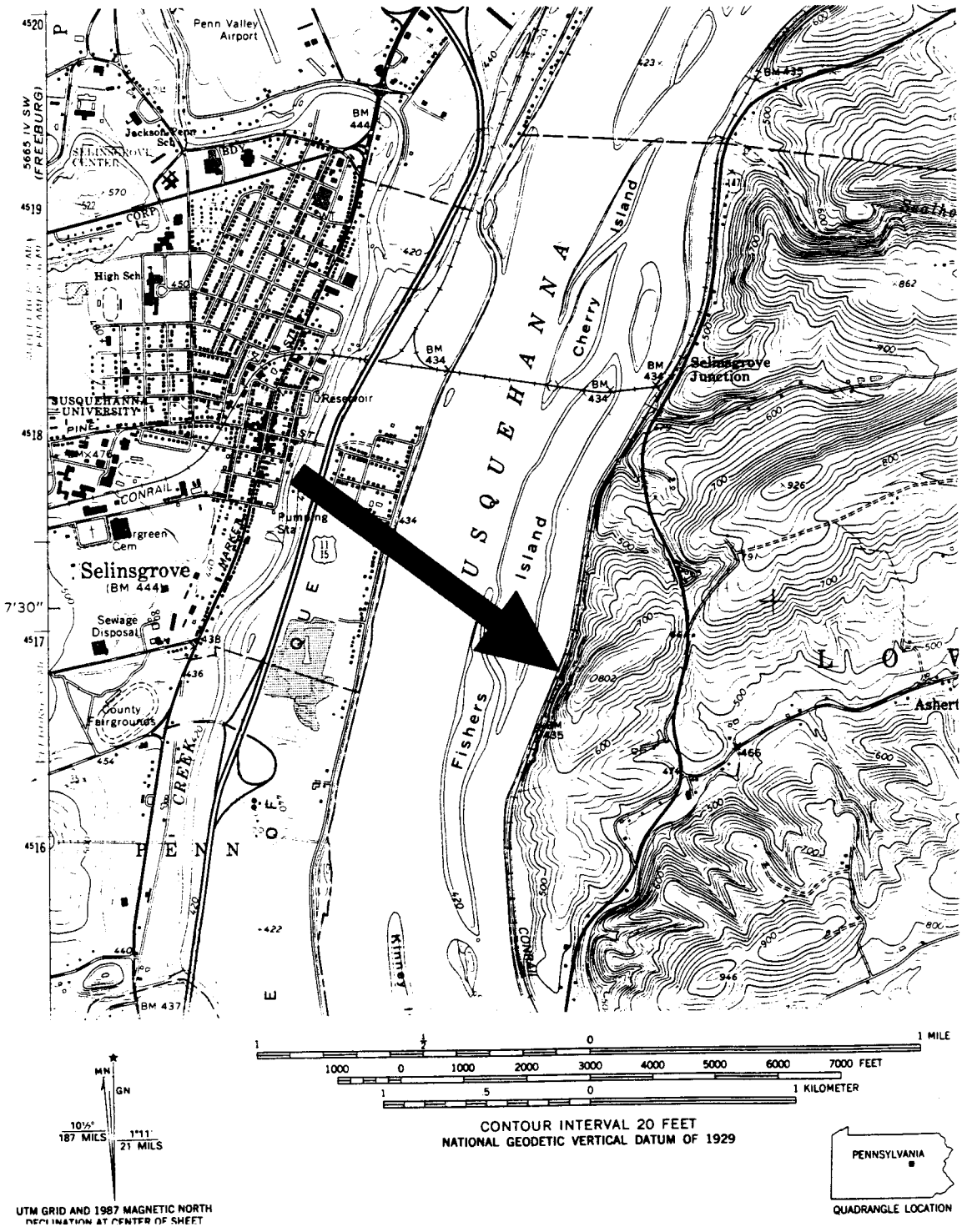

Figure 4.26. 7.5 minute quadrangle map of Sunbury, PA showing the railroad cut along the Susquehanna River of the Selinsgrove Junction outcrop.

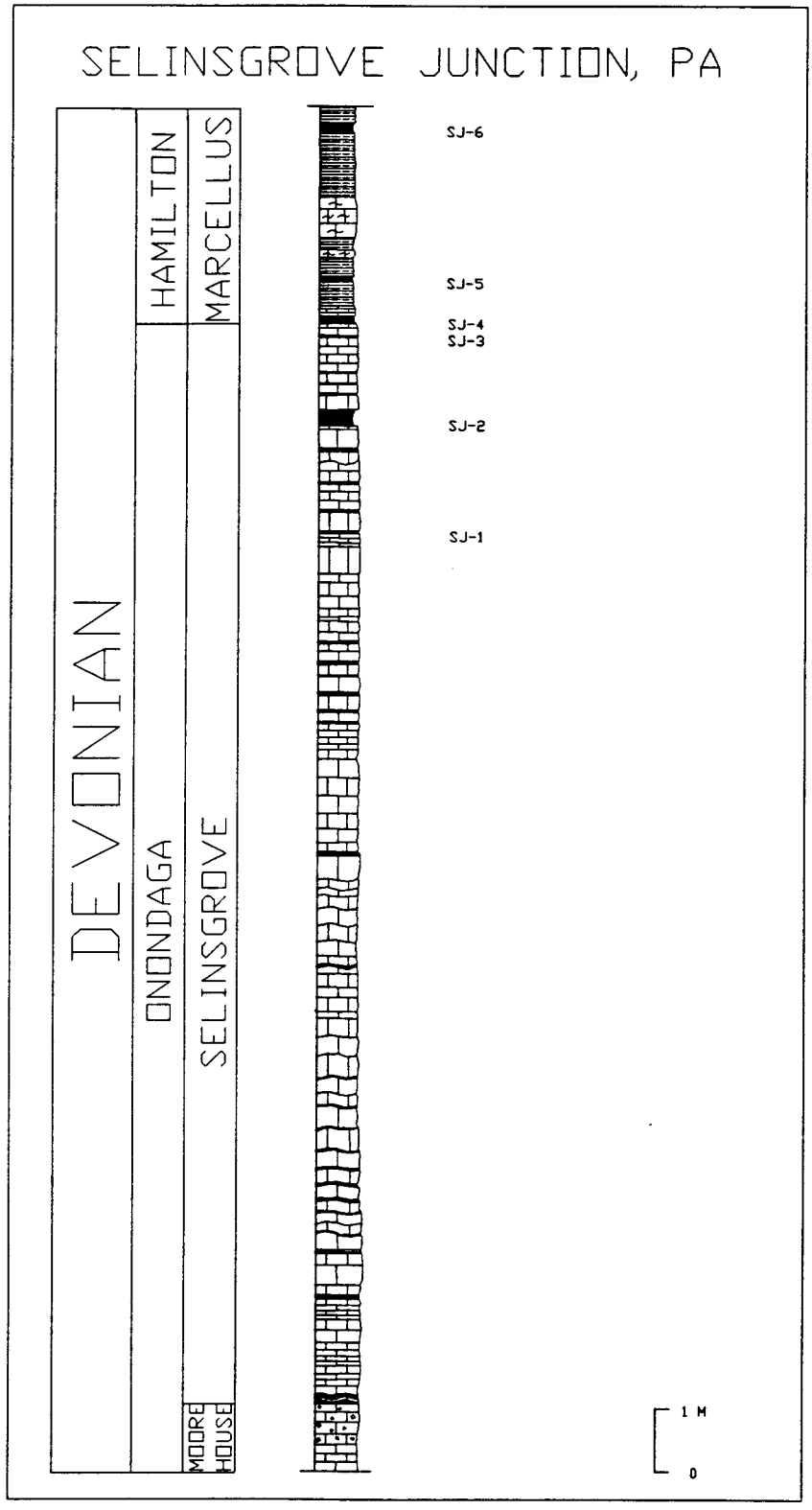

Figure 4.27. Stratigraphic column of the outcrop at Selinsgrove Junction, PA constructed by this investigator.

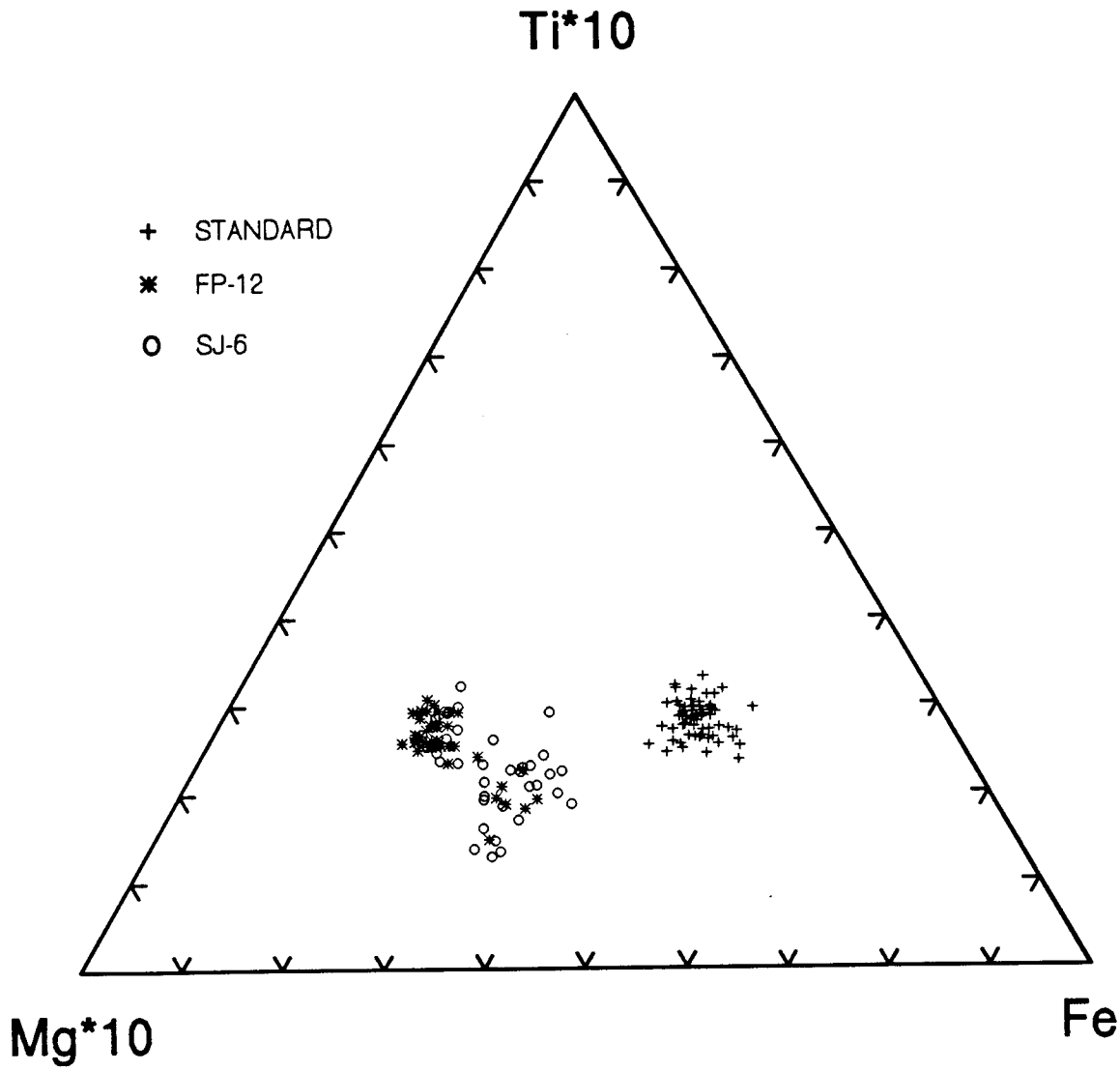

Figure 4.28. Ternary diagram of Mg*10-Ti*10-Fe. The symbols used are: pluses indicate the Yellowstone rhyolite standard; asterisks indicate bentonite FP-12; and circles indicate bentonite SJ-6.

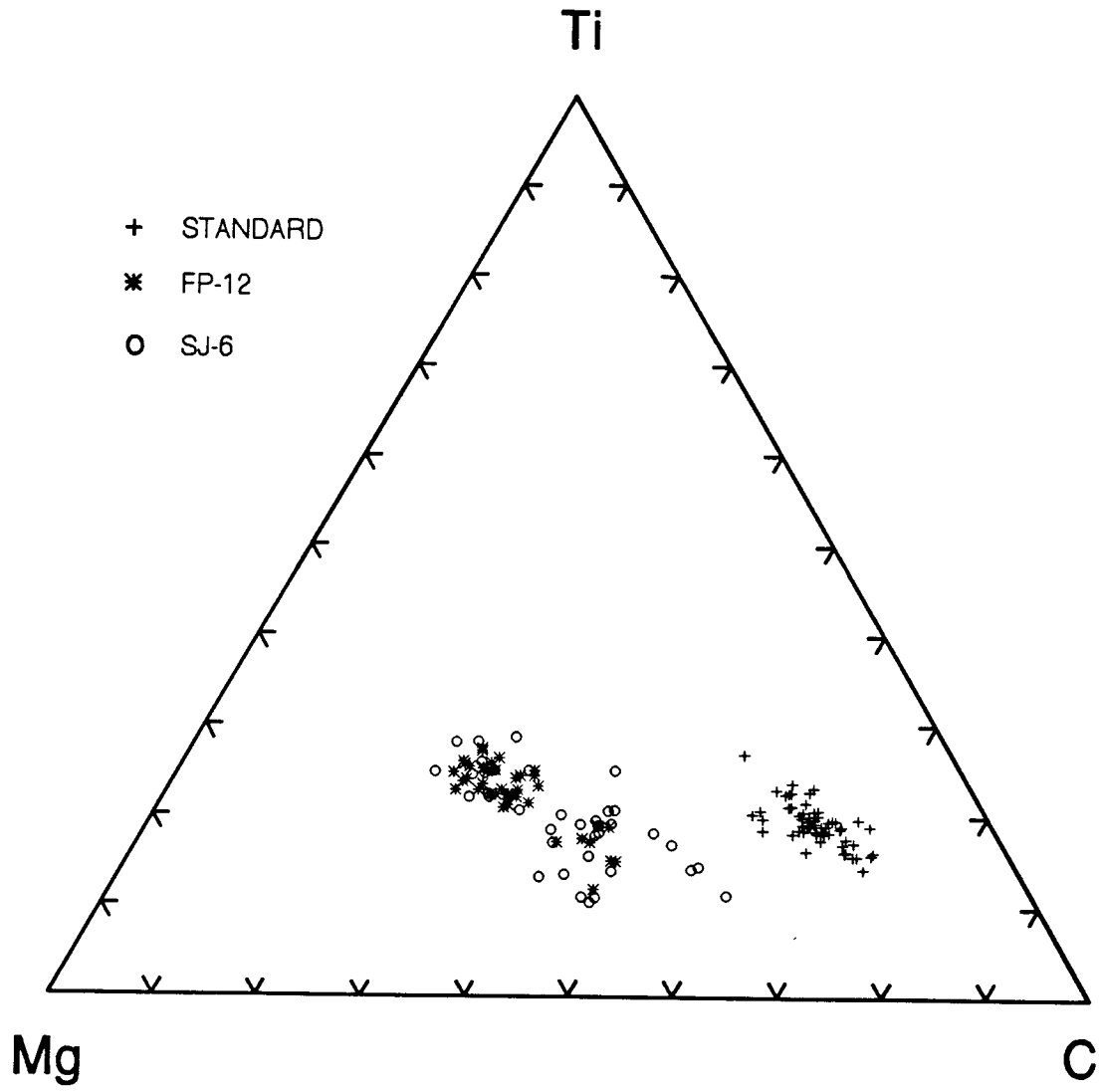

Figure 4.29. Ternary diagram of Mg-Ti-Cl. Symbols used are: pluses indicate the Yellowstone rhyolite standard; asterisks indicate bentonite FP-12; and circles indicate bentonite SJ-6.

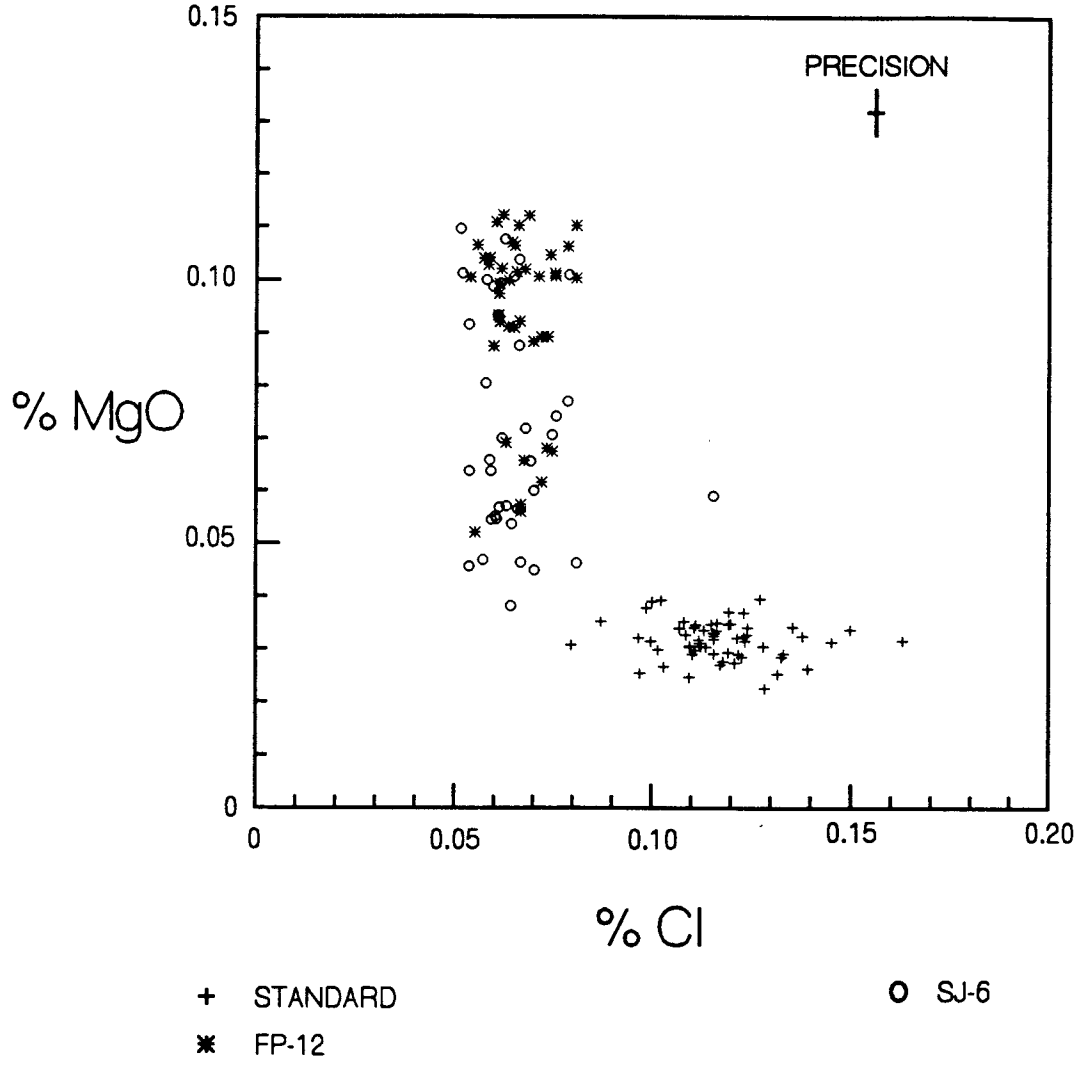

Figure 4.30. X-Y plot of wt % MgO vs Cl. The symbols used are: pluses indicate the Yellowstone rhyolite standard; asterisks indicate bentonite FP-12; and circles indicate bentonite SJ-6.

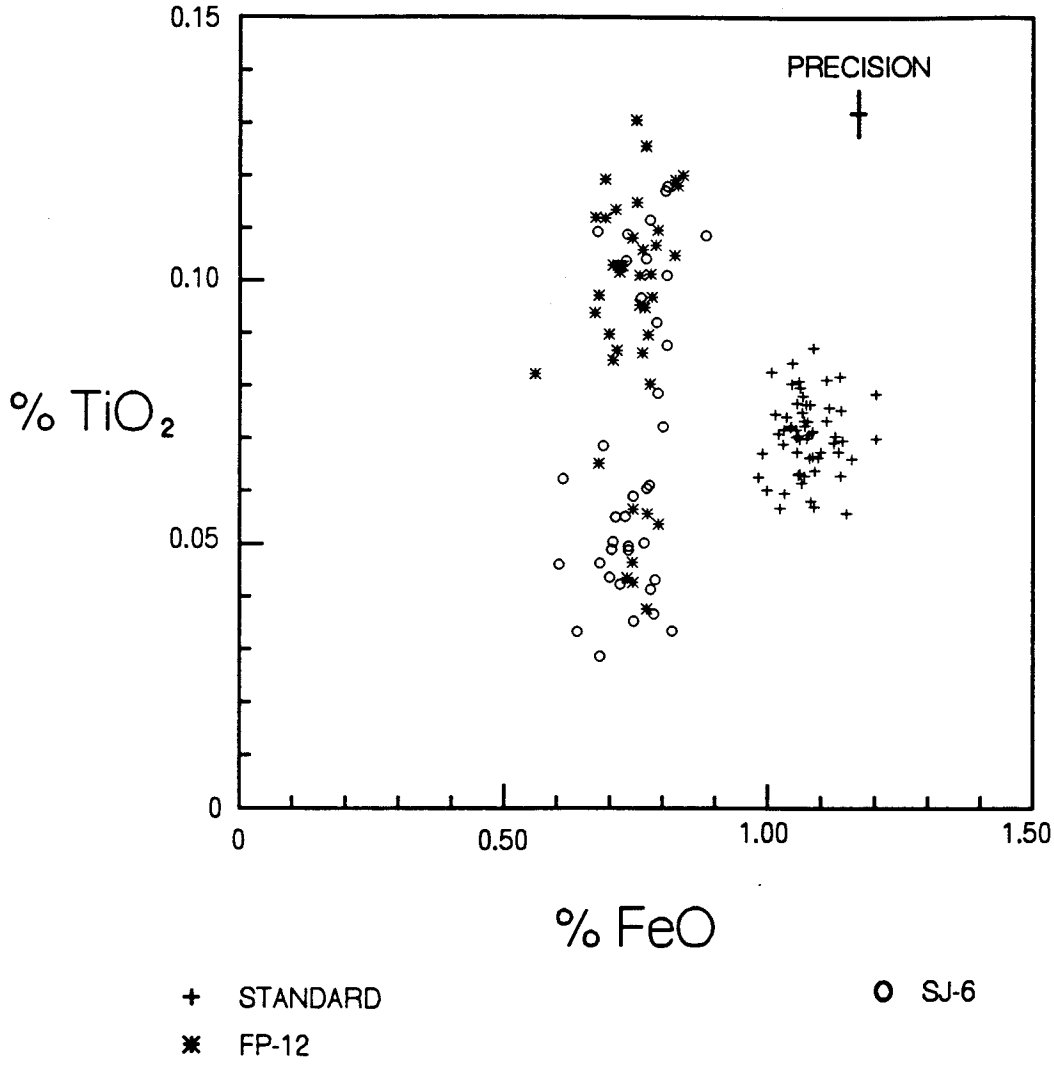

Figure 4.31. X-Y plot of wt % TiO_2 vs FeO. Symbols used are: pluses indicate the Yellowstone rhyolite standard; asterisks indicate bentonite FP-12; and circles indicate bentonite SJ-6.

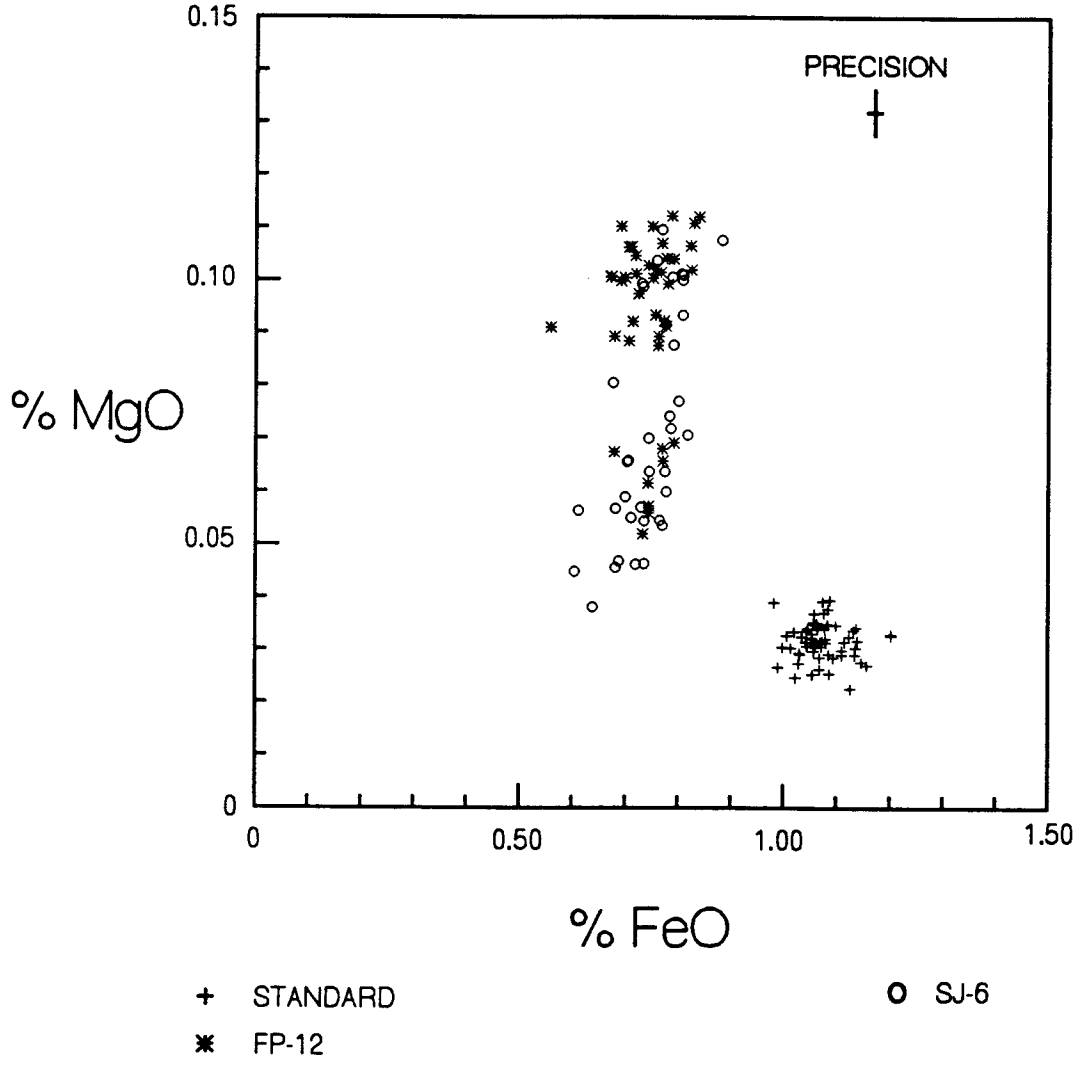

Figure 4.32. X-Y plot of wt % MgO vs FeO. The symbols used are: pluses indicate the Yellowstone rhyolite standard; asterisks indicate bentonite FP-12; and circles indicate bentonite SJ-6.

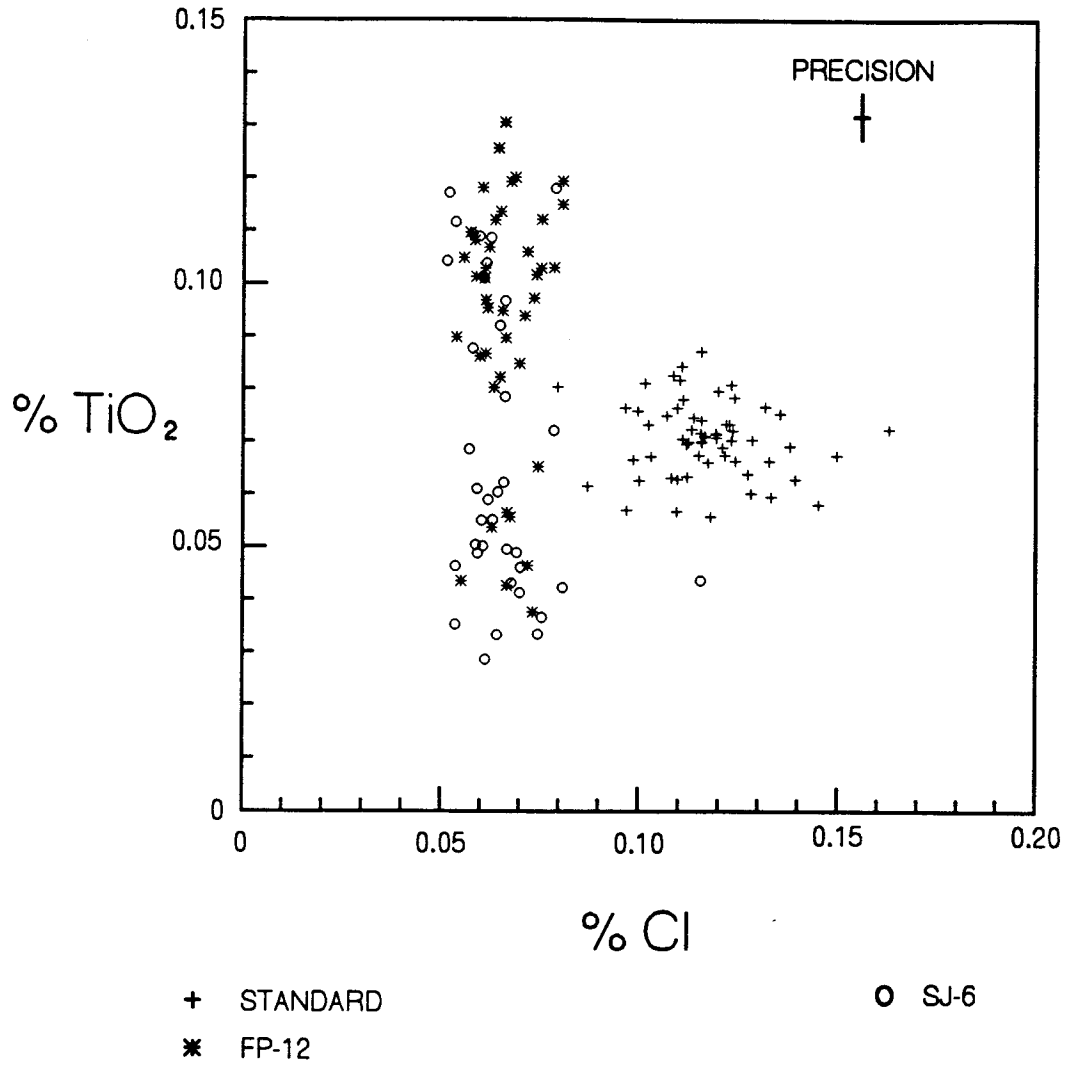

Figure 4.33. X-Y plot of wt % TiO_2 vs Cl. Symbols used are: pluses indicate the Yellowstone rhyolite standard; asterisks indicate bentonite FP-12; and circles indicate bentonite SJ-6.

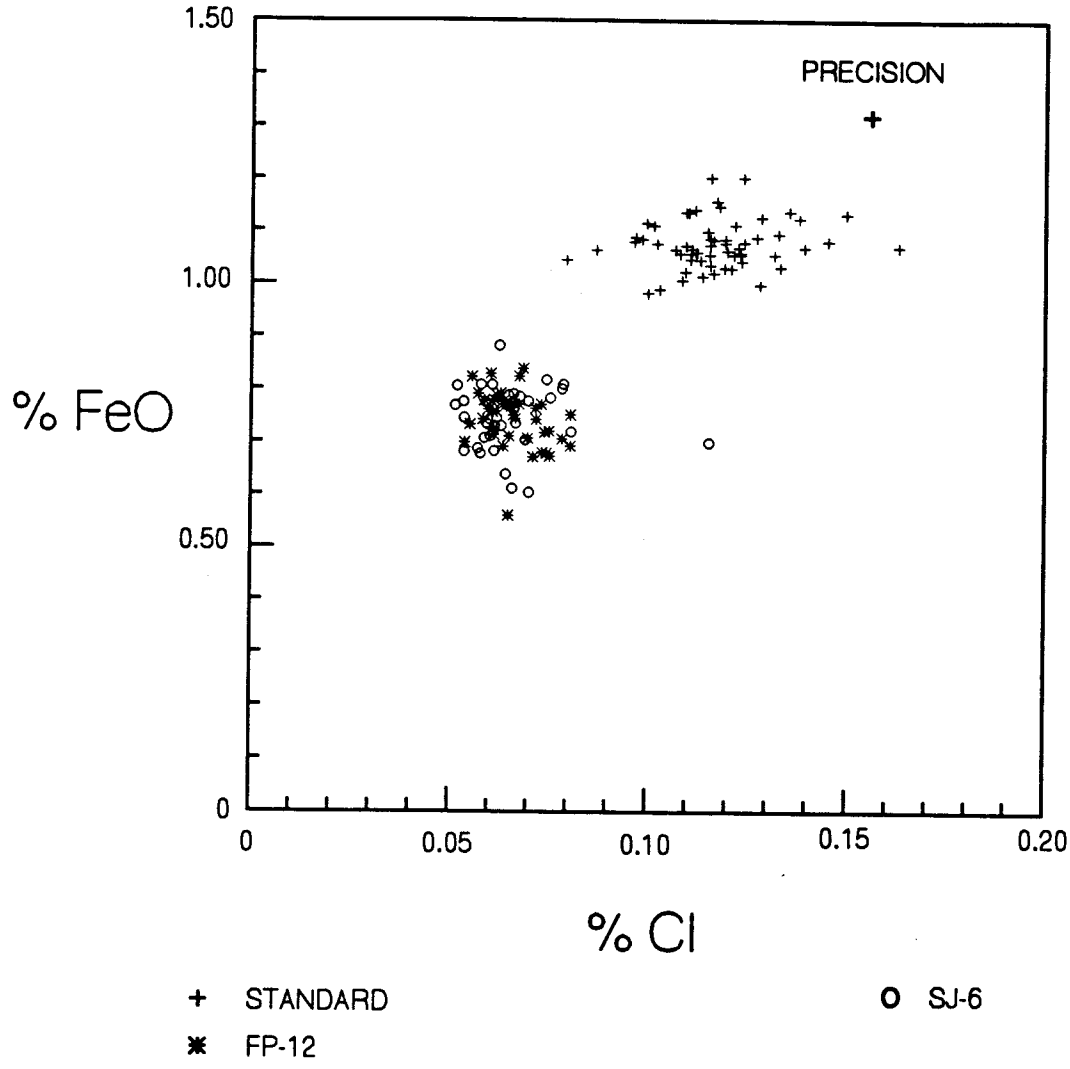

Figure 4.34. X-Y plot of wt % FeO vs Cl. Symbols used are: pluses indicate the Yellowstone rhyolite standard; asterisks indicate bentonite FP-12; and circles indicate bentonite SJ-6.

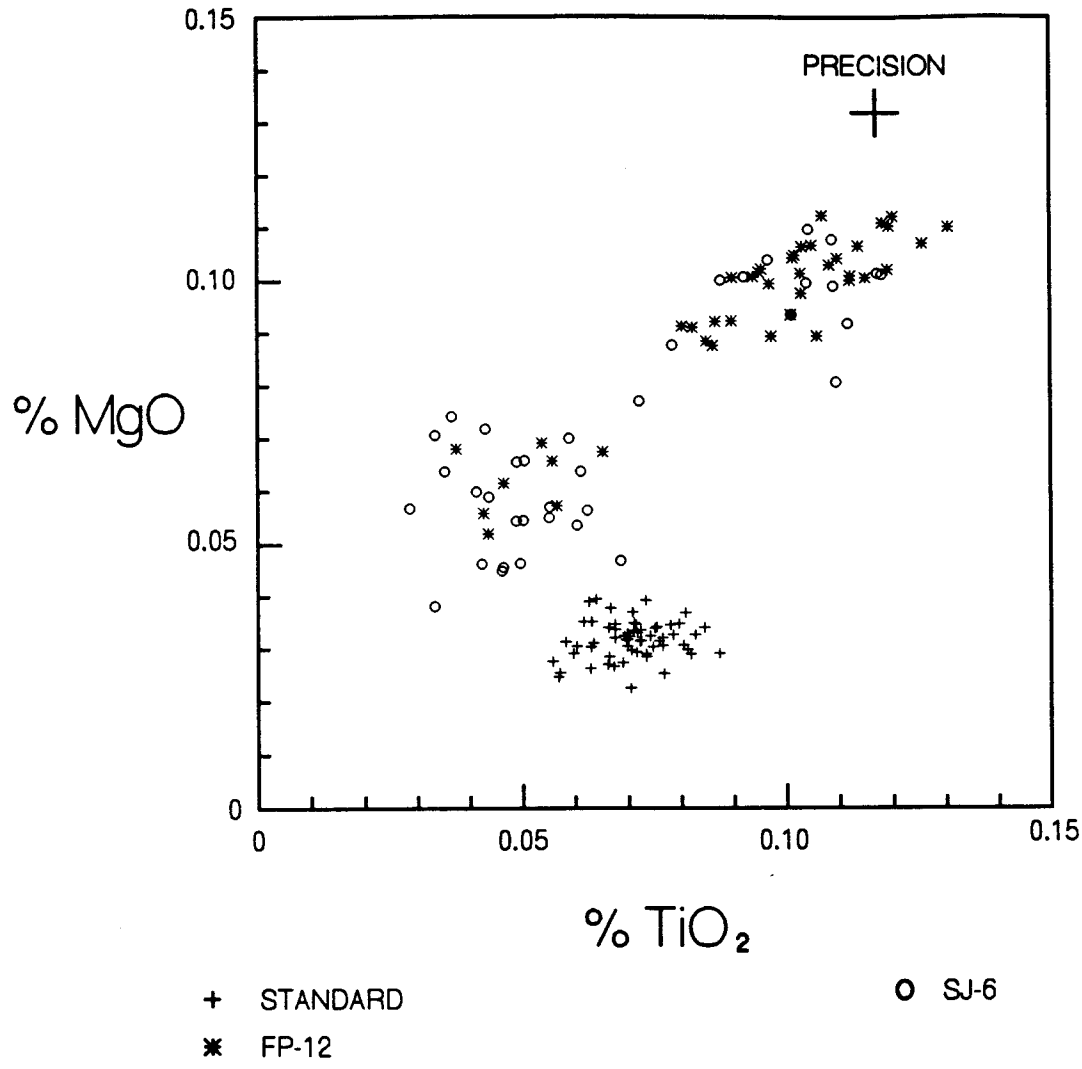

Figure 4.35. X-Y plot of wt % MgO vs TiO_2. The symbols used are: pluses indicate the Yellowstone rhyolite standard; asterisks indicate bentonite FP-12; and circles indicate bentonite SJ-6.

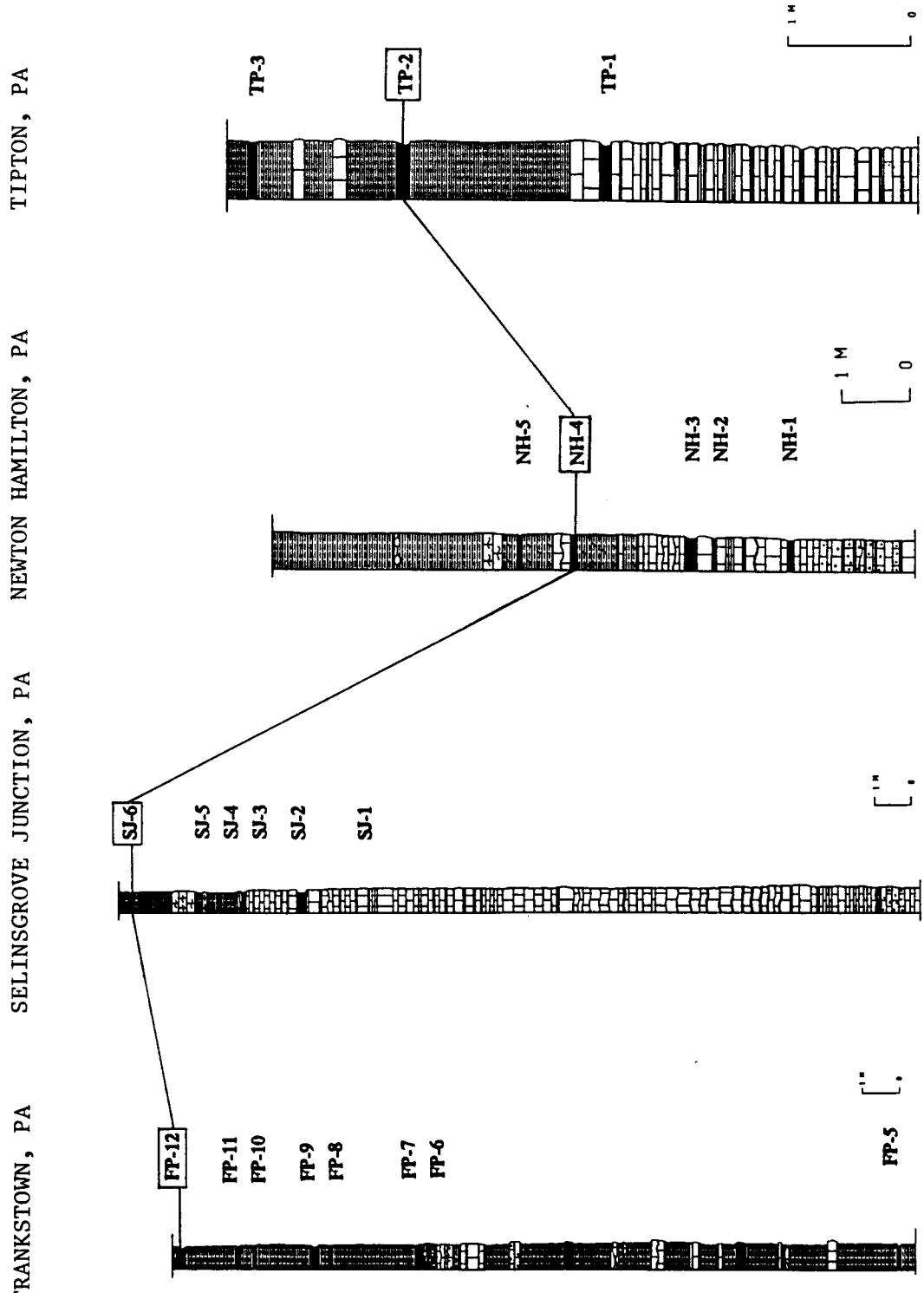

Figure 4.36. Stratigraphic columns of Frankstown, PA, Tipton, PA, Newton Hamilton, PA, and Selinsgrove Junction, PA. Bentonites that geochemically correlate are connected with a solid line.

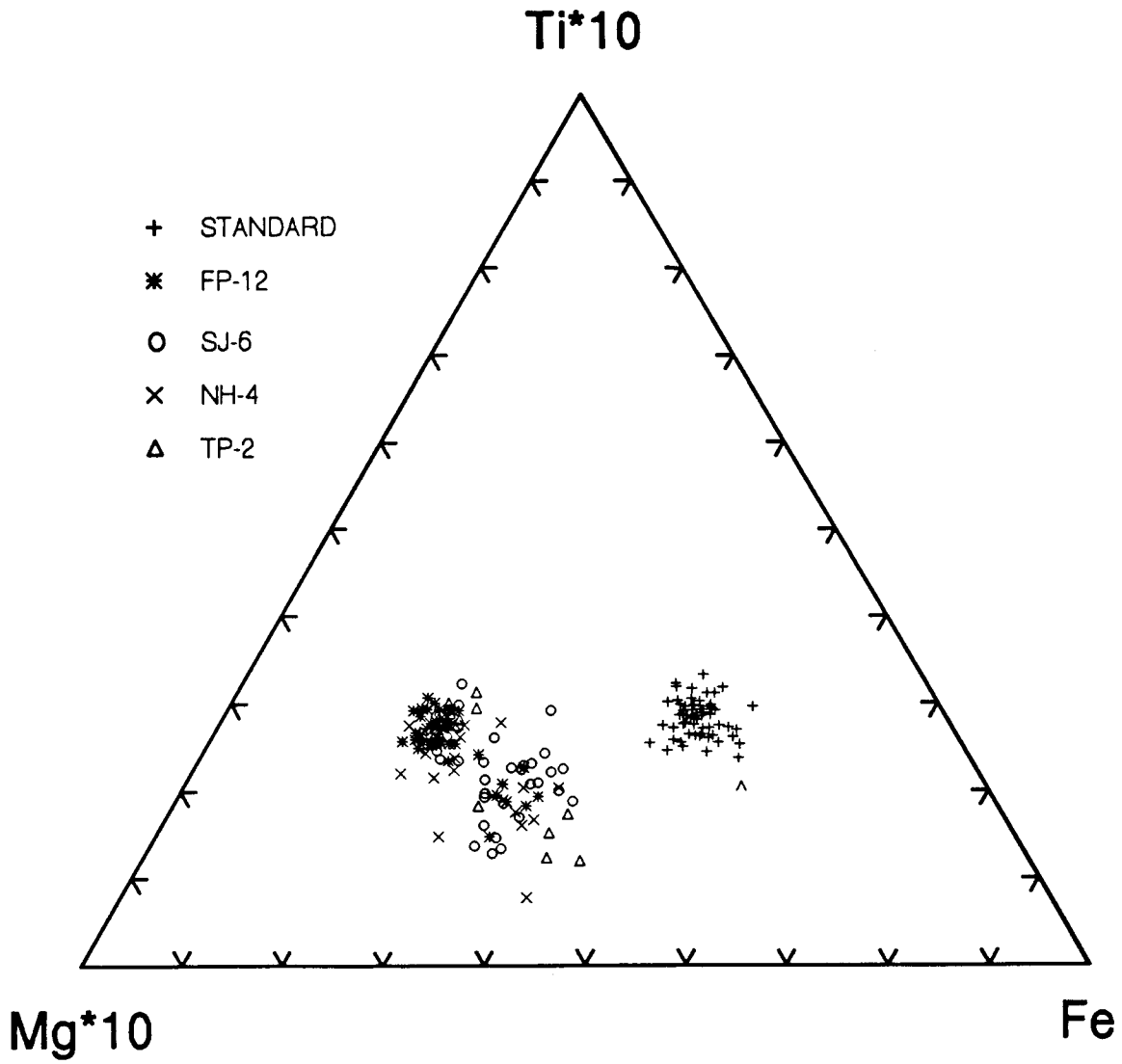

Figure 4.37. Ternary diagram of Mg*10-Ti*10-Fe showing all four localities that have been geochemically correlated. The symbols used are: pluses indicate the Yellowstone rhyolite standard; asterisks indicate bentonite FP-12; circles indicate bentonite SJ-6; X's indicate bentonite NH-4; and triangles indicate bentonite TP-2.

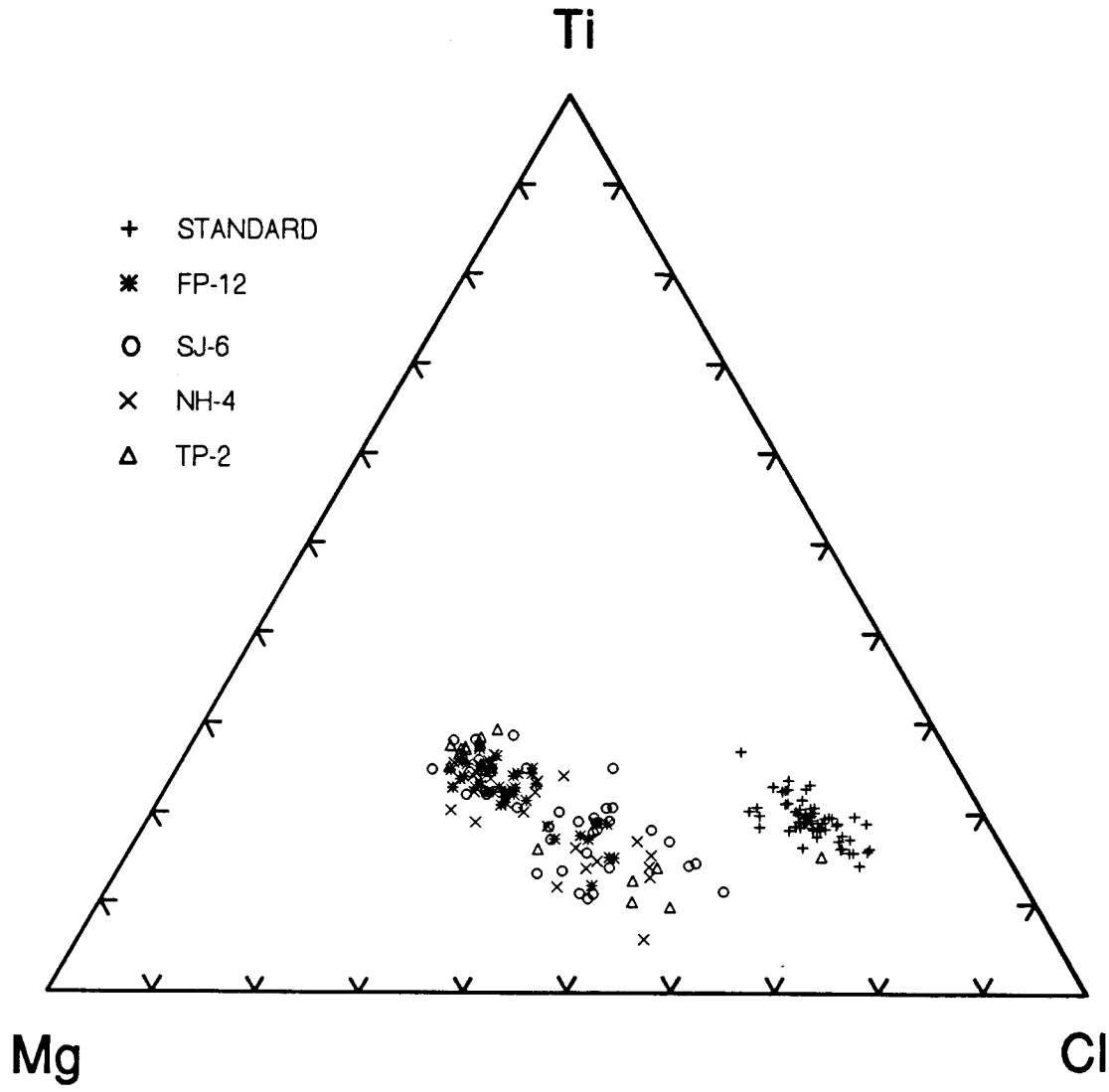

Figure 4.38. Ternary diagram of Mg-Ti-Cl showing all four localities that have been geochemically correlated. The symbols used are: pluses indicate the Yellowstone rhyolite standard; asterisks indicate bentonite FP-12; circles indicate bentonite SJ-6; X's indicate bentonite NH-4; and triangles indicate bentonite TP-2.

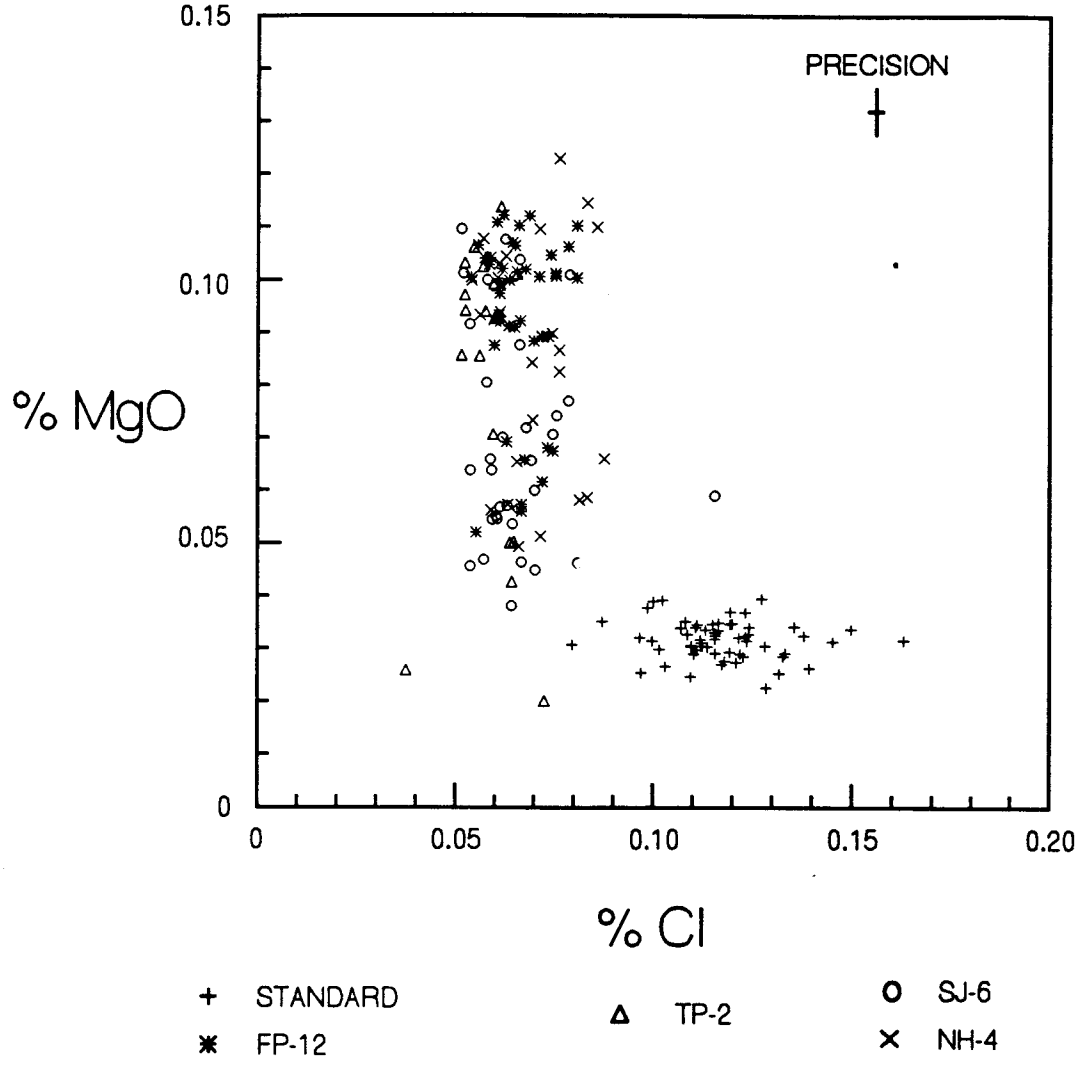

Figure 4.39. X-Y plot of wt % MgO vs Cl of all four localities that have been geochemically correlated. The symbols used are: pluses indicate the Yellowstone rhyolite standard; asterisks indicate bentonite FP-12; circles indicate bentonite SJ-6, X's indicate bentonite NH-4; and triangles indicate bentonite TP-2.

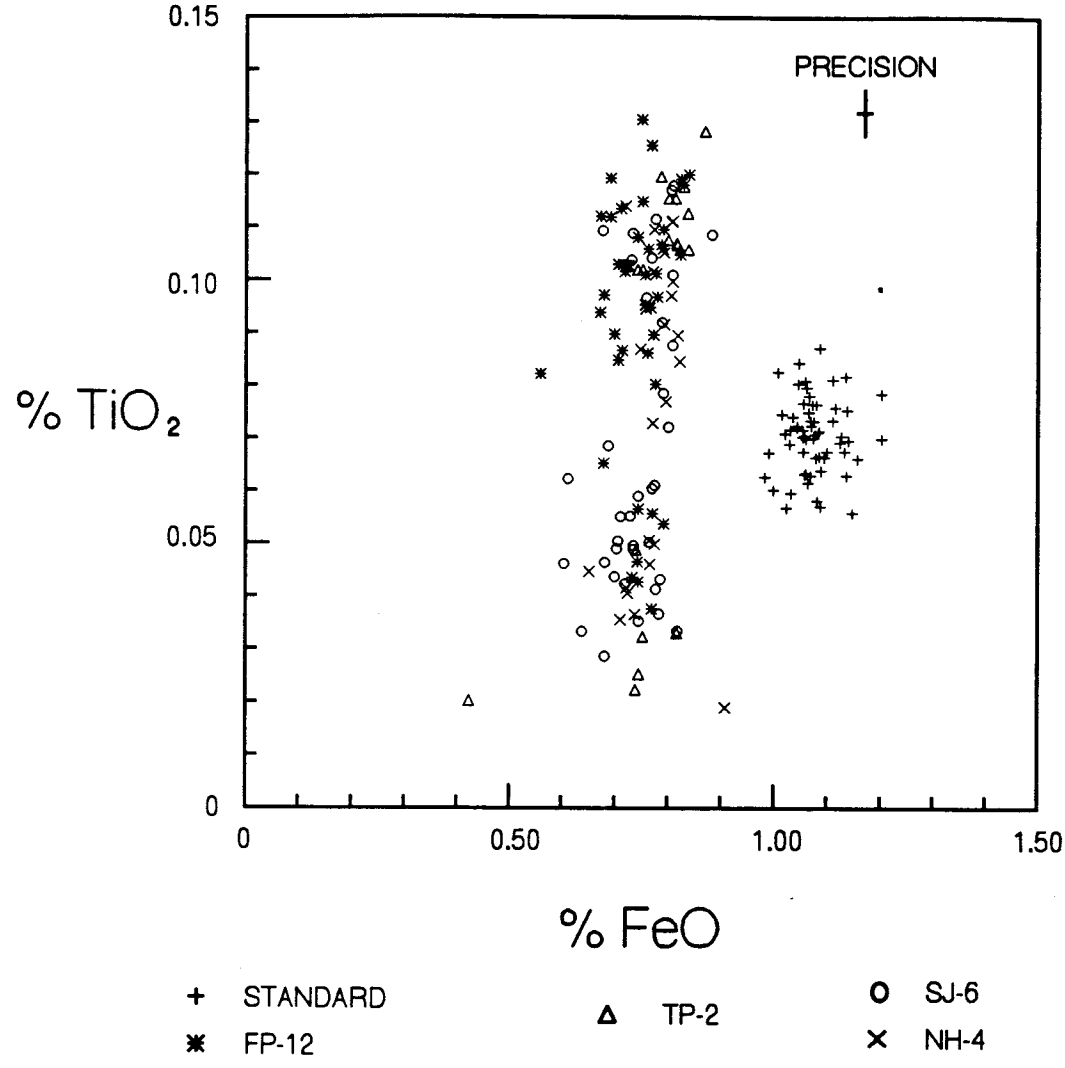

Figure 4.40. X-Y plot of wt % TiO_2 vs FeO of all four localities that have been geochemically correlated. The symbols used are: pluses indicate the Yellowstone rhyolite standard; asterisks indicate bentonite FP-12; circles indicate bentonite SJ-6; X's indicate bentonite NH-4; and triangles indicate bentonite TP-2.

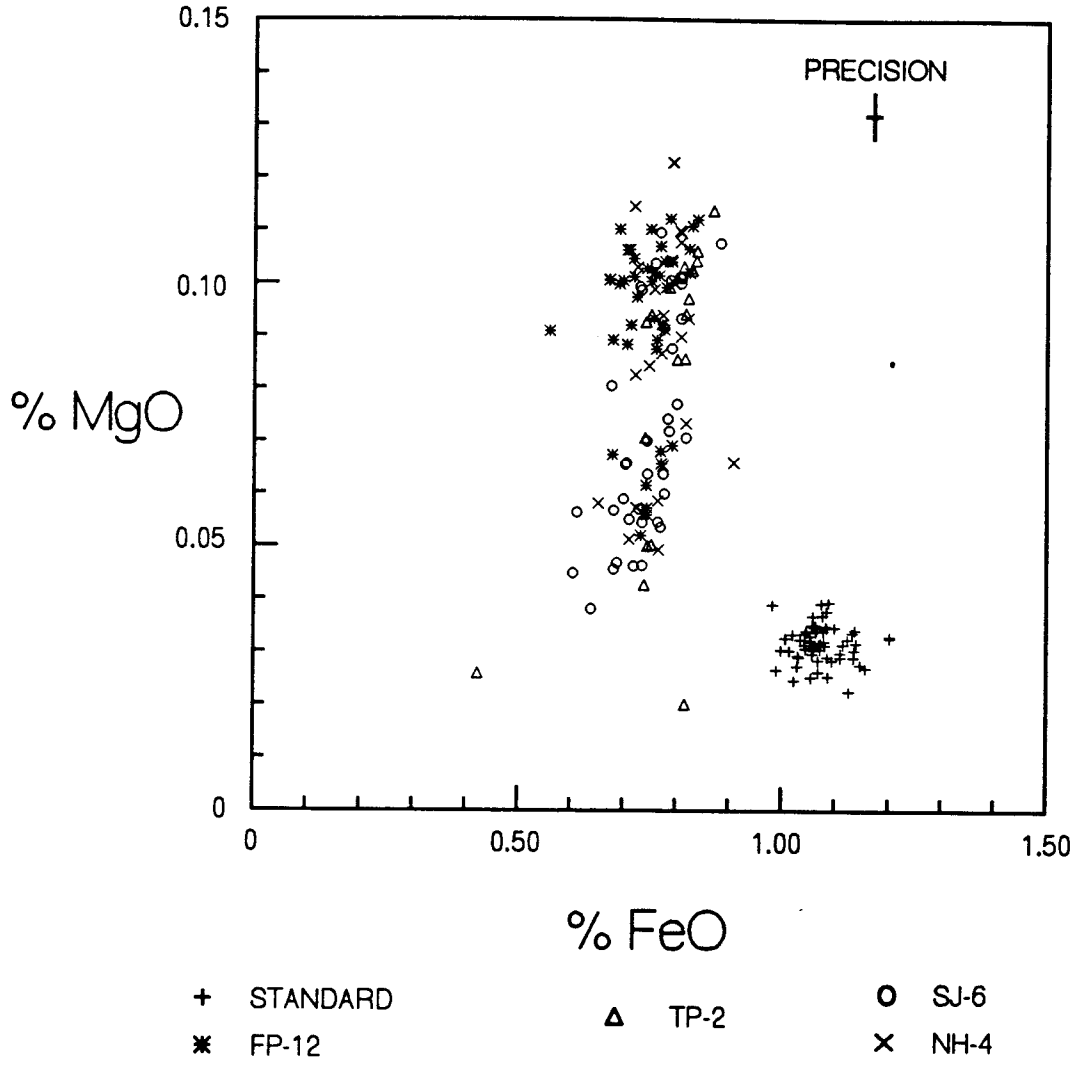

Figure 4.41. X-Y plot of wt % MgO vs FeO of all four localities that have been geochemically correlated. The symbols used are: pluses indicate the Yellowstone rhyolite standard; asterisks indicate bentonite FP-12; circles indicate bentonite SJ-6; X's indicate bentonite NH-4; and triangles indicate bentonite TP-2.

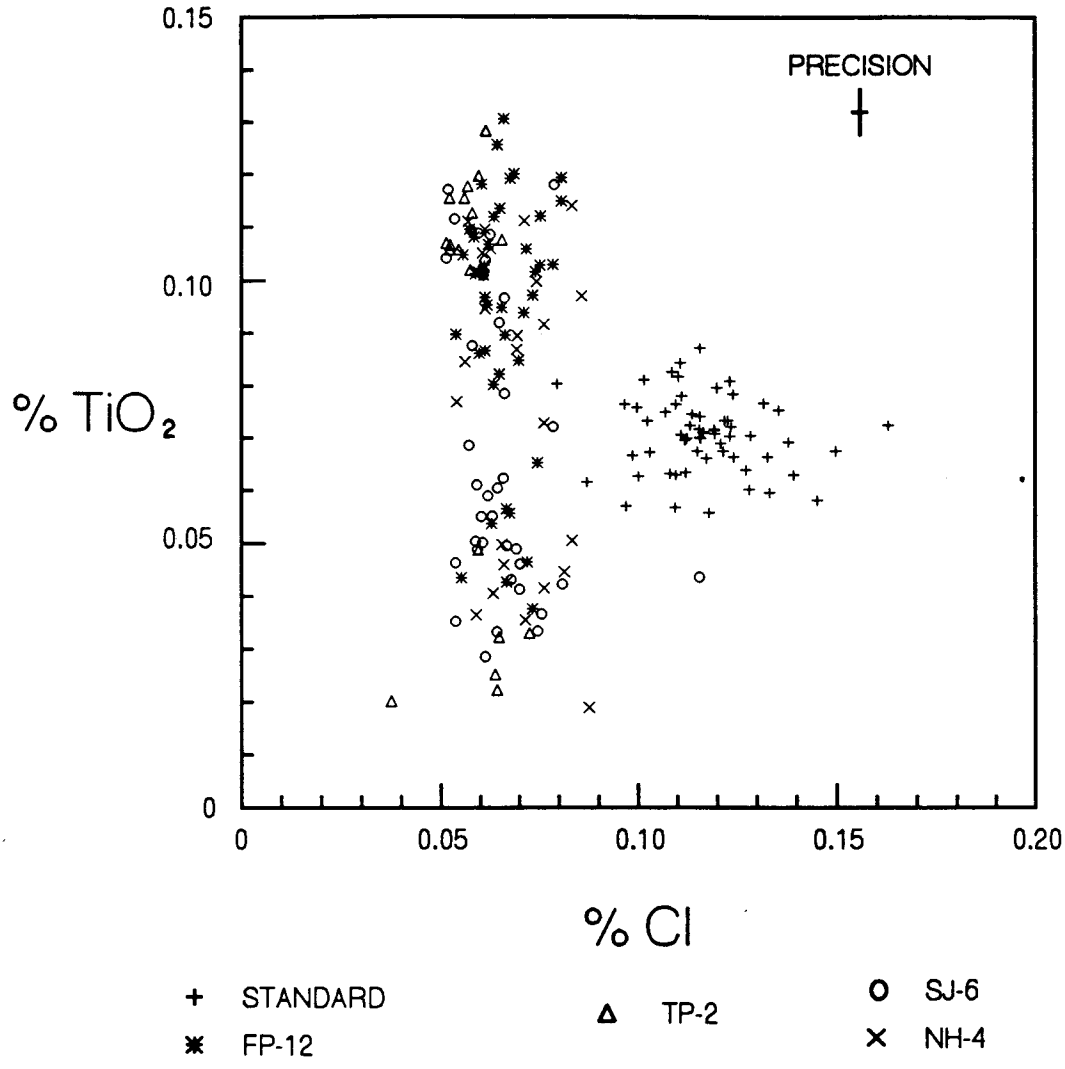

Figure 4.42. X-Y plot of wt % TiO_2 vs Cl of all four bentonite localities that have been geochemically correlated. The symbols used are: pluses indicate the Yellowstone rhyolite standard; asterisks indicate bentonite FP-12; circles indicate bentonite SJ-6; X's indicate bentonite NH-4; and triangles indicate bentonite TP-2.

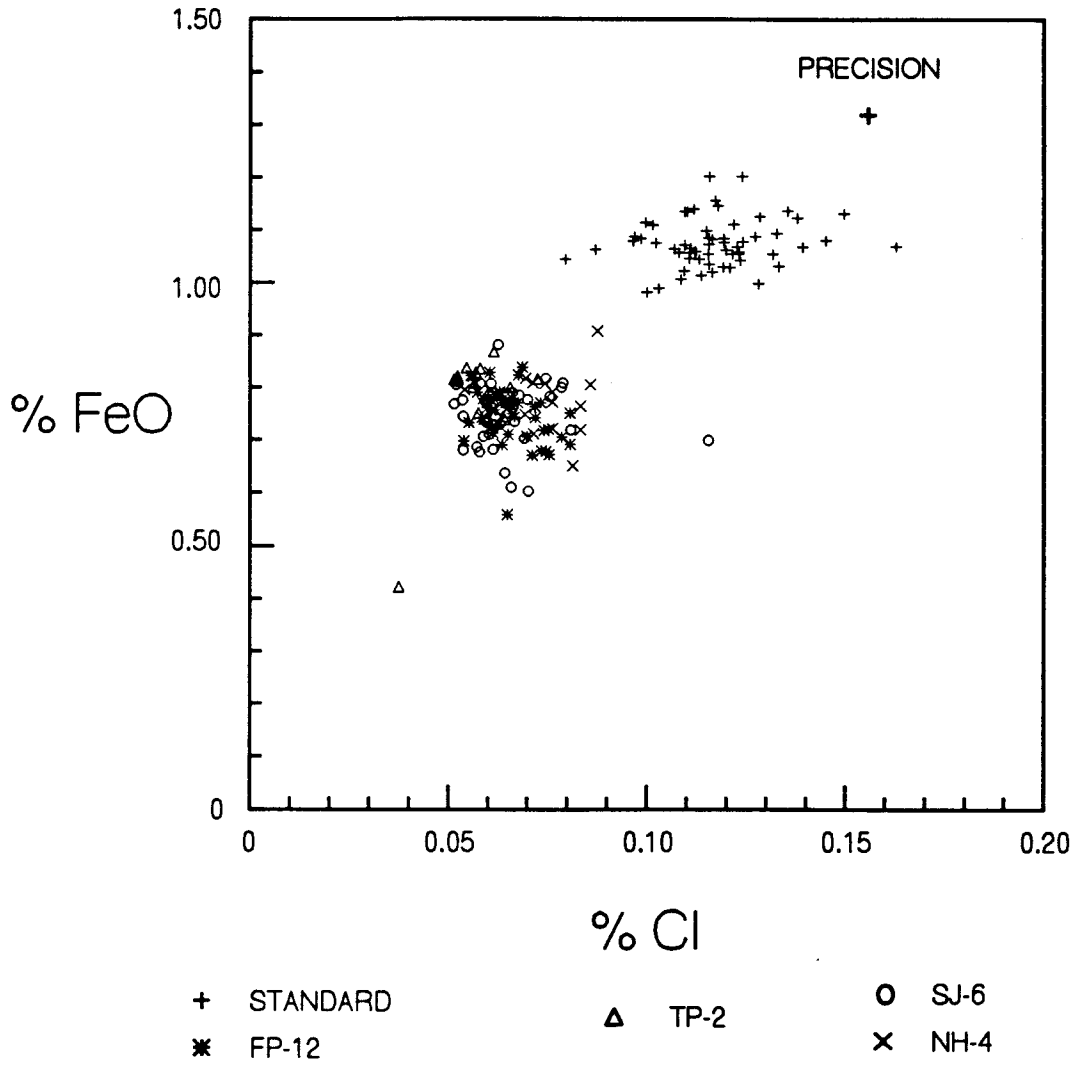

Figure 4.43. X-Y plot of wt % FeO vs Cl of all four localities that have been geochemically correlated. Symbols used are: pluses indicate the Yellowstone rhyolite standard; asterisks indicate benonite FP-12; circles indicate bentonite SJ-6; X's indicate bentonite NH-4; and triangles indicate bentonite TP-2.

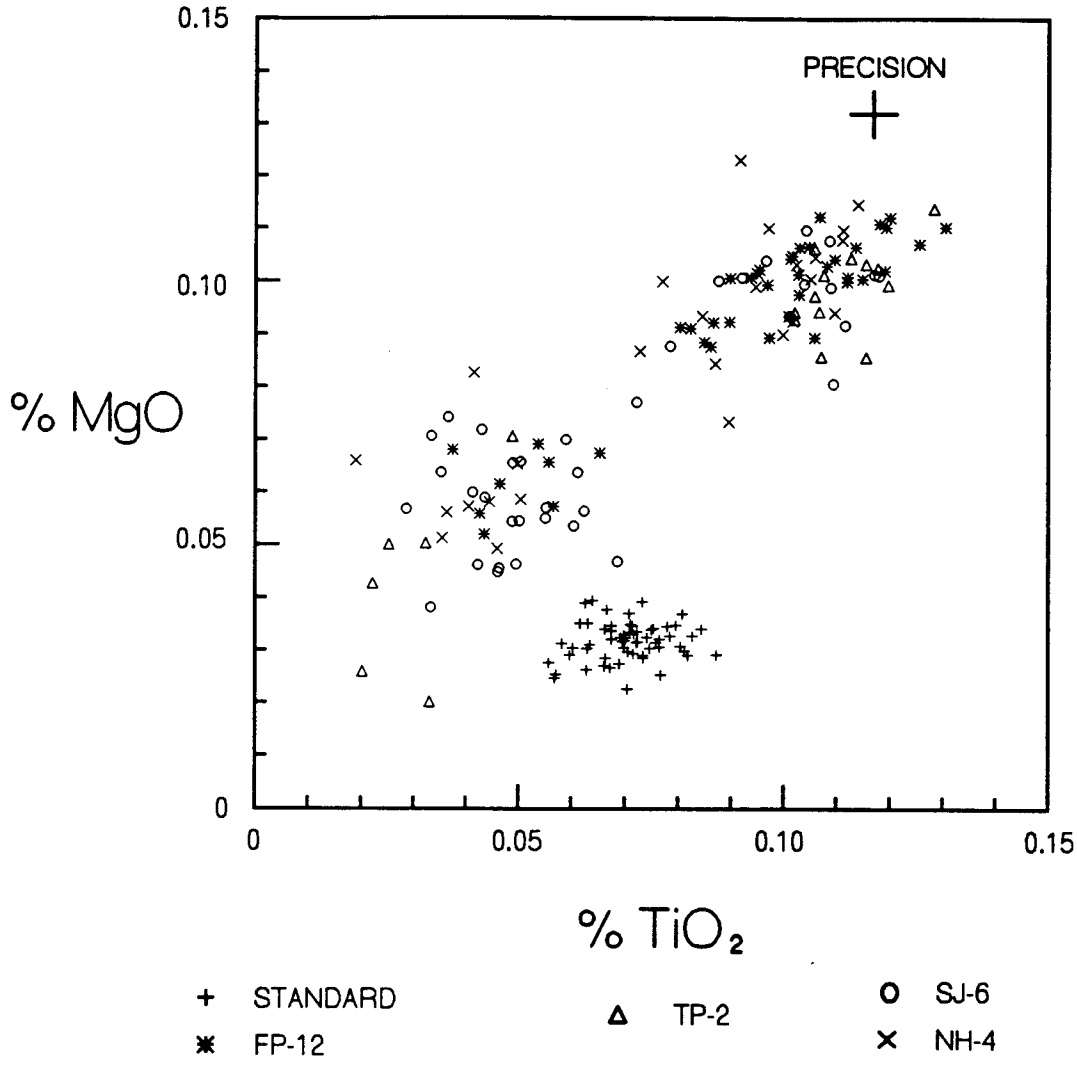

Figure 4.44. X-Y plot of wt % MgO vs TiO_2 of all four localities that have been geochemically correlated. The symbols used are: pluses indicate the Yellowstone rhyolite standard; asterisks indicate bentonite FP-12; circles indicate bentonite SJ-6; X's indicate bentonite NH-4; and triangles indicate bentonite TP-2.

4.2 CORRELATIONS TO BENTONITE FP-9

Two localities out of the fourteen sampled each contained a bentonite layer that geochemically correlated to the bentonite FP-9 at Frankstown, PA. These two localities are Newton Hamilton, PA and Midway, PA (Figure 4.45). These three localities create an east/west transect of 113 km in south central Pennsylvania. This distance of 113 km does not account for the shortening (≈35 km estimated from the Geological map of Pennsylvania, Berg et al., 1980) that has occurred in this fold and thrust belt of the Appalachians.

Newton Hamilton, PA

The bentonite at Newton Hamilton (40° 23′ 00" N, 77° 51′ 01" W) which correlates to bentonite FP-9 is bentonite NH-3 (Figure 4.45). It occurs 60 cm from the top of the Selinsgrove limestone, and was designated by Way et al. (1986) as being Tioga-B (Figure 3.4).

The geochemical analyses of melt inclusions that occur within this bentonite indicate that it is equivalent to bentonite FP-9 wich is consistent with the proposed correlation of Way et al. (1986; Figures 3.4 and 4.68). This is demonstrated by the ternary diagrams of Mg*10-Ti*10-Fe and Mg-Ti-Cl (Figure 4.46 and 4.47) and the X-Y plots of MgO vs Cl, TiO_2 vs FeO, MgO vs FeO, TiO_2 vs Cl, FeO vs Cl, and MgO vr TiO_2 (Figures 4.48 - 4.56).

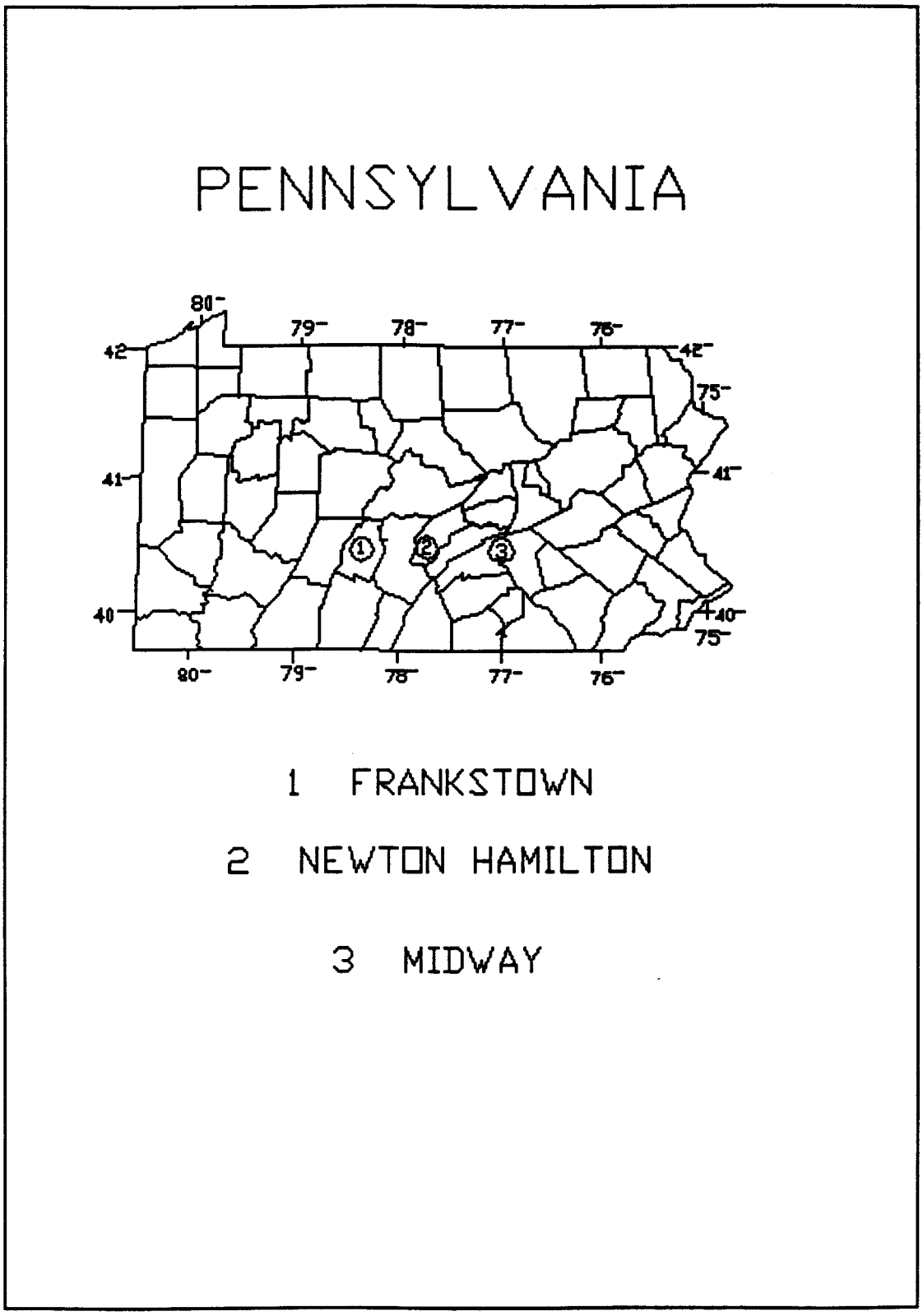

Figure 4.45. Map of Pennsylvania showing the locations of Frankstown, Newton Hamilton, and Midway.

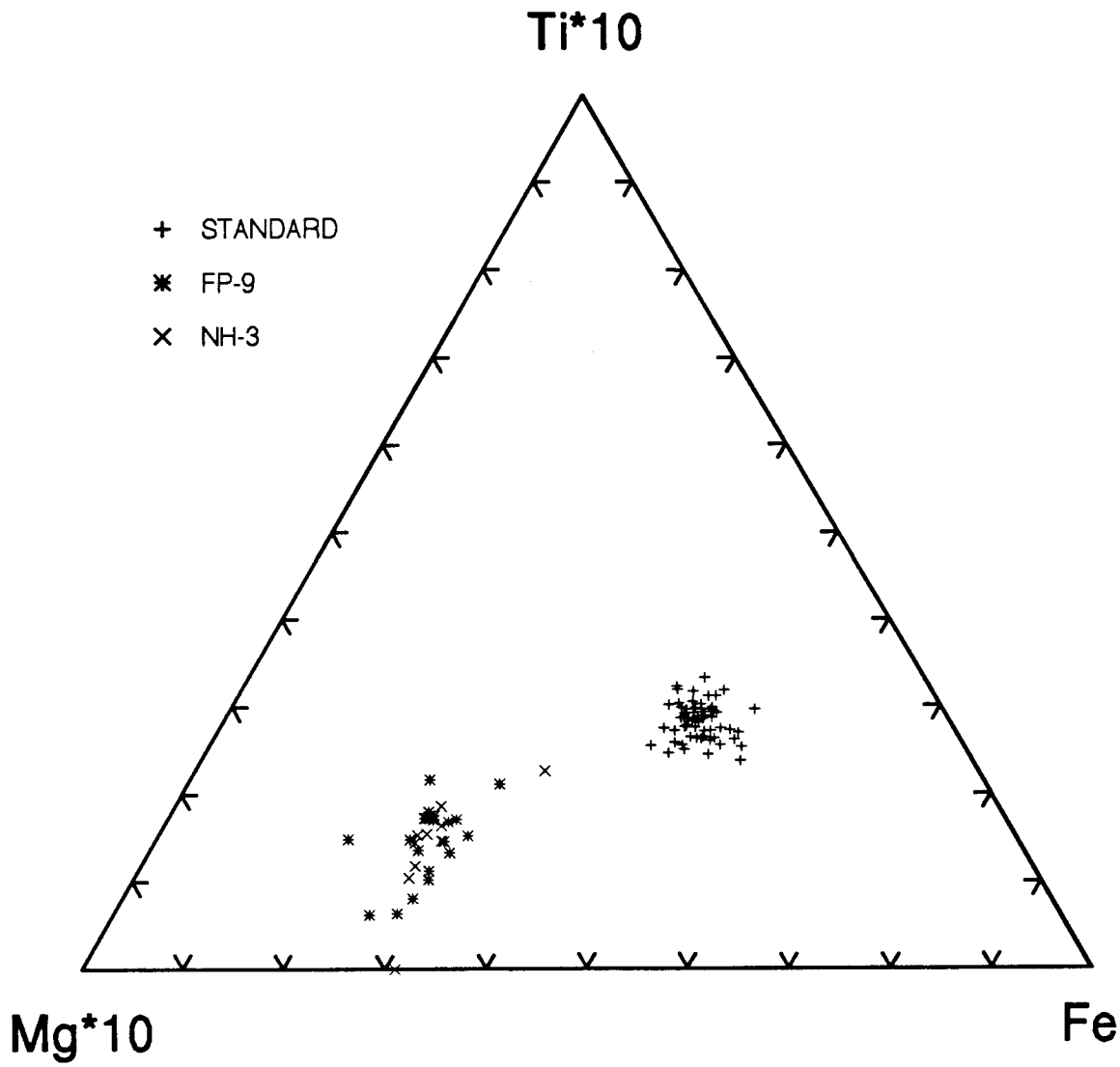

Figure 4.46. Ternary diagram of Mg*10-Ti*10-Fe. Symbols used are: pluses indicate the Yellowstone rhyolite standard; asterisks indicate the bentonite FP-9; and X's indicate the bentonite NH-3.

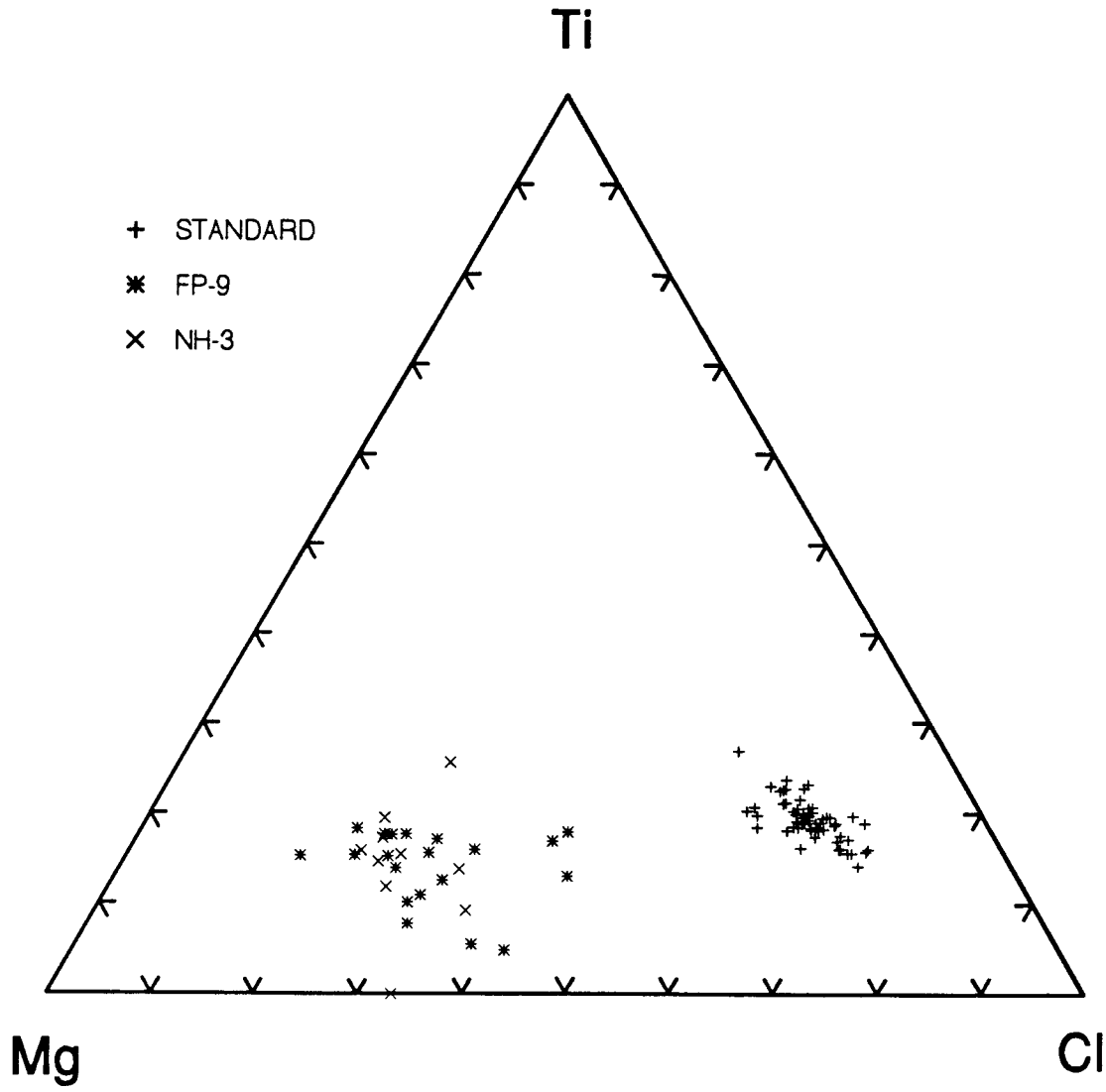

Figure 4.47. Ternary diagram of Mg-Ti-Cl. Symbols used are: pluses indicate the Yellowstone rhyolite standard; asterisks indicate bentonite FP-9; and X's indicate bentonite NH-3.

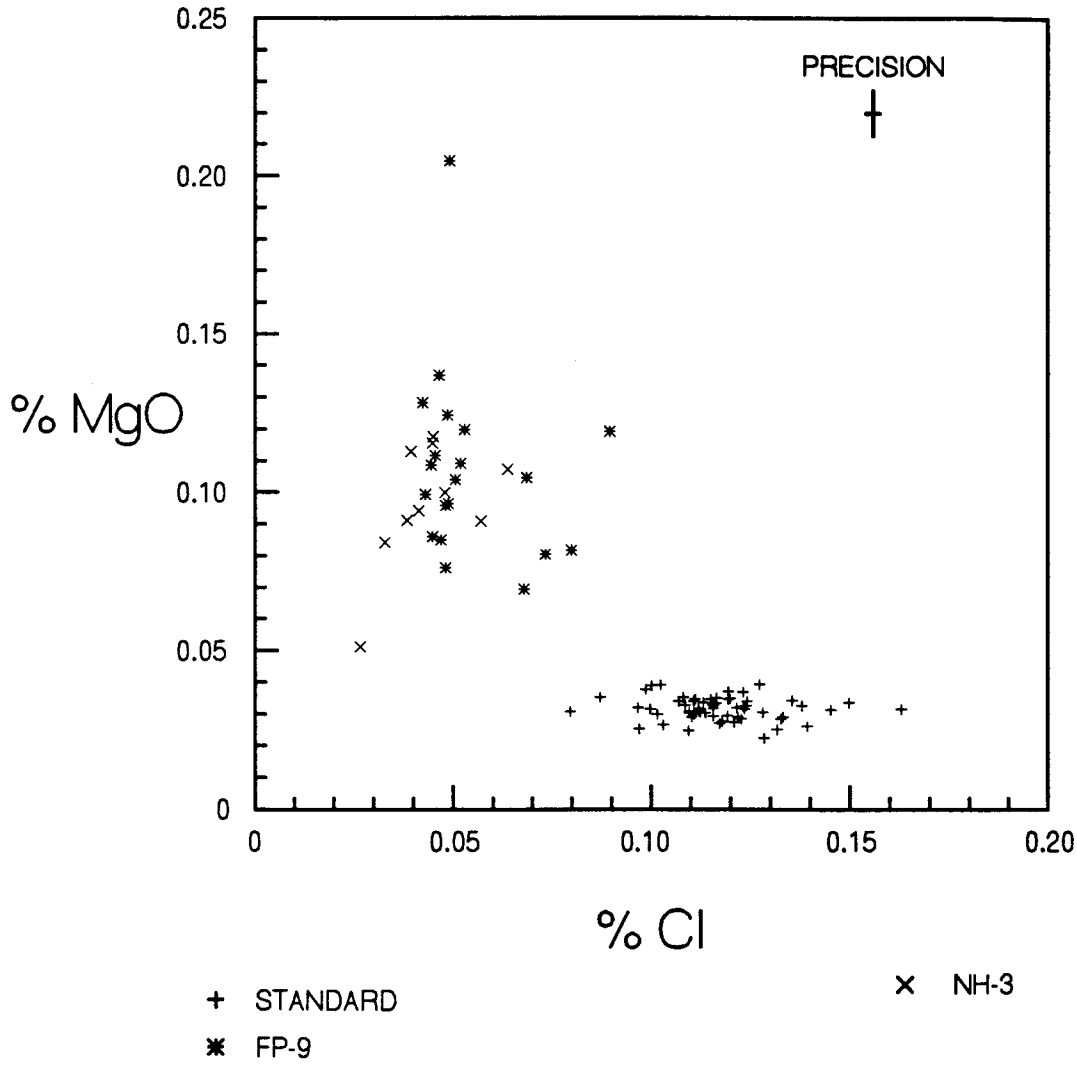

Figure 4.48. X-Y plot of wt % MgO vs Cl. Symbols used are: pluses indicate the Yellowstone rhyolite standard; asterisks indicate bentonite FP-9; and X's indicate bentonite NH-3.

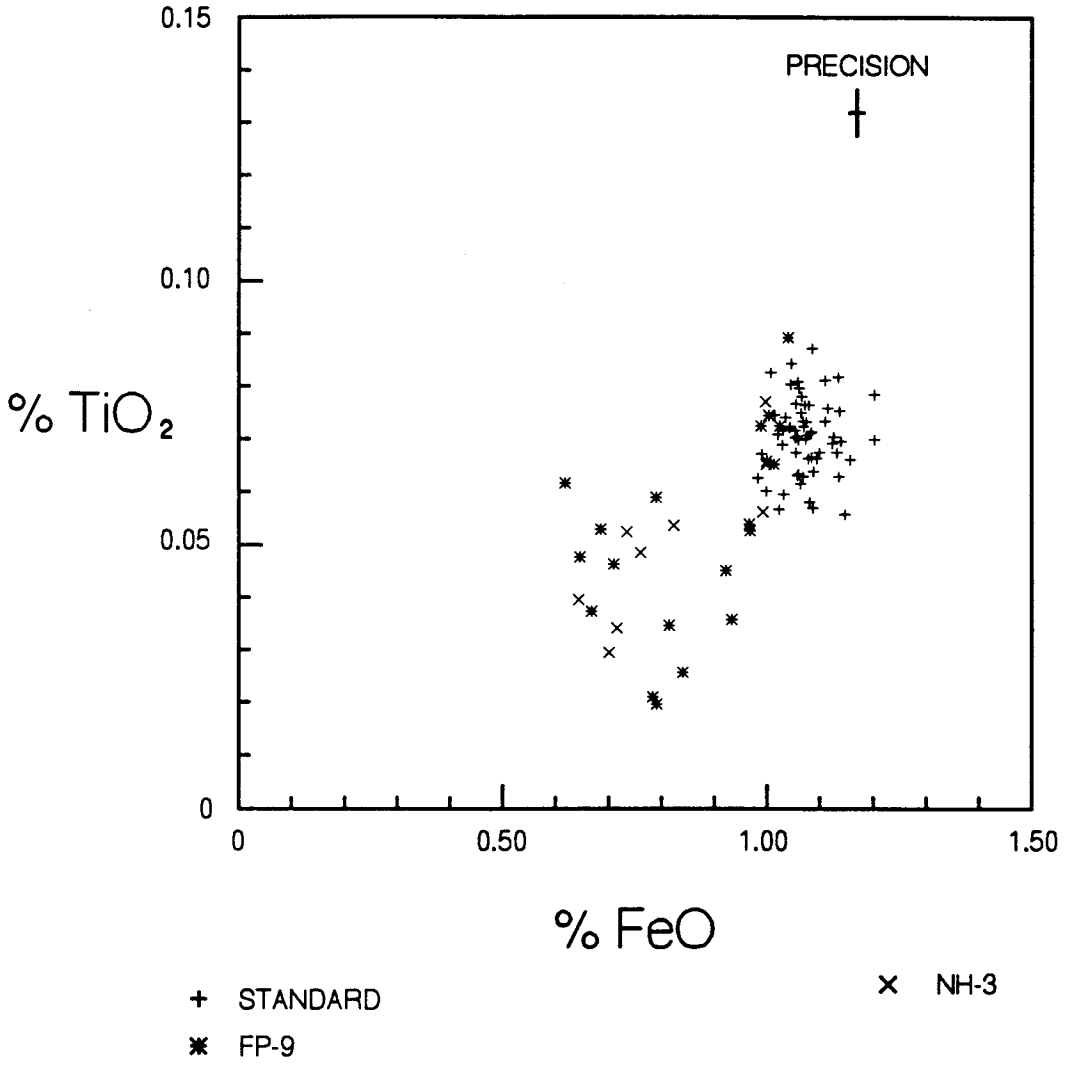

Figure 4.49. X-Y plot of wt % TiO_2 vs FeO. Symbols used are: pluses indicate the Yellowstone rhyolite standard; asterisks indicate bentonite FP-9; and X's indicate bentonite NH-3.

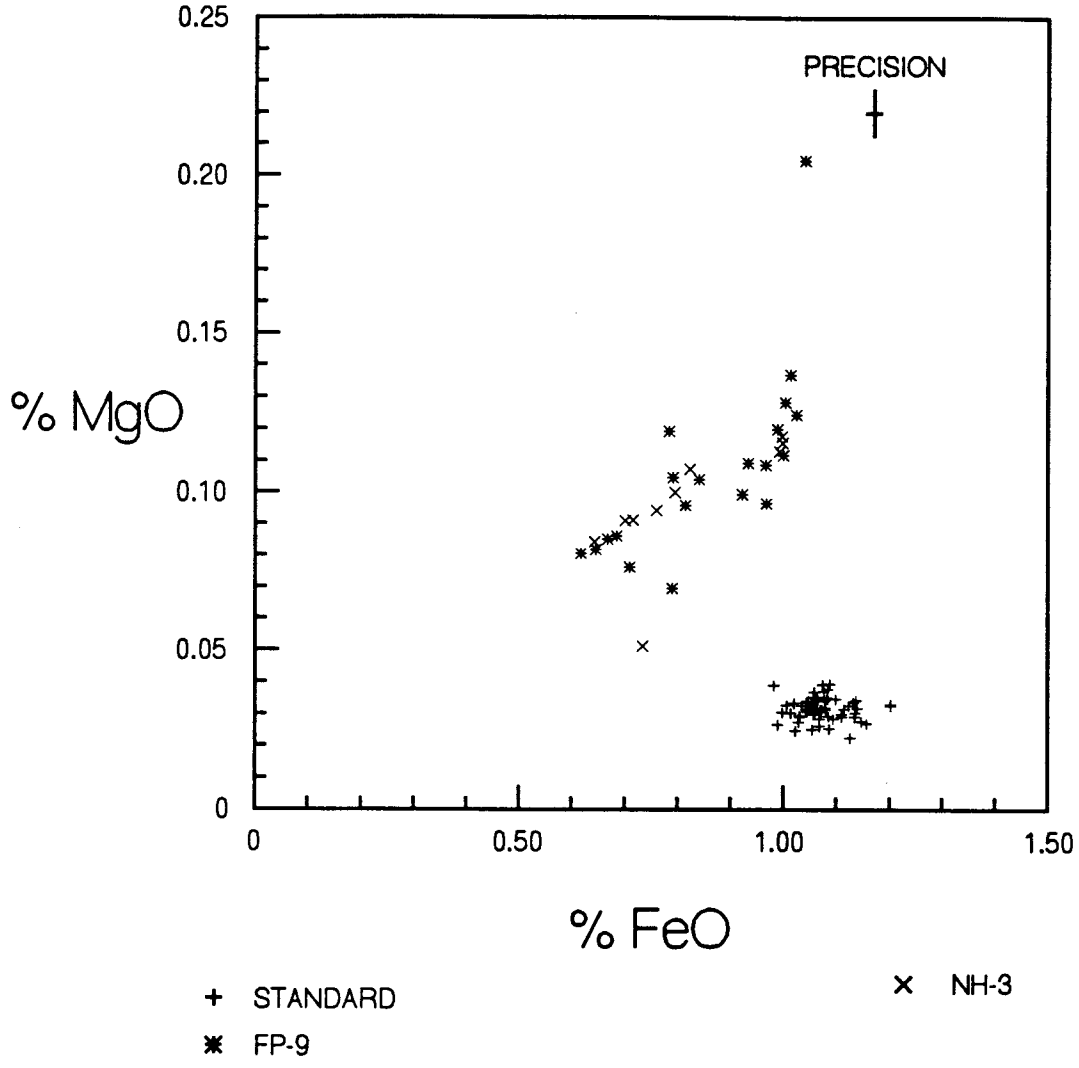

Figure 4.50. X-Y plot of wt % MgO vs FeO. Symbols used are: pluses indicate the Yellowstone rhyolite; asterisks indicate bentonite FP-9; and X's indicate bentonite NH-3.

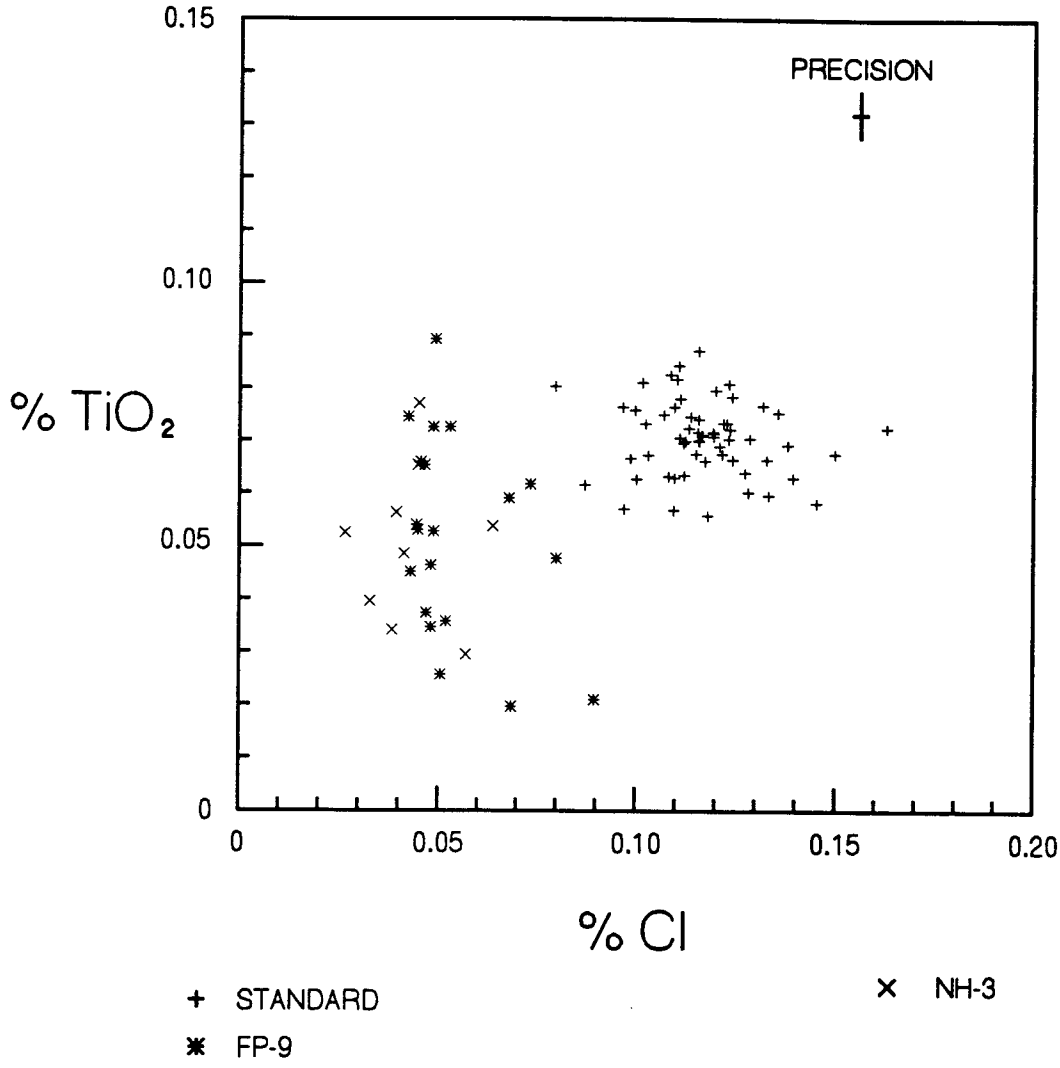

Figure 4.51. X-Y plot of wt % TiO_2 vs Cl. Symbols used are: pluses indicate the Yellowstone rhyolite standard; asterisks indicate bentonite FP-9; and X's indicate bentonite NH-3.

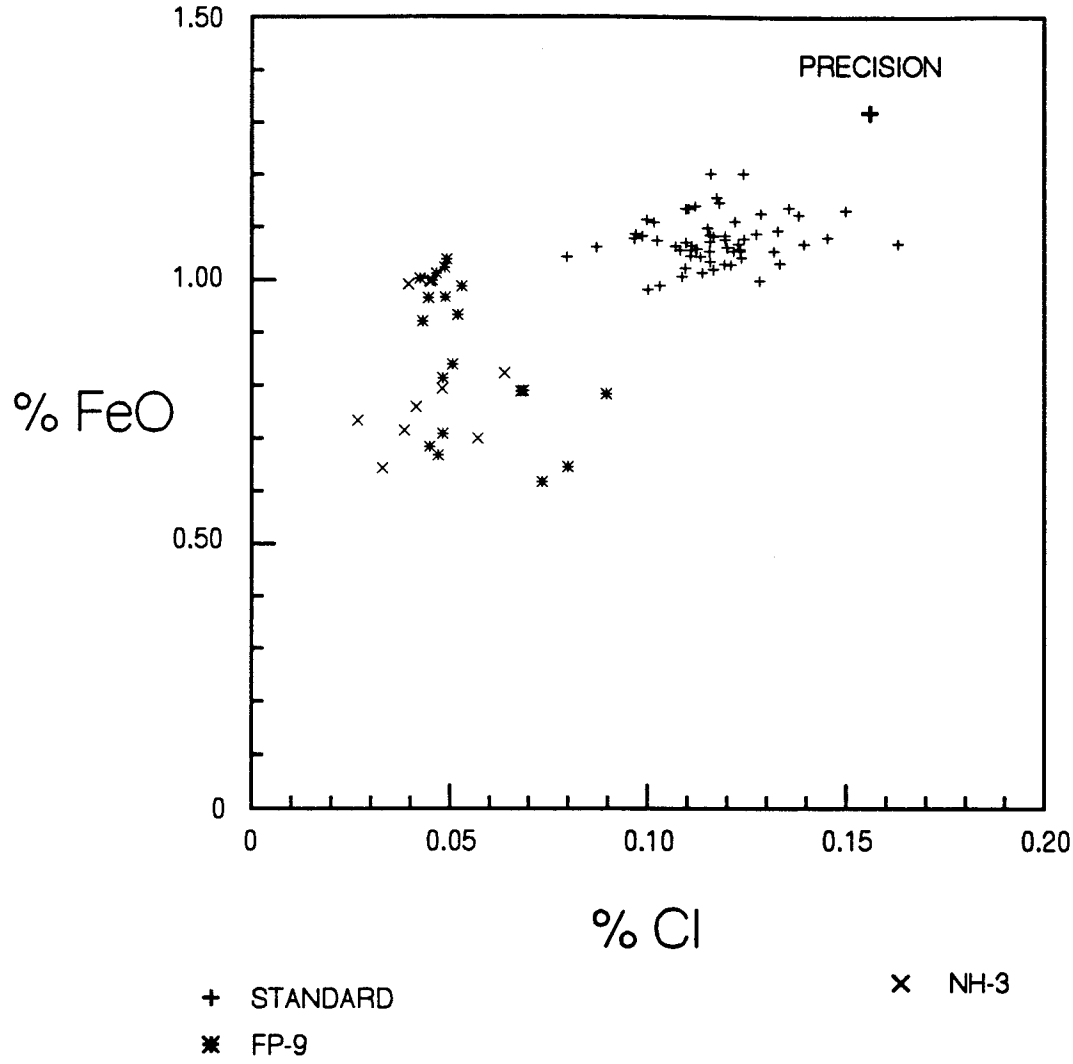

Figure 4.52. X-Y plot of wt % Feo vs Cl. Symbols used are: pluses indicate the Yellowstone rhyolite standard; asterisks indicate bentonite FP-9; and X's indicate bentonite NH-3.

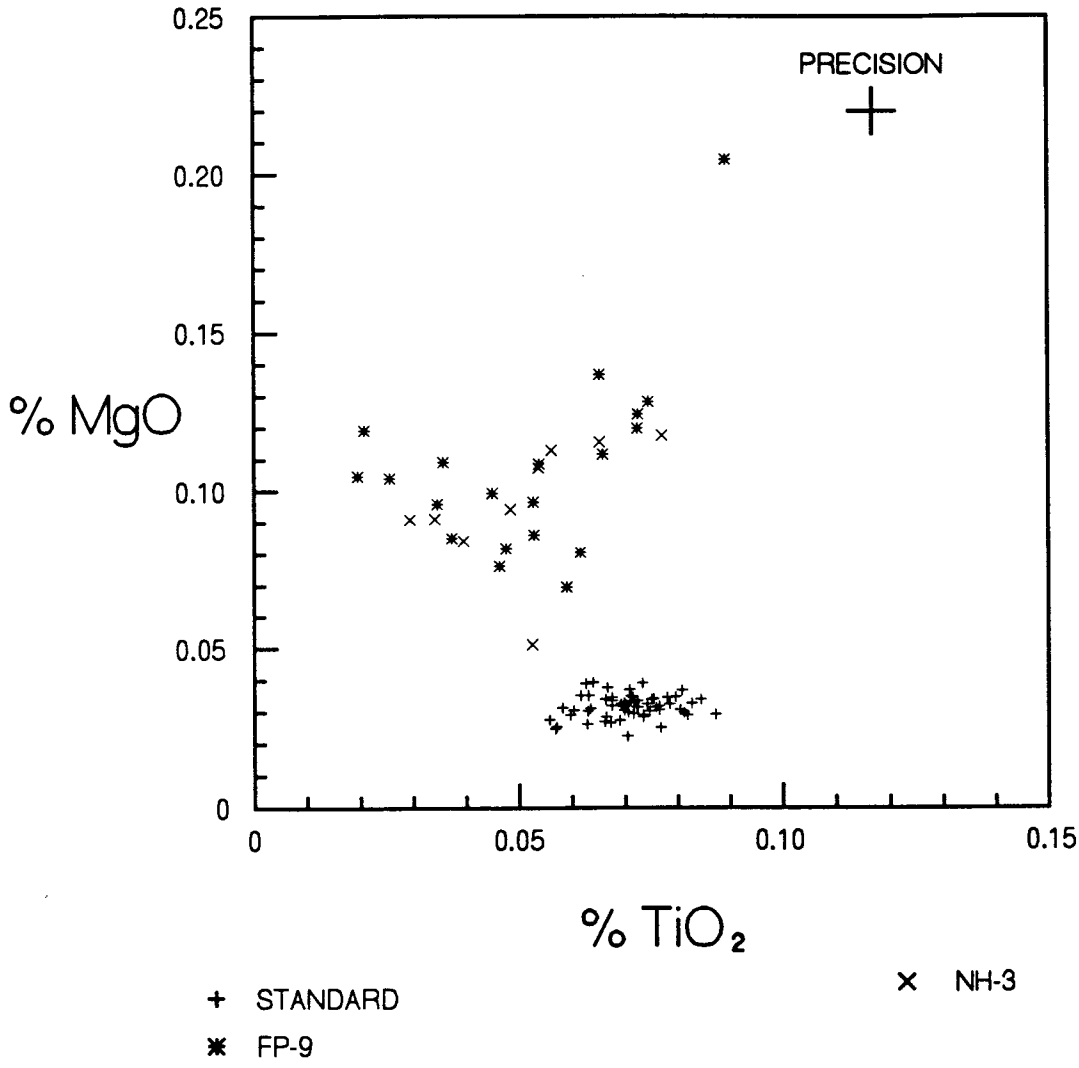

Figure 4.53. X-Y plot of wt % MgO vs TiO_2. Symbols used are: pluses indicate the Yellowstone rhyolite standard; asterisks indicate the bentonite FP-9; and X's indicate bentonite NH-3.

Midway, PA

The outcrop at Midway (41° 27′ 30"N, 77° 02′ 10"W) is an abandoned quarry located on the north side (westbound lane) of U.S. Route 322 1/8 mile before the Midway exit ramp (Figure 4.54). The author recognized five bentonites at this location (Figure 4.56) in contrast to the nine reported by Way et al. (1986, Figure 3.7).

All of the bentonites recognized at this location occur within the Selinsgrove limestone (Figures 4.55 and 4.56). They are dark gray in color and exist as a soft clay. The geochemical analyses of melt inclusions indicate that bentonite MW-1 correlates with bentonite FP-9 (Figure 4.65). This correlation is demonstrated by the ternary diagrams of Mg*10-Ti*10-Fe and Mg-Ti-Cl (Figure 4.57 and 4.58) and X-Y plots of MgO vs Cl, TiO_2 vs FeO, MgO vs FeO, TiO_2 vs Cl, FeO vs Cl, and MgO vs TiO_2 (Figures 4.58 - 4.64).

Whereas the bentonites at these two localities (i.e., Newton Hamilton and Midway) occur within the Selinsgrove limestone member, the equivalent bentonite at Frankstown, PA (i.e., FP-9) occurs within the Marcellus shale formation. This implies that between Midway and Frankstown this bentonite crosses a facies change. This implies that the sediment source for the Marcellus shale was transported along strike vice across strike (i.e, from the north or the south vice from the east) or may be craton derived (i.e., from the west).

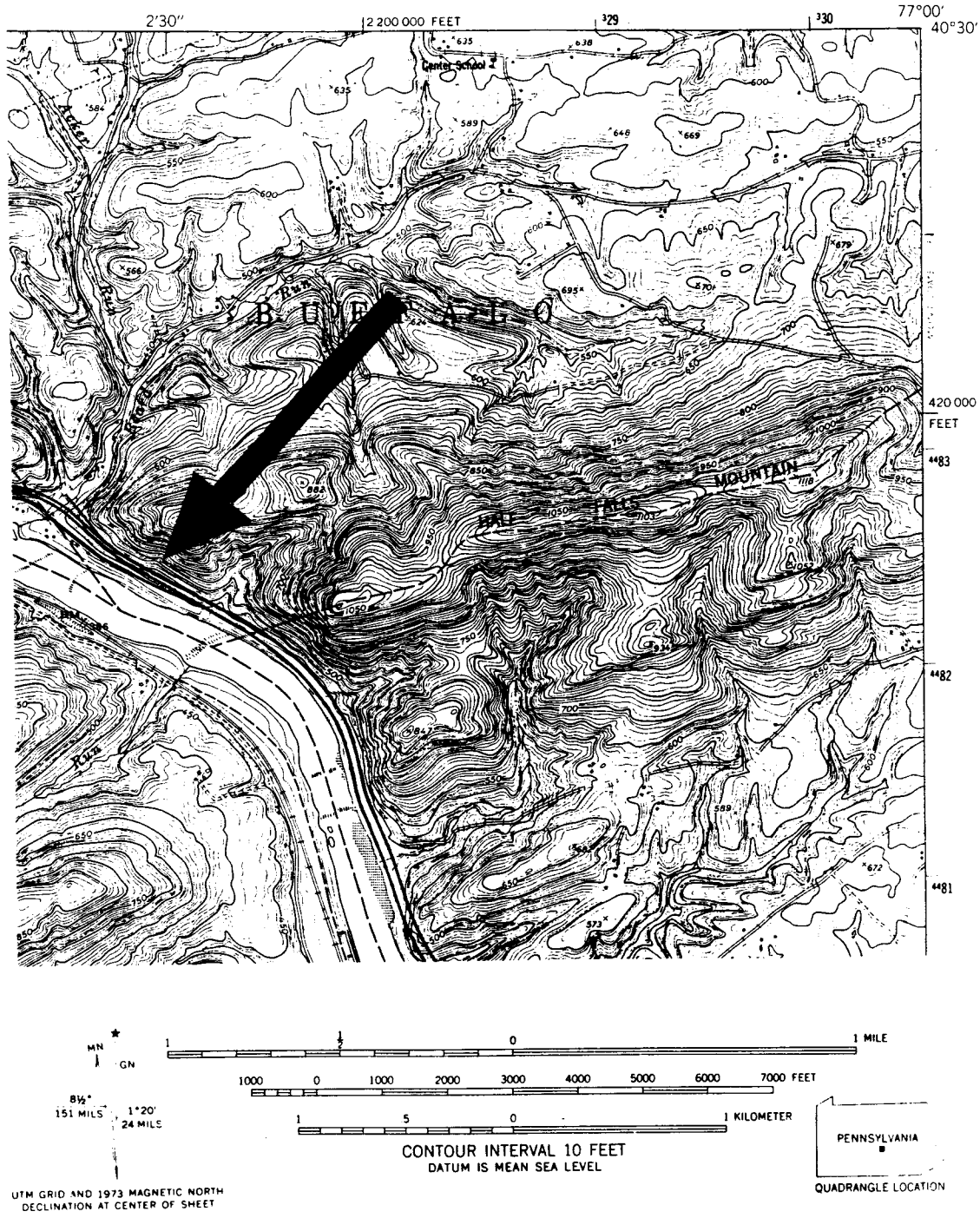

Figure 4.54. 7.5 minute quadrangle map of Duncannon, PA showing the location of the Midway outcrop.

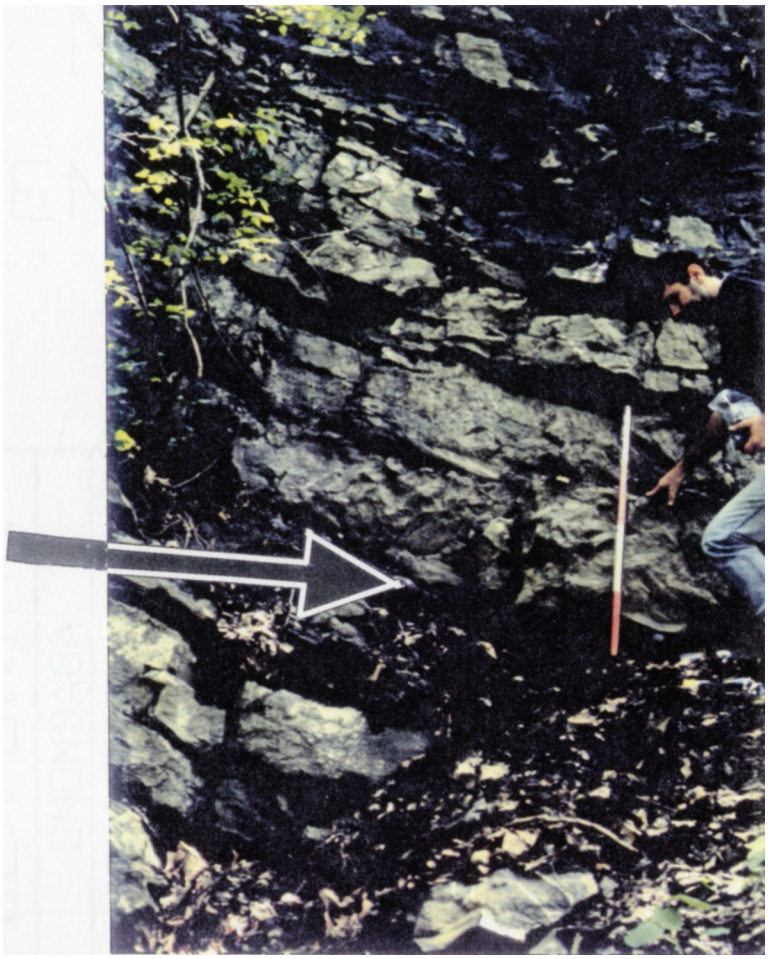

Figure 4.55. Photograph of the outcrop at Midway, PA. Note the arrow indicating bentonite MW-1. The scale bar is in feet.

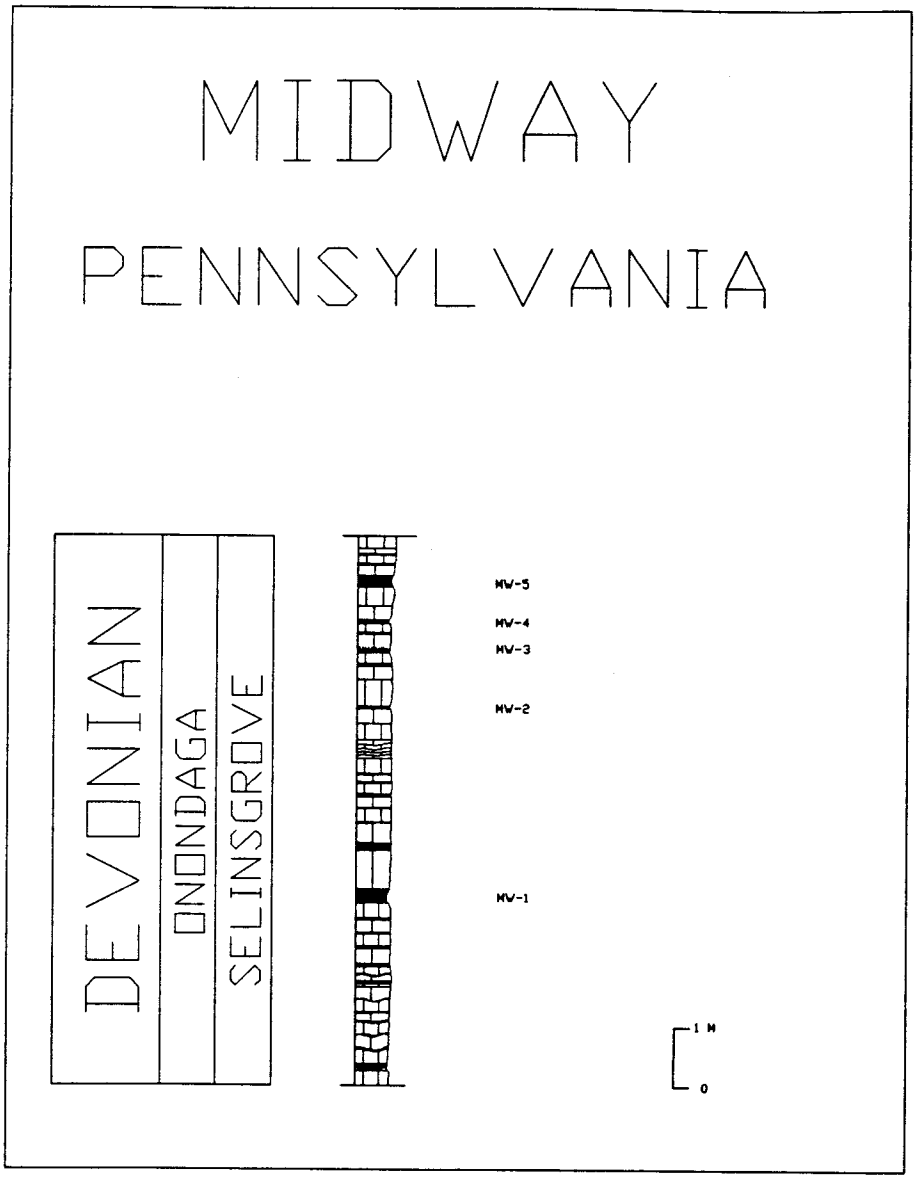

Figure 4.56. Stratigraphic column of the outcrop at Midway, PA constructed by this investigator.

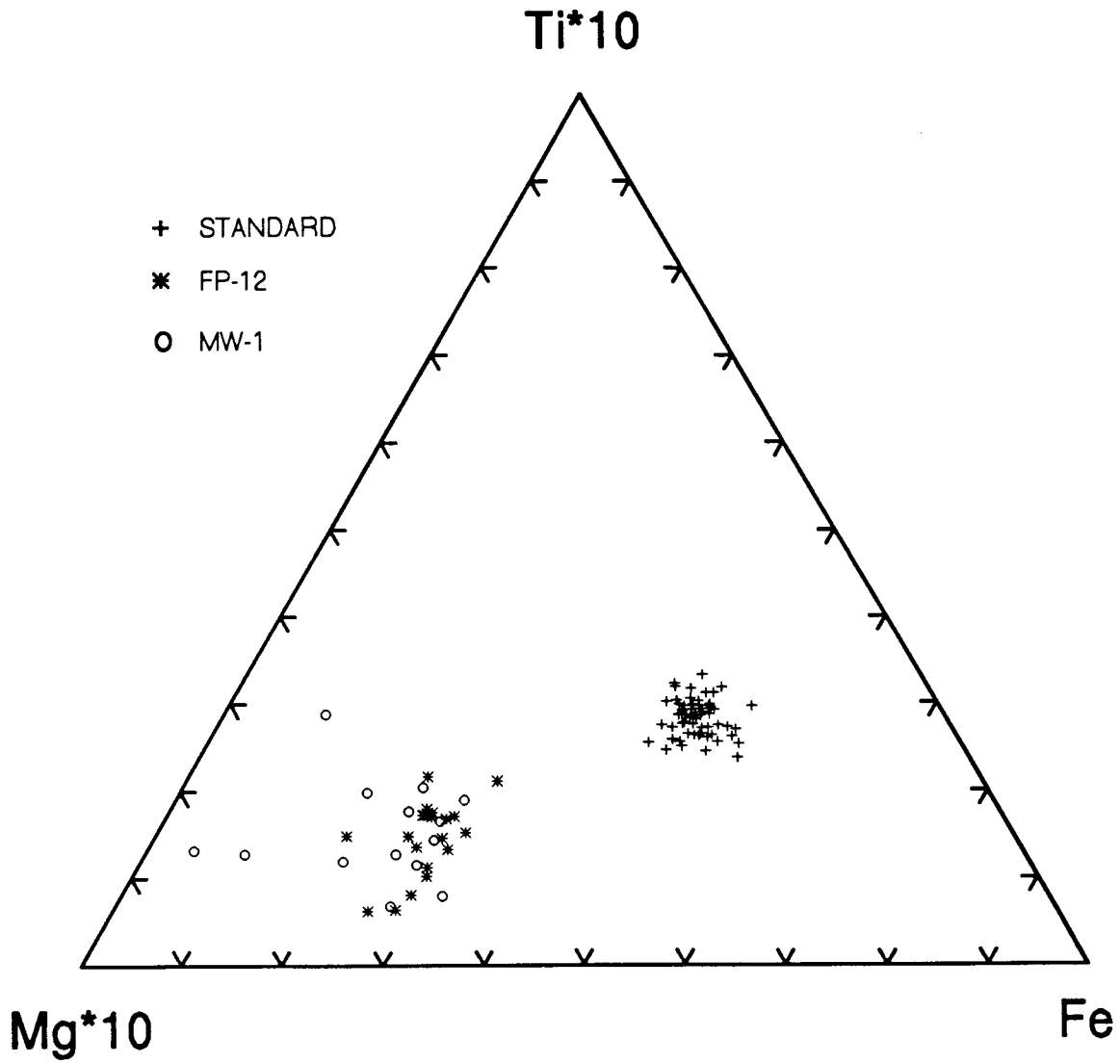

Figure 4.57. Ternary diagram of Mg*10-Ti*10-Fe. Symbols used are: pluses indicate the Yellowstone rhyolite standard; asterisks indicate the bentonite FP-9; and circles indicate the bentonite MW-1.

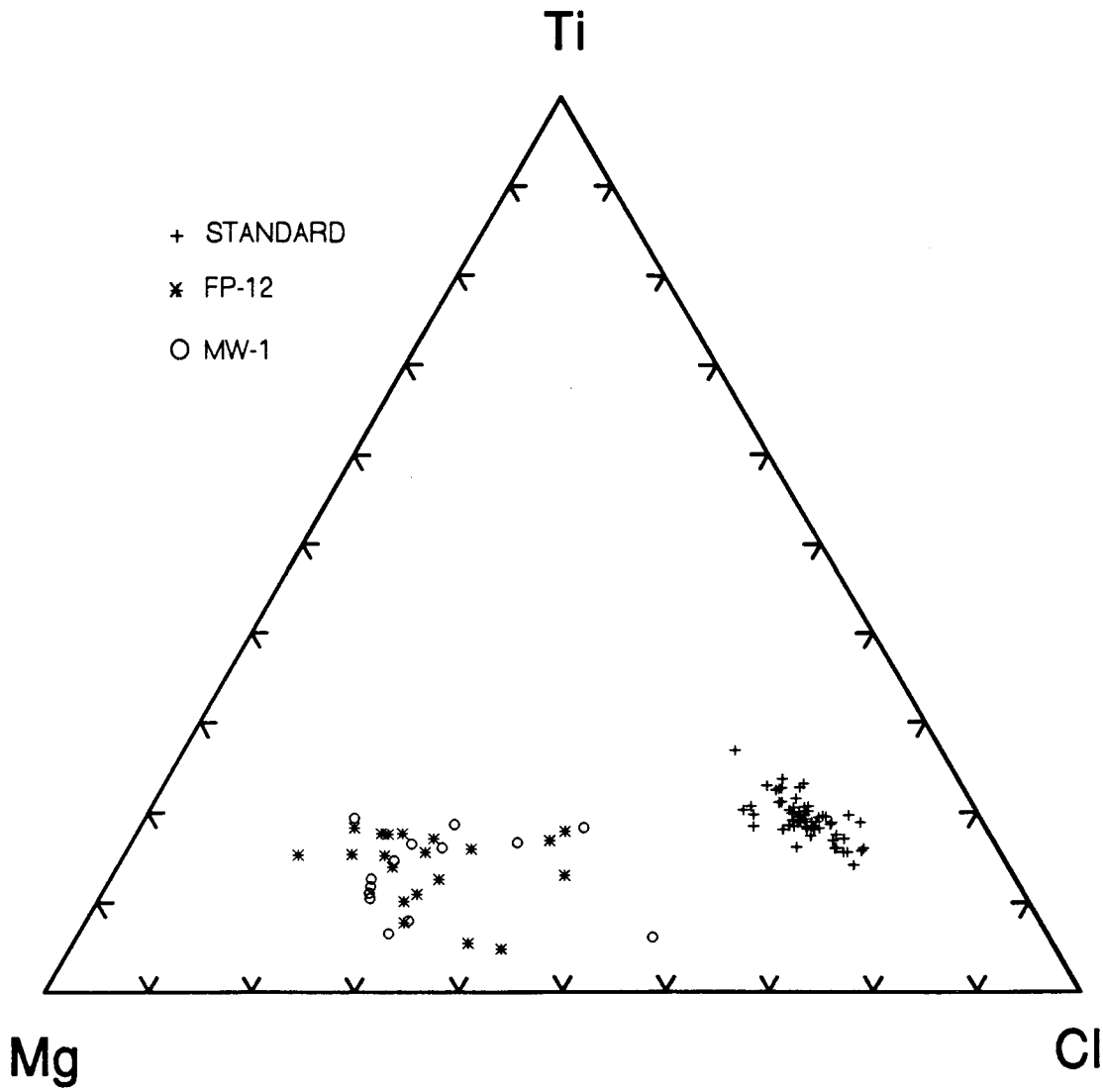

Figure 4.58. Ternary diagram of Mg-Ti-Cl. Symbols used are: pluses indicate the Yellowstone rhyolite standard; asterisks indicate bentonite FP-9; and circles indicate bentonite MW-1.

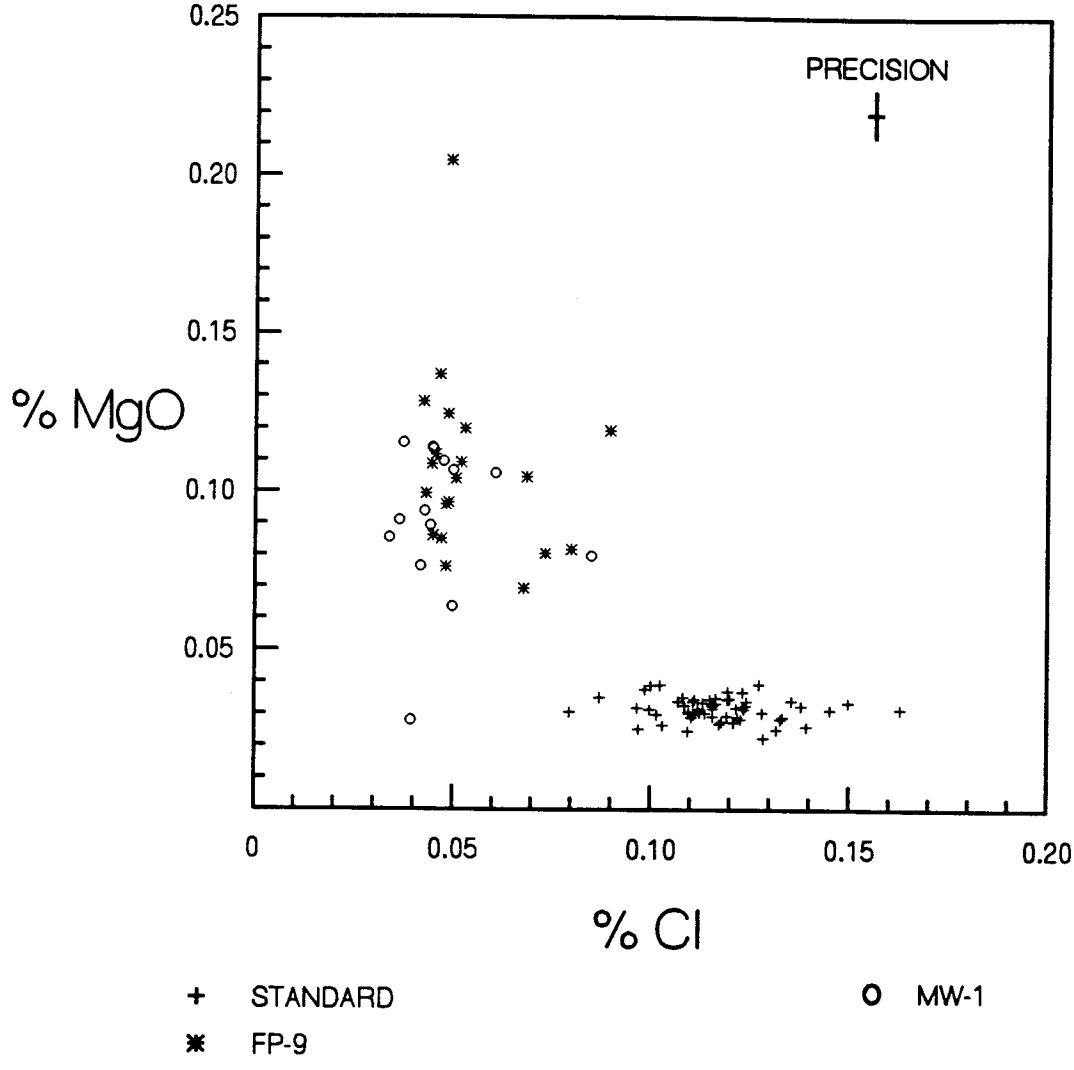

Figure 4.59. X-Y plot of wt % Mgo vs Cl. Symbols used are: pluses indicate the Yellowstone rhyolite standard; asterisks indicate bentonite FP-9; and circles indicate bentonite MW-1.

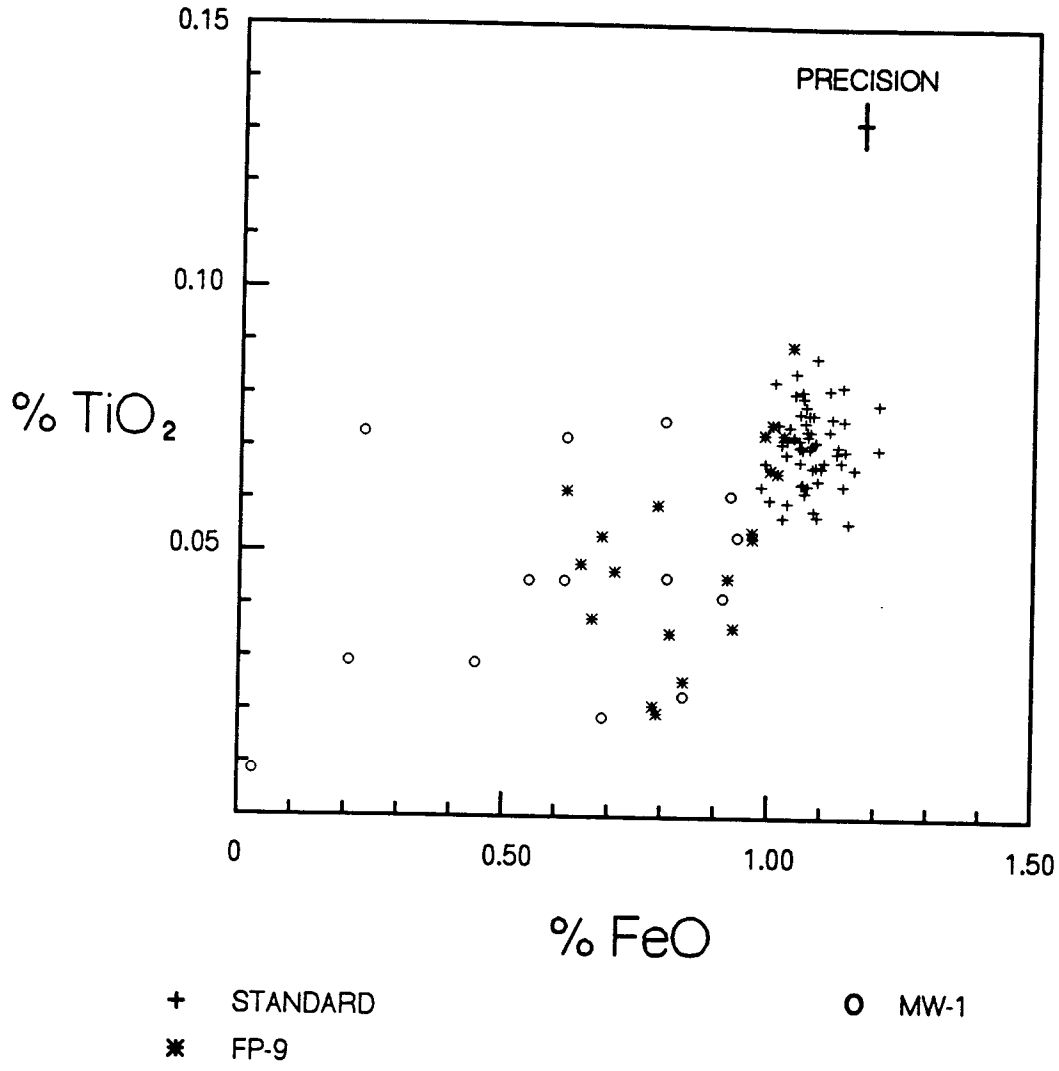

Figure 4.60. X-Y plot of wt % TiO_2 vs FeO. Symbols used are: pluses indicate the Yellowstone rhyolite standard; asterisks indicate bentonite FP-9; and circles indicate bentonite MW-1.

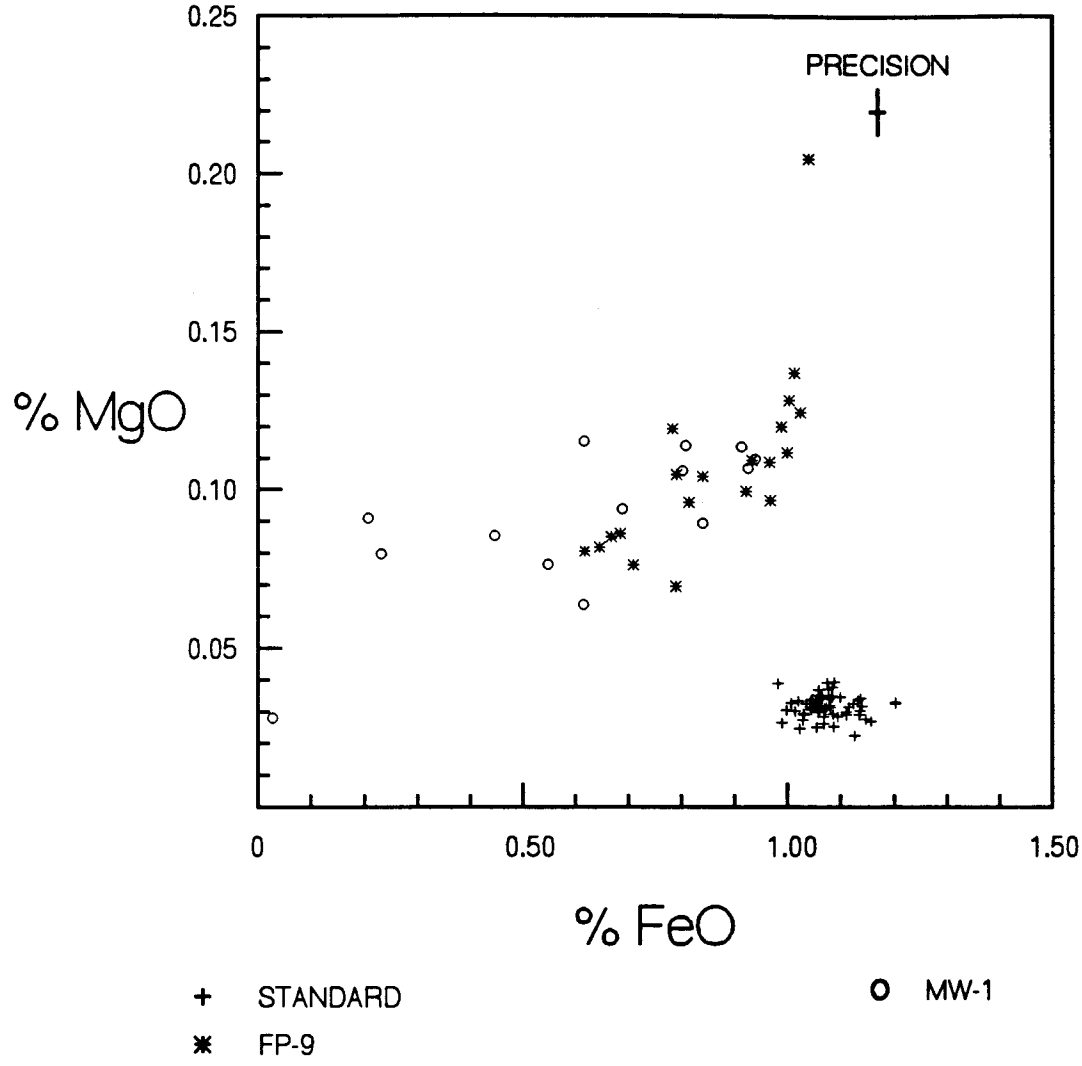

Figure 4.61. X-Y plot of wt % MgO vs FeO. Symbols used are: pluses indicate the Yellowstone rhyolite standard; asterisks indicate bentonite FP-9; and circles indicate bentonite MW-1.

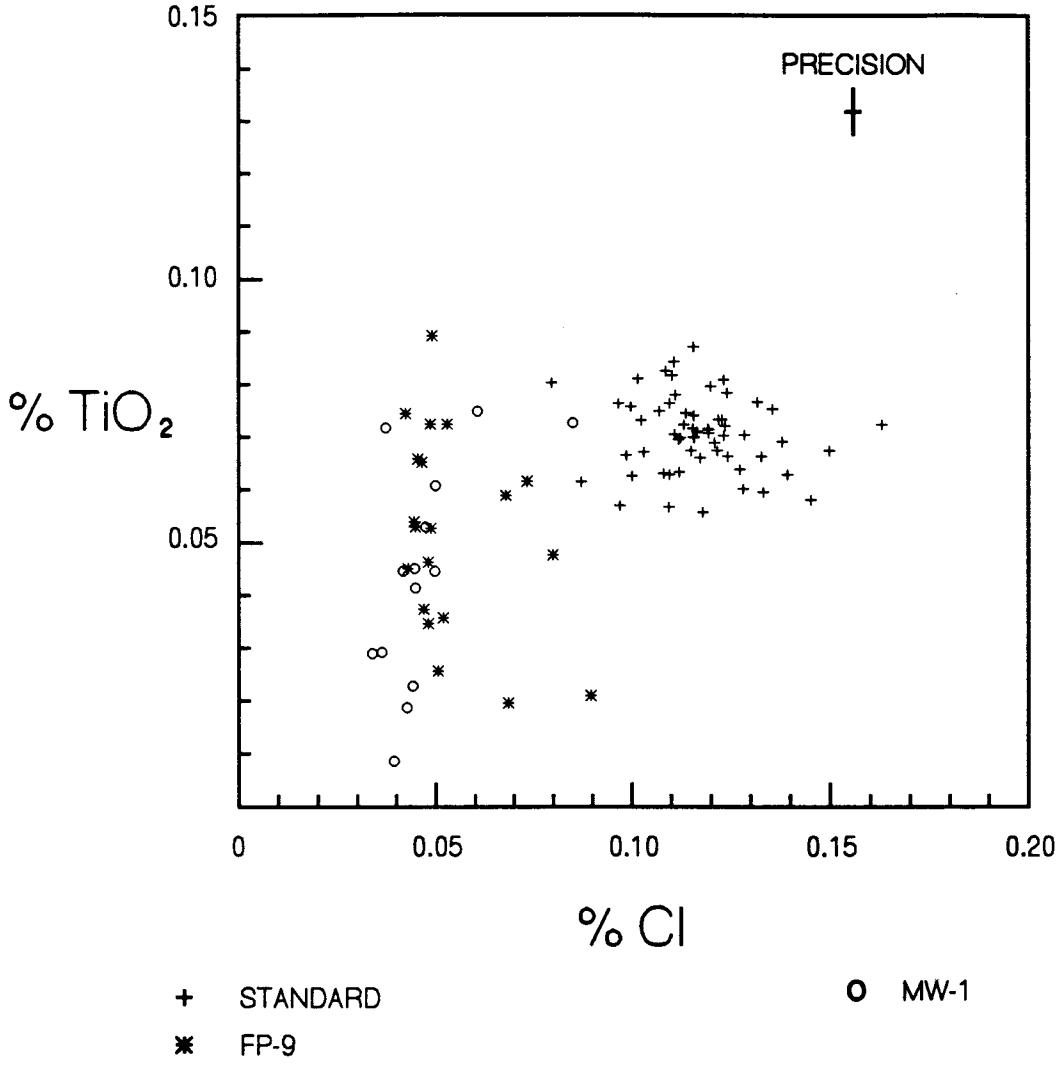

Figure 4.62. X-Y plot of wt % TiO_2 vs Cl. Symbols used are: pluses indicate the Yellowstone rhyolite standard; asterisks indicate bentonite FP-9; and circles indicate bentonite MW-1.

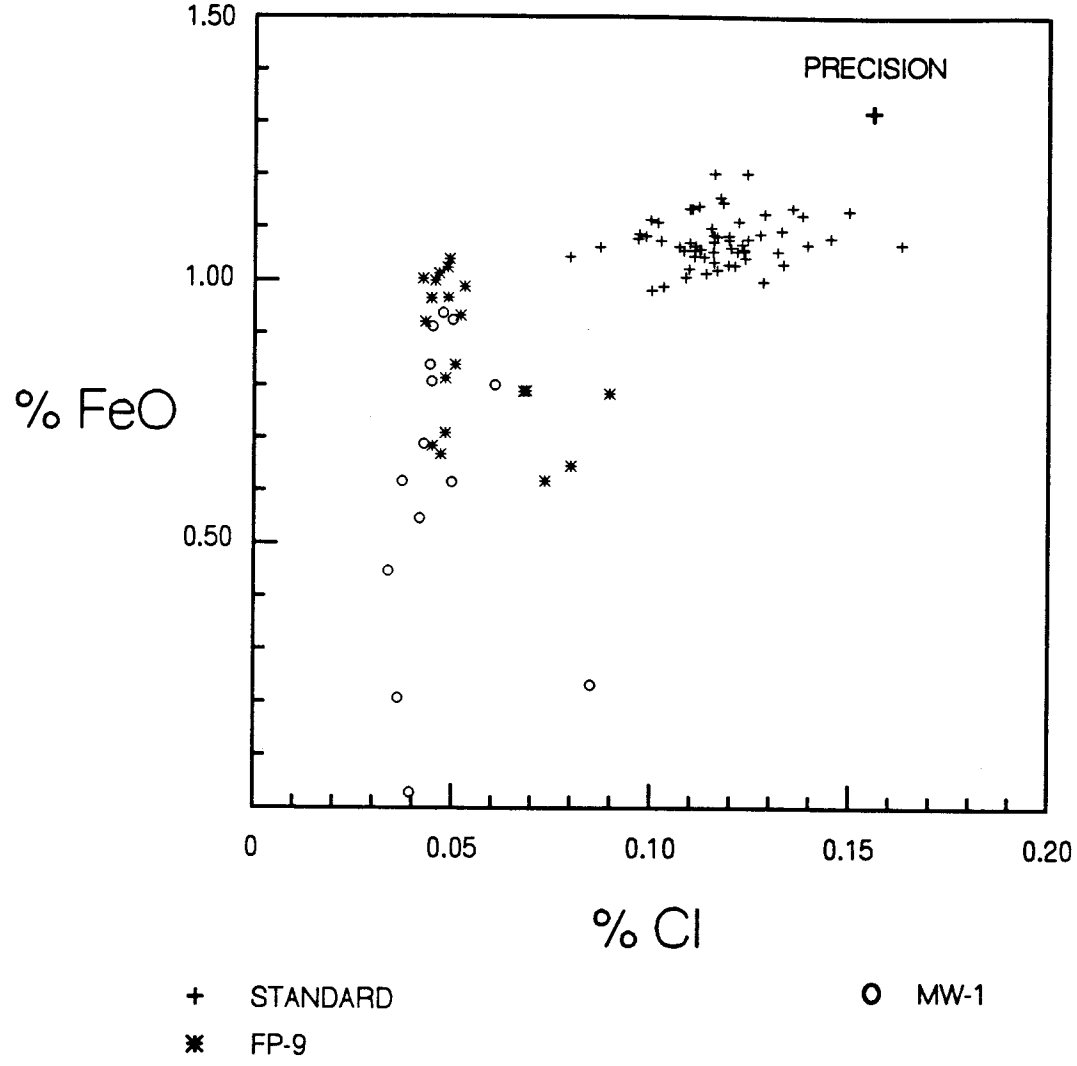

Figure 4.63. X-Y plot of wt % FeO vs Cl. Symbols used are: pluses indicate the Yellowstone rhyolite standard; asterisks indicate bentonite FP-9; and circles indicate bentonite MW-1.

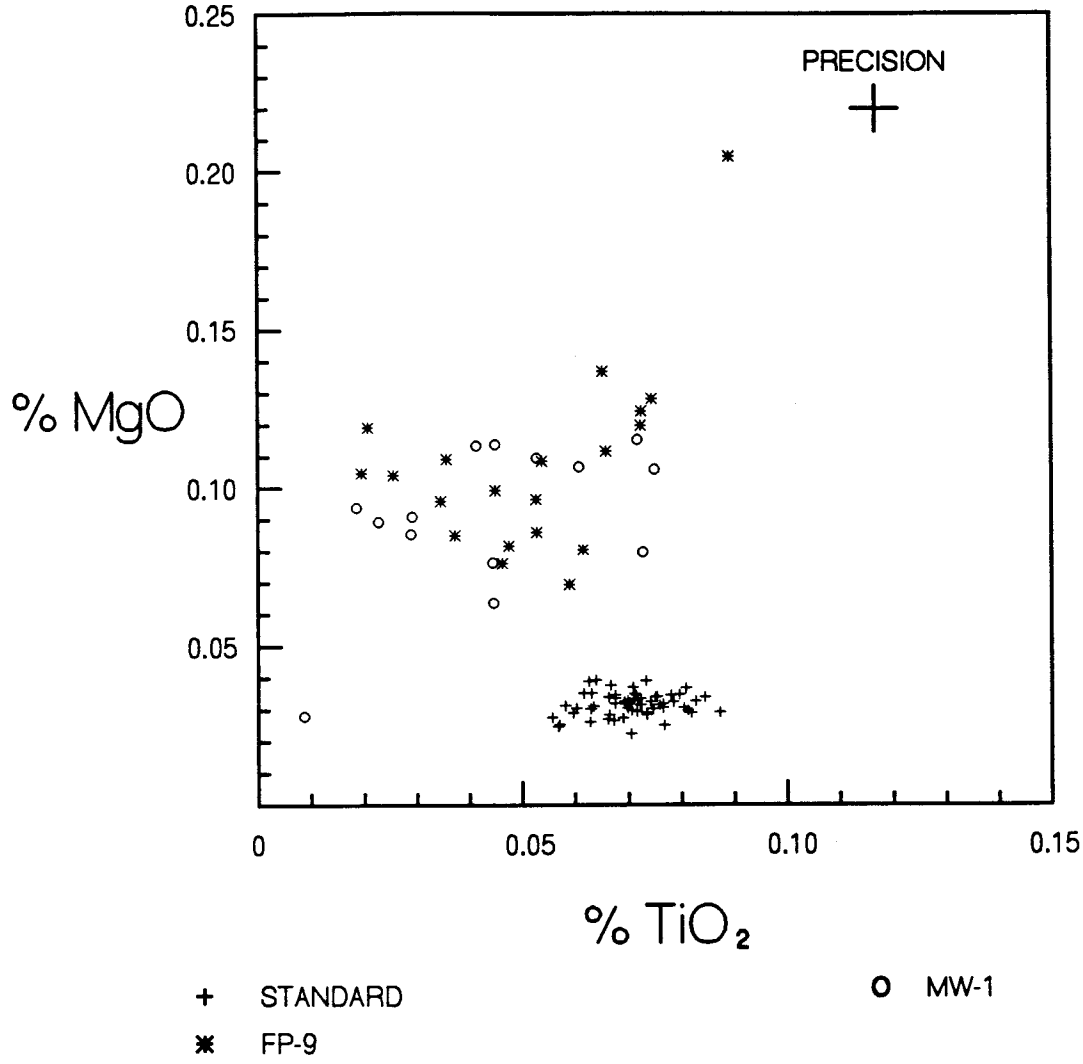

Figure 4.64. X-Y plot of wt % MgO vs TiO_2. Symbols used are: pluses indicate the Yellowstone rhyolite standard; asterisks indicate bentonite FP-9; and circles indicate bentonite MW-1.

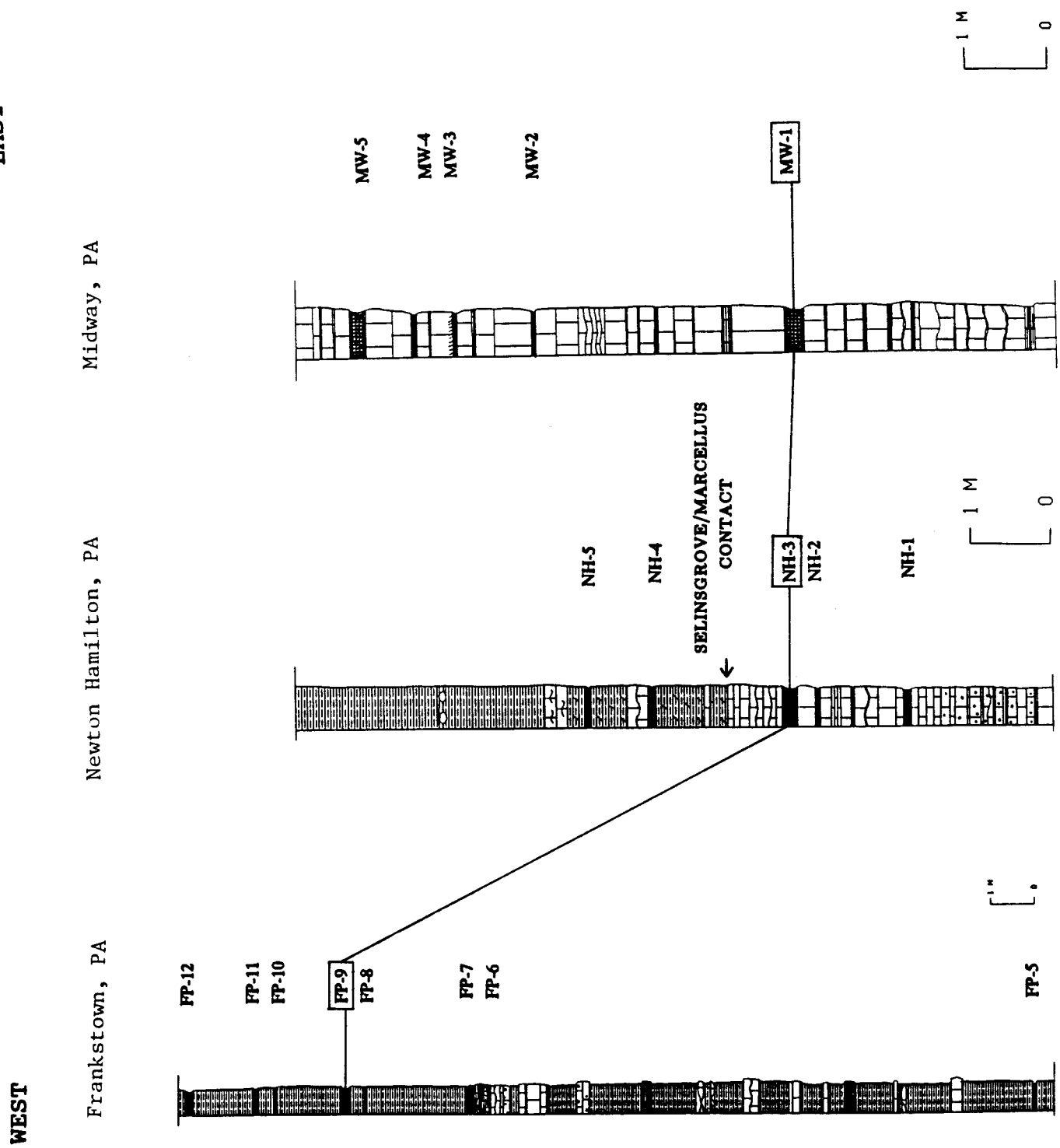

Figure 4.65. Stratigraphic columns of Frankstown. PA, Newton Hamilton, PA, and Midway, PA. Bentonites that geochemically correlate are connected with a solid line.

4.3 TEN OTHER LOCALITIES

Of the ten other localities sampled, only one locality contained a bentonite layer that has melt inclusion bearing quartz phenocrysts (Table 4.1). This locality is the General Crushed Stone quarry in Jamesville, NY (Figure 3.1). Only two quartz phenocrysts containing melt inclusions were found in the bentonite JV-1 from this locality. This bentonite occurs within the Onondaga limestone at the contact of the Moorehouse and Seneca members (Figure 4.69). The data from the geochemical analyses of these two melt inclusions suggest that this bentonite is equivalent to bentonite FP-9. This is indicated by the ternary diagrams of Mg*10-Ti*10-Fe and Mg-Ti-Cl (Figures 4.70 and 4.71) along with X-Y plots of MgO vs Cl, TiO_2 vs FeO, MgO vs FeO, TiO_2 vs Cl, FeO vs Cl, and MgO vs TiO_2 (Figures 4.72 - 4.77). The Cl to F ratios from apatite phenocrysts at this locality compared with those from bentonite NH-3 (Roden, 1989) also support this correlation. Although this data is suggestive that bentonite JV-1 correlates to bentonite FP-9, more work is required to confirm this.

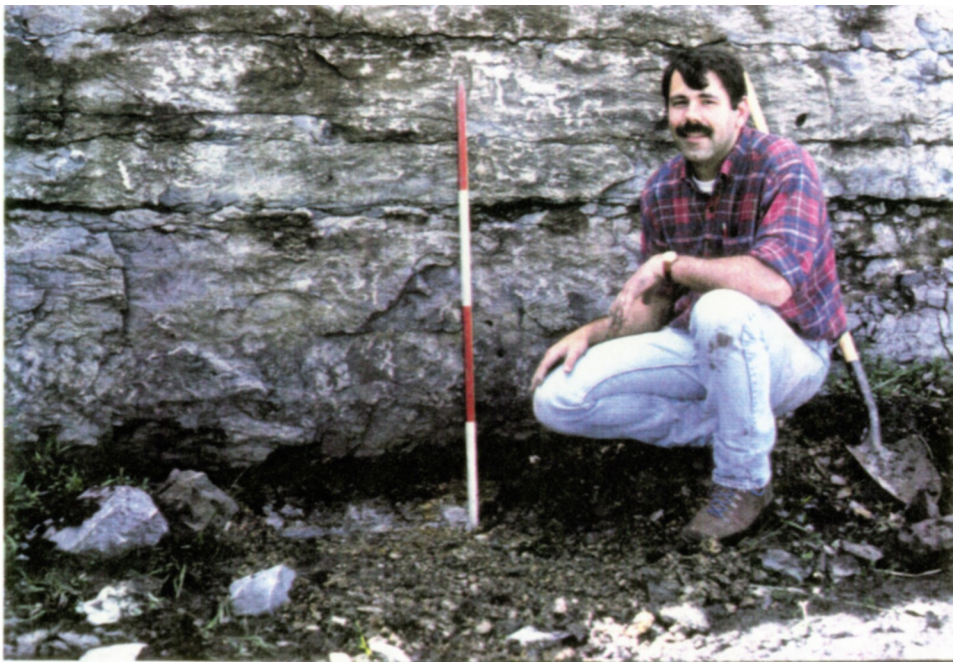

Figure 4.66. Photograph of bentonite JV-1 at the Jamesville locality. The markings on the scale bar are in feet.

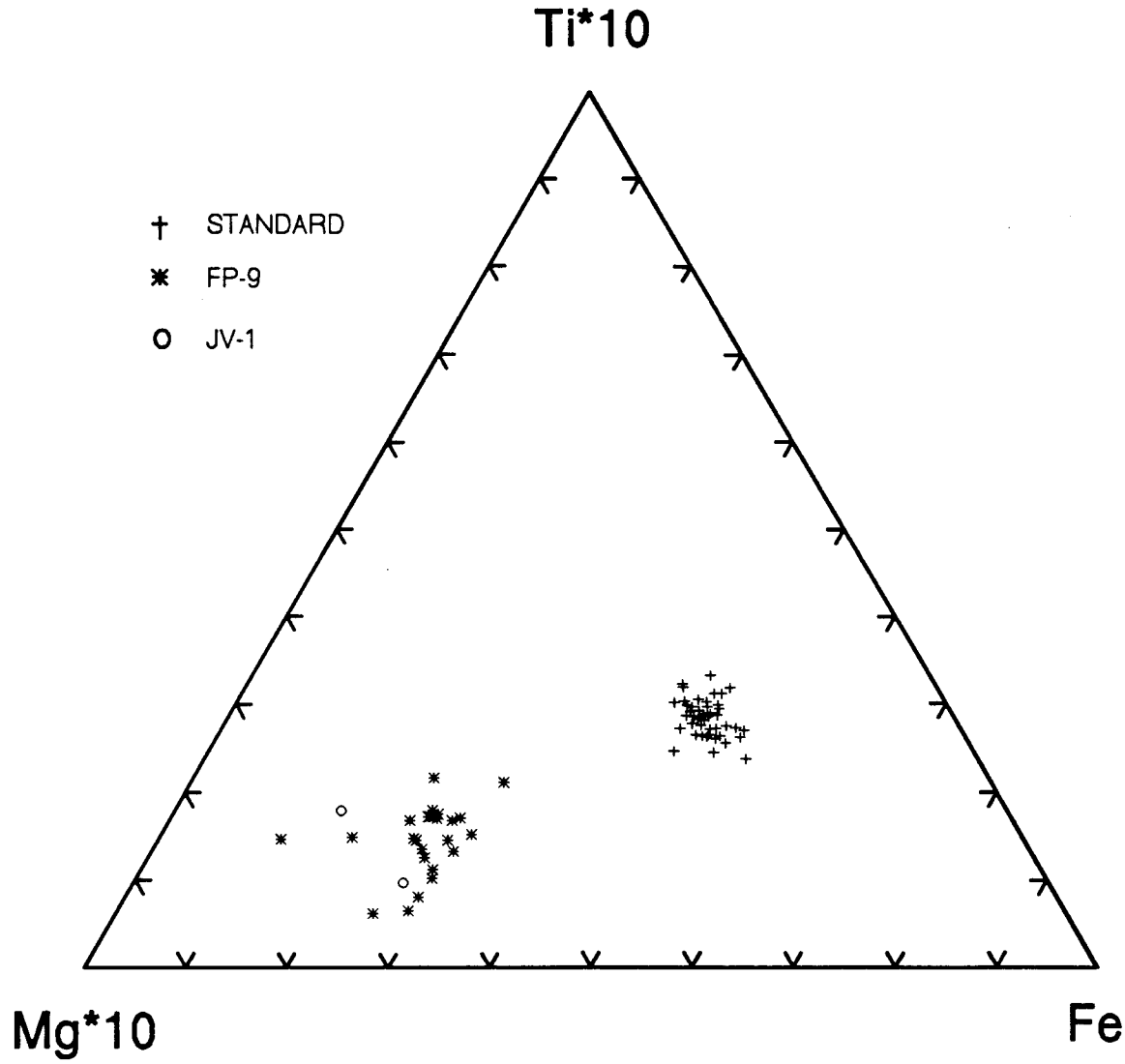

Figure 4.67. Ternary diagram of Mg*10-Ti*10-Fe. Symbols used are: pluses indicate the Yellowstone rhyolite standard; asterisks indicate bentonite FP-9; and circles indicate bentonite JV-1.

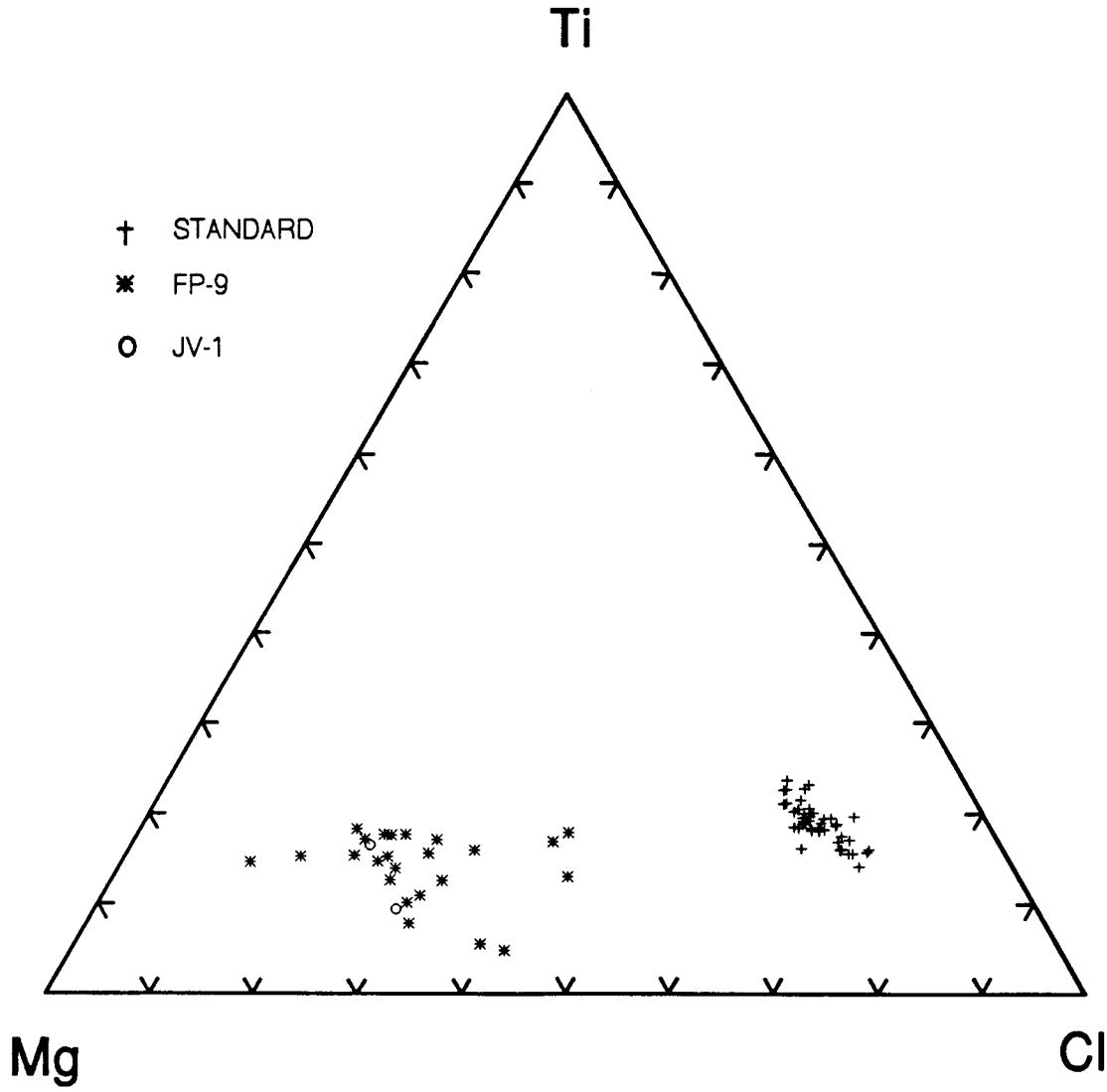

Figure 4.68. Ternary diagram of Mg-Ti-Cl. Symbols used are: pluses indicate the Yellowstone rhyolite standard; asterisks indicate bentonite FP-9; and circles indicate bentonite JV-1.

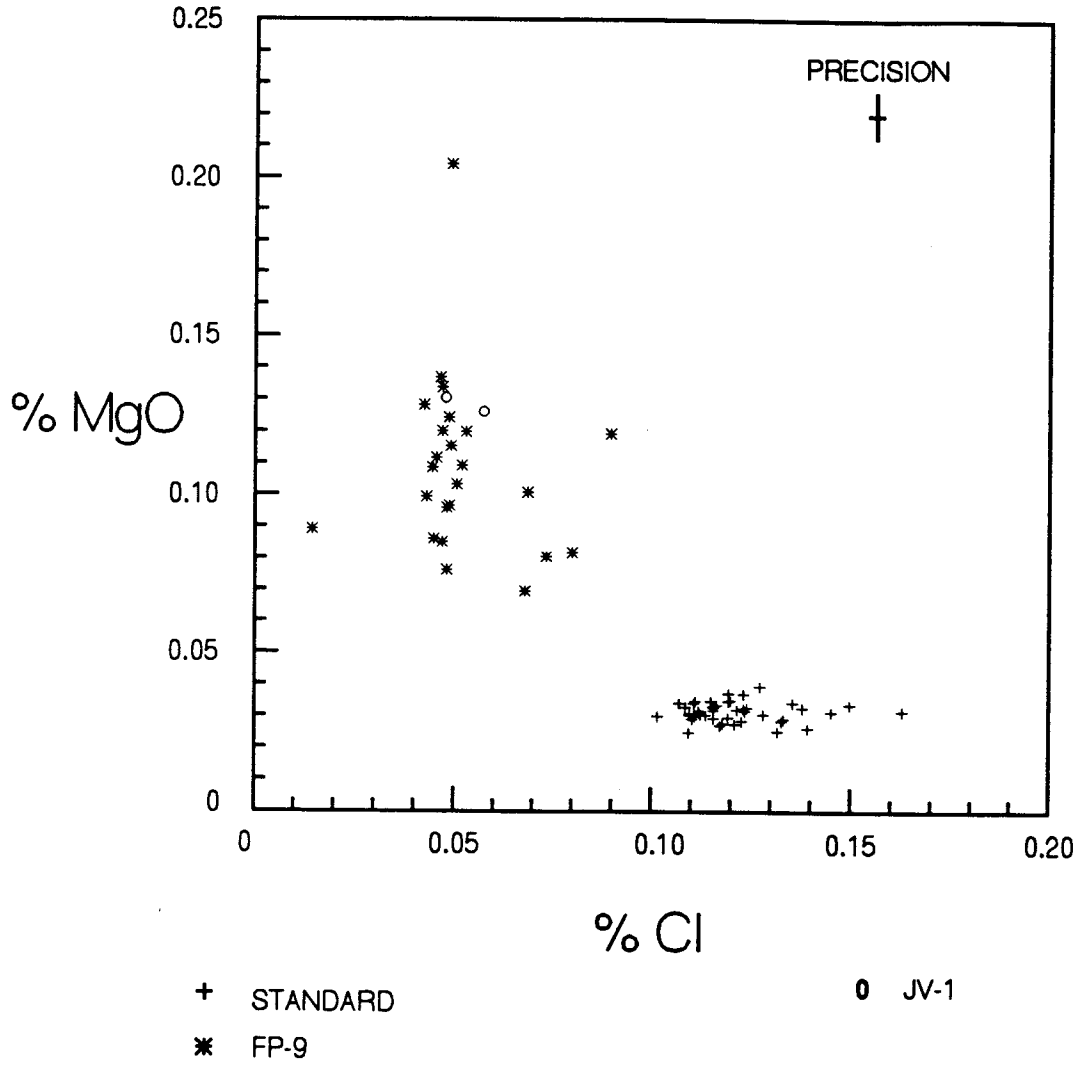

Figure 4.69. X-Y plot of wt % MgO vs Cl. Symbols used are: pluses indicate the Yellowstone rhyolite standard; asterisks indicate bentonite FP-9; and circles indicate bentonite JV-1.

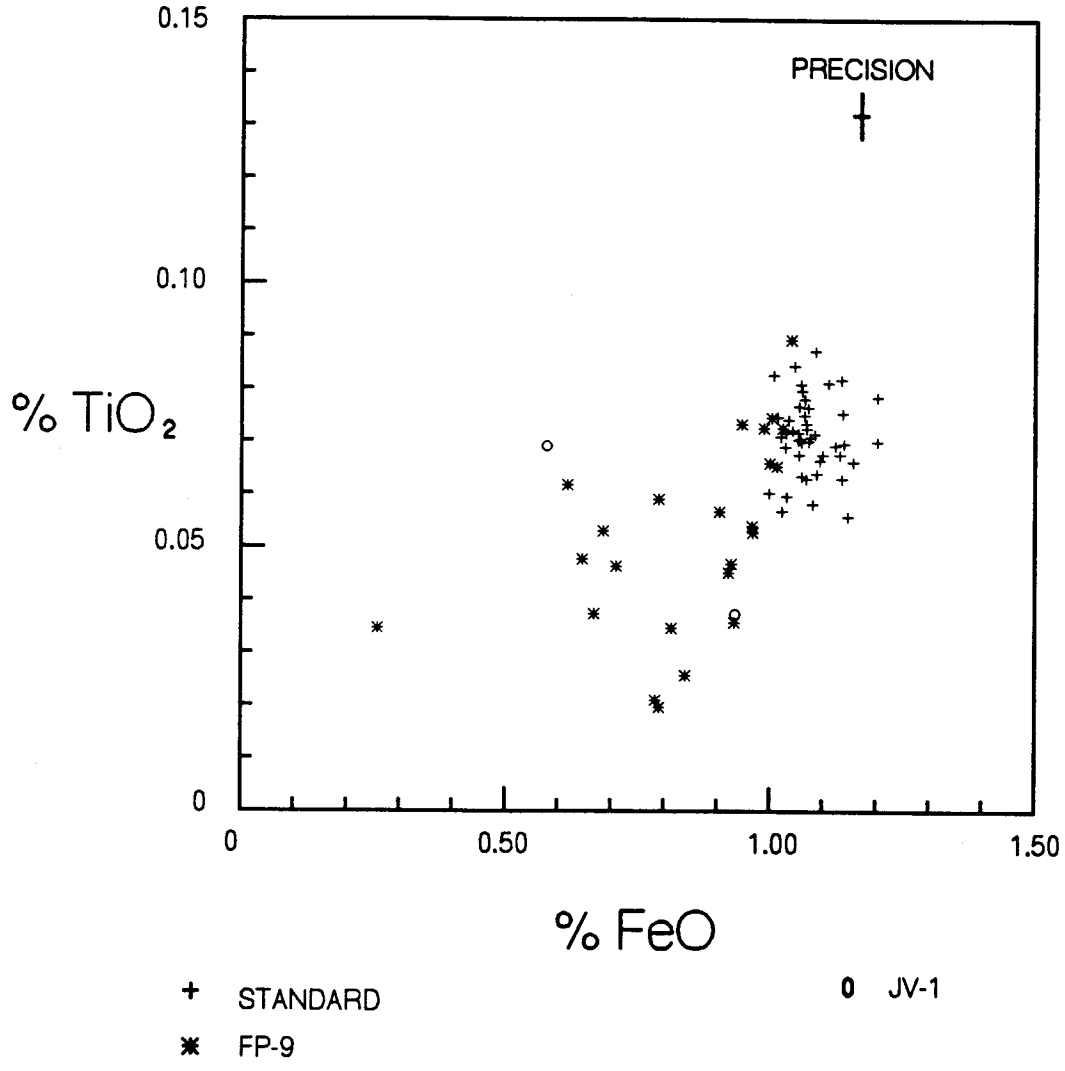

Figure 4.70. X-Y plot of wt % TiO_2 vs FeO. Symbols used are: pluses indicate the Yellowstone rhyolite standard; asterisks indicate bentonite FP-9; and circles indicate bentonite JV-1.

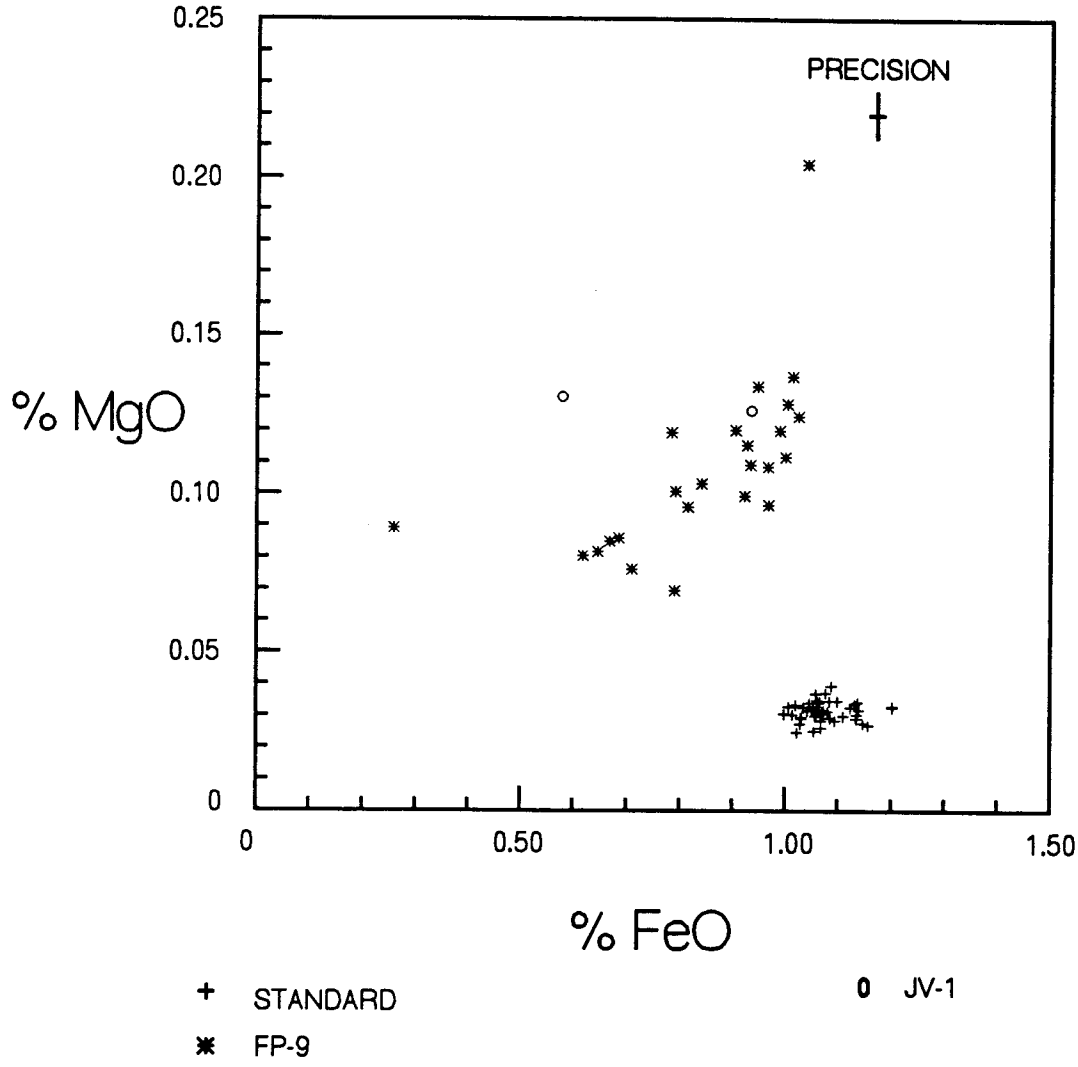

Figure 4.71. X-Y plot of wt % MgO FeO. Symbols used are: pluses indicate the Yellowstone rhyolite standard; asterisks indicate bentonite FP-9; and circles indicate bentonite JV-1.

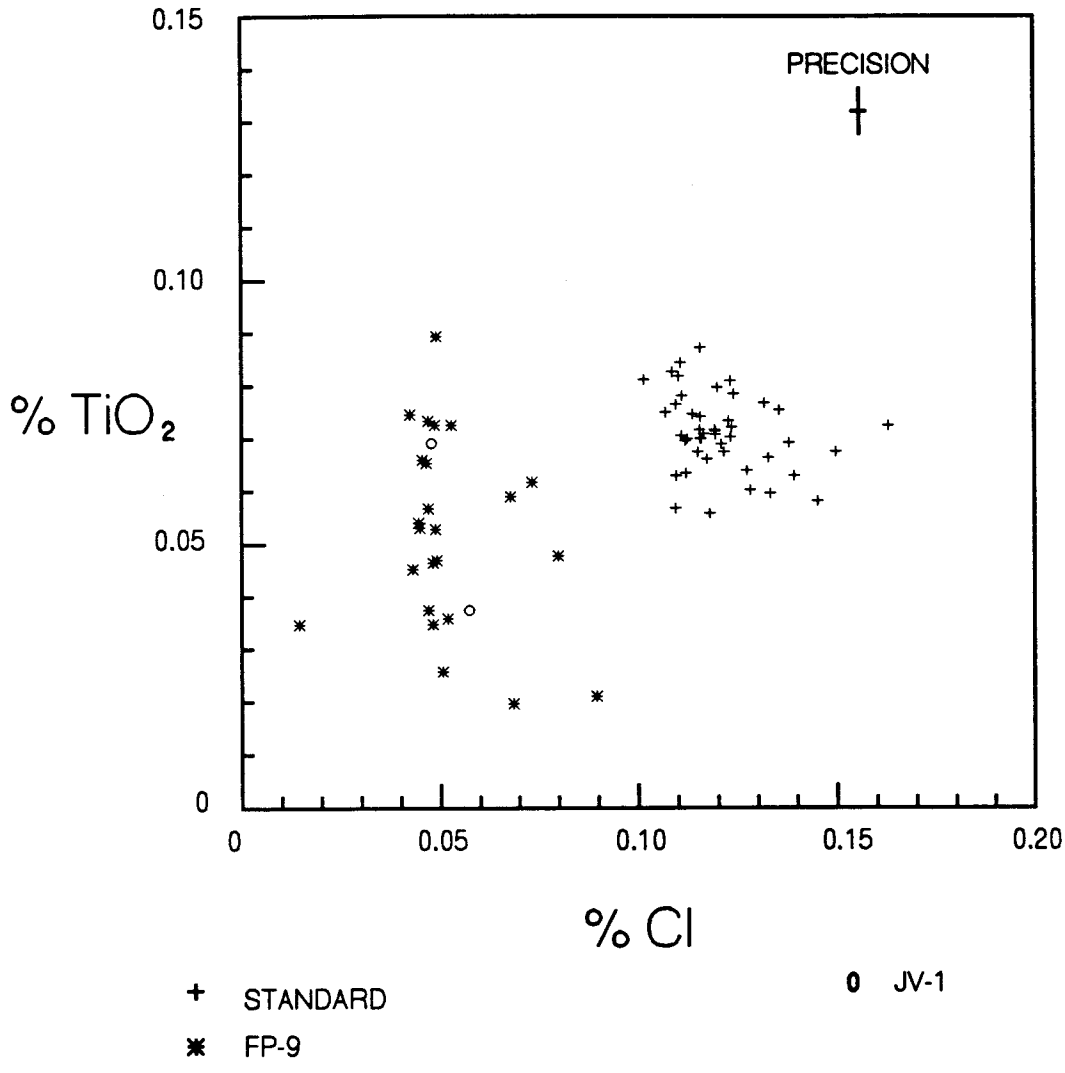

Figure 4.72. X-Y plot of wt % TiO_2 vs Cl. Symbols used are: pluses indicate the Yellowstone rhyolite standard; asterisks indicate bentonite FP-9; and circles indicate bentonite JV-1.

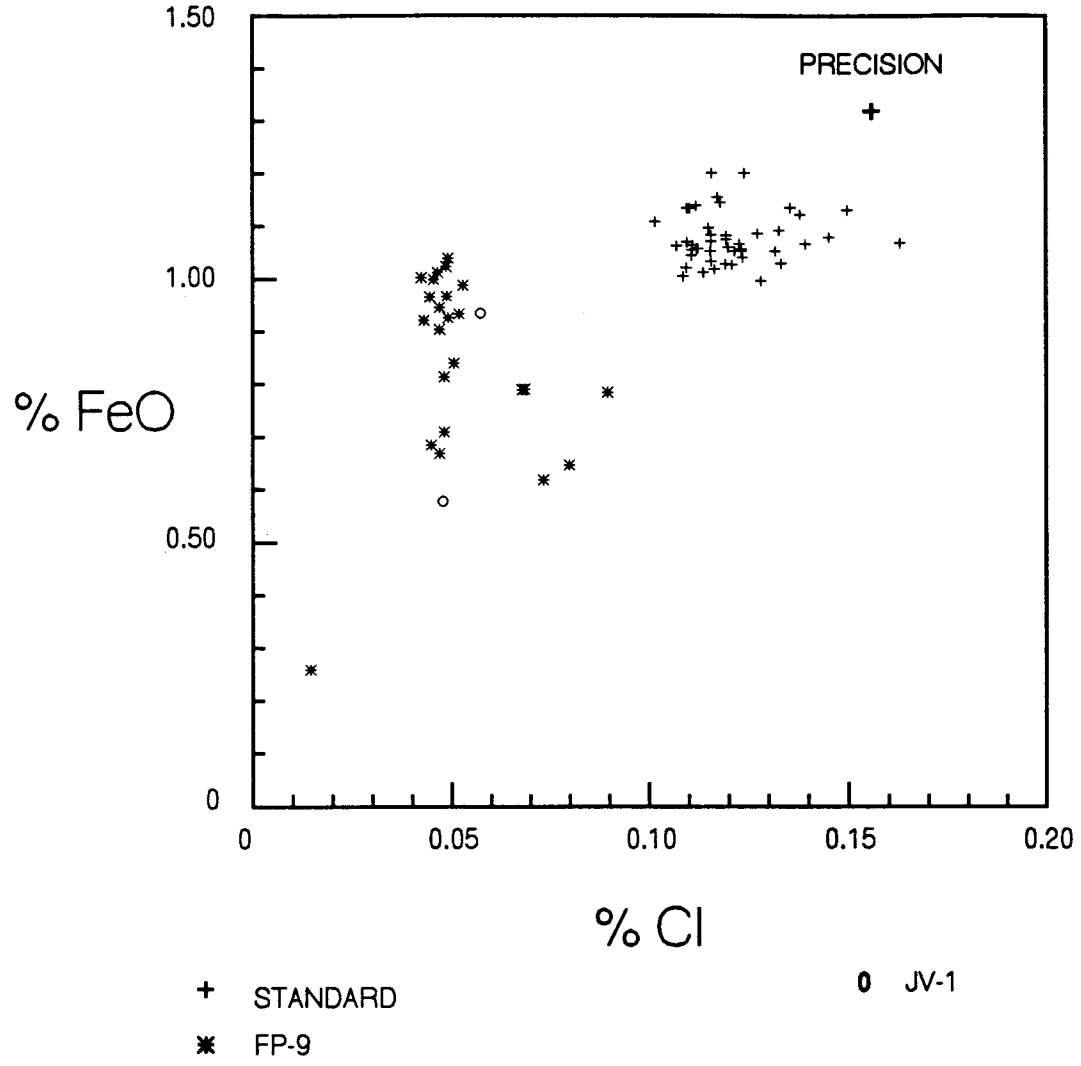

Figure 4.73. X-Y plot of wt % FeO vs Cl. Symbols used are: pluses indicate the Yellowstone rhyolite standard; asterisks indicate bentonite FP-9; and circles indicate bentonite JV-1.

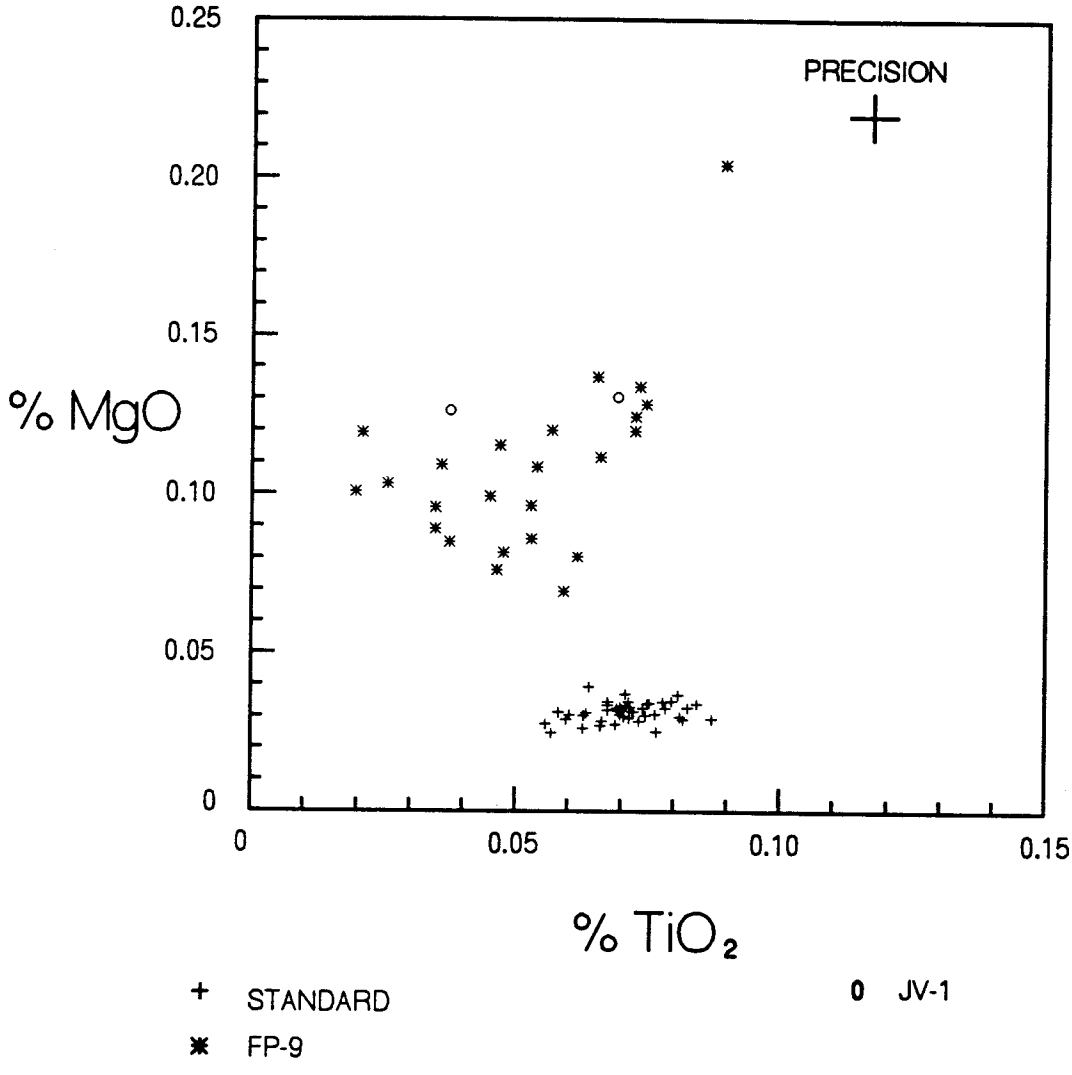

Figure 4.74. X-Y plot of wt % MgO vs TiO_2. Symbols used are: pluses indicate the Yellowstone rhyolite standard; asterisks indicate bentonite FP-9; and circles indicate bentonite JV-1.

TABLE 4.1 Amounts of quartz present in prepared samples.

SAMPLE	AMOUNT OF QUARTZ PRESENT	AMOUNT OF QUARTZ WITH MELT INCLUSIONS
FRANKSTOWN		
FP-12	Abundant	Fairly Abundant
FP-11	Rare	Absent
FP-10	Fairly Rare	Absent
FP-9	Abundant	Fairly Abundant
FP-8	Abundant	Moderate
FP-7	Fairly Rare	Absent
FP-6	Abundant	Absent
FP-5	Fairly Rare	Absent
FP-4	Absent	Absent
FP-3	Absent	Absent
FP-2	Absent	Absent
FP-1	Absent	Absent
SELINSGROVE JUNCTION		
SJ-6	Abundant	Fairly Abundant
SJ-5	Moderate	Absent
SJ-4	Moderate	Absent
SJ-3	Abundant	Absent
SJ-2	Abundant	Absent
SJ-1	Moderate	Absent
NEWTON HAMILTON		
NH-5	Moderate	Absent
NH-4	Abundant	Fairly Abundant
NH-3	Abundant	Fairly Abundant
NH-2	Moderate	Absent
NH-1	Moderate	Absent
TIPTON		
TP-3	Abundant	Absent
TP-2	Abundant	Fairly Abundant
TP-1	Abundant	Absent
MIDWAY		
MW-5	Abundant	Absent
MW-4	Moderate	Absent
MW-3	Rare	Absent
MW-2	Rare	Absent
MW-1	Abundant	Fairly Abundant
JAMESVILLE		
JV-1	Moderate	Rare

TABLE 4.1 (Continued).

CHERRY VALLEY		
CV-1	Moderate	Absent
LANCASTER		
LC-1	Moderate	Absent
SENECA FALLS		
SC-1	Moderate	Absent
MARCELLUS		
MC-1	Moderate	Absent
EAST STROUDSBURG		
ES-1	Moderate	Absent
BOWMANSTOWN		
BM-1	Abundant	Absent
BM-2	Moderate	Absent
DALMATIA		
DM-1	Moderate	Absent
DM-2	Moderate	Absent
EVERETT		
EV-1	Rare	Absent
EV-2	Rare	Absent
EV-3	Rare	Absent
CASTALIA		
CS-1	Moderate	Absent
CS-2	Moderate	Absent

Note: All samples are archived at the Department of Geological Sciences, State University of New York at Albany.

5.1 STATISTICAL ANALYSES

Sarna-Wojcicki et al. (1987) incorporated the use of statistical analyses in the correlation of Cenozoic tephra layers by definig a correlation coefficient. The SIMINAL method compares compositions of samples by deriving a similarity coefficient given by:

$$d_{(A,B)} = \frac{\sum_{i=1}^{n} [R_i]}{n}$$

where $d_{(A,B)}$ is the similarity coefficient for comparison between samples A and B, i is the element number, n is the number of elements, R_i is the concentration ratio of $X_{i(A)}/X_{i(B)}$ if the concentration of element i in sample B is larger or $X_{i(B)}/X_{i(A)}$ if the concentration of element i in sample A is larger, $X_{i(A)}$ is the concentration of element A, and $X_{i(B)}$ is the concentration of element B. This method is an excellent tool to provide confidence in a relation that is based on a set of parameters that vary around a single point or a cluster of points (i.e., a mean sample analysis point).

Due to the bimodal distribution of MgO and TiO_2 in bentonites FP-12, NH-4, SJ-6, and TP-2 (as seen in Figure 4.43), only the elemental abundances of Cl and FeO could be compared by this method. The analyses required an equal number of samples of each bentonite to be compared. To obtain an equal number of samples (limited to 18 samples

analyzed for bentonite TP-2), a random table of numbers was used to obtain 18 samples of bentonites FP-12, SJ-6, and NH-4, by the method described by Moore and McCabe (1989). The data used are shown in Tables 5.1 - 5.5. The similarity coefficients were then determined for bentonites NH-4, SJ-6, and TP-2 compared with bentonite FP-12 (Tables 5.6 - 5.8). From these matrixes a frequency distribution for each was constructed (Figures 5.1 - 5.3). Note the similarity of each frequency distribution and estimated means of 90.7 for bentonites FP-12 and SJ-6, 90.1 for bentonites FP-12 and NH-4, and 89.2 for bentonite FP-12 and TP-2. A separate matrix was constructed (Table 5.9) using simple random sample of a population of 10 analyses of bentonite FP-12 compared with bentonite FP-9 (which of course should not be correlated). A frequency distribution of these data (Figure 5.4) yielded an extremely different distribution compared with Figures 5.1 - 5.3. The estimated mean of 79.5 was obtained as compared with 90.7, 90.1, and 89.2 in the others.

This method of comparison resolves the highly similar bentonites of FP-12, SJ-6, NH-4, and TP-2 (Figures 5.1 - 5.3), as contrasted with the dissimilar comparison of bentonite FP-12 with bentonite FP-9 (Figure 5.4).

This statistical inference along with the graphical representations in Chapter 4, leaves little doubt as to the distinctiveness of bentonites FP-12, SJ-6, NH-4, and TP-2 compared with other bentonites analyzed.

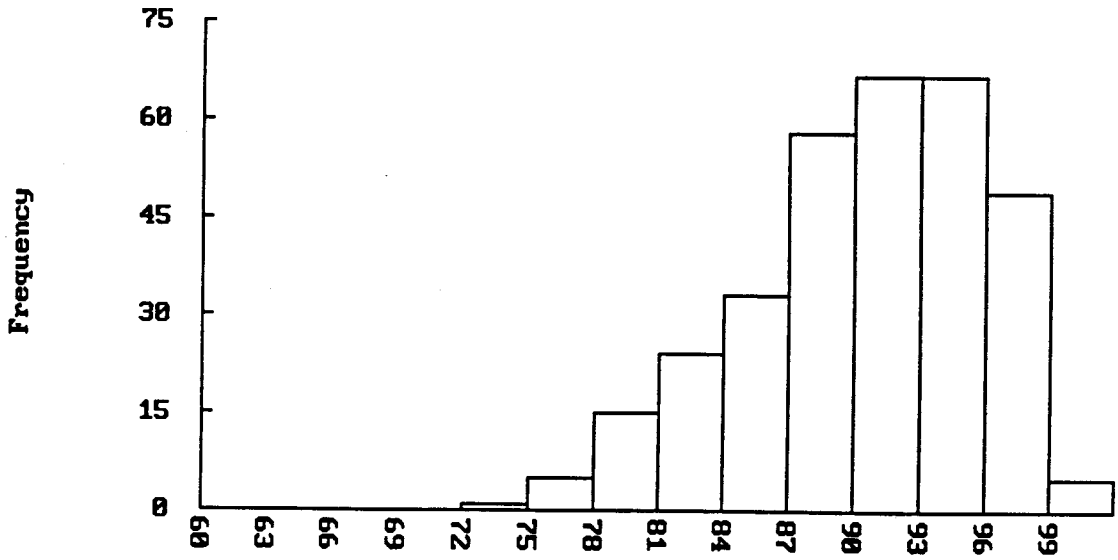

Figure 5.1. Frequency distribution of the correlation matrix between bentonite FP-12 and bentonite NH-4.

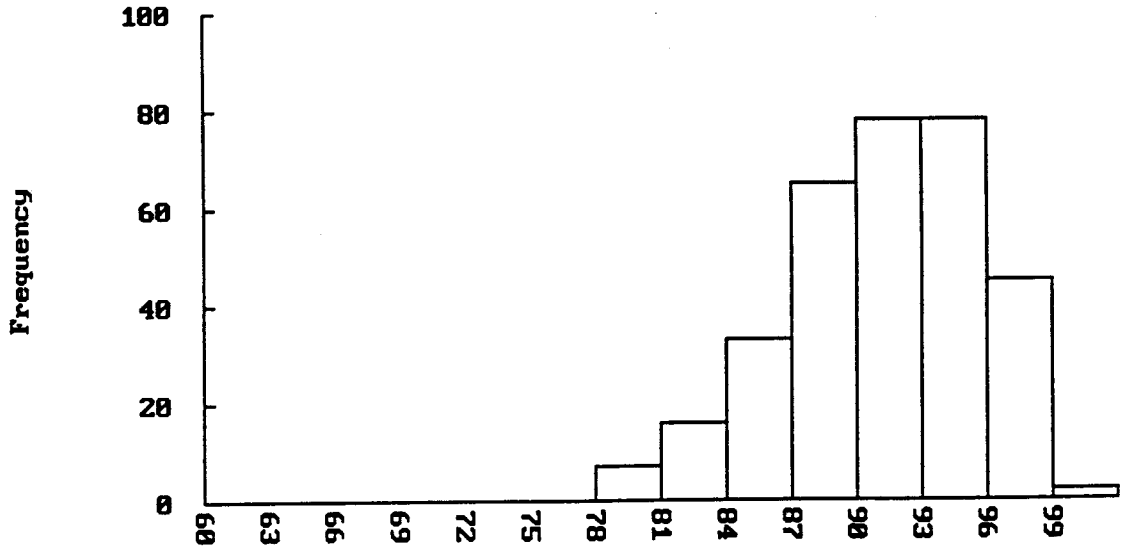

Figure 5.2. Frequency distribution of the correlation matrix between bentonite FP-12 with bentonite SJ-6.

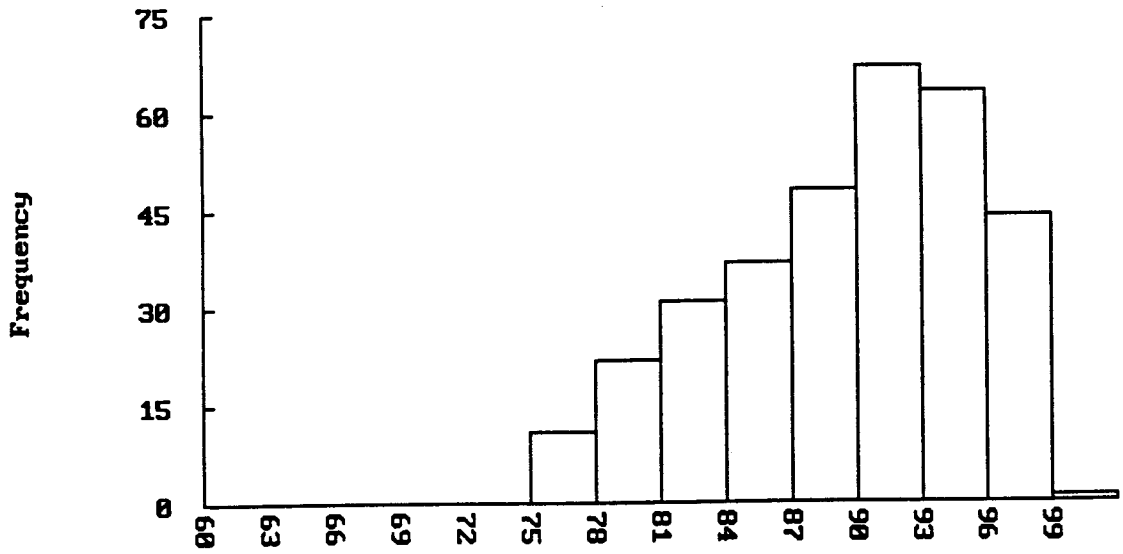

Figure 5.3. Frequency distribution of the correlation matrix between bentonite FP-12 and bentonite TP-2.

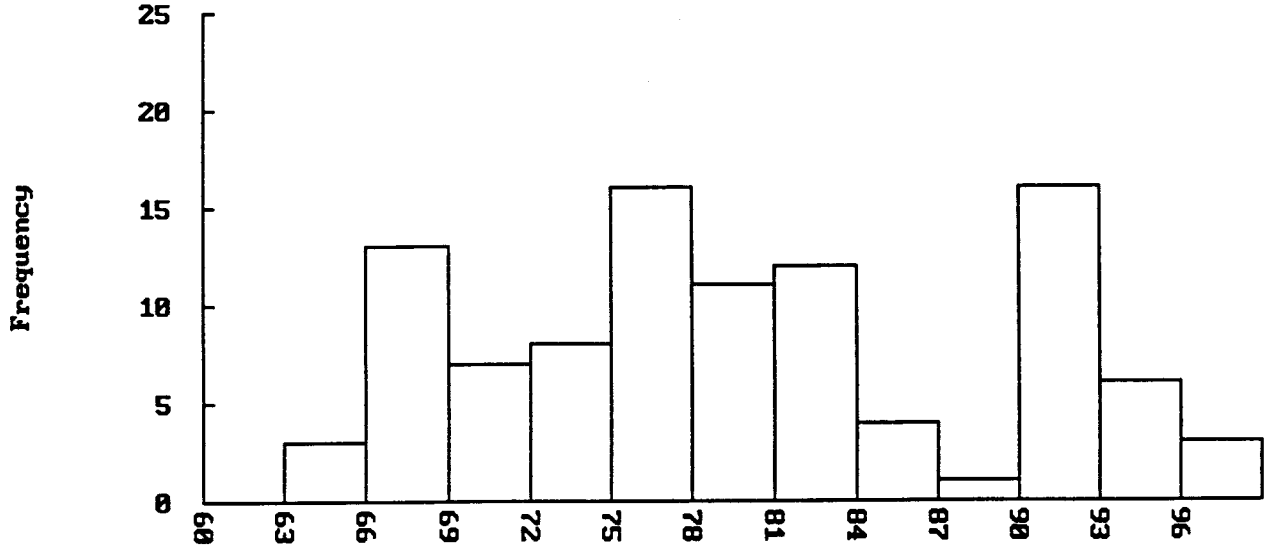

Figure 5.4. Frequency distribution of the correlation matrix between bentonite FP-12 and bentonite FP-9.

Table 5.1. Cl and FeO values of bentonite FP-12 used for statistical analyses.

SAMPLE	Cl	FeO
1	0.0612	0.7256
2	0.0742	0.7184
3	0.0712	0.6725
4	0.0808	0.7518
5	0.0636	0.7765
6	0.0629	0.7924
7	0.0721	0.7435
8	0.0614	0.7800
9	0.0605	0.8295
10	0.0574	0.7913
11	0.0699	0.7449
12	0.0733	0.7710
13	0.0636	0.6915
14	0.0754	0.6730
15	0.0747	0.6794
16	0.0599	0.7675
17	0.0718	0.7637
18	0.0665	0.7728

Table 5.2. Cl and FeO values of bentonite SJ-6 used for statistical analyses.

SAMPLE	Cl	FeO
1	0.0614	0.6825
2	0.0650	0.7886
3	0.0693	0.7044
4	0.0515	0.7693
5	0.0590	0.7070
6	0.0597	0.7334
7	0.0702	0.6047
8	0.0668	0.7364
9	0.0644	0.6391
10	0.0645	0.7704
11	0.0605	0.7111
12	0.0680	0.7864
13	0.0537	0.7768
14	0.0747	0.8186
15	0.0757	0.7844
16	0.0539	0.7457
17	0.0609	0.8088
18	0.0607	0.7652

Table 5.3. Cl and FeO values of bentonite NH-4 used for statistical analyses.

SAMPLE	Cl	FeO
1	0.0814	0.6525
2	0.0715	0.8093
3	0.0697	0.8187
4	0.0859	0.8065
5	0.0612	0.7268
6	0.0746	0.8084
7	0.0763	0.7224
8	0.0591	0.7392
9	0.0613	0.7739
10	0.0633	0.7252
11	0.0876	0.9081
12	0.0570	0.8080
13	0.0598	0.7722
14	0.0607	0.7931
15	0.0763	0.7928
16	0.0834	0.7199
17	0.0716	0.7121
18	0.0695	0.7491

Table 5.4. Cl and FeO values of bentonite TP-2 used for statistical analyses.

SAMPLE	Cl	FeO
1	0.0726	0.8169
2	0.0599	0.7428
3	0.0596	0.7412
4	0.0644	0.7397
5	0.0639	0.7461
6	0.0569	0.8291
7	0.0581	0.8371
8	0.0597	0.7863
9	0.0562	0.8009
10	0.0523	0.8135
11	0.0576	0.7516
12	0.0616	0.8689
13	0.0649	0.7532
14	0.0523	0.8221
15	0.0516	0.8158
16	0.0525	0.8169
17	0.0547	0.8384
18	0.0656	0.8005

Table 5.5. Cl and FeO values of bentonite FP-9 used for statistical analyses.

SAMPLE	Cl	FeO
1	0.0529	0.9883
2	0.0491	1.0402
3	0.0487	1.0244
4	0.0686	0.7916
5	0.0466	1.0129
6	0.0680	0.7897
7	0.0733	0.6185
8	0.0799	0.6468
9	0.0424	1.0035
10	0.0456	0.9992

Table 5.6. Correlation matrix using the SIMINAL method between bentonite FP-12 and bentonite NH-4. Element ratios used are Cl and FeO. A 100 indicates a perfect correlation and numbers trending towards zero indicate less of a correlation.

		NH-4																	
		1	2	3	4	5	6	7	8	9	10	11	12	13	14	15	16	17	18
	1	83	88	88	81	99	86	90	97	97	98	75	91	96	95	86	86	92	92
	2	91	93	91	88	91	94	98	88	88	92	82	83	87	86	94	95	98	95
	3	92	91	91	83	89	89	93	87	96	91	78	82	86	85	89	89	97	94
	4	93	91	89	94	86	93	95	86	87	87	88	82	86	85	95	96	92	93
	5	81	92	93	85	95	91	88	94	98	96	79	93	97	97	91	84	90	94
	6	80	93	94	86	95	91	87	94	98	95	80	94	96	98	91	83	89	93
	7	88	96	94	88	91	94	96	91	91	93	82	86	90	89	94	92	98	98
	8	80	91	92	84	96	89	87	96	99	95	78	95	98	99	89	83	89	92
	9	76	91	93	84	93	89	83	93	96	92	80	96	96	98	87	80	86	89
FP-12	10	76	89	90	82	93	87	83	95	96	91	76	99	97	97	88	79	85	89
	11	85	93	93	85	94	91	92	94	94	98	79	91	93	92	91	88	95	98
	12	87	96	95	90	89	97	95	88	92	90	84	87	91	90	97	91	95	96
	13	86	87	88	80	96	85	90	93	93	97	74	88	92	91	85	86	93	92
	14	95	89	87	86	87	91	96	85	84	88	80	79	83	83	92	92	95	91
	15	94	90	88	86	88	92	96	86	85	89	80	90	94	83	92	92	96	92
	16	79	89	90	82	96	88	86	97	98	95	76	95	99	98	88	83	88	92
	17	87	97	95	89	90	95	94	90	92	92	83	87	91	90	95	90	96	97
	18	83	94	95	87	93	92	90	92	96	95	81	91	95	94	89	86	93	96

Table 5.7. Correlation matrix using the SIMINAL method between bentonite FP-12 and bentonite SJ-6. Element ratios used are Cl and FeO. A 100 indicates a perfect correlation and numbers trending towards zero indicate less of a correlation.

		SJ-6																
		1	2	3	4	5	6	7	8	9	10	11	12	13	14	15	16	17	18
	1	97	93	93	89	97	98	85	95	92	95	98	91	91	85	87	93	95	97
	2	89	89	96	81	89	89	89	94	88	90	90	91	82	94	95	84	85	88
	3	92	88	96	80	89	88	94	93	93	93	90	91	81	88	90	83	84	87
	4	83	88	90	81	84	86	84	90	82	89	85	90	82	92	95	83	84	87
	5	92	98	91	90	92	94	84	95	91	93	96	92	90	92	90	90	96	97
	6	92	91	90	89	92	94	83	94	89	97	93	96	92	91	91	90	97	96
	7	88	92	95	84	88	91	89	96	88	93	90	94	85	94	95	87	88	91
	8	94	97	89	91	93	96	82	93	89	97	95	95	94	89	90	92	98	98
	9	90	94	86	89	91	94	80	90	85	93	93	92	91	90	87	89	98	96
FP-12	10	90	94	89	93	93	93	79	89	85	93	92	92	96	87	87	94	96	97
	11	92	96	96	87	92	94	88	99	93	97	93	97	88	90	92	90	92	94
	12	86	93	93	85	86	88	87	95	85	94	87	95	86	96	98	85	89	91
	13	98	93	95	85	95	94	89	95	96	94	96	90	87	85	86	89	91	93
	14	90	86	94	78	87	85	91	90	90	86	87	88	80	93	93	81	82	84
	15	91	87	95	79	88	86	91	91	90	87	88	89	80	91	93	82	83	85
	16	92	95	89	93	95	98	82	93	88	96	96	93	94	87	88	94	97	99
	17	87	94	94	85	87	90	88	95	87	94	89	96	88	95	96	86	90	92
	18	90	98	94	88	90	92	86	97	90	98	91	98	90	92	93	89	94	95

Table 5.8. Correlation matrix using the SIMINAL method between bentonite FP-12 and bentonite TP-2. Element ratios used are Cl and FeO. A 100 indicates a perfect correlation and numbers trending towards zero indicate less of a correlation.

		TP-2																	
		1	2	3	4	5	6	7	8	9	10	11	12	13	14	15	16	17	18
	1	87	98	98	97	97	90	91	95	91	87	90	91	95	87	87	87	88	92
	2	89	90	89	92	91	82	82	86	83	79	87	83	91	79	79	79	80	89
	3	90	87	87	91	90	81	81	85	81	78	85	82	90	78	77	78	79	88
	4	91	86	86	89	89	81	81	85	82	79	86	81	90	78	78	79	79	88
	5	91	95	95	97	98	92	92	96	93	91	94	93	97	88	88	89	89	97
	6	92	94	94	96	96	93	91	97	94	90	93	95	96	90	90	90	91	97
	7	95	91	91	94	94	84	85	89	85	82	89	86	94	81	81	82	82	92
	8	90	96	96	95	96	93	94	98	94	91	95	95	96	90	90	90	91	96
	9	91	94	94	92	92	97	98	97	95	92	93	97	92	93	92	93	95	94
FP-12	10	88	95	95	91	92	97	97	98	98	94	97	92	92	94	93	94	95	93
	11	92	95	94	98	98	87	88	92	89	85	93	89	98	84	84	85	85	96
	12	97	89	89	92	92	85	86	90	86	83	88	86	93	83	82	83	83	93
	13	86	94	94	96	96	86	87	91	87	84	91	88	95	83	83	84	84	92
	14	89	85	85	88	87	78	79	82	79	76	82	80	88	76	75	76	76	86
	15	90	86	86	89	88	79	79	83	80	77	84	80	89	76	76	77	77	86
	16	88	98	98	95	95	94	94	99	95	91	97	93	95	90	90	91	91	94
	17	96	90	90	93	93	86	86	90	87	83	89	87	95	83	83	84	84	93
	18	93	93	93	96	96	89	90	94	91	87	82	91	98	90	86	87	87	98

Table 5.9. Correlation matrix using the SIMINAL method between bentonite FP-12 and bentonite FP-9. Element ratios used are Cl and FeO. A 100 indicates a perfect correlation and numbers trending towards zero indicate less of a correlation.

		FP-9									
		1	2	3	4	5	6	7	8	9	10
	1	80	75	75	92	74	91	84	83	71	74
	2	72	68	68	92	67	91	92	91	65	67
	3	71	67	67	91	66	90	80	93	63	66
	4	71	67	67	90	66	90	86	92	64	66
FP-12	5	81	73	76	95	75	96	83	81	72	75
	6	82	77	77	96	76	96	82	82	73	76
	7	74	70	70	95	69	94	91	89	66	69
	8	83	77	78	94	76	95	82	80	73	76
	9	86	80	81	92	79	92	79	77	76	79
	10	86	81	81	92	80	92	78	77	76	79

Due to the spread of all elements in samples that graphically correlate with bentonite FP-9 (i.e., bentonites NH-3 and MW-1), it is not possible to use this method of statistical to infer correlation between these bentonites. The only determination of correlation between these bentonites can be inferred from their characteristic spread of data in graphical representations (Figures 4.47 - 4.56, 4.60 - 4.67).

6.1 INFORMATION ON BIMODAL DISTRIBUTION OF ELEMENTS

As seen in Figures 4.37 - 4.44, there is a bimodal distribution of elemental abundances in bentonites FP-12 and its equivalents (i.e., bentonites SJ-6, NH-4, and TP-2). There are at least two possible explanations for this observation: A) this bentonite layer may be composed of two or more distinct eruptions; or B) this bentonite layer is composed of a single eruption from a large heterogeneous (i.e., zoned) magma chamber.

To attempt to determine if this may be the product of two or more distinct eruptions, detailed sample collection from layers observed within the bentonite was performed. The bentonites SJ-6 and FP-12 were observed to be layered with zones of distinct mineralogy, color, and degree of lithification (Figure 6.1). Bentonite SJ-6 was carefully sampled in five distinct zones (Figure 6.2). Zone #1 (Figure 6.2) is composed of a brown-gray micaceous layer rich in biotite and quartz with small amounts of zircon. Zone #2 (Figure 6.2) is a 2.5-inch thick layer of lithified black shale that grades into a wavy 1-2 inch chert layer (zone #3). Zone #4 (Figure 6.2) consists of another brown-gray micaceous layer rich in biotite, but quartz and zircons are absent. Zone #5 (Figure 6.2) is a dark gray cherty layer measuring about 2.5 inches in thickness that grades into a lithified black shale. Quartz phenocrysts are

Figure 6.1. Close-up photograph of bentonite SJ-6 showing the observable layers within this bentonite. Note that the scale on the ruler is in inches.

LAYERING WITHIN BENTONITE SJ-6

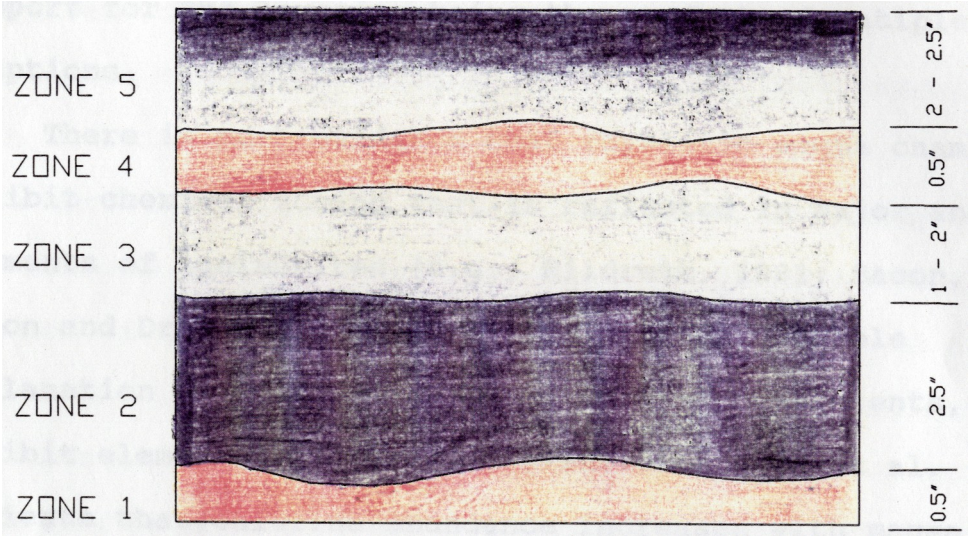

ZONE 1. Brown-gray micaceous layer

ZONE 2. Black lithofied layer

ZONE 3. Dark gray cherty layer

ZONE 4. Brown-gray micaceous layer

ZONE 5. Dark gray chert at base grading to a black shale

Figure 6.2. Schematic digram showing the internal zoning within bentonite SJ-6.

rare or absent in all zones with the exception of zone #1. Zone #1 contained abundant quartz phenocrysts with melt inclusions that, when analyzed, yielded both distributions of elemental abundances (e.g., Figures 4.37 - 4.35). With melt inclusions of both elemental abundance distributions occuring only in zone #1 and no other zones, there is no support for the layering being the product of mutiple eruptions.

There is much evidence that rhyolitic magma chambers exhibit chemical zoning that is reflected in major and trace elements of ignimbrites (e.g., Hildreth, 1981; Bacon, 1983; Bacon and Druitt, 1988). This is another possible explanation why bentonite FP-12, and its equivalents, exhibit elemental bimodal distribution. Stix et al. (1988) indicate that chlorine abundance increases with magma chamber depth. However, it is believed that the plinian phase of an eruption is localized within the upper portion of the magma chamber (Duffield and Ruiz, 1992). The similarity of chlorine abundance from both populations of melt inclusions contained in bentonite FP-12 and its equivalents would be consistent with the dynamics of a plinian eruption demonstrated by Duffield and Ruiz (1992). They suggest that the plinian phase of an eruption is limited to a source in the upper portion of the magma chamber and, therefore, no zoning of chlorine would be observed if one is only sampling the upper portion of the magma chamber. The bimodal distribution of MgO and TiO_2 may

be explained by the plinian eruption of a heterogeneous magma chamber caused by replenishment prior to eruption. This would provide a heterogeneous magma chamber due to the addition of new magma. This new magma could provide a heterogeneous chamber (i.e., zoned) with elements varying due to the additional magma not completly mixing prior to eruption. This mechanism provides for chemical zoning throughout the magma chamber and not just that associated with changing depth.

More investigation is required prior to making firm conclusions about the dynamics involved in explaining the bimodal distribution of elements in bentonite FP-12 and its equivalents. This may include more detailed sampling of this bentonite layer at other localites and investigations of more recent ash falls (i.e., historic eruptions such as Mount Pinatubo).

6.2 SUMMARY

The data presented in this study supports the following conclusions.

- Bentonites can be correlated over significant distances by using the geochemical analyses of melt inclusions that occur in quartz phenocrysts as a geochemical fingerprint.
- Out of fourteen locations that were previously reported as being the Tioga bentonites and equivalent to those occurring at Frankstown, PA, only four localities actually proved to contain bentonite layers that can be demonstrated to be the same (i.e., Tioga) bentonite.
- The Tioga group of bentonites most likely consist of more than the seven major bentonites than previously reported.
- The sediment source for the Marcellus shale was most likely transported along strike (i.e., from the north or south) vice across strike (i.e, from the east) or is craton derived (i.e., from the west). This is observed by the bentonite FP-9 and its equivalent occurring in shale in the west (i.e., Frankstown) and transgressing into limestone in the east (i.e., Midway).

REFERENCES

Bacon, C. R., 1983, Eruptive history of Mount Mazama and Crater Lake Caldera, Cascade Range, U. S. A. Journal Volcanol. Geotherm. Res., v. 18, pp. 57-115.

Bacon, C. R., and Druitt, T. H., 1988, Compositional Evolution of the Zoned Calkalkaline Magma Chamber of Mount Mazama, Crater Lake, Oregon. Contrib. Mineral. Petrol., v. 98, pp. 224-256.

Boucot, A. J., 1969, Geology of the Moose River and Roach River Synclinoria, North-Western Maine. Maine Geological Survey Bulletin, No. 21.

Boucot, A. J., Field, M. T., Fletcher, R., Forbes, W. H., Naylor, R. S., and Pavlides, L., 1964, Reconnaissance Bedrock Geology of the Presque Isle Quadrangle, Maine. Maine Geological Map Survey, Quadrangle Map Series No. 2.

Bradley, D. C., 1989, Tectonics of the Acadian Orogeny in New England and Adjacent Canada. Journal of Geology, v. 91, pp. 381-400.

Brett, C., 1991, In: Dynamic Stratigraphy and Depositional Environments of the Hamilton Group (Middle Devonian) in New York State, Part II, E. Landing and C. Brett editors. N.Y.S. Museum Bulletin No. 469.

Dennison, J. M., 1961, Stratigraphy of the Onesquethaw stage of the Devonian in West Virginia and Bordering States. West Virginia Geol. and Econ. Survey Bulletin No. 22, 87 p.

Dennison, J. M. and Textoris, D. A., 1970, Devonian Tioga tuff in Northeast United States. Bulletin Volcanologique, v. 34, pp. 289-294.

Dennison, J. M. and Textoris, D. A., 1971, Devonian Tioga Tuff. Virginia Div. of Mineral Res. Inf. Circular 1b, pp. 64-68.

Dennison, J. M. and Textoris, D. A., 1978, Tioga Bentonite Time-Marker Associated with Devonian Shales in the Appalachian Basin. In: Proceedings of the First Eastern Gas Shales Symposium, G. L. Scott, W. K. Overbet, Jr., A. E. Hunt, and C. A. Komar, editors, October 17-19, 1977, Morganstown West Virginia, U. S. Dep of Energy, Morganstown Energy Research Center, Pub. MERC/SP-77-5, pp. 166-182.

Dennison, J. M. and Textoris, D. A., 1987, Paleowind and Depositional Tectonics Interpreted from Tioga Ash Bed. Appalachian Basin Industrial Association Spring Meeting Program, May 7-8, 1987, 25 p.

Droste, J. B. and Shaver, R. H., 1975, Jeffersonville Limestone (Middle Devonian) of Indiana: Stratigraphy, Sedimentation, and Relation to Silurian Reef-Bearing Rocks. Amer. Association of Petroleum Geologists Bulletin, v. 59, pp. 1217-1221.

Druitt, T. H., Anderson, A. T., and Nagle, F., 1982, Water in Rhyolitic Magma, Bishop, California (abst.). EOS, v. 63, p 451.

Duffield, W. A. and Ruiz, J., 1992, Compositional gradients in Large Reservoirs of Silicic Magma as Evidenced by Ignimbrites versus Taylor Creek Rhyolite lava Domes. Contrib. Mineral. Petrol., v. 110, pp. 192-210.

Ebright, J. R., Fettke, C. R., and Ingham, A. I., 1949, East Fork Wharton gas field, Potter County, Pennsylvania. Penn. Geol. Survey, 4th series Bulletin M-30, 43 p.

Epstein, J. B., 1986, The Valley and Ridge Province of Eastern Pennsylvannia-Strtatigraphic and Sedimetologic contributions and Problems. Geolgical Journal, v. 21, pp. 283-306.

Feldman, H. R., 1980, Level-Bottom brachiopod Communities in the Middle Devonian of New York. Lethaia, v. 13, pp. 27-46.

Fettke, C. R., 1931, Physical Characteristics of the Oriskany Sandstone and subsurface studies in the Tioga Gas field, Potter County, Pennsylvania. Penn. Geol. Survey, 4th Series Bulletin 102-B, pp. 1-9.

Gates, O. and Moench, R. H., 1981, Bimodal Silurian and Lower Devonian Volcanic Rock Assemblages in the Machias-Eastport area, Maine. U. S. G. S. Professional Paper 1184.

Hall, J., 1843, Geology of New York. Albany, State of New York Part 4, 683 p.

Hall, B. A., 1970, Stratigraphy of the Southern end of the Munsungun Anticlinorium, Maine. Maine Geological Survey Bulletin No. 22.

Hanson, B. Z., Delano, J. W., Schirnick, C., and VonKiparsky, W., 1991, The Occurrence of Melt Inclusions in Quartz Phenocrysts from K-bentonites in the Helderberg Group of New York State and their Potential use in Stratigraphic Correlation. Geological Society of America, Abstracts with Programs, v.24 No. 3.

Hervig, R. L., Dunbar, N. W., Westrich, H. R., and Kyle, P. R., 1989, Pre-eruptive water content of Rhyolitic Magmas as Determined by Ion Microprobe analyses of Melt Inclusions in Phenocrysts. Journal of Vocanology and Geothermal Research, v. 36, pp. 293-302.

Hervig, R. L. and Dunbar, N. W., 1992, Cause of Chemical zoning in the Bishop (California) and Bandelier (New Mexico) Magma Chambers. Earth and Planetary Science Letters, v. III, pp. 97-108.

Hildreth, W., 1981, Gradients in Silicic Magma Chambers: Implications for lithospheric Magmatism. Journal of Geophysical Research, v. 86, pp. 10153-10192.

Hon, R., Acheson, D., III, and Schulman, J., 1981, Geochemical and Petrologic Correlation of Acadian Magmatic Rocks in Northwest and North-Central Maine. Geologial Society Abstracts With Programs, v. 13.

Inners, J. D., 1975, The Stratigraphy and Paleontology of the Onesquethaw Stage in Pennsylvania and Adjacent States. Ph.D. dissertation, University of Massachusetts.

Knight, W. C., 1898, Bentonite. Engineering and Mining Journal, v. 66, pp. 491.

Laurent, R. and Belanger, J., 1984, Geochemistry of Silurian-Devonian Alkaline Basalt Suites from the Gaspe Peninsula, Quebec Appalachians. Maritime Sediments and Atlantic Geology, v. 20, pp. 67-78.

Lindstrom, D. J., Delano, J. W., Hanson, B. Z., and Waechter, J. W., 1992, Geochemical Stratigraphy of the Devonian Sediments in New York and Pennsylvania using Glass-bearing Quartz Phenocrysts. Geological Society of America, Abstracts with Programs, v. 24, No. 3.

Lyons, P. C., Outerbridge, W. F., Congdon, R. P., Evans, H. T., Jr., and Slucher, E. R., 1992, "Fingerprinting" of Kaolinized volcanic ash beds (Tonsteins) as a Tool in the Correlation of Coal beds in the Appalachian Basin. Geological Society of America, Abstracts with Programs, v. 24. No. 3.

McKerrow, W. S. and Zeigler, A. M., 1971, The Lower Silurian Paleogeography of New Brunswick and Adjacent Areas. Journal of Geology, v. 79, pp. 635-646.

Meents, W. F. and Swan, D. H., 1965, Grand Tower Limestone (Devonian) of Southern Illinois. Illinois Geological Survey Circular 389, 34 p.

Melson, W. G., 1983, Monitoring the 1980-1982 Eruptions of Mount St. Helens: Compositions and Abundances of Glass. Science, v. 221, pp. 1387-1391.

Moore, D. S. and McCabe, G. P., 1987, Introduction to the Practice of Statistics. W. H. Freeman and Company, publishers.

Oliver, W. A., Jr., 1954, Stratigraphy of the Onondaga Limestone (Devonian) in central New York. Geological Society of America Bulletin, v. 65, pp. 621-652.

Oliver, W. A., Jr., 1956, Stratigraphy of the Onondaga Limestone (Devonian) in Eastern New York. Geological Society of America Bulletin, v. 67, pp. 1441-1474.

Oliver, W. A., Jr., DeWitt, W., Jr., Dennison, J. M., Hoskins, D. M., and Huddle, J. W., 1967, The Appalachian Basin, United States. In: International Symposium on the Devonian System, D. H. Oswald, editor, Alberta Society of Petroleum Geologists, v. 1, pp. 1001-1040.

Oliver, W. A., Jr., DeWitt, W., Jr., Dennison, J. M., Hoskins, D. M., and Huddle, J. W., 1969, Correlations of Devonian rock units in the Appalachian Basin. United States Geological Survey, Oil and Gas Investigations Chart OC-64.

Osberg, P. H., Tull, J. F., Robinson, P., Hon, R., and Butler, R. J., 1989, The Acadian Orogen. In: The Geology of North America, v. F-2, The Appalachian-Ouachita Orogen in the United States, The Geological Society of America, publishers.

Osbourne, R., 1992, Personal communication. New York State Department of Transportation.

Pinette, S. R., 1983, Stratigraphy, Structure, Metamorphism, and Volcanic Petrology of Islands in East Penobscot Bay, Maine. Master's Thesis, Orono, University of Maine.

Rankin, D. W., 1968, Volcanism Related to Tectonism in the Piscataquis volcanic Belt, an Island Arc of Early Devonian age in North-Central Maine. In: Studies of Appalachian Geology, Zen, E., White, W. S., Hadley, J. B., and Thompson, J. B., Jr., editors. Northern and Maritime, New York, Interscience publishers, pp. 355-370.

Rickard, L. V., 1964, Correlation of the Devonian rocks of New York State. N.Y.S. Museum and Science Service, Map and Chart Series No. 4.

Rickard, L. V., 1964, Correlation of the Silurian and Devonian rocks of New York State. N.Y.S. Museum and Science Service, Map and Chart Series No. 4.

Roden, M.K., 1989, Apatite Fission-Track Thermochronology of the Central and Southern Appalachian Basin. Ph.D. dissertation, Renssalaer Polytechnic Institute.

Roden, M. K., Parrish, R. K., and Miller, D. S., 1990, The Absolute age of the Eifelian Tioga ash bed, Pennsylvania. Journal of Geology, v. 98, pp. 282-295.

Roedder, E., 1984, Fluid Inclusions. In: Rev. in Mineralogy, v. 12, Mineralogical Society of America.

Roen, J. B. and Hosterman, J. W., 1982, Misuse of the term "Bentonite" for ash beds of Devonian age in the Appalachian Basin. Geological Society of America Bulletin, v. 93, pp. 921-925.

Rutherford, M. J., Sigurdson, H., Carey, S., and Davis, A., 1985, The May 18, 1980 Eruption of Mount St. Helens 1, Melt composition and Experimental phase Equilibria. Journal of Geophysical Research, v. 90, B 4, pp. 2929 -2947.

Sanford, 1976, Devonian Stratigraphy of the Hudson Platform. Canadian Geological Survey, Mem. No. 379.

Sargent, S. L., and Hon, R., 1981, Dockendorf group; Early Devonian Calcalkaline volcanism of "Andean-Type" in Northeastern Maine. Geological Society of America Abstracts with Programs, v. 13.

Schirnick, C., 1990, Origin, Sedimentary Geochemistry, and Correlation of Middle and Late Ordovician K-Bentonites: Constraints from Melt Inclusions and Zircon Morphology. Master's thesis, State Univ. of New York at Albany.

Schirnick, C. and Delano, J. W., 1990, Rhyolitic Melt Inclusions within Paleozoic K-Bentonites. Geological Society of Am., Abstracts with Programs v. 22, No. 7.

Schirnick, C. and Delano, J. W., 1991, Rhyolitic Melt Inclusions in Quartz Phenocrysts of Paleozoic Bentonites and Volcanic Ashes: Tectonic Constraints and Stratigraphic Correlations. Geological Society of America, Abstracts with Programs, v. 23, No. 1.

Shride, A. F., 1976, Stratigraphy and Correlation of Newbury Volcanic Complex, Northeastern Massachusetts. In: Contributions to Stratigraphy of New England, Page, L. R., editor. Geological Society of America Memoir 148, pp. 147-177.

Smith, R. C. and Way, J. H., 1983, The Tioga Ash Beds at Selinsgrove Junction. In: Silurian Depositional History and Alleghanian Deformation in the Pennsylvania Valley and Ridge. R. P. Nickelson and E. Cotter, leaders, Guidebook for the 48th Annual Field Conference of Pennsylvania Geologists.

Stix, J., Goff, F., Gorton, M. P., Heiken, G., and Garcia, S. R., 1988, Restoration of Compositional Zonation in the Bandelier Silicic Magma Chamber Between Two Caldera-Forming Eruptions: Geochemistry and Origin of the Cerro Toledo Rhyolite, Jemez Mountains, New Mexica. Journal of Geophysical Research, v. 93 No. B 6, pp. 6129-6147.

Way, J. H., Smith, R. C., and Roden, M. K., 1986, Detailed Correlations across 175 miles of the Valley and Ridge of Pennsylvania using 7 ash beds in the Tioga Zone. In: Guidebook for 51st Annual Field Conference of Pennsylvania Geologists, W. D. Sevan, editor, Pennsylvania Geological Survey, pp. 55-72.

Weaver, C. E., 1956, Mineralogy of the Middle Devonian Tioga K-Bentonite. American Mineralogist, v. 41, pp. 359 -362.

MAPS USED

Berg,T. M., Edmunds, W. E., Geyer, A. R., Glover, A. D., Hoskins, D. M., Miles, C. E., Kuchinski, J. G., MacLahlan, D. B., Root, S. I., Sevon, W. D., and Socolow, A. A., 1980, Geologic Map Of Pennsylvania.

U. S. G. S., 1959, 7.5 Minute Quadrangle Topographical Map of Newton Hamilton, PA, N4022.5-W7745/7.5.

U. S. G. S., 1963, 7.5 Minute Quadrangle Topographical Map of Frankstown, PA, N4022.5-W7815/7.5

U. S. G. S., 1963, 7.5 Minute Quadrangle Topographical Map of Tipton, PA, NE/4 Altoona 15' Quadrangle, 40078-F3-024.

U. S. G. S., 1965, 7.5 Minute Quadrangle Topographical Map of Sunbury, PA, SE/4 Sunbury 15' Quadrangle 40076-G7-TF-024.

U. S. G. S., 1973, 7.5 Minute Quadrangle Topographical Map of Duncannon, PA, NE/4 New Bloomfield 15' Quadrangle N4022.5-W7700/7.5

Appendix A. Electron microprobe values obtained for the Yellowstone rhyolite standard (USNM 72854). Columns of MgH, TiR, AlK, Cl, and FeG (left of vertical line) indicate the weight fraction of the elemental oxides without the Bence-Albee matrix corrections and columns of MgO, TiO_2, Al_2O_3, Cl, and FeO (right of vertical line) indicate the weight % of each elemental oxide after correction with its beta factor.

STANDARD

SAMPLE	MgH	TiR	AlK	Cl	FeG	MgO	TiO2	Al2O3	Cl	FeO
1	0.0301	0.0672	11.5003	0.1047	0.9897	0.0323	0.0703	11.5000	0.1233	1.0544
2	0.0307	0.0684	11.4710	0.0979	0.9870	0.0331	0.0718	11.5000	0.1156	1.0542
3	0.0298	0.0645	11.4956	0.1032	0.9895	0.0320	0.0675	11.5000	0.1216	1.0546
4	0.0340	0.0668	11.3406	0.1000	0.9968	0.0371	0.0709	11.5000	0.1194	1.0769
5	0.0284	0.0670	11.5229	0.0957	0.9971	0.0305	0.0700	11.5000	0.1125	1.0602
6	0.0289	0.0606	11.4915	0.0952	0.9945	0.0311	0.0635	11.5000	0.1122	1.0603
7	0.0337	0.0759	11.2884	0.1028	0.9750	0.0369	0.0809	11.5000	0.1233	1.0583
8	0.0296	0.0669	11.4887	0.0962	1.0066	0.0318	0.0701	11.5000	0.1156	1.0735
9	0.0303	0.0660	11.3520	0.0972	1.1142	0.0330	0.0700	11.5000	0.1160	1.2026
10	0.0247	0.0622	11.3007	0.0980	1.0677	0.0270	0.0663	11.5000	0.1174	1.1576
11	0.0280	0.0707	11.3985	0.0958	0.9436	0.0304	0.0747	11.5000	0.1138	1.0143
12	0.0320	0.0790	12.1110	0.1110	1.1890	0.0327	0.0785	11.5000	0.1241	1.2029
13	0.0340	0.0800	12.0820	0.1070	1.0470	0.0348	0.0797	11.5000	0.1199	1.0618
14	0.0390	0.0650	12.2280	0.1150	1.0860	0.0394	0.0640	11.5000	0.1274	1.0883
15	0.0290	0.0610	12.2940	0.1210	1.0350	0.0292	0.0597	11.5000	0.1333	1.0315
16	0.0260	0.0640	12.2400	0.1260	1.0680	0.0263	0.0629	11.5000	0.1394	1.0691
17	0.0280	0.0580	12.5050	0.1090	1.1710	0.0277	0.0558	11.5000	0.1180	1.1473
18	0.0250	0.0590	12.4970	0.1010	1.0430	0.0247	0.0568	11.5000	0.1094	1.0226
19	0.0340	0.0740	12.5480	0.1060	1.0450	0.0335	0.0710	11.5000	0.1166	1.0204
20	0.0300	0.0750	12.5930	0.1110	1.0590	0.0294	0.0717	11.5000	0.1194	1.0304
21	0.0310	0.0630	12.5780	0.1190	1.0250	0.0305	0.0603	11.5000	0.1281	0.9985
22	0.0340	0.0770	12.2810	0.1230	1.1400	0.0342	0.0755	11.5000	0.1356	1.1373
23	0.0340	0.0790	12.1770	0.1000	1.0590	0.0345	0.0781	11.5000	0.1112	1.0656
24	0.0320	0.0750	12.1690	0.1040	1.0280	0.0325	0.0742	11.5000	0.1157	1.0350
25	0.0310	0.0730	12.1640	0.1110	1.0350	0.0315	0.0722	11.5000	0.1236	1.0425
26	0.0300	0.0640	12.2230	0.0990	1.1340	0.0303	0.0630	11.5000	0.1097	1.1367
27	0.0300	0.0730	12.4380	0.1020	1.0730	0.0298	0.0706	11.5000	0.1111	1.0570
28	0.0310	0.0700	12.0970	0.1000	1.1280	0.0317	0.0697	11.5000	0.1119	1.1405
29	0.0340	0.0720	12.1200	0.1070	1.0730	0.0347	0.0715	11.5000	0.1196	1.0847
30	0.0280	0.0670	12.1380	0.1190	1.0640	0.0285	0.0664	11.5000	0.1328	1.0942
31	0.0250	0.0780	12.2270	0.1190	1.0530	0.0253	0.0768	11.5000	0.1318	1.0552
32	0.0320	0.0700	12.1650	0.1240	1.1160	0.0325	0.0693	11.5000	0.1380	1.1240
33	0.0280	0.0740	12.1260	0.1100	1.0580	0.0285	0.0735	11.5000	0.1228	1.0690
34	0.0310	0.0730	12.1270	0.1460	1.0590	0.0316	0.0725	11.5000	0.1630	1.0699
35	0.0330	0.0680	12.1130	0.1340	1.1200	0.0337	0.0676	11.5000	0.1498	1.1329
36	0.0340	0.0680	12.1150	0.1030	1.0870	0.0347	0.0676	11.5000	0.1151	1.0993
37	0.0310	0.0590	12.2100	0.1310	1.0770	0.0314	0.0582	11.5000	0.1453	1.0907
38	0.0280	0.0610	11.9110	0.0970	1.1040	0.0291	0.0619	11.5000	0.1103	1.1356
39	0.0330	0.0640	11.9730	0.0980	1.0220	0.0341	0.0645	11.5000	0.1106	1.0458
40	0.0320	0.0630	12.0640	0.0970	0.9930	0.0327	0.0627	11.5000	0.1087	1.0068
41	0.0290	0.0610	11.9960	0.0900	1.0870	0.0299	0.0613	11.5000	0.1016	1.1102
42	0.0330	0.0750	12.0280	0.0950	1.0450	0.0339	0.0751	11.5000	0.1070	1.0645
43	0.0290	0.0690	12.2800	0.1050	1.0880	0.0292	0.0672	11.5000	0.1158	1.0855
44	0.0270	0.0700	12.2010	0.1090	1.0250	0.0274	0.0691	11.5000	0.1210	1.0293
45	0.0300	0.0770	12.1010	0.0960	1.0590	0.0306	0.0766	11.5000	0.1097	1.0722
46	0.0327	0.0655	11.8732	0.1090	1.0455	0.0340	0.0664	11.5000	0.1243	1.0789
47	0.0282	0.0734	12.0190	0.1062	1.0897	0.0290	0.0735	11.5000	0.1219	1.1109
48	0.0218	0.0699	11.9359	0.1133	1.0973	0.0226	0.0705	11.5000	0.1285	1.1264
49	0.0325	0.0721	11.9626	0.1002	1.0214	0.0335	0.0724	11.5000	0.1132	1.0444
50	0.0299	0.0603	12.0004	0.0706	1.0237	0.0308	0.0605	11.5000	0.0797	1.0452
51	0.0347	0.0726	12.2745	0.1056	1.0849	0.0349	0.0712	11.5000	0.1165	1.0829
52	0.0313	0.0632	12.0368	0.0962	1.0387	0.0321	0.0632	11.5000	0.1062	1.0573
53	0.0293	0.0719	11.3054	0.0807	0.9959	0.0320	0.0766	11.5000	0.0967	1.0793
54	0.0344	0.0625	11.2771	0.0821	0.9979	0.0377	0.0667	11.5000	0.0986	1.0842
55	0.0323	0.0581	11.3412	0.0730	0.9848	0.0352	0.0617	11.5000	0.0872	1.0639
56	0.0358	0.0688	11.2835	0.0854	0.9901	0.0392	0.0734	11.5000	0.1025	1.0751
57	0.0288	0.0713	11.3015	0.0833	1.0292	0.0315	0.0759	11.5000	0.0998	1.1158
58	0.0232	0.0534	11.2567	0.0806	0.9993	0.0255	0.0571	11.5000	0.0970	1.0877
59	0.0242	0.0627	11.2109	0.0853	0.9052	0.0267	0.0673	11.5000	0.1030	0.9893
60	0.0355	0.0586	11.2478	0.0831	0.9016	0.0390	0.0627	11.5000	0.1001	0.9821

Appendix B. Electron microprobe values obtained for bentonite FP-12. Columns of MgH, TiR, AlK, Cl, and FeG (left of vertical line) indicate the weight fraction of the elemental oxides without Bence-Albee matrix corrections and the columns of MgO, TiO_2, Al_2O_3, Cl, and FeO (right of the vertical line) indicate the weight % of each elemental oxide after correction with its beta factor.

FP-12

SAMPLE	MgH	TiR	AlK	Cl	FeG	MgO	TiO2	Al2O3	Cl	FeO
1	0.0981	0.1075	11.3909	0.0548	0.6612	0.1064	0.1136	11.5000	0.0651	0.7112
2	0.0884	0.0959	11.2137	0.0507	0.6641	0.0974	0.1029	11.5000	0.0612	0.7256
3	0.1019	0.1132	11.4155	0.0681	0.6452	0.1103	0.1194	11.5000	0.0808	0.6925
4	0.0924	0.0921	10.9073	0.0598	0.6395	0.1047	0.1016	11.5000	0.0742	0.7184
5	0.1027	0.1130	11.3214	0.0575	0.7757	0.1121	0.1201	11.5000	0.0688	0.8395
6	0.0933	0.0895	11.3545	0.0550	0.7107	0.1016	0.0949	11.5000	0.0656	0.7669
7	0.0946	0.1021	11.3620	0.0492	0.6892	0.1029	0.1082	11.5000	0.0586	0.7432
8	0.1025	0.1247	11.4905	0.0561	0.7043	0.1103	0.1306	11.5000	0.0661	0.7510
9	0.0957	0.0916	11.7466	0.0618	0.6447	0.1007	0.0939	11.5000	0.0712	0.6725
10	0.0909	0.0878	12.1895	0.0552	0.7100	0.0922	0.0867	11.5000	0.0613	0.7137
11	0.0852	0.0946	11.2765	0.0508	0.6965	0.0934	0.1010	11.5000	0.0610	0.7568
12	0.0939	0.0901	11.3652	0.0520	0.7029	0.1021	0.0954	11.5000	0.0620	0.7578
13	0.1015	0.1159	12.4386	0.0693	0.6832	0.1009	0.1122	11.5000	0.0754	0.6730
14	0.0960	0.1105	11.8750	0.0558	0.6702	0.0999	0.1120	11.5000	0.0636	0.6915
15	0.0976	0.1148	12.0144	0.0717	0.7372	0.1004	0.1150	11.5000	0.0808	0.7518
16	0.1052	0.1047	12.2313	0.0710	0.7050	0.1063	0.1030	11.5000	0.0786	0.7062
17	0.0862	0.0849	12.0390	0.0621	0.6948	0.0885	0.0849	11.5000	0.0699	0.7071
18	0.0847	0.0765	11.4616	0.0538	0.7264	0.0913	0.0803	11.5000	0.0636	0.7765
19	0.1018	0.0995	11.2083	0.0515	0.7204	0.1123	0.1069	11.5000	0.0622	0.7875
20	0.0625	0.0498	11.1465	0.0518	0.7209	0.0693	0.0538	11.5000	0.0629	0.7924
21	0.0543	0.0421	10.8818	0.0579	0.6603	0.0617	0.0466	11.5000	0.0721	0.7435
22	0.0910	0.0911	11.3206	0.0513	0.7207	0.0994	0.0969	11.5000	0.0614	0.7800
23	0.0965	0.0975	11.1857	0.0461	0.7518	0.1066	0.1049	11.5000	0.0558	0.8235
24	0.1002	0.1097	11.1729	0.0499	0.7564	0.1108	0.1182	11.5000	0.0605	0.8295
25	0.0952	0.1030	11.3050	0.0479	0.7301	0.1041	0.1097	11.5000	0.0574	0.7913
26	0.0961	0.0958	11.3865	0.0495	0.7236	0.1043	0.1013	11.5000	0.0589	0.7786
27	0.0491	0.0384	10.8329	0.0535	0.6586	0.0560	0.0427	11.5000	0.0669	0.7449
28	0.0465	0.0399	11.0330	0.0451	0.6606	0.0521	0.0435	11.5000	0.0554	0.7336
29	0.0633	0.0358	11.4682	0.0621	0.7217	0.0682	0.0376	11.5000	0.0733	0.7710
30	0.0968	0.1161	11.7210	0.0586	0.7893	0.1021	0.1192	11.5000	0.0677	0.8251
31	0.0627	0.0545	11.7693	0.0587	0.7410	0.0658	0.0557	11.5000	0.0675	0.7714
32	0.0976	0.1148	12.0144	0.0717	0.7372	0.1004	0.1150	11.5000	0.0808	0.7518
33	0.0960	0.1105	11.8750	0.0558	0.6702	0.0999	0.1120	11.5000	0.0636	0.6915
34	0.1015	0.1159	12.4386	0.0693	0.9832	0.1009	0.1122	11.5000	0.0754	0.9685
35	0.1085	0.1007	14.7265	0.0706	0.6724	0.0911	0.0823	11.5000	0.0649	0.5594
36	0.0884	0.0811	10.8591	0.0433	0.6196	0.1006	0.0899	11.5000	0.0540	0.6991
37	0.0533	0.0530	9.7561	0.0538	0.5410	0.0675	0.0654	11.5000	0.0747	0.6794
38	0.0620	0.0693	8.5733	0.0466	0.4757	0.0894	0.0973	11.5000	0.0736	0.6798
39	0.0445	0.0451	9.5940	0.0473	0.5829	0.0573	0.0566	11.5000	0.0668	0.7444
40	0.0836	0.1007	9.6455	0.0459	0.6062	0.1071	0.1257	11.5000	0.0644	0.7700
41	0.0585	0.0591	8.2509	0.0365	0.5128	0.0876	0.0862	11.5000	0.0599	0.7615
42	0.0600	0.0730	8.2944	0.0440	0.5170	0.0894	0.1059	11.5000	0.0718	0.7637
43	0.0709	0.0708	9.4967	0.0466	0.5990	0.0923	0.0897	11.5000	0.0665	0.7728
44	0.0790	0.0823	9.6332	0.0536	0.5666	0.1014	0.1028	11.5000	0.0753	0.7207

Appendix C. Electron microprobe values obtained from bentonite SJ-6. The columns of MgH, TiR, AlK, Cl, and FeG (left of the vertical line) indicate the weight fraction of the elemental oxides without Bence-Albee matrix corrections and the columns of MgO, TiO_2, Al_2O_3, Cl, and FeO (right of the vertical line) indicate the weight % of each elemental oxide after correction with its beta factor.

SJ-6

SAMPLE	MgH	TiR	AlK	Cl	FeG	MgO	TiO2	Al2O3	Cl	FeO
1	0.0817	0.0752	11.5157	0.0564	0.7439	0.0877	0.0786	11.5000	0.0663	0.7915
2	0.0960	0.0917	11.4160	0.0559	0.7083	0.1039	0.0967	11.5000	0.0663	0.7602
3	0.0518	0.0588	11.3378	0.0552	0.5659	0.0565	0.0624	11.5000	0.0659	0.6115
4	0.0514	0.0266	11.1826	0.0507	0.6229	0.0568	0.0286	11.5000	0.0614	0.6825
5	0.0936	0.0879	11.1901	0.0551	0.7395	0.1034	0.0946	11.5000	0.0667	0.8097
6	0.0644	0.0556	11.3415	0.0520	0.6897	0.0702	0.0590	11.5000	0.0621	0.7451
7	0.0597	0.0457	11.2288	0.0575	0.6456	0.0657	0.0490	11.5000	0.0693	0.7044
8	0.1033	0.1009	11.6450	0.0443	0.7312	0.1096	0.1043	11.5000	0.0515	0.7693
9	0.0599	0.0471	11.2332	0.0489	0.6482	0.0659	0.0505	11.5000	0.0590	0.7070
10	0.0923	0.1044	11.5392	0.0509	0.6907	0.0989	0.1089	11.5000	0.0597	0.7334
11	0.0924	0.0991	11.4820	0.0522	0.6853	0.0995	0.1039	11.5000	0.0616	0.7313
12	0.0738	0.0710	11.8211	0.0686	0.7735	0.0772	0.0723	11.5000	0.0786	0.8017
13	0.0389	0.0411	10.7209	0.0556	0.5291	0.0448	0.0461	11.5000	0.0702	0.6047
14	0.0984	0.1180	12.0349	0.0701	0.7959	0.1011	0.1180	11.5000	0.0789	0.8103
15	0.0462	0.0506	12.2797	0.0606	0.7380	0.0465	0.0496	11.5000	0.0668	0.7364
16	0.0345	0.0309	11.1641	0.0531	0.5823	0.0382	0.0333	11.5000	0.0644	0.6391
17	0.0530	0.0527	11.4815	0.0536	0.6847	0.0571	0.0553	11.5000	0.0632	0.7307
18	0.0419	0.0630	11.0481	0.0467	0.6202	0.0469	0.0686	11.5000	0.0572	0.6878
19	0.0454	0.0526	10.4635	0.0498	0.6579	0.0536	0.0605	11.5000	0.0645	0.7704
20	0.0972	0.1007	11.1559	0.0516	0.8038	0.1077	0.1087	11.5000	0.0626	0.8828
21	0.0494	0.0507	11.0662	0.0494	0.6423	0.0552	0.0551	11.5000	0.0605	0.7111
22	0.0486	0.0299	8.3445	0.0419	0.5356	0.0720	0.0431	11.5000	0.0680	0.7864
23	0.0720	0.0855	8.7848	0.0338	0.5780	0.1013	0.1172	11.5000	0.0521	0.8061
24	0.0716	0.0998	10.9782	0.0470	0.6071	0.0806	0.1094	11.5000	0.0580	0.6776
25	0.0851	0.1064	11.4675	0.0455	0.7270	0.0917	0.1117	11.5000	0.0537	0.7768
26	0.0498	0.0242	8.6980	0.0480	0.5811	0.0708	0.0335	11.5000	0.0747	0.8186
27	0.0561	0.0284	9.3351	0.0522	0.5976	0.0743	0.0366	11.5000	0.0757	0.7844
28	0.0349	0.0328	9.3334	0.0558	0.5489	0.0462	0.0423	11.5000	0.0810	0.7206
29	0.0578	0.0328	11.1871	0.0445	0.6809	0.0639	0.0353	11.5000	0.0539	0.7457
30	0.0929	0.0836	11.4739	0.0492	0.7576	0.1001	0.0877	11.5000	0.0581	0.8090
31	0.0598	0.0588	11.5698	0.0506	0.7328	0.0639	0.0612	11.5000	0.0592	0.7760
32	0.0566	0.0400	11.6414	0.0603	0.7388	0.0601	0.0414	11.5000	0.0701	0.7776
33	0.0437	0.0456	11.8252	0.0470	0.6578	0.0457	0.0464	11.5000	0.0538	0.6816
34	0.0563	0.0428	11.7911	0.1006	0.6744	0.0590	0.0437	11.5000	0.1155	0.7008
35	0.0884	0.0983	11.7041	0.0526	0.7726	0.0934	0.1011	11.5000	0.0609	0.8088
36	0.0518	0.0477	11.7510	0.0516	0.7058	0.0545	0.0489	11.5000	0.0595	0.7359
37	0.0503	0.0475	11.3861	0.0510	0.7111	0.0546	0.0502	11.5000	0.0607	0.7652

Appendix D. Electron microprobe values obtained from bentonite NH-4. Columns of MgH, TiR, AlK, Cl, and FeG (left of the vertical line) indicate weight fraction of the elemental oxide without the Bence-Albee matrix corrections and columns of MgO, TiO_2, Al_2O_3, Cl, and FeO (right of the vertical line) indicate weight % of each elemental oxide after correction with its beta factor.

NH-4

SAMPLE	MgH	TiR	AlK	Cl	FeG	MgO	TiO2	Al2O3	Cl	FeO
1	0.0572	0.0450	12.1386	0.0730	0.6464	0.0582	0.0446	11.5000	0.0814	0.6525
2	0.1076	0.1121	12.1269	0.0640	0.8010	0.1097	0.1113	11.5000	0.0715	0.8093
3	0.0554	0.0490	11.6742	0.0719	0.7300	0.0587	0.0505	11.5000	0.0834	0.7662
4	0.0714	0.0894	12.0155	0.0618	0.8029	0.0734	0.0896	11.5000	0.0697	0.8187
5	0.1061	0.0961	11.9145	0.0756	0.7483	0.1101	0.0971	11.5000	0.0859	0.7695
6	0.1067	0.1088	12.7808	0.0578	0.7581	0.1032	0.1025	11.5000	0.0612	0.7268
7	0.0904	0.1030	12.4228	0.0684	0.8196	0.0899	0.0998	11.5000	0.0746	0.8084
8	0.0760	0.0393	11.3607	0.0640	0.6698	0.0827	0.0416	11.5000	0.0763	0.7224
9	0.0878	0.0817	11.6208	0.0483	0.7794	0.0934	0.0846	11.5000	0.0563	0.8218
10	0.0515	0.0343	11.3208	0.0464	0.6830	0.0562	0.0365	11.5000	0.0555	0.7392
11	0.0907	0.0891	11.3320	0.0514	0.7015	0.0989	0.0946	11.5000	0.0614	0.7585
12	0.0875	0.1049	11.5070	0.0521	0.7268	0.0940	0.1097	11.5000	0.0613	0.7739
13	0.0521	0.0379	11.2312	0.0525	0.6648	0.0573	0.0406	11.5000	0.0633	0.7252
14	0.0584	0.0456	11.0246	0.0535	0.6980	0.0655	0.0498	11.5000	0.0657	0.7757
15	0.4540	0.0435	11.3755	0.0555	0.7124	0.4933	0.0460	11.5000	0.0661	0.7673
16	0.0951	0.0990	11.2433	0.0522	0.7253	0.1045	0.1060	11.5000	0.0629	0.7904
17	0.0596	0.0177	11.1554	0.0722	0.8268	0.0660	0.0191	11.5000	0.0876	0.9081
18	0.0988	0.1046	11.3233	0.0477	0.7467	0.1078	0.1112	11.5000	0.0570	0.8080
19	0.0869	0.0982	11.6251	0.0513	0.7327	0.0924	0.1017	11.5000	0.0598	0.7722
20	0.0701	0.0754	8.6280	0.0387	0.5585	0.1004	0.1052	11.5000	0.0607	0.7931
21	0.0675	0.0534	8.3466	0.0334	0.5427	0.1000	0.0770	11.5000	0.0542	0.7967
22	0.0875	0.0670	8.7901	0.0495	0.5688	0.1230	0.0918	11.5000	0.0763	0.7928
23	0.0627	0.0541	8.9275	0.0503	0.5627	0.0868	0.0729	11.5000	0.0763	0.7723
24	0.0843	0.0862	9.0902	0.0560	0.5341	0.1146	0.1141	11.5000	0.0834	0.7199
25	0.0362	0.0258	8.7229	0.0461	0.5070	0.0513	0.0356	11.5000	0.0716	0.7121
26	0.0631	0.0668	9.2352	0.0474	0.5646	0.0844	0.0871	11.5000	0.0695	0.7491

Appendix E. Electron microprobe values obtained from bentonite TP-2. Columns of MgH, TiR, AlK, Cl, and FeG (left of the vertical line) indicate the wieght fraction of elemental oxides without the Bence-Albee matrix corrections and columns of MgO, TiO_2, Al_2O_3, Cl, and FeO (right of vertical line indicate weight % of each elemental oxide after correction with its beta factor.

TP-2

SAMPLE	MgH	TiR	AlK	Cl	FeG	MgO	TiO2	Al2O3	Cl	FeO
1	0.0188	0.0317	11.5298	0.0618	0.7687	0.0202	0.0331	11.5000	0.0726	0.8169
2	0.0883	0.0997	11.7538	0.0520	0.7126	0.0929	0.1021	11.5000	0.0599	0.7428
3	0.0645	0.0457	11.2652	0.0496	0.6815	0.0708	0.0488	11.5000	0.0596	0.7412
4	0.0390	0.0209	11.2761	0.0536	0.6807	0.0427	0.0223	11.5000	0.0644	0.7396
5	0.0465	0.0241	11.4639	0.0541	0.6981	0.0501	0.0253	11.5000	0.0639	0.7461
6	0.0945	0.1115	11.3968	0.0479	0.7712	0.1025	0.1178	11.5000	0.0569	0.8291
7	0.0939	0.1041	11.1147	0.0477	0.7594	0.1044	0.1127	11.5000	0.0581	0.8371
8	0.0928	0.1148	11.5404	0.0509	0.7406	0.0994	0.1197	11.5000	0.0597	0.7863
9	0.0807	0.1118	11.6423	0.0483	0.7610	0.0857	0.1156	11.5000	0.0562	0.8009
10	0.0981	0.1128	11.7450	0.0454	0.7798	0.1032	0.1156	11.5000	0.0523	0.8135
11	0.0899	0.1001	11.8073	0.0502	0.7243	0.0941	0.1021	11.5000	0.0576	0.7516
12	0.1055	0.1222	11.4538	0.0521	0.8123	0.1138	0.1284	11.5000	0.0616	0.8689
13	0.0469	0.0310	11.5231	0.0552	0.7084	0.0503	0.0324	11.5000	0.0649	0.7532
14	0.0920	0.1029	11.6993	0.0452	0.7850	0.0972	0.1059	11.5000	0.0523	0.8221
15	0.0234	0.0188	11.1603	0.0310	0.3855	0.0259	0.0203	11.5000	0.0376	0.4232
16	0.0815	0.1044	11.7358	0.0447	0.7814	0.0858	0.1071	11.5000	0.0516	0.8158
17	0.0890	0.1035	11.6755	0.0453	0.7784	0.0942	0.1067	11.5000	0.0525	0.8169
18	0.0988	0.1011	11.4950	0.0464	0.7866	0.1062	0.1059	11.5000	0.0547	0.8384
19	0.0946	0.1033	11.5522	0.0560	0.7548	0.1012	0.1076	11.5000	0.0656	0.8005

Appendix F. Electron microprobe values obtained from bentonite FP-9. Columns of MgH, TiR, AlK, Cl, and FeG (left of the vertical line) indicate wieght fraction of the elemental oxides without Bence-Albee matrix corrections and columns of MgO, TiO_2, Al_2O_3, Cl, and FeO (right of the vertical line) indicate weight % of each elemntal oxide after correction with its beta factor.

FP-9

SAMPLE	MgH	TiR	AlK	Cl	FeG	MgO	TiO2	Al2O3	Cl	FeO
1	0.0752	0.0470	12.1973	0.0434	0.7073	0.0762	0.0464	11.5000	0.0482	0.7105
2	0.0907	0.0337	11.6902	0.0417	0.7778	0.0959	0.0347	11.5000	0.0483	0.8152
3	0.1151	0.0714	11.8473	0.0463	0.9556	0.1201	0.0725	11.5000	0.0529	0.9883
4	0.1894	0.0849	11.4360	0.0415	0.9709	0.2047	0.0894	11.5000	0.0491	1.0402
5	0.1171	0.0701	11.6165	0.0418	0.9712	0.1246	0.0726	11.5000	0.0487	1.0244
6	0.0808	0.0510	11.5840	0.0385	0.6484	0.0862	0.0530	11.5000	0.0450	0.6858
7	0.0987	0.0250	11.6967	0.0438	0.8024	0.1043	0.0257	11.5000	0.0507	0.8405
8	0.0984	0.0190	11.6116	0.0588	0.7502	0.1047	0.0197	11.5000	0.0686	0.7916
9	0.1292	0.0633	11.6579	0.0401	0.9638	0.1370	0.0654	11.5000	0.0466	1.0129
10	0.0631	0.0551	11.2200	0.0563	0.7232	0.0695	0.0591	11.5000	0.0680	0.7897
11	0.1169	0.0211	12.1079	0.0802	0.7756	0.1193	0.0210	11.5000	0.0897	0.7849
12	0.0779	0.0613	11.9519	0.0647	0.6033	0.0806	0.0617	11.5000	0.0733	0.6185
13	0.0828	0.0495	12.4963	0.0737	0.6597	0.0819	0.0477	11.5000	0.0799	0.6468
14	0.0957	0.0537	12.2471	0.0442	0.9674	0.0966	0.0528	11.5000	0.0489	0.9678
15	0.1076	0.0549	12.2435	0.0403	0.9656	0.1086	0.0540	11.5000	0.0446	0.9663
16	0.0841	0.0379	12.2086	0.0424	0.6665	0.0851	0.0374	11.5000	0.0470	0.6689
17	0.0986	0.0459	12.2515	0.0390	0.9220	0.0995	0.0451	11.5000	0.0431	0.9221
18	0.1096	0.0369	12.4014	0.0476	0.9450	0.1092	0.0358	11.5000	0.0520	0.9336
19	0.1236	0.0738	11.9020	0.0373	0.9748	0.1284	0.0746	11.5000	0.0424	1.0035
20	0.1112	0.0673	12.2845	0.0414	1.0018	0.1119	0.0659	11.5000	0.0456	0.9992

Appendix G. Electron microprobe values obtained from bentonite MW-1. Columns of MgH, TiR, AlK, Cl, and FeG (left of the vertical line) indicate the weight fraction of elemental oxides without Bence-Albee matrix corrections and the columns of MgO, TiO_2, Al_2O_3, Cl, and FeO indicate weight % of each elemental oxide after correction with its beta factor.

MW-1

SAMPLE	MgH	TiR	AlK	Cl	FeG	MgO	TiO2	Al2O3	Cl	FeO
1	0.0987	0.0578	11.4260	0.0422	0.8627	0.1068	0.0609	11.5000	0.0500	0.9251
2	0.0902	0.0185	11.8766	0.0376	0.6677	0.0939	0.0188	11.5000	0.0429	0.6888
3	0.0979	0.0712	11.4106	0.0512	0.7474	0.1060	0.0751	11.5000	0.0608	0.8025
4	0.0809	0.0282	11.6856	0.0293	0.4266	0.0856	0.0290	11.5000	0.0340	0.4473
5	0.1067	0.0433	11.5586	0.0383	0.7627	0.1141	0.0451	11.5000	0.0449	0.8085
6	0.0916	0.0302	12.4368	0.0334	0.2108	0.0910	0.0292	11.5000	0.0364	0.2077
7	0.1131	0.0723	12.1145	0.0335	0.6103	0.1154	0.0718	11.5000	0.0374	0.6172
8	0.1102	0.0413	11.9789	0.0398	0.8925	0.1137	0.0415	11.5000	0.0450	0.9129
9	0.0616	0.0444	11.9544	0.0440	0.6011	0.0637	0.0447	11.5000	0.0498	0.6161
10	0.0272	0.0087	11.9563	0.0349	0.0281	0.0281	0.0088	11.5000	0.0395	0.0288
11	0.0789	0.0473	12.7625	0.0395	0.5703	0.0764	0.0446	11.5000	0.0419	0.5475
12	0.1075	0.0533	12.1093	0.0426	0.9283	0.1097	0.0530	11.5000	0.0476	0.9393
13	0.0773	0.0725	11.9825	0.0753	0.2273	0.0797	0.0728	11.5000	0.0851	0.2324
14	0.0864	0.0227	11.9333	0.0391	0.8193	0.0895	0.0229	11.5000	0.0444	0.8412

Appendix H. Electron microprobe values obtained from bentonite NH-3. Columns of MgH, TiR, AlK, Cl, and FeG (left of vertical line) indicate elemental oxides without Bence-Albee matrix corrections and columns of MgO, TiO_2, Al_2O_3, Cl, and FeO (right of vertical line) indicate each elemental oxide after correction with its beta factor.

NH-3

SAMPLE	MgH	TiR	AlK	Cl	FeG	MgO	TiO2	Al2O3	Cl	FeO
1	0.1115	0.0750	11.7020	0.0390	0.9525	0.1178	0.0771	11.5000	0.0451	0.9973
2	0.0908	0.0480	11.8993	0.0364	0.7385	0.0943	0.0486	11.5000	0.0414	0.7604
3	0.0812	0.0391	11.8941	0.0290	0.6256	0.0844	0.0396	11.5000	0.0330	0.6444
4	0.0947	0.0000	11.6962	0.0415	0.7595	0.1001	0.0000	11.5000	0.0480	0.7956
5	0.0442	0.0465	10.6552	0.0210	0.6386	0.0513	0.0525	11.5000	0.0267	0.7343
6	0.1073	0.0623	11.4738	0.0381	0.9348	0.1156	0.0654	11.5000	0.0450	0.9982
7	0.0867	0.0334	11.7468	0.0334	0.6864	0.0912	0.0342	11.5000	0.0385	0.7159
8	0.1057	0.0541	11.5680	0.0338	0.9365	0.1129	0.0563	11.5000	0.0396	0.9919
9	0.0778	0.0259	10.5587	0.0445	0.6048	0.0911	0.0295	11.5000	0.0571	0.7018
10	0.1037	0.0533	11.9301	0.0563	0.8024	0.1074	0.0538	11.5000	0.0639	0.8241